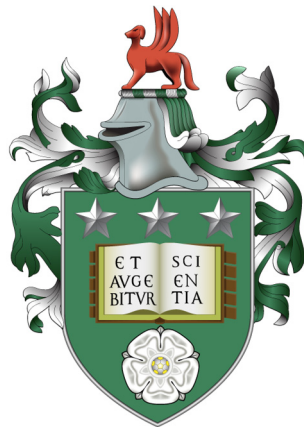


# **Implications of Large-Scale Bioenergy Deployment for Land, Climate and Biodiversity**

**Charlotte Maya Weaver**



**University of Leeds**

School of Chemical and Process Engineering

School of Earth and Environment

This dissertation is submitted for the degree of

*Doctor of Philosophy*

September 2022



## **Declaration of Authorship**

The candidate confirms that the work submitted is her own and that appropriate credit has been given where reference has been made to the work of others.

Charlotte Maya Weaver

2022

This copy has been supplied on the understanding that it is copyright material, and that no quotation may be published without proper acknowledgment. The right of Charlotte Maya Weaver to be identified as Author of this work has been asserted by her in accordance with the Copyright, Designs and Patents Act 1988.

© 2022 The University of Leeds and Charlotte Maya Weaver



## Acknowledgements

I would firstly like to thank my three supervisors: Piers Forster, for all the questions answered, the opportunities provided to me, and his unwavering faith in me from the start, and Dominick Spracklen and Catherine Bale for their additional guidance, expertise, and support throughout the years. I would also like to acknowledge the EPSRC Centre for Doctoral Training (CDT) in Bioenergy and the United Bank of Carbon (UBoC) for giving me the opportunity and funding to carry out this PhD.

I want to express my deepest gratitude to Antti-Ilari Partanen, Nadine Mengis, and Damon Matthews at Concordia University in Montreal, for showing me how to set up and run the University of Victoria (UVic) climate model; their guidance, technical expertise, and overall kindness helped form the basis of *Chapter 4*. Thanks also to Christophe Simmons and Lawrence Mysak for all the extra advice on the UVic model. Regarding *Chapter 5*, I'd like to thank Amy Molotoks for introducing me to analyses using the Alliance for Zero Extinction database, and to Chris Smith and Camille Leclerc for their advice and efforts on future work in climate implications for biodiversity. I'm also very grateful to Richard Rigby, who I always felt I could go to for any IT issue.

I feel extremely lucky to have been part of the Bioenergy CDT, largely due to the people I have met. In particular, I'd like to thank Jenny Jones, James McKay, Emily Bryan-Kinns, and Andrew Ross who always went out of their way to organise everything. Importantly, I couldn't have done this PhD without my colleagues and friends. Special thanks to Daisy Thomas, Iram Razaq, Nicola Wood, Jennifer Spragg, and Richard Birley for being truly great friends from the start. I will miss our many tea breaks! I'd also like to thank the cohort in the year above, in particular Hana Mandová, Luke Conibear, Lee Roberts and Robert White, for all the great chats and always being willing to pass down your wisdom. In addition to the CDT, I feel very grateful to have been part of the School of Earth and Environment, where I met so many wonderful people. A huge thank you to Anya Schlich-Davies, Sarah Shallcross, Laura Arenas-Calle, Laura Kiely, Anne Barber, and Josie McSherry for being amazing friends over the last few years. Thanks also to the UBoC team, including Cat Scott, Anna Gugan, Hazel Mooney, Will Rolls, Tom Sloan, Judith Ford, and Jonathan Wild, who have ignited my interest in trees, and who provided great company during my write up.

I also want to thank all my friends and family outside of work, who I couldn't have done this PhD without. Special mention to Silka, Harriet, Yasmine, Asha, and Hannah for being there for me always. Also, to Gail and Paul for all the support and wonderful meals towards the end of my PhD. Finally, a massive thank you to Stu for the constant love and encouragement, and for being a rock through it all. And to my parents, who have always inspired and motivated me to chase my aspirations.

## Abstract

Large-scale second-generation bioenergy production with carbon capture and storage (BECCS) is considered a crucial component in many climate change mitigation pathways limiting global warming to 1.5–2 °C. However, land requirements for lignocellulosic cropland expansion could pose threats to the Sustainable Development Goal (SDG) agenda. Two major concerns regarding impacts of land-use changes are potential implications for climate and biodiversity. Yet, with regards to bioenergy, these two areas remain relatively understudied, largely due to a lack of suitable data resources and the overall complexity involved in calculating these impacts. As a result, most literature on land-use impacts of bioenergy focuses on present day first-generation bioenergy cropland and/or tends to be at the regional or local scale.

The aim of this thesis is to explore the global impacts of large-scale bioenergy deployment (300 EJyr<sup>-1</sup> by 2100) on climate and biodiversity, in the aims of furthering our knowledge of bioenergy's role within SDGs 13: "Climate Action", and 15: "Life on Land". By implementing sophisticated land-use scenarios into an Earth system climate model and two species richness models, this work identifies potential biogeochemical and biogeophysical climate effects and biodiversity impacts resulting from global cultivation of second-generation energy cropland over the 21<sup>st</sup> century. At the global scale, findings suggest major climate benefits from large-scale BECCS production, whereby substitution of fossil fuel emissions via BECCS leads to a cooling effect (–0.44 °C by 2100) which is significantly dominant over the biogeochemical warming effect from land conversion (+0.0087 °C by 2075–2100). At the regional scale, however, both biogeochemical and biogeophysical climate effects are more significant (reaching up to 0.1 °C and -0.09 °C in some regions by 2075–2100, respectively) and vary widely across the globe, influenced by changes in polar amplification, soil carbon, surface albedo, evapotranspiration, sensible and latent heat fluxes, and soil temperatures.

Bioenergy expansion is also expected to cause significant habitat loss in biodiversity hotspots, particularly across tropical regions of Africa, Asia, and Latin America, with the largest numbers and percentages of endemic species extinctions occurring in Madagascar and the Philippines, respectively. Mexico contains the highest number of threatened endangered and critically endangered species in comparison to all other countries, accounting for more than half of the total species impacted by cropland expansion in North America. In total, approximately

12,300–15,500 endemic species and 557 endangered and critically endangered species are expected to be lost due to second-generation bioenergy production by 2100.

Sustainability measures will be needed alongside large-scale bioenergy deployment to combat potential trade-offs with sustainability goals. For instance, water protection and forest conservation policies can be implemented to reduce unsustainable water withdrawals and deforestation. However, findings in this work indicate that, while global impacts of water protection on land-use changes are small, the expansion of non-irrigated rainfed cropland into nearby forests could cause further threats to biodiversity and exacerbate biogeophysical climate effects. Site-specific understanding of human and environmental water consumption, increased irrigation efficiency through improvements in water storage and transport, and better land management practices can help increase yields and reduce the need for large areas of rainfed cropland.

On the other hand, implementation of a global forest protection scheme (REDD+) significantly reduces implications of bioenergy expansion for both climate and biodiversity. Although, cropland ‘leakage’ onto other equally biodiverse ecosystems may occur. Furthermore, current conservation initiatives tend to focus on reductions in greenhouse gas emissions, often overlooking the broader range of ecosystem services provided by forests, such as biogeophysical effects (e.g., water regulation, soil protection), ecological functions, and cultural values. Sustainable delivery of second-generation bioenergy will require a more holistic representation of these ecosystem services in future land management and conservation schemes, aided by shared knowledge between local stakeholders (e.g., landowners, local governments, and indigenous communities), researchers, and policy advisors.



# Contents

<b>List of Figures</b> .....	<b>xv</b>
<b>List of Tables</b> .....	<b>xxiii</b>
<b>Abbreviations</b> .....	<b>xxv</b>
<b>Chapter 1 Introduction</b> .....	<b>1</b>
1.1    Anthropogenic Climate Change .....	1
1.2    The Role of Bioenergy in Future Mitigation Pathways.....	3
1.3    Sustainability of Large-Scale Bioenergy Deployment .....	5
1.4    Research Aims.....	9
1.5    Thesis Structure .....	10
<b>Chapter 2 Theoretical Background and Literature Review</b> .....	<b>13</b>
2.1    Overview .....	13
2.2    The Role of Bioenergy in Climate Change Mitigation.....	13
2.2.1    Global Status of Bioenergy .....	13
2.2.1.1    Traditional Bioenergy .....	14
2.2.1.2    Modern bioenergy .....	15
2.2.2    Biomass Feedstocks and Energy Production .....	15
2.2.2.1    First-generation biomass .....	15
2.2.2.2    Second-generation biomass.....	16
2.2.2.3    Third-generation biomass .....	17
2.2.3    Decarbonisation via Second-Generation Bioenergy Expansion .....	18
2.2.3.1    A Transition from First- to Second-Generation Bioenergy .....	18
2.2.3.2    Bioenergy with Carbon Capture and Storage (BECCS) .....	19
2.2.3.3    Future Mitigation Pathways .....	20
2.2.3.4    BECCS Deployment in Future Mitigation Pathways.....	22
2.2.3.5    Global Carbon Cycle Responses to CDR and BECCS .....	24
2.2.3.6    Land-Use Changes in Future Mitigation Pathways .....	26
2.2.4    Sustainability Implications of Large-Scale Bioenergy Deployment.....	31
2.3    Impacts of Bioenergy Expansion on Climate .....	32
2.3.1    Climate Impacts of Deforestation .....	32
2.3.1.1    Biogeochemical Impacts of Deforestation .....	32

2.3.1.2	Biogeophysical Impacts of Deforestation.....	34
2.3.2	Calculating Biogeochemical and Biogeophysical Climate Impacts .....	34
2.3.2.1	Ground-Based and Observational Techniques .....	35
2.3.2.2	Modelling Techniques .....	36
2.3.2.2.1	Dynamic Global Vegetation Models (DGVMs) .....	36
2.3.2.2.2	Global Climate Models (GCMs).....	37
2.3.2.3	TCRE Methodology .....	38
2.3.3	Global and Regional Climate Impacts of Deforestation.....	39
2.3.4	Climate Impacts of Historical Land-Use Changes .....	40
2.3.5	Lessons from First-Generation Bioenergy Expansion.....	42
2.3.6	Climate Impacts of Second-Generation Bioenergy Within Future Pathways .	45
2.3.7	Isolated Impacts of Bioenergy Expansion in Future Mitigation Pathways .....	50
2.3.7.1	Regional Impacts .....	50
2.3.7.2	Global Impacts.....	51
2.4	Impacts of Bioenergy Expansion on Biodiversity .....	53
2.4.1	Impacts of First-Generation Bioenergy Expansion .....	54
2.4.2	Impacts of Indirect Land-Use Change.....	55
2.4.3	Impacts of Second-Generation Bioenergy Expansion.....	56
2.4.3.1	An Improvement on First-Generation Bioenergy? .....	56
2.4.3.2	Measuring Impacts of Second-Generation Bioenergy Production on Biodiversity .....	57
2.4.3.2.1	Land-Use Impacts .....	58
2.4.3.2.2	Climate Impacts .....	61
2.4.3.2.3	Critical Analysis of Biodiversity Modelling Techniques.....	63
2.4.3.2.4	Accounting for Species Vulnerability and Irreplaceability .....	66
2.5	Sustainability Measures and Conservation Schemes .....	67
2.5.1	Land Conservation.....	67
2.5.1.1	Existing Land Conservation Schemes .....	67
2.5.1.2	Land Conservation in Future Impact Assessments.....	70
2.5.2	Water Conservation .....	71
2.5.2.1	Current Water Requirements and Conservation Schemes.....	71
2.5.2.2	Water Conservation in Future Impact Assessments .....	73
2.6	Conclusions from the Literature.....	74

<b>Chapter 3 Methods: The MAgPIE Land-Use Model and Scenarios .....</b>	<b>77</b>
3.1 Overview .....	77
3.2 Introduction to the MAgPIE Scenarios .....	77
3.2.1 MAgPIE Land-Use Optimisation Model .....	77
3.2.2 MAgPIE Land-Use Scenarios .....	79
3.2.2.1 NoBio .....	80
3.2.2.2 Bio .....	81
3.2.2.3 Bio-REDD .....	82
3.2.2.4 Bio-WaterProt .....	83
3.3 Land-Use Changes Within the MAgPIE Scenarios .....	83
3.3.1 Global Land-Use Change .....	83
3.3.2 Regional Land-Use Change .....	85
3.3.3 Comparison to Other Pathways .....	86
3.4 Uncertainties in Land-Use Modelling .....	89
3.5 Advantages of Using the MAgPIE Land-Use Scenarios .....	90
<b>Chapter 4 Impacts of Bioenergy Expansion on Climate .....</b>	<b>91</b>
4.1 Overview .....	91
4.2 Method .....	92
4.2.1 Model Description .....	92
4.2.2 Experimental Setup .....	94
4.2.2.1 Land-Use Data Input .....	94
4.2.2.2 Fossil Fuel Data Input .....	96
4.2.2.3 Other Inputs and Forcings .....	98
4.2.3 Simulations .....	99
4.3 Results .....	103
4.3.1 Land-Use Dynamics .....	103
4.3.1.1 Land Impacts in Relation to Climate-Carbon Cycle Feedbacks .....	103
4.3.1.2 Land-Use Changes in TL and PC Simulations .....	105
4.3.1.3 Isolated Impacts of Bioenergy and Conservation Schemes .....	107
4.3.2 Surface Air Temperature and Atmospheric CO <sub>2</sub> Dynamics .....	108
4.3.3 Transient Climate Response to Cumulative Carbon Emissions (TCRE) .....	110
4.3.4 Impacts of Land-Use Changes on Surface Climate .....	112
4.3.4.1 Global Impacts .....	112
4.3.4.2 Regional Impacts .....	114

4.3.5	Climate Impacts from Land-Use Change Explained .....	117
4.3.5.1	Carbon Fluxes from Land-Use Change .....	117
4.3.5.2	Biogeophysical Effects from Land-Use Change .....	121
4.3.5.2.1	Impacts of Bioenergy on Biogeophysical Effects .....	125
4.4	Discussion .....	126
4.4.1	Importance of Land Representations .....	126
4.4.1.1	Model Representations of Land-Use Changes .....	126
4.4.1.2	Effects of Present-Day Land Distributions.....	127
4.4.2	Biogeochemical and Biogeophysical Climate Impacts .....	130
4.4.2.1	Climate Impacts of Total Land-Use Change .....	130
4.4.2.2	Isolated Climate Impacts of Bioenergy .....	132
4.4.3	Biogeochemical Impacts in More Detail .....	134
4.4.3.1	A Comparison to Integrated Assessment Model Studies .....	134
4.4.3.2	A Comparison to Climate Model Studies.....	136
4.4.3.3	Soil Carbon Dynamics.....	138
4.4.3.4	Impacts of Nitrogen and Phosphorous Cycling .....	139
4.4.4	Biogeophysical Impacts in More Detail .....	141
4.4.4.1	A Comparison to Climate Model Studies.....	141
4.4.4.2	Impacts of Excluding Cloud Dynamics.....	142
4.4.4.3	A Key Missing Component in Climate Assessments and Policies.....	142
4.5	Summary and Conclusions.....	144
<b>Chapter 5 Impacts of Bioenergy Expansion on Biodiversity .....</b>		<b>147</b>
5.1	Overview .....	147
5.2	Materials and Methods.....	148
5.2.1	Data .....	148
5.2.1.1	Land-Use Change .....	148
5.2.1.2	Biodiversity .....	148
5.2.1.2.1	Biodiversity Hotspots.....	149
5.2.1.2.2	Alliance for Zero Extinction (AZE) Sites .....	150
5.2.2	Experiments.....	151
5.2.2.1	Biodiversity Hotspot Analysis.....	151
5.2.2.1.1	Origins of the Endemics-Area Relationship Model .....	151
5.2.2.1.2	Habitat Loss in Biodiversity Hotspots .....	154
5.2.2.1.3	Species Extinctions in Biodiversity Hotspots .....	156

5.2.2.2	AZE Analysis.....	157
5.3	Results .....	158
5.3.1	Biodiversity Hotspot Analysis .....	158
5.3.1.1	Habitat Extent at Present Day .....	158
5.3.1.2	Future Global Habitat Loss .....	158
5.3.1.3	Regional Habitat Loss .....	159
5.3.1.4	Endemic Species Extinctions Due to Habitat Loss .....	164
5.3.1.4.1	Global Species Loss.....	164
5.3.1.4.2	Species Loss Within Hotspots .....	165
5.3.2	AZE analysis.....	167
5.3.2.1	Impacts of Cropland Expansion on AZE sites .....	167
5.4	Discussion .....	171
5.4.1	Impacts on Species Classes.....	171
5.4.2	Regional Threats .....	173
5.4.2.1	Africa .....	173
5.4.2.2	Asia .....	175
5.4.2.3	Latin America .....	177
5.4.3	Impacts of Bioenergy on Biodiversity .....	179
5.4.3.1	Isolated Impacts of Bioenergy Expansion.....	179
5.4.3.2	Impacts of Bioenergy in Future Mitigation Pathways .....	180
5.4.4	Impacts of a REDD+ Scheme .....	182
5.4.5	Impacts of a Water Protection Scheme .....	186
5.4.6	Limitations in Methodological Approaches.....	187
5.5	Summary and Conclusions .....	190
<b>Chapter 6 Conclusions and Future Work.....</b>		<b>193</b>
6.1	Summary of Findings .....	193
6.2	Contributions to Knowledge.....	196
6.3	Limitations and Future Recommendations.....	199
6.3.1	Modelling and Metrics .....	200
6.3.2	Policies and Conservation Schemes.....	201
6.4	Closing Comments .....	203
<b>References .....</b>		<b>205</b>



## List of Figures

<b>Figure 1.1:</b> Drivers of observed warming between 1850 and 2020; reproduced from Eyring et al. (2021).....	1
<b>Figure 1.2:</b> Global bioenergy consumption in 409 future scenarios; reproduced from Smith et al. (2019). Data is from the Integrated Assessment Modelling Consortium (IAMC) Scenario Explorer developed for the SR15 (Rogelj, Shindell, et al., 2018; Huppmann et al., 2019). Figure (a) shows bioenergy deployment over the 21 <sup>st</sup> century for the entire database (in grey) and the four illustrative pathways from SR15 (coloured). Figure (b) displays global area of energy cropland versus bioenergy consumption in 2100, whereby colours represent the carbon price in 2100 (in 2010 USD per tCO <sub>2</sub> ). Higher carbon prices generally result in greater bioenergy deployment.....	4
<b>Figure 1.3:</b> Synergies and trade-offs between bioenergy and 11 linked sustainable development goals (SDGs). Length of bars indicate the strength of the synergies and trade-offs, and shading indicates confidence in impact assessments. This graph represents a combination of findings from various literature (van Leeuwen, 2017; GBEP, 2018; Roy et al., 2018). .....	5
<b>Figure 2.1:</b> Total global primary energy supply in 2019, split into percentages of renewable energy supplies, and end-use sectors of bioenergy deployment. This figure has been adapted from WBA (2021) using values from REN21 (2021).....	14
<b>Figure 2.2:</b> Bioenergy conversion technologies; created using findings from EUBIA (2020), Costa and Piazzullo (2018), and IEA (2009). .....	16
<b>Figure 2.3:</b> Global CO <sub>2</sub> emissions for SSP scenarios, and corresponding CO <sub>2</sub> concentrations for 2100. Highlighted lines indicate selected pathways from the CMIP6 ScenarioMIP project. This figure has been adapted from Rogelj, Popp, et al. (2018) using concentration values from the IIASA SSP database (IIASA, 2018b). .....	22
<b>Figure 2.4:</b> Decarbonisation characteristics in 1.5 °C (1.9 W m <sup>-2</sup> ) scenarios following SSP1, SSP2, SSP4 and SSP5 pathways; reproduced from Rogelj, Popp, et al. (2018). Figure (a) shows primary energy from biomass with CCS (BECCS), (b) shows primary energy from coal without CCS, and (c) shows the annual amount of CO <sub>2</sub> stored by CCS in 1.5 °C (1.9 W m <sup>-2</sup> ) scenarios. Shaded areas indicate the range per SSP, solid lines are the marker scenarios for each SSP, and dashed yellow lines indicate scenarios that are not markers.....	23

<b>Figure 2.5:</b> Changes in land and ocean carbon storage in response to CO <sub>2</sub> (a) and climate change (b); reproduced from Arias et al. (2021). .....	26
<b>Figure 2.6:</b> Land-use changes in 1.5 °C and 2 °C pathways based on the Shared Socioeconomic Pathways, for 2030 and 2050 relative to 2010; adapted from Rogelj, Shindell, et al. (2018). Four archetype pathways are shown, comprising three 1.5°C-consistent pathways based on SSPs 1 (S1), 2 (S2) and 5 (S5), developed by the AIM, MESSAGE-GLOBIOM, and REMIND-MAgPIE models, respectively. In addition, a scenario with low energy demand (LED) is included. ....	29
<b>Figure 2.7:</b> Biogeochemical and biogeophysical impacts of land conversion from forest to energy cropland, and their influences on climate (i.e., warming or cooling). Image icons used to create this figure have been taken from Freepnging (2022) and are licensed by Creative Commons (2022). ....	33
<b>Figure 2.8:</b> Changes in mean global annual surface air temperature (°C) in response to historical anthropogenic land-use changes, estimated in a range of studies using observations, DGVMs and GCMs; reproduced from Jia et al. (2019). Values are for certain years in the period 1990–2014 relative to years in 1700–1920. ....	41
<b>Figure 2.9:</b> Changes in energy cropland area (a) and cumulative LUC emissions (b) in SSP scenarios following RCP2.6, calculated from five different integrated assessment models; reproduced from Popp et al. (2017). Coloured lines indicate marker model results for each SSP, shaded areas indicate range of data across the timeline, and the grey line in Figure (b) represents historical trends. ....	46
<b>Figure 2.10:</b> LUC emissions and corresponding biogeochemical effects on temperature, calculated for RCP2.6 scenarios in a range of studies using GCMs and DGVMs. Values are for the period 2099-2100 relative to 2000-2006. ....	47
<b>Figure 2.11:</b> Changes in mean global annual surface air temperature (°C) in response to future anthropogenic land-use changes, estimated in a range of studies using DGVMs and GCMs; reproduced from Jia et al. (2019). Values are for the period 2099-2100 relative to 2000-2006. ....	49
<b>Figure 3.1:</b> Summary of the MAgPIE scenarios. These scenarios have been created by authors Humpenöder et al. (2018a), and generally follow the SSP2 ‘middle-of-the-road’ pathway, detailed by Popp et al (2017). ....	80
<b>Figure 3.2:</b> Second-generation bioenergy demand in the MAgPIE scenarios between 2005 and 2100. Bioenergy demand is also provided for other SSP2 scenarios following RCP2.6 and	



RCP1.9 pathways. Values for the SSP-RCP pathways have been taken from the online SSP database (IIASA, 2018b). .....	81
<b>Figure 3.3:</b> Global land-use changes for each land type in the MAgPIE scenarios, between 2005 and 2100.....	84
<b>Figure 3.4:</b> Regional bioenergy-induced land-use changes within the bioenergy scenarios (Bio, Bio-REDD and Bio-WaterProt compared to NoBio), in 2100 relative to 2005. Values are percentages of grid cells undergoing land cover changes.....	86
<b>Figure 3.5:</b> Global land-use changes in the MAgPIE scenarios. These have been overlaid by the author onto trajectories previously calculated by Popp et al. (2017) for each SSP following RCP2.6 using different integrated assessment models. Values are presented for the period 2005 to 2100. ....	87
<b>Figure 4.1:</b> Architecture diagram of the UVic ESCM v2.9 and inputs and outputs. The model consists of 4 components: Atmosphere, land, ocean, and ocean sediment. Arrows inside the model diagram represent the coupling of these components- the colour of each arrow matches the colour of the symbol on the component being coupled. Inputs include cropland and pasture land-use fractions, CO <sub>2</sub> emissions, and sulphate aerosol forcing. Cropland here is a combination of food/feed cropland (including first-generation energy cropland), and second-generation energy cropland. Outputs include various biogeochemical and biogeophysical effects.....	93
<b>Figure 4.2:</b> Global mean grid cell fraction trajectories of cropland (a) and pasture (b) inputs for the UVic ESCM, taken from the cropland and pasture variables in the MAgPIE scenarios (shown previously in Chapter 3, Section 3.3). Cropland here encompasses food/feed cropland (including first-generation energy cropland) and second-generation energy cropland. Values have been calculated as average fractions of the whole globe (including land and ocean grid cells), to indicate global interpolation between historical data ('Hist'), taken from the HYDE 3.1 dataset (Goldewijk et al., 2011), and future data, taken from the MAgPIE scenarios. Scenario trajectories in black and grey represent non-interpolated data, whereas coloured trajectories are the newly interpolated scenarios used as input for the UVic simulations. ....	95
<b>Figure 4.3:</b> Architecture diagram of the four types of simulations used for each scenario in this study. This figure is linked to <b>Figure 4.1</b> and illustrates the inputs (i.e., land-use data and prescribed fossil fuel emissions) and outputs (i.e., annual average global terrestrial carbon TC and surface air temperature T) for the historical and future simulations, as well how the outputs have been used to calculate LUC emissions and biogeochemical and biogeophysical climate impacts of LUC within the scenarios. Abbreviations in these calculations are linked to those	

provided in <b>Table 4.1</b> , <b>Table 4.3</b> , and <b>Table 4.4</b> . The method here has been adapted from that in Simmons and Matthews (2016).....	101
<b>Figure 4.4:</b> Regional land-use changes in Bio, BioPC and BioPC minus Bio (BioPC–Bio) simulations, in 2100 relative to 2005. BioPC indicates Values are percentages of grid cells undergoing land cover changes. ....	104
<b>Figure 4.5:</b> Trajectories of land-use change for five different plant functional types in the UVic ESCM simulations. Values are in area and percentage units relative to 2005. ....	106
<b>Figure 4.6:</b> Spatial land-use changes for C3/C4 grasses, forest and shrubland in the UVic model as a result of bioenergy expansion; for 2100 relative to 2005. Values are calculated as the difference between Bio (e.g., Bio-BioPC) and NoBioBE (NoBioBE-NoBioBEPC) simulations and are percentages of grid cells undergoing land cover changes. ....	108
<b>Figure 4.7:</b> Global annual mean projections for surface air temperature (a), CO <sub>2</sub> concentration (b), yearly CO <sub>2</sub> emissions (c) and cumulative CO <sub>2</sub> emissions (d), for the UVic simulations between years 2005 and 2100. Additionally, findings for SSP2 RCP2.6 scenarios are included, taken from the online SSP database (IIASA, 2018b). Values in (a) and (c) have been calculated relative to the pre-industrial base period 1850–1900, as demonstrated in the work of Rogelj, Shindell, et al. (2018). Cumulative and yearly CO <sub>2</sub> emissions are made up of LUC emissions calculated from this study and input fossil fuel emissions shown in <b>Table 4.1</b> . ....	109
<b>Figure 4.8:</b> Transient climate response for MAgPIE scenarios compared to the RCP scenarios (a) and the SSP2 scenarios (b). Annual-average surface air temperatures from 1850-1990 are plotted against cumulative CO <sub>2</sub> emissions since 1976. Graph (a1) shows a close-up of the MAgPIE TCRE results compared to the RCP 2.6 TCRE results. Results for the SSP scenarios have been taken from the SSP database (IIASA, 2018b). Results for the RCP scenarios in (a) have been extracted from Figure SPM.10 in Gray (2007) using software by GetData (2019). Historical values are extracted from Figure 2.3 in Rogelj et al (2018). ....	111
<b>Figure 4.9:</b> Annual-average global biogeophysical (BGP) and biogeochemical (BGC) impacts of LUC on surface temperature for all 5 scenarios between 2005 and 2100. Light blue lines represent impacts in the tropical (25°S to 25°N) region, light green lines represent results for the extratropical (lower=65°S to 25°S and upper=25°N to 65°N) regions, and dark blue lines show the global impacts. Tropical values are calculated as yearly averages over the tropics. Extratropical values are calculated as yearly averages of the lower and upper regions together. Black lines denote the combined (BGC + BGP) impacts of LUC on surface temperature. BGP and BGC temperature changes were obtained using the calculations: $T_{PC(LUC+FF)} - T_{FF}$ and $T_{LUC+FF} - T_{PC(LUC+FF)}$ respectively, as shown previously in <b>Table 4.4</b> . ....	113

**Figure 4.10:** The spatial distribution of biogeophysical and biogeochemical impacts on surface temperature for the MAgPIE scenarios. Results have been plotted for the 25-year average of the period 2075–2100 compared to the 15-year average of the period 1995–2010. Biogeochemical and biogeophysical temperature changes were obtained using the calculations:  $T_{PC(LUC + FF)} - T_{FF}$  and  $T_{LUC + FF} - T_{PC(LUC + FF)}$  respectively, as shown previously in **Table 4.4**. Tropical and extratropical regions are illustrated by dotted lines at latitudes: 65°S, 25°S, 25°N and 65°N. .... 115

**Figure 4.11:** Projections of changes in vegetation carbon (a), soil carbon (b), land carbon (c) and cumulative LUC emissions (d) for the UVic simulations, between years 2005 and 2100. Plain lines represent TL simulations, and dotted lines represent PC simulations. LUC emissions in (d) are calculated as the difference between terrestrial carbon storage for PC and TL simulations ( $TC_{PC(LUC + FF)} - TC_{LUC + FF}$ ), multiplied by the carbon-CO<sub>2</sub> conversion factor 3.67. .... 118

**Figure 4.12:** Projections of cumulative LUC emissions in the UVic simulations, for the five plant functional types (broad leaf trees, needle leaf trees, C3 grasses, C4 grasses and shrubland) and soil. .... 119

**Figure 4.13:** Projections of changes in soil temperature, sensible heat flux and P-E. Findings are shown for TL and PC simulations ((a), (c), (e), (g)) and the differences between them ( $LUC + FF - PC(LUC + FF)$ ) indicating their relative contributions to biogeophysical effects leading to surface cooling or warming ((b), (d), (f), (h)). .... 122

**Figure 4.14:** Spatial projections of changes in soil temperature, sensible heat flux and P-E in the Bio scenario. Findings are shown for TL and PC simulations ((a), (c), (e), (g)) and the differences between them ( $LUC + FF - PC(LUC + FF)$ ) indicating their relative contributions to biogeophysical effects leading to surface cooling or warming ((b), (d), (f), (h)). Results are for the 25-year average of the period 2075–2100 compared to the 15-year average of the period 1995–2010. .... 123

**Figure 4.15:** Impacts of bioenergy (alone and with REDD+ and water protection policies included) on biogeophysical effects. Results have been calculated as the differences between the three scenarios Bio, Bio-REDD and Bio-WaterProt, and the NoBioBE scenario. They have been plotted for the 25-year average of the period 2075–2100 compared to the 15-year average of the period 1995–2010. .... 125

**Figure 4.16:** Spatial land-use changes occurring in the UVic model simulations, resulting from inputs (cropland and pasture) for the Bio MAgPIE scenario; calculated for 2100 relative to 2005. Corresponding changes in UVic forest cover are provided alongside changes in forest in

the original MAgPIE scenario. Values are percentages of grid cells undergoing land cover changes. .... 128

**Figure 4.17:** A comparison of global annual biogeochemical and biogeophysical changes in surface air temperature (°C) in response to land-use changes between this study and previous work. Results for this study are for the five MAgPIE land-use scenarios, and are shown as the average for the period 2075-2100 compared to 2005, and the maximum absolute values (within the period 2005-2100) compared to 2005. They are indicated by five different symbols (a star, square, asterisk, dot, and cross). For comparison, previous findings assessed in the work of Jia et al. (2019) (see **Figure 2.11** in Chapter 2) have been included. These comprise of historical absolute values (taken from years within the period 1990-2014 compared to years in the period 1700-1920) and future values (either for 2099 or 2100 compared to years in the period 2000-2006) (Chase et al., 2000; Betts, 2001; Chase et al., 2001; Zhao and Pitman, 2002; Gibbard et al., 2005; Feddema, 2005; Brovkin et al., 2006; Betts et al., 2007; Findell et al., 2009; Arora and Boer, 2010; Kvalevåg et al., 2012; Lawrence et al., 2012; De Noblet-Ducoudré et al., 2012; Houghton et al., 2012; IPCC, 2013; Zhang et al., 2013; Jones et al., 2013; Boysen et al., 2014; Davies-Barnard et al., 2014; Carvalhais et al., 2014; Pugh et al., 2015; Devaraju et al., 2015; Hansis et al., 2015; Hua et al., 2015; Avitabile et al., 2016; Simmons and Matthews, 2016; Li et al., 2017; Tharammal et al., 2018; Lawrence et al., 2018). Note: Results from the work of Simmons and Matthews (2016) have been recalculated by the author, and included in this plot, since the work of Jia et al. (2019) was published. .... 131

**Figure 4.18:** Projections of cumulative and yearly LUC emissions in the UVic simulations, in addition to findings for the original MAgPIE scenarios (as shown in Humpenöder et al. (2018a)), SSP2 data from the online SSP database (Riahi et al., 2017; IIASA, 2018), and historical data from the works of Houghton et al. (2012), Friedlingstein et al. (2010), and Canadell et al. (2007). .... 135

**Figure 4.19:** LUC emissions and corresponding biogeochemical effects on temperature, calculated in this study and for RCP2.6 scenarios in a range of studies using GCMs and DGVMs. Results in this study are shown as the average for the period 2075–2100, and maximum values (between 2005 and 2100, relative to 2005). Literature findings are for the period 2099–2100 relative to 2000-2006. .... 137

**Figure 4.20:** Spatial representations of soil carbon storage in the BioPC (a) and Bio (b) simulations, and corresponding soil CO<sub>2</sub> emissions (c). Soil CO<sub>2</sub> emissions have been calculated as the difference between terrestrial carbon storage in the Bio and BioPC simulations ( $TC_{PC(LUC+FF)} - TC_{LUC+FF}$ ), multiplied by the carbon-CO<sub>2</sub> conversion factor 3.67. .... 139

<b>Figure 5.1:</b> Biodiversity hotspots and their outer limits, as defined in the works of Mittermeier et al. (2005) and Conservation International (2011). .....	149
<b>Figure 5.2:</b> Sites of critically endangered and endangered species provided in the Alliance for Zero Extinction (AZE) database (AZE, 2010). Coloured dots represent AZE sites inside (yellow) and outside (purple) the biodiversity hotspots shown in <b>Figure 5.1</b> . .....	150
<b>Figure 5.3:</b> The three scales of species-area curve, recreated using findings in Rosenzweig (2001) and Rosenzweig (2003a). Island SARs are bounded by the intraprovincial SAR of their province and the interprovincial SAR on which their province lies. ....	152
<b>Figure 5.4:</b> Relationships between proportions of primary forest species found in secondary forests and different ages of secondary forest. Proportions have been taken from the work of Chazdon et al. (2009) for (a) plants, (b) amphibians, (c) birds, (d) mammals and (e) reptiles. ....	155
<b>Figure 5.5:</b> Total land-use change in the MAgPIE scenarios across 35 biodiversity hotspots in 2100, relative to 2005. ....	159
<b>Figure 5.6:</b> Percentage of primary forest loss (P-blue) and secondary forest loss (SL-red) and gain (SG-green) in the MAgPIE Bio scenario, for 2100 relative to 2005. ....	160
<b>Figure 5.7:</b> Percentage change in primary and secondary forest in the MAgPIE scenarios for each biodiversity hotspot, by 2100 relative to 2005. ....	161
<b>Figure 5.8:</b> Primary (a) and secondary (b) forest loss in the MAgPIE scenarios, for each biodiversity hotspot, by 2100 relative to 2005. ‘I.Os’ stand for Indian Ocean islands, and ‘W.A’ stands for West Africa. ....	163
<b>Figure 5.9:</b> Global numbers of plant (a) and vertebrate (b) extinctions in the MAgPIE scenarios, calculated using z values: 0.15, 0.2 and 0.25, and secondary forest ages: 10, 20 and 40 years old. ....	164
<b>Figure 5.10:</b> Alliance for zero extinction (AZE) sites of endangered and critically endangered species (red dots), overlaid onto changes in energy (a) and food/feed (b) cropland, in the MAgPIE Bio scenario, between 2005 and 2100. In the figure key, upward and downward arrows represent increase and loss in cropland. ....	169
<b>Figure 5.11:</b> Numbers of threatened species, per class, in both the hotspot (a) and AZE (b) analyses. Values for the hotspots were calculated using parameters: z = 0.2 and secondary forest age = 20 years old. In the hotspot analysis values represent extinctions by 2100 relative to 2005, whereas in the AZE analysis, values represent number of impacted species by 2100 relative to 2010. ....	172

- Figure 5.12:** Regional numbers of threatened species, in both the hotspot (a) and AZE (b) analyses. Values for the hotspots were calculated using parameters:  $z = 0.2$  and secondary forest age = 20 years old..... 174
- Figure 5.13:** Changes in energy and food/feed cropland area in each biodiversity hotspot, for each MAgPIE scenario, between 2005 and 2100. .... 176
- Figure 5.14:** Number of plant (a) and tetrapod (b) extinctions versus second-generation bioenergy demand in 2100 compared to 2005. Graph (a) shows projections for the MAgPIE scenarios and the RCP pathways provided in the work of Jantz et al. (2015). Graph (b) additionally shows results for the RCP-SSP hybrid scenarios found by Chaudhary and Mooers (2017). ‘Bioenergy demand’ includes bioenergy produced from traditional and modern feedstock and includes bioenergy with and without carbon capture and storage depending on the scenario. Bioenergy demand values, for comparison to results by Jantz et al. (2015), have been taken from the work of van Vuuren et al. (2011). Values for RCP 2.6 SSP1 IMAGE, RCP 3.4 SSP4 GCAM and RCP 6 SSP4 GCAM have been taken from the SSP database (IIASA, 2018b)..... 181
- Figure 5.15:** Alliance for Zero Extinction sites inside (yellow dots) and outside (purple pots) biodiversity hotspots, overlaid onto changes in primary (P-blue) and secondary forest (SL/SG- red/green) between 2005 and 2100. .... 183
- Figure 5.16:** Percentage reductions in energy “E” (a) and food/feed “F/F” (b) cropland intensity due to the implementation of a REDD+ policy, calculated as the difference between cropland expansions in the Bio-REDD and Bio scenarios between 2005 and 2100. Increases in cropland expansion from REDD+ are not shown. Yellow and purple dots are the AZE sites inside and outside of biodiversity hotspots, respectively. .... 185
- Figure 6.1:** Findings in this study for the relationship between bioenergy expansion and SDGs 13 and 15, alongside results indicated in existing literature, as previously discussed in Chapter 1 (Figure 1.3). Overall, bioenergy expansion could counteract with aims in SDGs 13 (medium confidence), and 15 (high confidence). Length of bars indicate the strength of the synergies and trade-offs, and shading indicates confidence in impact assessments. Results other than those from this study have been taken from the works of van Leeuwen (2017), GBEP (2018), Roy et al. (2018). .... 199

## List of Tables

<b>Table 2.1:</b> Literature findings for biodiversity impacts of global land conversion for second-generation energy cropland using different biodiversity indicators; based off findings in Immerzeel et al (2014) and example studies provided in the table.....	59
<b>Table 4.1:</b> CO <sub>2</sub> emission and removal values taken from the SSP database for the REMIND-MAgPIE SSP2 RCP2.6 scenario for years 2005 to 2100. Fossil fuel and industry emissions ('FF') are highlighted in green alongside LUC emissions and CCS removals in this scenario (IIASA, 2018b). Additional CO <sub>2</sub> emissions ('BE') have been calculated and added to FF for the NoBioBE scenario (represented as 'FF + BE') and are highlighted in blue. Positive values represent emissions, whereas negative values represent removal of emissions.....	96
<b>Table 4.2:</b> Procedure for calculating the weighted average amount of CO <sub>2</sub> emissions per EJ of fossil fuel energy production. ....	98
<b>Table 4.3:</b> A summary of the simulations used for each scenario in this study. 'Spatial land use' refers to land-use data used for historical (HYDE 3.1 dataset) and future (MAgPIE scenarios) simulations. Prescribed CO <sub>2</sub> emissions are the input fossil fuel and industry CO <sub>2</sub> emissions (with added emissions for absence of bioenergy in NoBioBE), released directly to the atmosphere from a yearly emissions data file. Prescribed CO <sub>2</sub> concentration refers to simulations in which atmospheric CO <sub>2</sub> is forced to follow a specified CO <sub>2</sub> concentration trend. The method in this table has been adapted from that in Simmons and Matthews (2016). Emissions forcings in column 3 are linked to identifying abbreviations provided previously in Table 4.1. ....	100
<b>Table 4.4:</b> Calculations of global net cumulative LUC emissions, biogeochemical temperature change, and biogeophysical temperature change. In the formulae, TC denotes the annual-average global terrestrial carbon content and T the annual-average surface air temperature. Subscripts indicate identifying abbreviations from the source simulation emissions forcings in Table 4.3, also shown in Table 4.3 and Figure 4.3. The method in this table has been adapted from that in Simmons and Matthews (2016). ....	102
<b>Table 4.5:</b> Global land use for the five scenarios in years 2050 and 2100 relative to 2005, in their original form taken from the MAgPIE model (represented by five land-use types) and in their new form in the UVic ESCM (represented by the UVic ESCM's five plant functional	

types). Values from the UVic simulations are calculated as the difference between TL and PC simulations.....	105
<b>Table 4.6:</b> Bioenergy-induced LUC and climate impacts calculated in this study for the original MAgPIE scenarios and UVic simulations, in addition to findings from Hallgren et al. (2013), for the year 2050 relative to 2000. Values are calculated by subtracting results for NoBioBE from results for the bioenergy scenarios.....	133
<b>Table 5.1:</b> Proportions of species from primary forests that can occur in nearby secondary forests ('Mixed'), and remaining proportions of species only found in primary forests ('Primary'), depending on the age of the secondary forest (10, 20 or 40 years old).....	156
<b>Table 5.2:</b> Numbers (and percentages) of species lost in 16 biodiversity hotspots, for each MAgPIE scenario, in 2100 compared to 2005. Species counts in 2005 have been taken from the work of Mittermeier et al (2005). Values are calculated using parameters: $z = 0.2$ and secondary forest age = 20 years.....	166
<b>Table 5.3:</b> Numbers of endangered and critically endangered AZE species impacted by energy and food/feed cropland expansion by 2100 in the MAgPIE scenarios.....	168
<b>Table 5.4:</b> Regional numbers of endangered and critically endangered AZE species impacted by cropland expansion in the MAgPIE scenarios.....	170



## Abbreviations

AD	Anaerobic <b>D</b> igestion
AFOLU	Agriculture, Forestry and <b>O</b> ther Land Use
AR	Assessment <b>R</b> eport
AZE	Alliance for <b>Z</b> ero Extinction
BECCS	Bioenergy with <b>C</b> arbon Capture and Storage
BGC	<b>B</b> io <b>G</b> eo <b>C</b> hemical
BGP	<b>B</b> io <b>G</b> eo <b>P</b> hysical
BII	Biodiversity Intactness <b>I</b> ndex
CBD	Convention on <b>B</b> iological Diversity
CCS	Carbon Capture and Storage
CDR	Carbon <b>D</b> ioxide <b>R</b> emoval
CH <sub>4</sub>	<b>M</b> ethane
CHP	Combined <b>H</b> eat and <b>P</b> ower
CMIP	Coupled <b>M</b> odel Intercomparison <b>P</b> roject
CO <sub>2</sub>	Carbon <b>D</b> ioxide
DAC	<b>D</b> irect Air Capture
DGVM	<b>D</b> ynamic <b>G</b> lobal <b>V</b> egetation <b>M</b> odel
EAR	Endemics-Area <b>R</b> elationship
ECPT	<b>E</b> cosystem Carbon <b>P</b> ayback <b>T</b> ime
EF	<b>E</b> nvironmental <b>F</b> low
EN	<b>E</b> ndangered
ESCM	<b>E</b> arth <b>S</b> ystem <b>C</b> limate <b>M</b> odel
ESM	<b>E</b> arth <b>S</b> ystem <b>M</b> odel
EW	<b>E</b> nhanced <b>W</b> eathering
FAO	<b>F</b> ood and <b>A</b> griculture <b>O</b> rganization
FF	<b>F</b> ossil <b>F</b> uel
GCAM	<b>G</b> lobal <b>C</b> hange <b>A</b> ssessment <b>M</b> odel
GCM	<b>G</b> lobal <b>C</b> limate <b>M</b> odel
GHG	<b>G</b> reen <b>H</b> ouse <b>G</b> as
GLDF	<b>G</b> lasgow <b>L</b> eaders' <b>D</b> eclaration on <b>F</b> orests
GLOBIO	<b>G</b> LOBal <b>B</b> IOdiversity Model

HadGEM	<b>Hadley Centre Global Environment Model</b>
HNV	<b>High Nature Value</b>
IEA	<b>International Energy Agency</b>
IIASA	<b>International Institute for Applied Systems Analysis</b>
iLUC	<b>Indirect Land-Use Change</b>
IMAGE	<b>Integrated Model to Assess the Global Environment</b>
IPBES	<b>Intergovernmental Science-Policy Platform on Biodiversity and Ecosystem Services</b>
IPCC	<b>Intergovernmental Panel on Climate Change</b>
IUCN	<b>International Union for Conservation of Nature</b>
LPJmL	<b>Lund-Potsdam-Jena managed Land</b>
LUC	<b>Land-Use Change</b>
LUCID	<b>Land-Use and Climate, Identification of Robust Impacts</b>
LW	<b>LongWave</b>
MAgPIE	<b>Model of Agricultural Production and its Impact on the Environment</b>
MEA	<b>Millenium Ecosystem Assessment</b>
MIROC	<b>Model for Interdisciplinary Research On Climate</b>
MIT	<b>Massachusetts Institute of Technology</b>
MOSES	<b>Met Office Surface Exchange Scheme</b>
MPI	<b>Max Planck Institute</b>
MSA	<b>Mean Species Abundance</b>
N	<b>Nitrogen</b>
N <sub>2</sub> O	<b>Nitrous Oxide</b>
NBSAP	<b>National Biodiversity Strategies and Action Plans</b>
NDC	<b>Nationally Determined Contributions</b>
NEE	<b>Net Ecosystem Exchange</b>
NPP	<b>Net Primary Productivity</b>
NYDF	<b>New York Declaration on Forests</b>
O <sub>3</sub>	<b>Ozone</b>
OA	<b>Ocean Alkalinisation</b>
P	<b>Phosphorous</b>
PC	<b>Prescribed Carbon</b>
P-E	<b>Precipitation - Evaporation</b>
PES	<b>Payments for Ecosystem Services</b>
PFT	<b>Plant Functional Type</b>

PIK	<b>P</b> otsdam <b>I</b> nstitute for <b>C</b> limate <b>I</b> mpact <b>R</b> esearch
PREDICTS	<b>P</b> rojecting <b>R</b> esponses of <b>E</b> cological <b>D</b> iversity <b>I</b> n <b>C</b> hanging <b>T</b> errestrial <b>S</b> ystems
RCP	<b>R</b> epresentative <b>C</b> oncentration <b>P</b> athway
REDD+	<b>R</b> educing <b>E</b> missions from <b>D</b> eforestation and <b>F</b> orest <b>D</b> egradation
REMIND	<b>R</b> Egional <b>M</b> odel of <b>I</b> Nvestment and <b>D</b> evelopment
SAR	<b>S</b> pecies- <b>A</b> rea <b>R</b> elationship
SAT	<b>S</b> urface <b>A</b> ir <b>T</b> emperature
SCS	<b>S</b> oil <b>C</b> arbon <b>S</b> equestration
SDG	<b>S</b> ustainable <b>D</b> evelopment <b>G</b> oal
SED	<b>S</b> tandard <b>E</b> uclidean <b>D</b> istance
SEforALL	<b>S</b> ustainable <b>E</b> nergy <b>f</b> or <b>A</b> LL
SH	<b>S</b> ensible <b>H</b> eat
SSP	<b>S</b> hare <b>S</b> ocioeconomic <b>P</b> athway
SW	<b>S</b> hort <b>W</b> ave
TCRE	<b>T</b> ransient <b>C</b> limate <b>R</b> Espnse to <b>C</b> umulative <b>C</b> arbon <b>E</b> missions
TRIFFID	<b>T</b> op-down <b>R</b> epresentation of <b>I</b> nteractive <b>F</b> oliage and <b>F</b> lora <b>I</b> ncluding <b>D</b> ynamics
UN	<b>U</b> nited <b>N</b> ations
UNEP	<b>U</b> nited <b>N</b> ations <b>E</b> nvironment <b>P</b> rogramme
UNFCCC	<b>U</b> nited <b>N</b> ations <b>F</b> ramework <b>C</b> onvention on <b>C</b> limate <b>C</b> hange
UVic	<b>U</b> niversity of <b>V</b> ictoria
WBA	<b>W</b> orld <b>B</b> ioenergy <b>A</b> ssociation
WG	<b>W</b> orking <b>G</b> roup
WWF	<b>W</b> orld <b>W</b> ildlife <b>F</b> und



# Chapter 1 Introduction

## 1.1 Anthropogenic Climate Change

Over the last decade, global warming has reached approximately 1.09 [0.95 to 1.20] °C above pre-industrial (1850–1900) levels. Though natural drivers play a small role in climate fluctuations, it is unequivocal that human influence is the main cause of this warming. Activities such as combustion of fossil fuels for energy and unsustainable land-use practices have resulted in large increases in atmospheric concentrations of greenhouse gases (GHGs). These, in turn, alter the Earth’s energy budget by absorbing and re-emitting radiation back towards Earth’s surface, where it is absorbed and creates a warming effect. Recent predictions in the Intergovernmental Panel on Climate Change Sixth Assessment Report indicate that warming caused by humans alone rose to 0.8 °C to 1.3 °C by 2010-2019 (relative to 1850–1900), largely due to increases in GHGs (IPCC, 2021; Eyring et al., 2021) (see **Figure 1.1**).

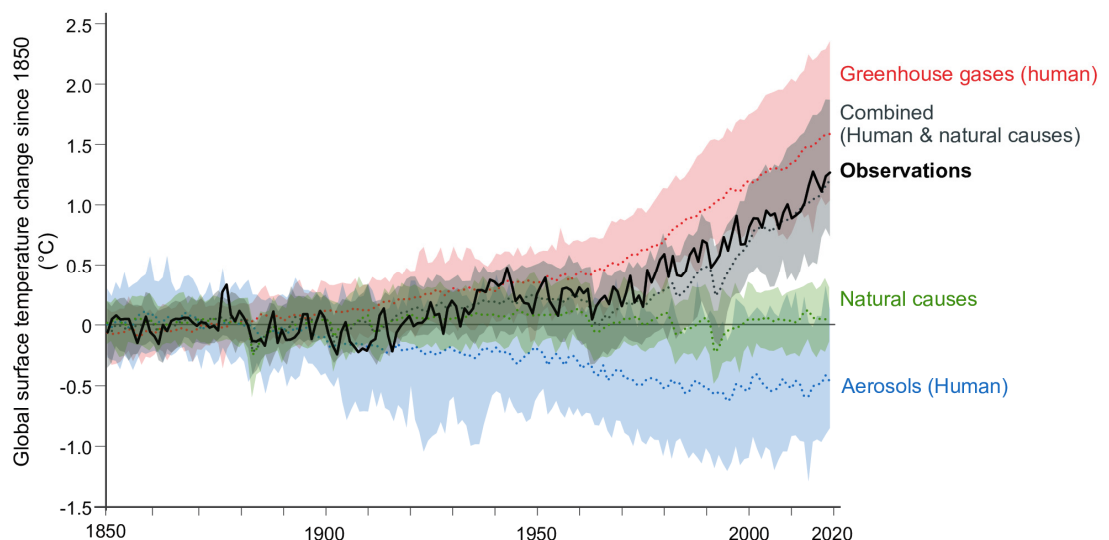


**Figure 1.1:** Drivers of observed warming between 1850 and 2020; reproduced from Eyring et al. (2021).

In comparison to other long-lived greenhouse gases (e.g., methane (CH<sub>4</sub>), nitrous oxide (N<sub>2</sub>O)), carbon dioxide (CO<sub>2</sub>) has the longest residence time because of its unreactive properties, whereby around 15 to 40% of emitted CO<sub>2</sub> can remain in the atmosphere longer than 1,000 years (Ciais et al., 2013). In 2020, global atmospheric concentrations of CO<sub>2</sub> reached 412 ppm, around 50% above pre-industrial (pre-1750) levels (Friedlingstein et al., 2020). Such high concentrations are unprecedented in the last 2 million years, with rates of increase at least 10 times faster than at any other point in the last 800,000 years (Canadell et al., 2022). While there is still some uncertainty in Earth's temperature response to CO<sub>2</sub> concentration levels, it is evident that if net-zero CO<sub>2</sub> emissions are not reached by 2050–2070, constraining global mean warming to Paris agreement goals of “well below 2 °C” by 2100 will become increasingly challenging (IPCC, 2021).

Increases in global temperatures will likely be accompanied by substantial changes to both natural and human systems. For instance, loss of Arctic sea ice extent during the season sea ice minimum could increase from 41%, measured for September 2020 (compared to 1981-2010; (National Snow and Ice Data Center, 2019)) to near total loss before 2050 (Fox-Kemper et al., 2021). In addition, sea levels could rise by half a metre or more by 2100 (Jevrejeva et al., 2014; Jackson et al., 2018; Fox-Kemper et al., 2021), more than double the increase seen between 1901 to 2010 (~0.19 m (IPCC, 2014)). Climate and weather extremes, including heatwaves, heavy precipitation events, cyclones, drought and fire weather are also expected to increase in frequency and intensity (Seneviratne et al., 2021).

These extremes will place many terrestrial, freshwater, coastal and marine ecosystems at high or very high risks of biodiversity loss. Common terrestrial species (~50,000 species studied) are predicted to lose  $\geq 50\%$  of their present ‘climatic range size’ — the probability of a species’ occurrence conditioned on climatic variables — by the 2080s (Warren et al., 2013). Depending on the global warming level, approximately 3–48% of terrestrial species are threatened with extinction over the century (Parmesan et al., 2022). Coastal and marine species will face progressively lower oxygen levels, as well as high increases in ocean acidification, with associated risks being intensified by ocean temperature extremes. In addition, polar ecosystems will be affected as the loss of sea ice reduces habitat extents (Parmesan et al., 2022). Climate change is also expected to impact human societies in a range of different areas, with the largest impacts being on human health. Health impacts include increased injuries and deaths due to more intense climate events, higher risks from waterborne or foodborne diseases, and more cases of undernutrition in poorer regions (IPCC, 2022a). Other impacts are changes to people’s

livelihoods; with people in urban and rural areas being affected differently, and threats to international and regional security, due to widespread population displacements and distress migration (McLeman, 2011).

Near-term mitigation actions that limit global warming to 1.5 °C would substantially reduce, though not eliminate, negative and potentially irreversible impacts related to climate change occurring in ecosystems and human systems, compared to higher warming levels (IPCC, 2022a). In addition to adaptation measures (e.g., early warning systems and structure measures for flooding, forest conservation and restoration, cultivar improvements, and water resource management), future mitigation efforts will require fundamental changes to several sectors, including energy supply and demand, transport, buildings, industry, and AFOLU (agriculture, forestry, and other land use). Decarbonisation of energy systems, by switching the use of fossil fuels to alternative forms of energy, will play a key role in reducing emissions from most of these sectors. Alternative sources include wind, solar, geothermal, nuclear, and hydro power, which although are important, have their drawbacks, such as intermittency issues, provision of electricity only, geographic limitations, safety issues, and upfront costs. Biomass for energy (or ‘Bioenergy’) is predicted to combat most of these issues and is therefore a key element of future mitigation pathways.

## 1.2 The Role of Bioenergy in Future Mitigation Pathways

Combining biomass conversion technologies with systems that capture and store CO<sub>2</sub> — otherwise known as BECCS — could deliver net negative emissions. Hence, BECCS plays a crucial role in future decarbonisation of the energy sector within 1.5 °C and 2 °C mitigation pathways, accounting for 10–37% of global primary energy by 2050 (Clarke et al., 2022). Previous IPCC reports have estimated bioenergy potentials of 0 to 561 EJ yr<sup>-1</sup> by 2100, whereby upper estimates are reflective of more ambitious 1.5–2°C scenarios (IPCC, 2012; Clarke et al., 2014; Smith et al., 2014; Fuss et al., 2014; IPCC, 2018) (see **Figure 1.2**). Uncertainty within findings represents the complexity of incorporating bioenergy at a large scale, with different integrated assessment models (IAMs) generating a variety of estimates dependent on certain societal and environmental factors, as well as governance context. Most ambitious pathways, however, phase out the use of fossil fuels, traditional woodfuel, and first-generation bioenergy crops (e.g., oil palm, sugarcane, soy), transitioning to more advanced

technologies able to convert second-generation bioenergy feedstocks (e.g., lignocellulosic energy crops, forest wood, and wastes).

By 2050, as much as 7 million km<sup>2</sup> of global land area is required to produce dedicated energy cropland in 1.5 °C pathways. Model estimates vary based on assumptions regarding the yield of bioenergy crops, price of bioenergy, cost of production, demand for land for other purposes, and implementation of policies (e.g., subsidies, taxes, constraints), which could all influence changes in land-use or bioenergy demand. Despite these variations, together findings indicate that extensive use of land will be needed to supply high bioenergy demands consistent with ambitious mitigation pathways.

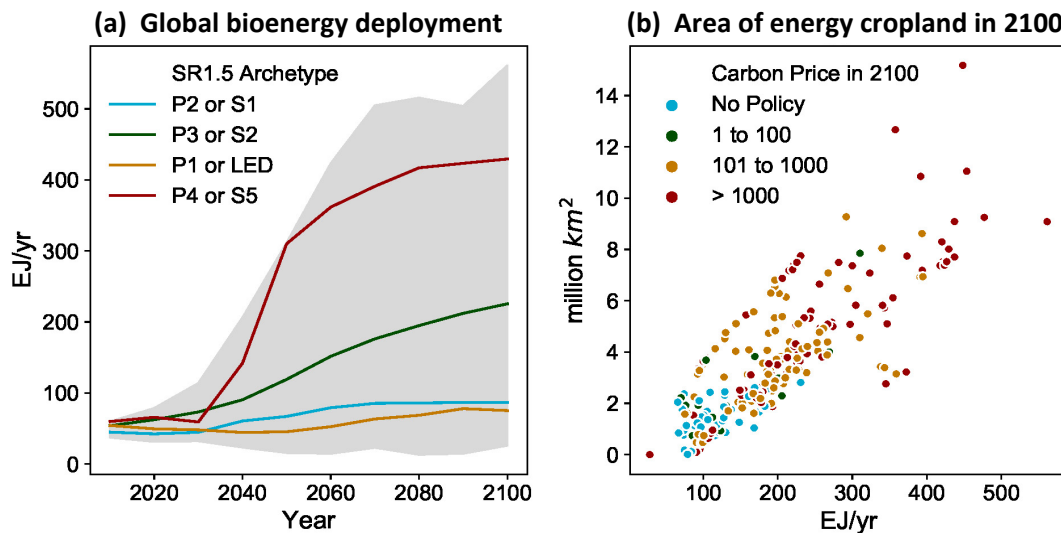


**Figure 1.2:** Global bioenergy consumption in 409 future scenarios; reproduced from Smith et al. (2019). Data is from the Integrated Assessment Modelling Consortium (IAMC) Scenario Explorer developed for the SR15 (Rogelj, Shindell, et al., 2018; Huppmann et al., 2019). Figure (a) shows bioenergy deployment over the 21<sup>st</sup> century for the entire database (in grey) and the four illustrative pathways from SR15 (coloured). Figure (b) displays global area of energy cropland versus bioenergy consumption in 2100, whereby colours represent the carbon price in 2100 (in 2010 USD per tCO<sub>2</sub>). Higher carbon prices generally result in greater bioenergy deployment.



## 1.3 Sustainability of Large-Scale Bioenergy Deployment

The expansion of large-scale bioenergy will likely have both co-benefits and adverse side-effects, dependent on factors such as the geographic region, scale of deployment, initial land use, type of land management practice, and type of feedstock used. Sustainable bioenergy deployment will require an overall synergistic relationship with the sustainable development goals (SDGs), created by the United Nations in 2015 (UN, 2015). The SDGs are a collection of 17 interlinked global goals designed in the aims of ‘meeting the needs of present and future generations through balancing economic, social, and environmental considerations’ (WCED, 1987; Roy et al., 2018). **Figure 1.3** demonstrates linkages between bioenergy and eleven related SDGs in terms of potential synergies and trade-offs that may occur with large-scale deployment.

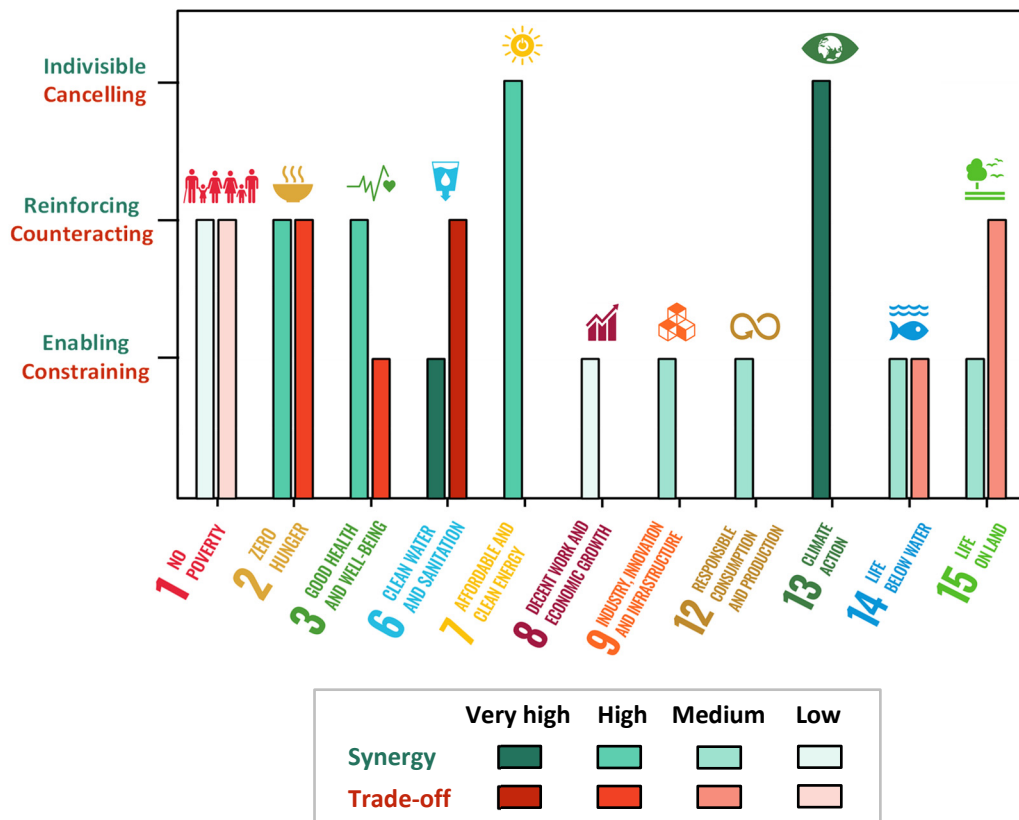


**Figure 1.3:** Synergies and trade-offs between bioenergy and 11 linked sustainable development goals (SDGs). Length of bars indicate the strength of the synergies and trade-offs, and shading indicates confidence in impact assessments. This graph represents a combination of findings from various literature (van Leeuwen, 2017; GBEP, 2018; Roy et al., 2018).

Inherently, the development of bioenergy fulfils aims outlined in SDG 7: access to affordable and clean energy (indivisible and high confidence; **Figure 1.3**) and SDG 13: combatting climate change (indivisible and very high confidence; **Figure 1.3**). However, sustaining bioenergy production depends on how it is perceived by society, with primary driving forces related to food security, employment and economic growth, energy security, and health, especially in developing regions (Domac et al., 2005). Multiple benefits have been found regarding these requisites. For instance, the transition to modern bioenergy could provide new employment opportunities and remove the need for laborious traditional fuelwood collection (SDGs 1 and 8) (Openshaw, 2010; FAO and UNEP, 2020). Reduced reliance on hard-to-reach fossil fuel reserves and local cultivation of biomass feedstocks could further boost local economies and provide energy security (SDGs, 7, 8) (Foust et al., 2017).

Improved knowledge of agricultural techniques for energy cropland cultivation may help increase food productivity, thus offsetting the food lost from bioenergy-induced land-use changes (SDGs 2 and 9) (Arndt et al., 2010; Negash and Swinnen, 2013). Additionally, the development of a renewable energy source has the potential to significantly reduce air pollution and thus improve global health (SDGs 3 and 12). Changes such as, transitioning from gasoline and diesel fossil fuels to biofuels for transport (Hill et al., 2006; Kularathne et al., 2019), incorporating CCS technologies in bioenergy power generation (IPCC, 2005; Shackley et al., 2009; Singh et al., 2011; P. Ashworth et al., 2012; Corsten et al., 2013), and reducing traditional biomass use in inefficient stoves, could help control air pollution and thus reduce airborne casualties and illnesses (WHO, 2018).

Environmental benefits are also possible. For instance, increased planting of perennial cropland in cleared agricultural landscapes could promote the mediation of dryland salinity, reduce eutrophication, and strengthen biodiversity (Davis et al., 2013; Cacho et al., 2018; Odgaard et al., 2019). Planting on low-carbon soil could also improve soil carbon sequestration (Bárcena et al., 2014; Immerzeel et al., 2014; Mello et al., 2014; Rowe et al., 2016; Schröder et al., 2018; Robertson et al., 2018; Whitaker et al., 2018).

However, important trade-offs are also likely to occur with regards to both socio-economic and environmental SDGs. One of the main impacts is competition for available land and other inputs such as water and fertilisers. As a result, food/feed cropland may shift to other areas leading to food price increases (SDGs 1 and 2), and water availability for drinking and sanitation use may be reduced (SDG 6) (Mondiale, 2008; Melillo, Gurgel, et al., 2009; Bailey,

2013; Gorter et al., 2013; Pahl-Wostl et al., 2013; J. Popp et al., 2014; Bárcena et al., 2014; Bonsch et al., 2015; Rulli et al., 2016; Chang et al., 2016; Kline et al., 2017; Franz et al., 2018; Mbow et al., 2019; Ai et al., 2021). Cropland expansion for bioenergy could also lead to land appropriation and dispossession, whereby rural, poor, and indigenous communities would be most affected (SDG 1). Other implications include emissions from harvesting, transporting and use of feedstock (SDGs 13), and CO<sub>2</sub> leakage incidents from CCS implementation (SDGs 7, 3, 12, and 13) (Berndes, 2002; Wang and Jaffe, 2004; Kim and Dale, 2005; Larson, 2006; Hertwich et al., 2008; Yee et al., 2009; Lardon et al., 2009; Apps et al., 2010; Stratton et al., 2010; Veltman et al., 2010; Van Der Voet et al., 2010; Chum et al., 2011; Siirila et al., 2012; Atchley et al., 2013; Creutzig et al., 2015; Staples et al., 2017; Daioglou et al., 2019).

Some of the potentially largest, yet less understood, trade-offs are environmental side-effects caused by land-use changes, such as forest loss, loss of freshwater ecosystems, and nutrient leakage from fertilisers (Popp, Lotze-Campen, et al., 2011; Behrman et al., 2015; Wiloso et al., 2016; Valdez et al., 2017; Harris et al., 2018; Harper et al., 2018; Hof et al., 2018). Loss of forests and other natural land are leading concerns within the sustainability sector because they provide multiple benefits. Two major benefits are climate regulation and habitat provision for biodiversity (Mittermeier et al., 2011; Smith et al., 2019; FAO, 2022). However, in relation to the overall global sustainability of bioenergy expansion, these two areas are relatively understudied. For example, low indication of negative climate effects from bioenergy expansion has been made in relation to the SDGs (i.e., SDG 13: ‘Climate Action’, see **Figure 1.3**), whereby SDG-bioenergy intercomparison studies tend to focus on its positive role in climate change mitigation (Roy et al., 2018; GBEP, 2018). More research has been carried out into trade-offs with SDG 15: ‘Life on Land’, suggesting both counteracting and enabling effects (see **Figure 1.3**). However, only medium confidence in this finding indicates that further work is also needed in this field.

One main cause for this gap in literature has been a lack of data on spatial projections of advanced second-generation energy cropland production. Thus, previous studies have mainly focussed on the overall impact of land-use changes on climate and biodiversity, treating energy and food/feed cropland as one variable. Where bioenergy impacts have been isolated, the literature tends to be at the regional or local scale, and generally focusses on first-generation energy cropland (Fitzherbert et al., 2008; Danielsen et al., 2009; VanLoocke et al., 2010; Beringer et al., 2011; Georgescu et al., 2011; Anderson et al., 2013; Tölle et al., 2014; Caiazza et al., 2014; Harding et al., 2016; Meijaard et al., 2018). The location and type of bioenergy

production is an important consideration in its sustainability as different regions and types of land vary in their suitability for cropland growth. For instance, the expansion of oil palm in Malaysia and Indonesia has led to significant loss of natural fertile land considered essential for biodiversity and climate regulation (Koh and Wilcove, 2008). On the other hand, conversion of abandoned land to perennial grasses and short-rotation crops across the US and Europe have shown to provide habitat and shelter for specific species, as well as a cooling impact which offsets warming from life cycle emissions of the fuel (Dauber et al., 2010; Georgescu et al., 2011; Meehan et al., 2011; Anderson et al., 2013; Caiazzo et al., 2014).

Recent advancements in IAM projections of second-generation energy cropland distribution have enabled new opportunities for analysing potential impacts of bioenergy expansion on sustainability indicators at a global and multiregional level. IAMs are useful for estimating simple changes in terrestrial-atmospheric carbon fluxes from possible land-use scenarios (biogeochemical effects), however they do not consider impacts from changing land characteristics, such as surface albedo, surface roughness, and energy balance (biogeophysical effects). In addition, IAMs have been used to create scenarios incorporating nature conservation (Beringer et al., 2011; Humpenöder et al., 2018a), however, are not able to directly determine co-benefits and trade-offs of land-use changes with regards to species loss or gains. By implementing spatial outputs from IAMs into climate and biodiversity models, predictions of potential bioenergy-induced land impacts on these two indicators can be assessed, though as of yet only few studies have attempted this (Heck et al., 2018; Harper et al., 2018; Muri, 2018; Tudge et al., 2021; Hanssen et al., 2022).

Preventing potential trade-offs and reconciling large-scale bioenergy production with the global SDG agenda will require additional sustainability measures, such as forest or water conservation schemes. Although, improvements in these areas may have negative consequences for other SDGs. In the context of bioenergy, these two fields have been well studied in previous literature (Popp, Dietrich, et al., 2011; Kraxner et al., 2013; Calvin et al., 2014; Bonsch et al., 2016; Obersteiner et al., 2016; Humpenöder et al., 2018a). However, there is little evidence of their influence on climate and biodiversity impacts from land-use changes. Understanding this interaction could indicate where and to what extent improvements may be needed within these protection schemes.

---

## 1.4 Research Aims

This thesis aims to determine potential implications of land-use changes associated with large-scale second-generation bioenergy deployment for two major sustainability concerns, climate and biodiversity, over the 21<sup>st</sup> century. In doing so, this work is intended to inform further insight into the relationship between bioenergy expansion and SDGs 13: “Climate Action”, and 15: “Life on Land”. The following chapters, summarised in Section 1.5, will aim to answer three main research questions:

- 1) What are the biogeochemical and biogeophysical climate effects of possible land-use changes from the expansion of global second-generation bioenergy over the 21<sup>st</sup> century, and which regions are most affected?
- 2) What are the potential impacts of second-generation bioenergy expansion on habitat loss and species counts across the globe?
- 3) What role do environmental protection measures, such as forest and water conservation schemes, play within the expansion of another large land-use sector and how will they influence impacts on climate and biodiversity?

To answer these questions, a combination of literature research, scenario analysis, and spatial and statistical modelling will be carried out.

## 1.5 Thesis Structure

The structure of this thesis consists of six chapters, which are thus as follows:

➤ ***Chapter 1: Introduction***

*Chapter 1* has provided a brief overview of the research topic, the context within it lies, gaps in current knowledge, and the overall aims of this thesis.

➤ ***Chapter 2: Theoretical Background and Literature Review***

*Chapter 2* discusses the existing literature within the research field. This chapter firstly presents a theoretical background of bioenergy and its role within future mitigation pathways. Following this, an in-depth review of climate and biodiversity literature is provided, focussing on land-related impacts from present day bioenergy production and future expansion. Lastly, gaps in the literature are further refined and provided towards the end of this chapter. These gaps inform the basis of work carried out in this thesis.

➤ ***Chapter 3: Land-Use Scenarios***

*Chapter 3* provides an overview of four scenarios used in this thesis. These scenarios are spatial representations of global land-use changes, three of which follow trajectories whereby second-generation bioenergy demand increases linearly from 0 EJ in 2010 to 300 EJ in 2100, reflecting the upper end of projections in 1.5 °C and 2 °C pathways. Two of these scenarios additionally incorporate forest and water protection schemes. A final scenario excludes bioenergy expansion and is therefore used as a control scenario for comparison. This data has been created by Humpenöder *et al* (2018a) using the Model of Agricultural Production and its Impact on the Environment (MAgPIE). In this chapter, the MAgPIE scenarios are compared to pathways previously outlined in IPCC assessment reports.

➤ ***Chapter 4: Impacts of Bioenergy Expansion on Climate***

In answering research questions 1 and 3 in Section 1.4, *Chapter 4* evaluates the impacts of second-generation bioenergy expansion on climate, focussing on the effects of land-use changes over the 21<sup>st</sup> century. This chapter outlines the climate model, experimental setup, and simulations used. By implementing the MAgPIE scenarios in the UVic Earth System

Climate Model (version 2.9), the work explores the interactions between land and the climate system at both the regional and global scale.

➤ ***Chapter 5: Impacts of Bioenergy Expansion on Biodiversity***

In addressing research questions 2 and 3 in Section 1.4, *Chapter 5* determines the impacts of global land-use changes from second-generation bioenergy expansion on biodiversity. Presented in this chapter are the data used to define spatial distributions of biodiversity and methods used to calculate the effects of habitat loss from land-use changes in the MAgPIE scenarios on species counts across the globe. This chapter consists of a two-part intercomparison assessment, incorporating both the Endemics-Area Relationship model in combination with biodiversity hotspots, and a spatial overlay analysis with sites from the Alliance for Zero Extinction database.

➤ ***Chapter 6: Conclusions and Future Work***

*Chapter 6* summarises and discusses the work carried out. This chapter provides key findings from the climate and biodiversity analyses in *Chapters 4* and *5*. The work is further discussed in terms of how it contributes to existing knowledge in the literature. Finally, limitations and future recommendations are provided regarding the assessments used, current policies and conservation schemes, and the overall sustainability of bioenergy expansion over the 21<sup>st</sup> century.





# Chapter 2 Theoretical Background and Literature Review

## 2.1 Overview

This chapter provides background knowledge of bioenergy, with regards to its status within the energy sector at present day, its role in future mitigations pathways, and the potential impact energy cropland expansion could have on the land system. Following this, a critical analysis of existing literature is carried out to determine potential impacts of global land-use change (LUC) on climate and biodiversity and the gaps in knowledge within these fields. A comprehensive understanding of current findings and methods, in addition to these gaps, will provide the basis for assessments executed in *Chapters 3, 4* and *5*.

## 2.2 The Role of Bioenergy in Climate Change Mitigation

### 2.2.1 Global Status of Bioenergy

“Biomass” refers to biological material, in particular plants and wastes. At present, energy production using biomass is roughly  $57 \text{ EJ yr}^{-1}$ , accounting for 12% of total primary energy and around 70% of all renewable energy production (WBA, 2021) (see **Figure 2.1**). This is made up of both traditional bioenergy and modern bioenergy.

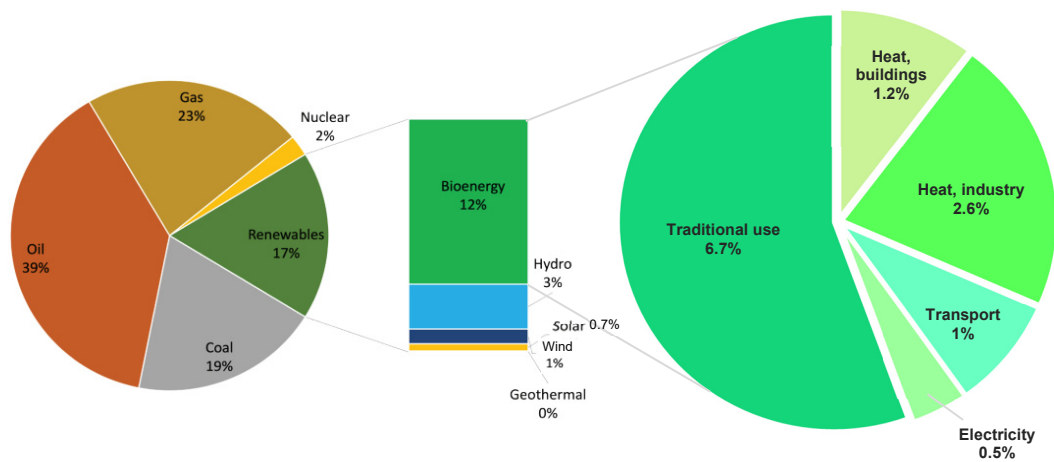


**Figure 2.1:** Total global primary energy supply in 2019, split into percentages of renewable energy supplies, and end-use sectors of bioenergy deployment. This figure has been adapted from WBA (2021) using values from REN21 (2021).

### 2.2.1.1 Traditional Bioenergy

Traditional bioenergy is the use of local solid biomass (or fuelwood) in open fires and low-efficiency cooking stoves in developing countries. This use of biomass is unsustainable, being mostly collected from natural forest that is not re-planted after use. In addition, it can lead to negative health impacts (e.g., smoke inhalation), social impacts (e.g., labour-intensive collection of biomass, often carried out by women and children) and environmental effects (e.g., forest degradation, and emissions of methane and black carbon). Recent estimates show that over 2.5 billion people still rely on traditional biomass as their principal source of energy, accounting for 56% (32 EJ) of total bioenergy production around 6.7% of the energy production altogether (IEA, 2017; IEA, 2020; WBA, 2021) (see **Figure 2.1**). Considering the rising population trends, actions to promote more sustainable use of biomass have been organised under the UN Sustainable Energy for All (SEforALL) initiative to ensure universal access to clean energy by 2030. This will involve the increasing use of “modern bioenergy”.

### 2.2.1.2 Modern bioenergy

Modern bioenergy is generated using both plants and wastes as feedstocks. If sustainably produced, using plants like this can be considered as “carbon neutral” because plants absorb CO<sub>2</sub> as they grow, thus offsetting the CO<sub>2</sub> emissions released when they are converted to biofuels and burned. Modern bioenergy already plays a prominent role, though mostly in the portfolios of only 26 countries (IEA, 2017). The largest global application of modern bioenergy is for heat consumption, accounting for 32% (18 EJ yr<sup>-1</sup>) of total bioenergy produced in 2019 (WBA, 2021) (see **Figure 2.1**). Provision of heat is largest for industrial processes (68%), followed by buildings (32%), with a small amount also utilised by agricultural and commercial applications. The remaining modern bioenergy production is for transport (8%; 5 EJ yr<sup>-1</sup>), and electricity (4%; 2 EJ yr<sup>-1</sup>).

## 2.2.2 Biomass Feedstocks and Energy Production

When used for modern energy production, biomass can be categorised into three main different generations of feedstocks, based on the properties of the biomass, the cultivation process used to acquire it, and the method used to convert it to bioenergy (i.e., chemical, biochemical, or thermochemical conversion).

### 2.2.2.1 First-generation biomass

First-generation biomass feedstocks are crops that can also be consumed as human food. Oil crops, such as soybean, oil palm and rapeseed, contain vegetable oils that can be extracted using esterification or hydrotreating to produce biodiesel or renewable diesel, respectively (Chongkhong et al., 2007; Aatola et al., 2009) (see **Figure 2.2**). Sugar (e.g., sugarcane) and starch (e.g., maize and wheat) crops contain simple sugars which can be converted into alcohols (ethanol and butanol) through hydrolysis and fermentation (Schwietzke et al., 2009; Cardona et al., 2010). In the transport sector, first-generation biofuels, particularly biodiesel and bioethanol, are widely deployed at full commercial scale, although the number of markets is limited. In 2018, around 100 billion litres of ethanol were produced worldwide, with approximately 85% of this represented by the United States and Brazil (WBA, 2020). Biodiesel production, on the other hand, was shared relatively evenly between the Americas, Asia, and Europe, equating to around 40 billion litres in 2018.

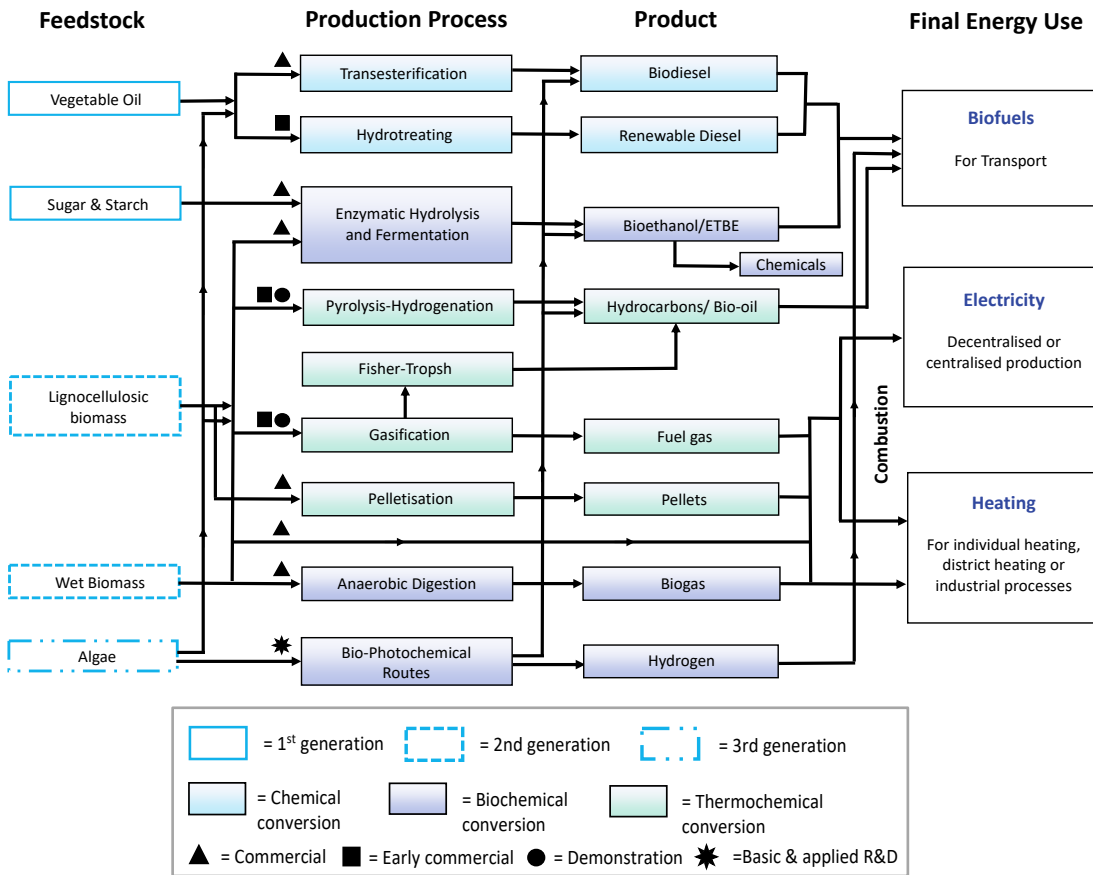


**Figure 2.2:** Bioenergy conversion technologies; created using findings from EUBIA (2020), Costa and Piazzullo (2018), and IEA (2009).

### 2.2.2.2 Second-generation biomass

Scaling up bioenergy use will require advanced feedstocks and technologies. Second-generation biomass feedstocks are non-edible lignocellulosic biomass; such as wood and residues from sustainably managed forests, purpose grown energy crops and municipal solid waste (Elliott Campbell et al., 2008; Daioglou et al., 2016; Pour et al., 2018; Peura et al., 2018; S. V. Hanssen et al., 2020; Goh et al., 2020), and wet wastes; for instance, sewage sludge, farm waste and food waste (Cantrell et al., 2008; Chua et al., 2013; Dung et al., 2014). In combination with a variety of thermochemical and biochemical technologies, these feedstocks can be used to produce heat, electricity, and biofuels for transport. For heat and electricity production, direct combustion and gasification are the main technologies used for lignocellulosic feedstocks (see **Figure 2.2**). Modern direct combustion technologies for heat

production range from small-scale biomass boilers and stoves to more efficient large-scale plants, often combined with electricity production in combined heat and power (CHP) systems. Combustion technologies are currently in commercial operation, and generally use roundwood and woody residues from forestry, agricultural residues, and purpose grown energy crops (e.g., miscanthus, poplar) as feedstocks (Lauri et al., 2019; Drax Group plc, 2021). Gasification for heat and electricity is still at the early commercial scale, due to its complexity and cost. If in the longer term gasification can be widely commercialised, it could provide greater efficiency, higher versatility in terms of feedstock used, and more affordable energy (IEA, 2009). For wet biomass feedstocks, fully commercialised anaerobic digestion (AD) can be used to produce heat and electricity. However, these technologies are generally less efficient than thermochemical approaches and often produce large amounts of CO<sub>2</sub>, requiring the produced fuels to undergo substantial upgrading (Melara et al., 2020).

Second-generation biofuels for transport can be produced using the same lignocellulosic feedstocks used in combustion technologies. Biochemical (hydrolysis and fermentation) or thermochemical (pyrolysis and gasification) conversion methods are slowly becoming commercialised, with around 67 second-generation biofuel plants currently operating around the world (Nguyen et al., 2017). A large proportion (35%) of cellulosic biofuel production is based in the US, though the potential for growth in European, Asian, South American, and African markets is high. Although second-generation feedstock can be readily produced by existing infrastructure and technology, energy production using this feedstock is more complex than first-generation processes. Investment requirements are therefore far greater than for corn-starch or sugarcane-based ethanol, and financial lenders can be hesitant to invest in new conversion technologies unless proven to be economically viable without subsidy (Bracmort, 2014; de Coninck et al., 2018).

### **2.2.2.3 Third-generation biomass**

Third-generation biomass refers to feedstocks derived from algae. Macro-algae (e.g., seaweed) can be treated as a lignocellulosic biomass, and hence can be used in all 2<sup>nd</sup> generation conversion methods to produce heat, electricity, and biofuels. Microalgae are microscopic photosynthetic organisms (e.g., diatoms, green algae, golden algae). The two main conversion routes for microalgae are transesterification, to produce biodiesel, and a variety of biophotochemical routes, which produce biofuels and hydrogen gaseous fuel. Microalgae have gained significant interest due to their ability to produce outstanding yields per hectare, and

their ability to grow in waste water. However, major challenges in cultivating macroalgae and microalgae, such as high water and fertiliser intake, and difficulties in sustaining growth over long periods, have meant that these methods are still at the ‘basic and applied research and development’ scale (Kumar et al., 2015).

## **2.2.3 Decarbonisation via Second-Generation Bioenergy**

### **Expansion**

#### **2.2.3.1 A Transition from First- to Second-Generation**

##### **Bioenergy**

For years, first-generation biofuels have been considered an attractive option for renewable energy production, with life cycle assessments calculating positive findings for both energy return on investment (Stromberg and Gasparatos, 2012) and fossil energy improvements (Menichetti and Otto, 2009). However, cropland expansion for first-generation biofuels is not possible alongside projected increases in food requirements, and studies show that combined changes in land use will exceed land and water planetary boundaries (Gerten et al., 2013; Steffen et al., 2015; Henry et al., 2018). In 2013, the combined global production of bioethanol and biodiesel required the use of around 0.413 million km<sup>2</sup> of fertile land, and 216 billion m<sup>3</sup> of freshwater (Rulli et al., 2016). In addition, significant areas of undisturbed land have been converted to first-generation biofuels, particularly in South America and Asia (Pena, 2008; Fargione et al., 2008; Lapola et al., 2010; Koh et al., 2011; Gao et al., 2011; Lima et al., 2011; Havlík et al., 2011; Carlson et al., 2012; Leal et al., 2017). For instance, between 1990 and 2005, over half of oil palm expansion in Malaysia and Indonesia occurred at the expense of primary forest (Koh and Wilcove, 2008).

Transitioning to dedicated second-generation bioenergy crops has been considered a potential solution for combatting these sustainability trade-offs, largely due to their ability to grow on marginal or abandoned agricultural land (Tilman et al., 2006; Zomer et al., 2008; Mehmood et al., 2017). In addition, substantial reductions in GHG emissions have been found when producing second-generation bioenergy compared to first-generation bioenergy, largely due to reductions in fossil fuel energy required (Wang, 2007; Highina et al., 2014). The combined availability of low-impact second-generation bioenergy feedstocks, such as dedicated energy crops, wastes and residues from agriculture and forestry, and wood from selective logging, is

still uncertain, with numerous sectors competing for this biomass (e.g., construction materials and chemicals). As cropland area is more easily quantifiable, many mitigation pathways consistent with 1.5–2 °C warming explicitly rely on dedicated second-generation bioenergy crops for provision of heat, electricity, and transport.

### **2.2.3.2 Bioenergy with Carbon Capture and Storage (BECCS)**

To reach global warming targets of 1.5–2 °C by 2100, additional carbon dioxide removal (CDR) strategies will be required to offset residual emissions and achieve global net negative emissions towards the end of the 21<sup>st</sup> century. Proposed options include reforestation/afforestation, direct air capture of CO<sub>2</sub> (DAC), ocean alkalisation (OA), soil carbon sequestration using biochar (SCS), enhanced weathering (EW), and carbon capture and storage combined with second-generation bioenergy production (BECCS). Multiple co-benefits have been identified for each CDR option, largely related to their potential contributions to sustainable development, enhancement of ecosystem functions and services and other societal goals (IPCC, 2019; Canadell et al., 2022). However, these benefits are context specific, and large limitations have also been found regarding CDR abatement costs, side effects, and potential for deployment by 2050 (de Coninck et al., 2018; Canadell et al., 2022).

In almost all pathways limiting global warming to 1.5–2 °C, BECCS contributes the largest part of CDR (Rogelj, Popp, et al., 2018). BECCS consists of three processes: planting lignocellulosic biomass; which captures atmospheric CO<sub>2</sub> through photosynthesis, using the biomass for bioenergy production (as described in Section 2.2.2), and capturing and sequestering the CO<sub>2</sub> emitted in geological reservoirs; most commonly saline aquifers (Canadell and Schulze, 2014). This chain of processes, in addition to subsequent cropland regrowth/replanting and substitution of fossil fuel use with bioenergy, results in overall net negative emissions.

Currently, five facilities across the world are actively using BECCS technologies, collectively capturing around 1.5 million tonnes of CO<sub>2</sub> per year (MtCO<sub>2</sub>yr<sup>-1</sup>). These include one large-scale corn to ethanol facility in Illinois, US (capturing up to 1 MtCO<sub>2</sub>yr<sup>-1</sup>), and four small ethanol production plants located in the US and Canada (Consoli, 2019). Three additional large-scale heat and power projects are also underway in the UK (Drax, 2020), Japan (Toshiba, 2019), and Norway (CCS Norway, 2020). Theoretically, the potential for BECCS expansion is

high, particularly for bioethanol production whereby the technology is already mature. However, there are still large uncertainties with regards to realistic carbon removal potentials, the ability to scale up such a complex technology, and broader sustainability considerations of using biomass. In addition, a major challenge will be harmonising aims for BECCS expansion in the long-term with short-term greenhouse gas-reduction priorities (Fajardy et al., 2019; Köberle, 2019).

### **2.2.3.3 Future Mitigation Pathways**

Integrated assessment models (IAMs) can be used to predict the role of BECCS in future mitigation pathways by combining energy, economy, and climate system models into one single framework. These pathways are constructed using assumptions around economic and population growth, demand in various GHG-emitting activities (such as transport, heating, industry, and agriculture), and strategies in limiting long-term temperature change to specified goals. Most of the global-level analysis on climate change mitigation has, to date, been based on results from IAMs; hence they inform the basis for IPCC reports. Though they are used extensively, research incorporating IAMs has been criticised for issues surrounding lack of transparency regarding model structures and input assumptions, over-reliance on certain technologies, and insufficient representation of real-world policies and processes such as innovation and behaviour. However, there is consensus that IAMs provide multiple benefits, namely their ability to account for numerous assumptions around costs, policies, performance characteristics, and availability of different fuels and technologies. With regards to BECCS, significant improvements in IAMs have already been seen, including better representations of lifecycle emissions, operating characteristics of BECCS power plants, and potential deployment constraints (Gambhir et al., 2019; Muratori et al., 2020).

Despite their limitations, over time the development of alternative future pathways using IAMs has become more sophisticated. This began with the creation of the Special Report on Emission Scenarios (SRES) based on possible emission trajectories (Nakićenović et al., 1998), and has moved towards exploring different climate futures using the Representative Concentration Pathways (RCPs). These are a set of six different greenhouse gas concentration trajectories (RCP1.9, RCP2.6, RCP3.4, RCP4.5, RCP6, and RCP8.5), spanning the range of year 2100 radiative forcing values found in the open literature, i.e., from 1.9–8.5W m<sup>-2</sup>. More recently, the development of the shared socio-economic pathways (SSPs) (O’Neill et al., 2014; O’Neill et al., 2015; Popp et al., 2017) has enabled further research into global climate change studies



as well as broader assessments of global sustainable development. The SSPs portray five different global futures with varying socio-economic challenges to mitigation and adaptation. For instance, SSP1 describes a sustainability pathway with low challenges for adaptation and mitigation, whereas in SSP3 both challenges are high due to regional rivalry. A more middle-of-the-road narrative is depicted in SSP2, which describes medium challenges in both mitigation and adaptation, representing a future in which development trends are not dissimilar to current patterns. Due to its lack of extremeness in any dimension, the SSP2 pathway has been utilised in many future global assessments in the literature (A. Popp, Weindl, et al., 2014; Bonsch et al., 2016; Krause et al., 2017; Humpenöder et al., 2018a).

The six IAMs used in the initial development of the RCPs and SSPs are AIM, GCAM, IMAGE, MESSAGE-GLOBIOM, REMIND-MAgPIE and WITCH-GLOBIOM, some of the most widely used models in global mitigation scenario analysis. These IAMs have a variety of differing characteristics, such as the degree of detail in describing global and regional energy systems (e.g., technologies and fuels), the depiction of energy demand in each sector (i.e., transport, buildings, industrial manufacturing and agriculture) of the economy in these regions, the availability of mitigation technologies and options, and the calculation of temperature change due to emissions from the energy system in each period (Gambhir et al., 2019). In addition to energy sectors, variation between IAMs can also exist within non-energy sectors such as land use and agriculture, responsible for emitting CO<sub>2</sub> as well as non-CO<sub>2</sub> gases.

The SSPs and RCPs can be used in conjunction with each other in a scenario matrix architecture (van Vuuren et al., 2014). This involves the implementation of climate policies in SSPs to achieve RCP-specific climate target levels, and thus determine the ability and efforts needed to mitigate climate change, in addition to associated contributions of the land sector (Kriegler et al., 2014; Popp et al., 2017). The combined SSP-RCP scenarios cover a wide spectrum of socio-economic and climate forcing pathways, with CO<sub>2</sub> concentration levels ranging between 380 ppm (for SSP1-RCP1.9) and 1090 ppm (for SSP5-RCP8.5) by 2100 (see **Figure 2.3**). Reaching concentration levels of 440 ppm CO<sub>2</sub>eq or less by 2100 will require substantial reductions in global GHG emissions, and most IAM scenarios rely heavily upon BECCS to achieve this goal. Scenarios with a radiative forcing target of 2.6 Wm<sup>-2</sup> (around 2 °C warming) are associated with GHG emissions reductions of 30-99% by 2050 compared to 2010. For the more ambitious 1.9 Wm<sup>-2</sup> target (around 1.5C warming), GHG emissions reduction levels reach near zero or below by 2050 (between 88 and 125% reductions since 2010) (IIASA, 2018b).

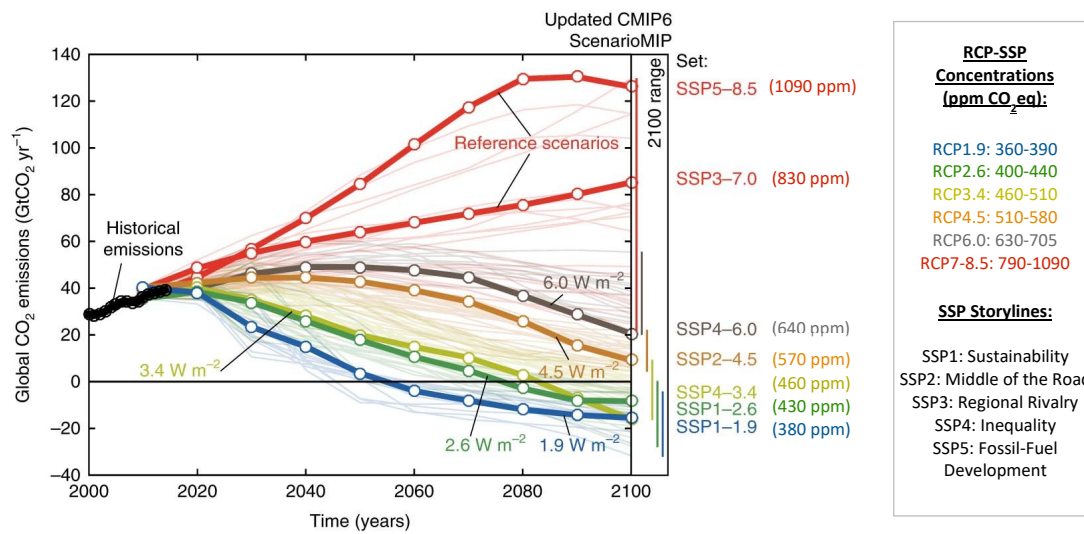


**Figure 2.3:** Global CO<sub>2</sub> emissions for SSP scenarios, and corresponding CO<sub>2</sub> concentrations for 2100. Highlighted lines indicate selected pathways from the CMIP6 ScenarioMIP project. This figure has been adapted from Rogelj, Popp, et al. (2018) using concentration values from the IIASA SSP database (IIASA, 2018b).

### 2.2.3.4 BECCS Deployment in Future Mitigation Pathways

While BECCS technologies have not been deployed as fast as projections have envisioned, IAMs continue to rely heavily on BECCS for reducing the costs of reaching climate change mitigation targets. This has led to a wide range of predicted bioenergy potentials across multi-model assessments. Early projections suggested potentials between 10 to 245 EJ yr<sup>-1</sup> in 2050 and 105 to 325 EJ yr<sup>-1</sup> in 2100 (IPCC, 2011; GEA, 2012; Smith et al., 2014). More recent reports, such as the IPCC Special Report on Global Warming of 1.5 °C (SR15) published in 2018, and the IPCC Sixth Assessment Report on Mitigation of Climate Change published in 2022, further indicate that BECCS deployment could increase up to around 80 to 450 EJ yr<sup>-1</sup> by 2100 in pathways with global warming targets of below 1.5–2 °C (RCP 1.9–2.6) (IIASA, 2018b; IPCC, 2018; Riahi et al., 2022).

These scenarios incorporate a clear shift away from fossil fuels without CCS by 2050, and an overall phase out of all fossil fuel energy by the end of the century (see **Figure 2.4** (a)). For pathways consistent with a 2 °C target (radiative forcing of 2.6 W m<sup>-2</sup>), a median of 3.3 GtC yr<sup>-1</sup> is removed from the atmosphere through BECCS (170EJ<sup>-1</sup> yr by 2100) by 2100. This

equates to around one third of present-day emissions from fossil fuel and industry and leads to cumulative negative emissions of 614 GtCO<sub>2</sub> by 2100 (Smith et al., 2016; Harper et al., 2018). Across 1.5 °C pathways, CO<sub>2</sub> sequestration from BECCS reaches roughly 5–30 GtCO<sub>2</sub>yr<sup>-1</sup> by 2100, where approximately 150–1,200 GtCO<sub>2</sub> is removed from the atmosphere during the 21<sup>st</sup> century, equivalent to around 4–30 years of current annual emissions (Rogelj, Popp, et al., 2018).

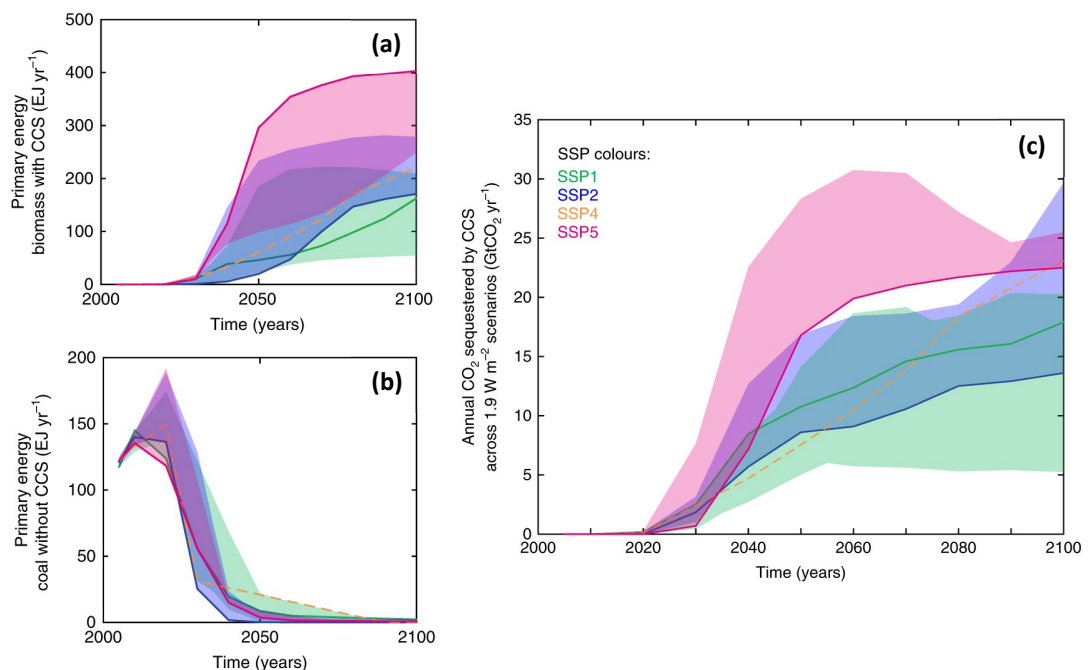


**Figure 2.4:** Decarbonisation characteristics in 1.5 °C ( $1.9 \text{ W m}^{-2}$ ) scenarios following SSP1, SSP2, SSP4 and SSP5 pathways; reproduced from Rogelj, Popp, et al. (2018). Figure (a) shows primary energy from biomass with CCS (BECCS), (b) shows primary energy from coal without CCS, and (c) shows the annual amount of CO<sub>2</sub> stored by CCS in 1.5 °C ( $1.9 \text{ W m}^{-2}$ ) scenarios. Shaded areas indicate the range per SSP, solid lines are the marker scenarios for each SSP, and dashed yellow lines indicate scenarios that are not markers.

Uncertainty across BECCS potentials and corresponding CO<sub>2</sub> sequestration levels is due to the different ways in which BECCS is modelled within the various IAMs, in terms of bioenergy feedstocks, logistics, conversion technologies, and environmental and socio-economic patterns. Concern around such uncertainties has been a driver for model intercomparison studies, such as the Energy Modelling Forum projects 27 and 33 (EMF -27 and -33), which determine the importance of bioenergy production in achieving future climate objectives (Rose

et al., 2014; Rose et al., 2020; Rose et al., 2022). Overall, most models indicate the use of residues and lignocellulosic energy crops (perennial grasses and woody crops) as biomass feedstock, with some additionally using managed forest (e.g., BET, GRAPE, IMACLIM-NLU, and MESSAGE-GLOBIOM). Nearly all models have the option to produce electricity from biomass-fuelled power plants with CCS, and some also incorporate liquid biofuel (e.g., AIM, COFFEE, GCAM MESSAGE-GLOBIOM, POLES, REMIND-MAgPIE, and TIAM-WORLD) and hydrogen options with CCS (e.g., COFFEE, DNE21+, IMACLIM-NLU, IMAGE, MESSAGE-GLOBIOM, POLES, and REMIND-MAgPIE). Some models also include biogas technology (e.g., BET, COFFEE, DNE21, FARM, GCAM, MESSAGE-GLOBIOM, POLES, and REMIND-MAgPIE), whereas fewer include biomass-based heat (e.g., AIM, COFFEE, FARM, MESSAGE-GLOBIOM, POLES, REMIND-MAgPIE, TIAM-WORLD).

One of the key aspects to BECCS potential within these models is the magnitude of biomass supply possible. This is determined by the feedstocks modelled and land conversions allowed, as well as associated impacts on emissions, land use, land management, and the agricultural market, which in turn affect issues such as land productivity, food security, water quality and scarcity, and biodiversity. Overall, studies show a wide range of possibilities regarding biomass supply (i.e., feedstocks, locations, and consequences), indicating a need for more detailed assessments of land-use projections from IAMs.

### **2.2.3.5 Global Carbon Cycle Responses to CDR and BECCS**

The effectiveness of BECCS as a mitigation option is largely dependent on its role within the carbon cycle. Earth system feedbacks can either amplify or reduce carbon sequestration potentials of different CDR methods and thus their effectiveness in reducing atmospheric CO<sub>2</sub> and mitigating climate change. Since the pre-industrial era, anthropogenic CO<sub>2</sub> emissions from fossil fuels and LUC have been redistributed between atmosphere (46% in 2010-2019), land (31%), and ocean (23%) carbon reservoirs due to carbon cycle processes (Canadell et al., 2022). The removal of CO<sub>2</sub> via BECCS and other CDR applications is expected to have varying impacts on these reservoirs depending on the extent of their application.

In high emissions scenarios (e.g., SSP5-8.5) with low BECCS or CDR, land and ocean carbon sinks absorb more CO<sub>2</sub> emissions (CO<sub>2</sub> fertilisation), however, the fraction of emissions removed from the atmosphere decreases with increased CO<sub>2</sub> concentrations. Hence, the more

CO<sub>2</sub> is emitted, the less efficient the ocean and land sinks become. In ambitious mitigation scenarios (e.g., RCP2.6, SSP1-2.6), as CDR application is ramped up and CO<sub>2</sub> emissions start to decline, the land and ocean sinks continue to take up CO<sub>2</sub> from the atmosphere, still responding to prior trajectories of rising CO<sub>2</sub> concentrations due to inertia (Tokarska and Zickfeld, 2015; Jones et al., 2016). Over time, uptake of CO<sub>2</sub> by the land and ocean begins to weaken and these reservoirs start to release CO<sub>2</sub> into the atmosphere, thus making CDR less effective. For scenarios reaching net negative emissions within the 21<sup>st</sup> century (e.g., RCP2.6, SSP1-2.6), this release could be decades or centuries later, whereas for scenarios with larger amounts of removal (e.g., SSP5-3.4-overshoot), it is much sooner and larger. Timings and magnitudes of this sink-to-source transition vary between land and ocean, with land predicted to become a source sooner than ocean. In general, CO<sub>2</sub> remaining in the atmosphere after an emission is larger than CO<sub>2</sub> remaining out of the atmosphere after a removal, due to asymmetries between land and ocean carbon fluxes from non-linearities in the carbon cycle response to CO<sub>2</sub> and temperature (Keller et al., 2018; Zickfeld et al., 2021).

In addition to CDR impacts, the effectiveness of BECCS can be determined by how energy crops respond to increases in CO<sub>2</sub> and climate change. As previously discussed, increases in atmospheric CO<sub>2</sub> concentrations result in CO<sub>2</sub> fertilisation and thus higher uptake of carbon in the land. This occurs particularly in tropical regions with extensive vegetation, such as the Amazon rainforest, the Democratic Republic of Congo and Southeast Asia (see **Figure 2.5**) (Arias et al., 2021). On the other hand, climate change is expected to lead to land carbon accumulation only in high latitudes and the northern hemisphere, with significant loss occurring in the tropics. Using carbon uptake as a proxy for vegetation growth, this suggests that energy crops (and other land types) are expected to grow more effectively in higher latitudes in future scenarios. Observations have shown that, even after the conversion of forest to cropland, net primary productivity (NPP) increases in high latitudes due to higher grassland productivity resulting from CO<sub>2</sub> fertilisation, despite cooler temperatures (Roy et al., 2001; Bathiany et al., 2010; Longobardi et al., 2016). In contrast, the counteracting effects of carbon responses to CO<sub>2</sub> and climate in the tropics suggests that bioenergy crops may grow less effectively in this region, particularly in parts of Latin America and Sub-Saharan Africa.

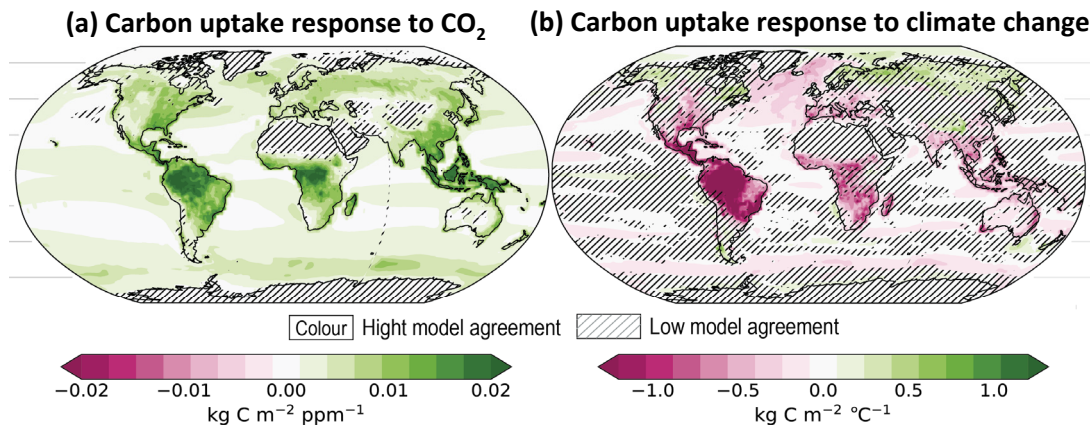


**Figure 2.5:** Changes in land and ocean carbon storage in response to CO<sub>2</sub> (a) and climate change (b); reproduced from Arias et al. (2021).

As shown in this section, the relationship between BECCS and the carbon cycle is complex, with numerous factors determining the effectiveness of this CDR method. Out of all biological CDR options (e.g., afforestation/reforestation, soil carbon sequestration, biochar), large-scale deployment of BECCS could have the strongest influence on the carbon cycle due to its large CO<sub>2</sub> removal potentials and substantial land requirements. However, this is dependent on type of feedstock, region, climate, and management practices. If not implemented carefully, disturbances to land could exacerbate the release of CO<sub>2</sub> from land to the atmosphere, further reducing the effectiveness of BECCS as a CDR method. More research into the impacts of bioenergy expansion on global land-use changes, as well as corresponding co-benefits and trade-offs, is thus needed.

### 2.2.3.6 Land-Use Changes in Future Mitigation Pathways

Cultivation of second-generation energy cropland, such as grasses (miscanthus) and fast-growing trees (eucalyptus, poplar) is included under the umbrella of the agriculture, forestry, and other land-use sector (AFOLU). AFOLU also comprises other biomass used for energy (e.g., woodfuel and first-generation energy cropland), food and feed cropland, other CDR strategies (e.g., afforestation and reforestation), wood for pulp and construction, and the supply of ecosystem services. Fulfilling all demands together, whilst limiting warming to below 1.5–2 °C will require changes in overall land use, as well as in agricultural and forestry practices (Smith et al., 2014; Popp et al., 2017; Rogelj, Shindell, et al., 2018).

---

At present, only 20% of the world's 13.4 billion hectares of land surface is suitable for crop production, due to availability of land resources and local natural conditions (Bruinsma, 2003). With half of this already cultivated, and a large portion of the remaining land currently beneath tropical forests (Delzeit et al., 2017), studies have suggested that there is almost no room for cropland expansion (Eitelberg et al., 2015). The effectiveness of another large land-use sector, such as BECCS, thus depends on whether it can co-exist among current land demands, and hence can vary depending on location and land-use prior to conversion (Clarke et al., 2014; Smith et al., 2014; Harper et al., 2018; Rose et al., 2022).

Future land-use interactions within the agricultural system will be strongly based on population dynamics and economic growth, as well as other basic socio-economic conditions such as dietary patterns and food demand, technological development in the crop and livestock sector, investments in agricultural technology, trade of agricultural goods, and interactions with other sectors (e.g., the bioenergy sector). Scenarios such as the SSPs and RCPs, are useful tools for understanding potential land-use dynamics, corresponding GHG emissions and land-based mitigation options under different sets of socio-economic and climate settings (Popp et al., 2017). IAMs which explicitly model land-use changes are well-suited to creating such scenarios, as they include a dedicated energy system, a land-use module, and economy and climate modules, which all interact together to determine supply, demand, and yields. As a result, competition occurs between land-use related activities such as food, livestock, and bioenergy crop production, based on either profit maximisation or cost minimisation, leading to land allocation across these categories, as well as pasture, grass, shrubland and other non-commercial forestland. Climate policy can be represented by introducing a carbon price that taxes fossil fuels, as well as greenhouse gas emissions associated with the production of biomass and its conversion into bioenergy. In some models, the carbon price is applied to carbon stocks held in the terrestrial system, hence replacement of carbon-rich ecosystems with bioenergy cropland could result in negative carbon balance (and thus land-use carbon emissions). In this case, strong incentives exist to either avoid deforestation or expand carbon stocks through afforestation/reforestation to achieve climate targets (A. Popp, Rose, et al., 2014; Harper et al., 2018).

Though the overall aims of IAMs are similar, the models' representations and parameterisations of biogeochemical, biogeophysical and socio-economic processes can vary significantly. This is particularly the case regarding land and water resources available for dedicated bioenergy crops, with some models considering all land available, some keeping land

types (e.g., managed forest and pasture) static, and some allocating bioenergy crops based on suitability of soil and climatic conditions, as well as competition with land needed for other agricultural activities and forest conservation. Crop irrigation also differs among models, whereby REMIND-MAGPIE has been noted for its flexibility in being able to shift production from irrigated to rainfed in response to economic or climate drivers for all types of crop production (A. Popp, Rose, et al., 2014). Other models (e.g., IMAGE) tend to consider irrigation for only food cropland, leaving bioenergy cropland to be rainfed, or implicitly consider both irrigated and rainfed croplands – i.e., they do not include them as technology choices (e.g., GCAM).

In general, land-use modelling using IAMs is a complex process. Consequently, the development of isolated spatial second-generation energy cropland distributions has been a slow development, with only few studies having investigated isolated impacts of bioenergy expansion in the past (Beringer et al., 2011; Hallgren et al., 2013; A. Popp, Rose, et al., 2014). Further, most of the existing literature and databases combine energy and non-energy cropland (food/feed cropland) into one ‘cropland’ variable (IIASA, 2009; IIASA, 2018a). Growing interest in global impacts of second-generation bioenergy suggests the need for more detailed spatial data and has led to a variety of more recent assessments in bioenergy’s role within the SSP and RCP pathways, discussed later in this chapter (Popp et al., 2017; Riahi et al., 2017; Heck et al., 2018; Harper et al., 2018; Muri, 2018; Rogelj, Popp, et al., 2018; Humpenöder et al., 2018a; Tudge et al., 2021; Hanssen et al., 2022).

Within these recent studies, limited harmonisation between IAMs has led to a broad range of outputs for land-use futures. Rogelj, Shindell, et al. (2018) provide a clear overview of LUC transitions produced in key SSP and RCP multi-model comparison assessments: Popp et al. (2017), Riahi et al. (2022) and Rogelj, Popp, et al. (2018) (see **Figure 2.6**). Across all model estimates for the SSPs, energy cropland is projected to increase by 0.42–5.08 million km<sup>2</sup> in 2 °C pathways and further by 0.92–7.21 million km<sup>2</sup> in 1.5 °C pathways by 2050 (relative to 2010). For the 2 °C pathways, this increases to up to 2.45–15.17 million km<sup>2</sup> by 2100 (Popp et al., 2017). Other studies have projected even more extensive energy cropland needed for large-scale bioenergy production, estimating areas of up to 14.07–15.25 million km<sup>2</sup> by 2050 in their scenarios (Melillo, Reilly, et al., 2009; Kicklighter et al., 2012; Hallgren et al., 2013).



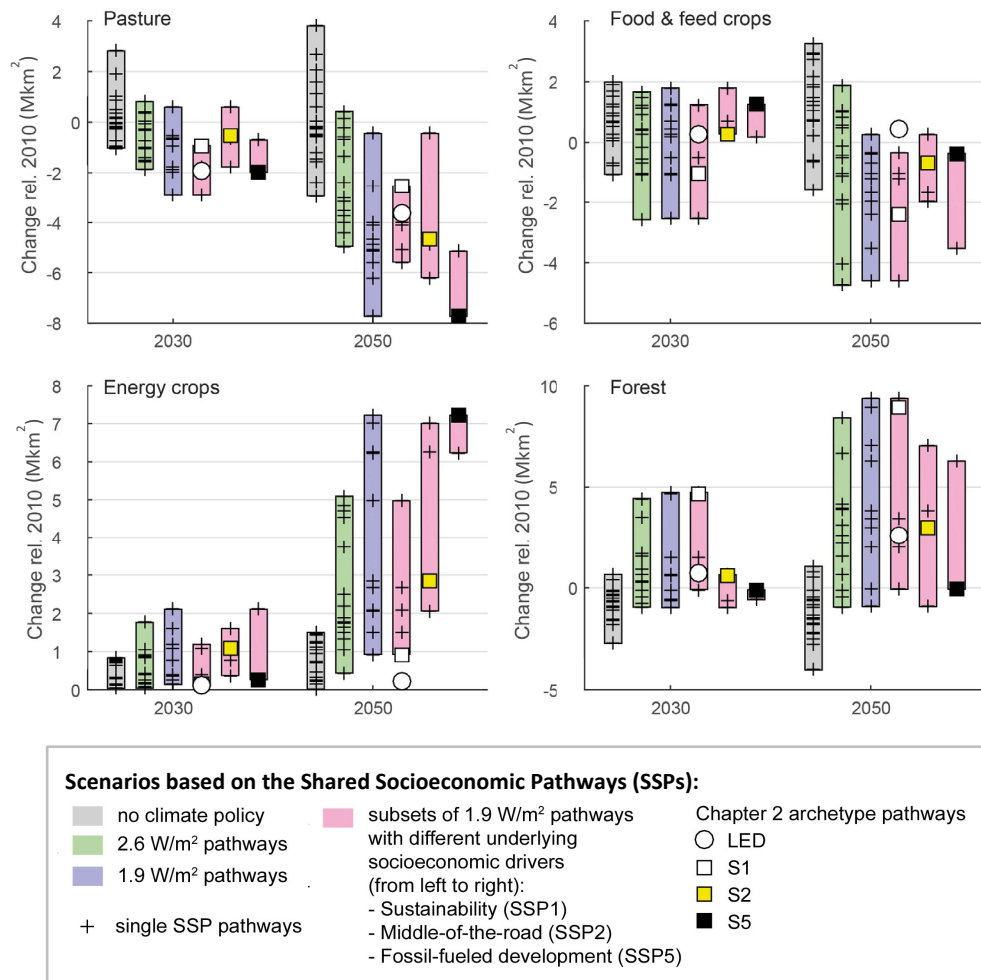


**Figure 2.6:** Land-use changes in 1.5 °C and 2 °C pathways based on the Shared Socioeconomic Pathways, for 2030 and 2050 relative to 2010; adapted from Rogelj, Shindell, et al. (2018). Four archetype pathways are shown, comprising three 1.5°C-consistent pathways based on SSPs 1 (S1), 2 (S2) and 5 (S5), developed by the AIM, MESSAGE-GLOBIOM, and REMIND-MAgPIE models, respectively. In addition, a scenario with low energy demand (LED) is included.

Substantial increases in energy cropland have consequences on other land-use types. By 2050, changes in pasture due to second-generation bioenergy and afforestation equate to around (–)4.95–(+0.43 million km<sup>2</sup> across 2 °C pathways, and (–)7.73–(–)0.44 million km<sup>2</sup> in 1.5 °C pathways. For most ambitious mitigation scenarios, the use of pasture or degraded land is not enough to fulfil required bioenergy potentials. Thus, in these scenarios, energy crop production competes with food/feed cropland for fertile land. Changes in food/feed cropland are estimated

as (-)4.75-(+)1.86 million km<sup>2</sup> by 2050 across all 2 °C and 1.5 °C pathways, whereby food/feed cropland generally includes first-generation bioenergy crops. Large reductions of these two land types are facilitated by intensification on agricultural land and in livestock production systems, as well as changes in human consumption patterns (Frank et al., 2017; Popp et al., 2017; Rogelj, Shindell, et al., 2018). Agricultural expansion is further reduced by restrictions in deforestation, as well as afforestation and reforestation measures, particularly in more ambitious pathways. The extent of these parameters, however, varies widely across different models in the literature, with forest extent ranging from -0.94 to 9.37 million km<sup>2</sup> across 1.5 °C and 2 °C pathways. In scenarios with high forest increase, significant loss of ‘other natural land’ tends to occur as it is utilised for agricultural expansion (Popp et al., 2017).

The SSP land dynamics have consequences for sustainable development. In most scenarios, BECCS and afforestation CDR strategies occur at the expense of land for food and feed crops (SSP1, SSP2, SSP4 and SSP5) and pastureland (SSP1, SSP2, SSP4 and SSP5) (Nijsen et al., 2012). However, in some scenarios, other natural land (SSP4) and unprotected forests (SSP2, SSP3 and SSP4) are also replaced. The highest losses of forest and other natural land have been observed in SSP3 due to limited land-use regulations, mainly within Middle Eastern, African and Latin American countries (Popp et al., 2017). In contrast, high regulations in land-use, improvements in agricultural productivity, low meat-based diets, and rapid global cooperation of climate change mitigation in SSP1 leads to abandonment of agricultural land and associated regrowth of natural vegetation in baseline and mitigation projections. In addition, food prices are impacted differently, whereby SSP1 shows global price decreases whereas SSP3 indicates strong increases, particularly in Middle Eastern and African countries and across Asia.

In general, findings indicate that following SSP1 could provide the most positive impacts on sustainable development. In reality, the future of global land-use dynamics will be more complex, with uncertainties across IAMs, and SSP/RCP pathways, indicating a wide range of possible land-use futures. Continuous research into land-use impacts on sustainable development is therefore vital, particularly with regards to second-generation bioenergy expansion.

## 2.2.4 Sustainability Implications of Large-Scale Bioenergy

### Deployment

Disparities between scenario estimates of bioenergy potentials, carbon sequestration potentials and corresponding land-use changes demonstrate the complexities of implementing second-generation bioenergy at a global scale. It is, however, evident that as bioenergy deployment increases to high levels, both trade-offs and co-benefits for e.g., food security, ecosystems, biodiversity, water use, and nutrients become more likely (de Coninck et al., 2018; IPCC, 2022a; IPCC, 2022b) (see *Chapter 1*, Section 1.3). One of, if not, the largest concerns is the potential impact unregulated land-use changes could have on forest cover across the globe. Over the last two decades, around 4.37 million km<sup>2</sup> (11%) of tree cover has been lost (WRI, 2022a). Within this, around 0.68 million km<sup>2</sup> of primary forests have been removed in the humid tropics, two-thirds of which can be attributed to commodity production (industrial-scale agriculture, mining, oil, and gas, etc.) (WRI, 2022b). The remaining one-third is related to shifting agriculture, the temporary clearance of forest for agriculture followed by tree regrowth (Curtis et al., 2018). Though ambitious mitigation pathways suggest mainly increases in forest extent over the century, lack of policy and regulatory measures in the real world could lead to significant forest loss.

Forests and other natural land provide a myriad of benefits that, if lost, would have major consequences for the planet. Climate regulation and habitat provision for biodiversity are two benefits that have gained considerable attention due to the significance and rapidity of changes occurring within these fields because of forest loss. However, as discussed in Section 1.3, in relation to second-generation bioenergy expansion these two fields are relatively understudied. Understanding the impacts of bioenergy-induced land-use change on climate and biodiversity could provide more insight into the sustainability of second-generation bioenergy expansion, particularly with regards to sustainable development goals 13: 'Climate Action' and 15: 'Life on Land'. By assessing previous literature in these two areas, gaps in knowledge can be identified to help build the foundation for research performed in this thesis.

## 2.3 Impacts of Bioenergy Expansion on Climate

Climate impact assessments of bioenergy or biofuels generally focus on greenhouse gas emissions occurring directly or indirectly during the life cycle of the fuel. Until recently these assessments have mostly targeted emissions from harvesting and transport, as well as fuel production, distribution, and combustion (Kim and Dale, 2005; Larson, 2006; Lardon et al., 2009; Yee et al., 2009; Stratton et al., 2010; Van Der Voet et al., 2010; Chum et al., 2011; Creutzig et al., 2015; Staples et al., 2017; Daioglou et al., 2019). Land-use changes for bioenergy production, however, may also alter fluxes of CO<sub>2</sub>, other GHGs, and aerosols (biogeochemical effects) which should be accounted for in these assessments. In addition, physical changes to the land surface can affect the surface energy balance, further impacting climate (biogeophysical effects). These effects are expected to be greatest and most detrimental following conversion of forest to cropland.

### 2.3.1 Climate Impacts of Deforestation

#### 2.3.1.1 Biogeochemical Impacts of Deforestation

Biogeochemical effects from deforestation generally lead to a warming at the surface and in the atmosphere (Houghton et al., 1983) (see **Figure 2.7**). Forests and other ecosystems play an important role in the global carbon cycle as they take in carbon dioxide (CO<sub>2</sub>) from the atmosphere. Around half of this carbon is returned to the atmosphere through respiration while the remaining half is fixed as plant biomass during photosynthesis, creating a carbon sink. Recent estimates by the Global Carbon Project indicate that the global land CO<sub>2</sub> sink was  $3.1 \pm 0.6 \text{ GtC yr}^{-1}$  during the decade 2012-2021, approximately 30% of total annual anthropogenic CO<sub>2</sub> emissions (Friedlingstein et al., 2022). Following deforestation, carbon from vegetation and soils is released into the atmosphere as CO<sub>2</sub>. As atmospheric CO<sub>2</sub> concentrations increase, deforested areas have less capacity to act as a CO<sub>2</sub> sink (see Section 2.2.3.5). In addition, more longwave (LW) infrared radiation is trapped at the surface resulting in increased surface temperatures (the greenhouse effect) (Strassmann et al., 2008; Arora and Boer, 2010).

Deforested areas are also more vulnerable to outside forces, whereby rising temperatures can lead to forest fires which emit more CO<sub>2</sub>, methane (CH<sub>4</sub>), ozone (O<sub>3</sub>)-producing compounds, black carbon and organic carbon aerosols (Pielke et al., 2002; Randerson et al., 2006; Heimann

and Reichstein, 2008; Pielke et al., 2011); further trapping LW infrared radiation at the surface. Additional warming can occur from cropland production, via emissions of  $N_2O$  and  $CH_4$  (Jia et al., 2019), increased soil carbon loss (Lal, 2004), and changes in aerosol emissions such as mineral dust aerosols and biogenic volatile organic compounds (BVOCs) which influence cloud reflectivity (albedo) (Heald and Geddes, 2016; Scott et al., 2017).

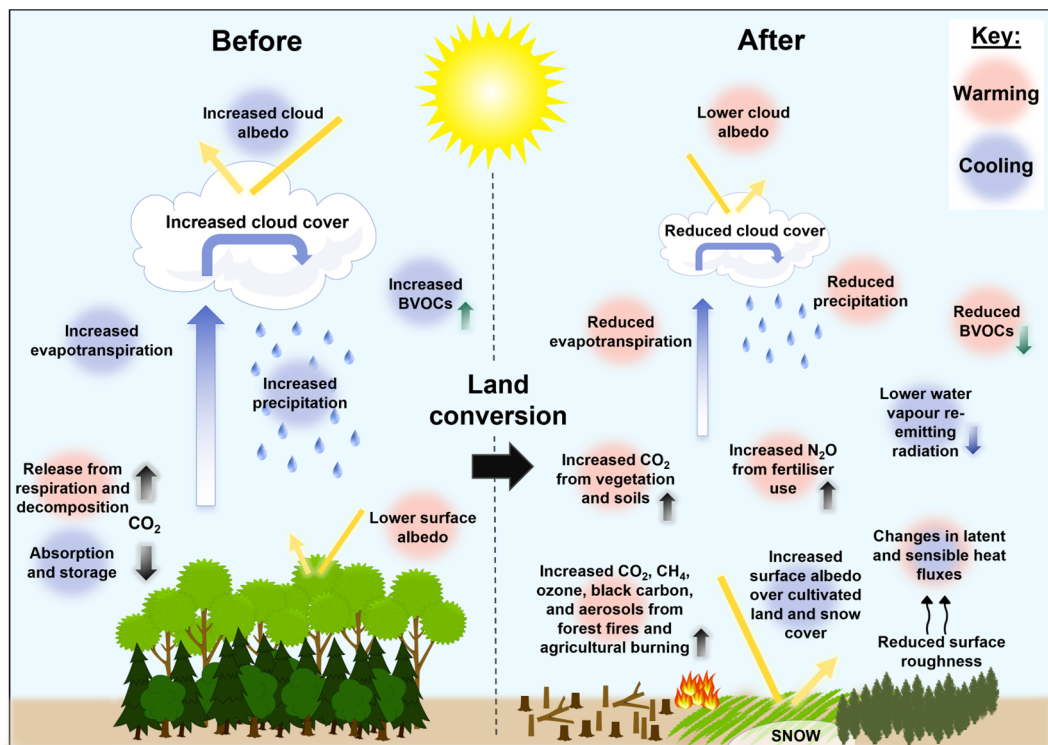


**Figure 2.7:** Biogeochemical and biogeophysical impacts of land conversion from forest to energy cropland, and their influences on climate (i.e., warming or cooling). Image icons used to create this figure have been taken from Freepnging (2022) and are licensed by Creative Commons (2022).

Out of all the GHGs,  $CO_2$  has the longest residence time in the atmosphere (see Section 1.1), and therefore has the largest positive radiative forcing. Hence, biogeochemical impacts are mainly related to fluxes of  $CO_2$  between land and atmosphere. In terms of global LUC (i.e., the conversion of forest to cropland, pasture to cropland, forest to pasture etc.), this involves changes in carbon stocks stored in different ecosystems. For instance, the carbon stored in tropical vegetation and soil is almost three times larger in forests than croplands or grasslands

(Devaraju et al., 2015). Therefore, most studies focus on the effects of changes in CO<sub>2</sub> emissions from LUC when analysing BGC impacts.

### **2.3.1.2 Biogeophysical Impacts of Deforestation**

Biogeophysical effects from deforestation can lead to either a warming or cooling (see **Figure 2.7**). Reduced surface roughness and lower canopy height from the conversion of forests (e.g., roughness length = 1m) to cropland (e.g., roughness length = 0.1–0.25m) generally results in decreases in energy transfer through turbulent fluxes (i.e., latent and sensible heat fluxes), though findings are mixed and have varying impacts on surface temperature (Bala et al., 2007; Pitman et al., 2009; Longobardi et al., 2016). Subsequent reductions in evapotranspiration lead to reduced cloud formation, and thus lower cloud albedo, allowing more incoming shortwave (SW) solar radiation to penetrate and an increased warming of the atmosphere and surface. Reductions in evapotranspiration also lower atmospheric water vapour, resulting in less LW infrared radiation being re-emitted to Earth's surface and thus a cooling effect.

Cooling also occurs in response to the higher surface albedo of cultivated land (around 0.15 to 0.26; Monteith and Unsworth (2008)) compared to forests (around 0.08 to 0.19; (Monteith and Unsworth (2008))), whereby lower amounts of SW solar radiation are absorbed by croplands. This is particularly the case at mid-to-high northern latitudes, where snow covers the ground in the winter season. The brighter snow cover on newly created open surface has a high albedo compared to the low albedo of boreal or temperate tree cover which would normally mask the snow (the snow-masking effect) (Bonan et al., 1992; Claussen et al., 2002; Bounoua et al., 2002; Matthews, 2004). In the tropics, the cooling from increased surface albedo of cropland may be offset by the warming from increased solar radiation due to reduced evapotranspiration (Shukla and Mintz, 1982; Spracklen et al., 2012).

## **2.3.2 Calculating Biogeochemical and Biogeophysical Climate Impacts**

Continuous improvements in observational data, land models and climate models have facilitated research into a range of methodologies for calculating national to global scale biogeochemical and biogeophysical climate impacts of land-use change. However, the majority of these approaches focus on biogeochemical impacts, due to challenges around measuring

biogeophysical effects, which are often neglected in climate impact assessments. Biogeophysical effects can act on top of ongoing biogeochemical climate effects, potentially exacerbating their impact, particularly at the local level. Thus, understanding these biogeophysical effects is of high importance in policy making to ensure proper planning. Evaluating and monitoring these impacts depends on which impact is being studied and at what scale. Typical methods include the use of ground-based and observational data (such as national GHG inventories, book-keeping techniques, weather station and eddy flux measurements, and remote sensing data) and models (such as the Carbon Budget Model, dynamic global vegetation models and Earth system models).

### 2.3.2.1 Ground-Based and Observational Techniques

In terms of biogeochemical impacts, country reporting of GHG inventories (GHGIs) are a requirement of the United Nations Framework Convention on Climate Change (UNFCCC), whereby fluxes are determined based on changes in carbon stocks (e.g., from forest inventories) or activity data (e.g., area of land management activity multiplied by emission factors) (Grassi et al., 2018; Jia et al., 2019). Further, the FAOSTAT has produced country level estimates of GHG emissions from agriculture (1961–2016) and land use (1990–2016), using a mixture of simple methods using default values (IPCC Tier 1) and more complex methods incorporating the carbon stock change method (IPCC Tier 3) based on country statistics of carbon stocks and forest area collected through the FAO FRA (Tubiello et al., 2013).

Bookkeeping and accounting carbon models use data on biomass density and rates of growth/decomposition from ground-based inventories (i.e., field measurements of carbon in trees and soils) to determine changes in biomass and soils that occur due to alterations in land activity. A limitation of these types of models, however, is that they do not explicitly include indirect effects of changing environmental conditions, and thus can overestimate carbon fluxes (Houghton et al., 2012; Hansis et al., 2015; Houghton and Nassikas, 2017).

Biogeophysical impacts can be determined using *in situ* observational data, such as weather station and eddy flux measurements. This high-resolution data has enabled analysis into forest biogeophysical impacts and the attribution of temperature changes to particular biogeophysical forcings (e.g., surface albedo, evapotranspiration, surface roughness), though only at the local scale (Lee et al., 2011; Luysaert et al., 2014; Broucke et al., 2015; Bright et al., 2017; Liao et al., 2018). Satellite remote sensing techniques have recently been used to extrapolate to larger

scales, creating global maps of forest cover effects on local climate (Zhang et al., 2014; Li et al., 2015; Alkama and Cescatti, 2016; Duveiller, Hooker, et al., 2018; Duveiller et al., 2020). Remote sensing data can provide high resolution estimates of biogeophysical effects that are 0.5-3 time more sensitive to forest cover change than in situ methods. However, they are limited in that they only provide local effects, rather than non-local effects (i.e., teleconnections), and thus have generally been applied to idealised forest change (Lawrence et al., 2022). Recent observation-based methodologies have been developed to calculate impacts from ongoing land use rather than focussing on climate sensitivities to idealised forest change, though these are also only at the local level (Alkama and Cescatti, 2016; Bright et al., 2017; Prevedello et al., 2019).

Satellite remote sensing data can similarly be used to calculate biogeochemical effects, though this only implicitly includes indirect and natural disturbance effects. In previous work, satellite remote sensing data methods have generally been used alongside models and land-cover change data to determine direct observational-based estimates of fluxes due to changes in forest area (Baccini et al., 2012; Tyukavina et al., 2015; Harris et al., 2015) or degradation (Baccini et al., 2017). However, the calculation of carbon fluxes from space has been stated as a notoriously difficult method (Stocker et al., 2019).

### **2.3.2.2 Modelling Techniques**

Types of models used in climate analyses include statistically-based extensions of forest inventory data, such as the Carbon Budget Model (Kurz et al., 2009), and mechanistic process-based models such as dynamic global vegetation models (DGVMs) used in global climate models (GCMs) (or Earth system models (ESMs)). For this work, which investigates global impacts of bioenergy in future land-use pathways, DGVMs and GCMs are most applicable.

#### **2.3.2.2.1 Dynamic Global Vegetation Models (DGVMs)**

Dynamic global vegetation models (DGVMs) can be used to assess biogeochemical processes dependant on the dynamics of vegetation structure and composition. Multiple DGVMs have been independently developed (e.g., LPJmL, TRIFFID) and have been applied to many global carbon cycle analyses and climate change assessments (Foley et al., 1996; Brovkin et al., 1997; Friend et al., 1997; Cox et al., 1998). DGVMs are useful tools for modelling large-scale vegetation dynamics, generally based on the assumption that competition between different



PFTs is determined by their relative competitiveness expressed in annual net primary productivity (NPP), and natural and disturbance-driven mortality (Brovkin et al., 2009). Further, they can simulate ecological processes (e.g., respiration, photosynthesis, growth, decomposition), driven by environmental conditions such as changes in CO<sub>2</sub>, climate variability, climate change, and nitrogen concentrations.

To model land carbon fluxes, DGVMs can be forced with increasing atmospheric CO<sub>2</sub> and changes in climate and are run with and without land-use changing. This process differentiates the anthropogenic effects from the indirect effects of climate and CO<sub>2</sub>, or the ‘land sink’; indirect effects are therefore explicitly included. It also accounts for the ‘lost additional sink capacity’ (LASC) after forest removal, which is the loss of possible surplus carbon uptake and storage which typically occurs in forests following increases in atmospheric CO<sub>2</sub> (CO<sub>2</sub> fertilisation) (Sitch et al., 2005; Pongratz et al., 2010; Ciais et al., 2013; Friedlingstein et al., 2022).

#### **2.3.2.2.2 Global Climate Models (GCMs)**

GCMs are increasingly used to calculate global climate impacts of land carbon fluxes, as well as biogeophysical processes (e.g., surface albedo, evapotranspiration, surface roughness). These models couple DGVMs, surface hydrology, and energy exchange modules with atmosphere, ocean, and sea ice modules, and can thus provide feedbacks between climate change, the carbon cycle, and physical changes in land characteristics. As with DGVMs, GCM experiments with and without LUC (prescribing CO<sub>2</sub> concentrations from simulations with LUC to simulations without LUC) can be used to diagnose anthropogenic effects on changes in climate. This approach was first outlined in the LUCID-CMIP5 project (MPI, 2009) and has since been used in various studies investigating historical and future land-use effects on climate (Pitman et al., 2009; Brovkin et al., 2013; Boysen et al., 2014). Examples of GCMs used for such analyses include MPI-ESM, CLIMBER-2.3, CanESM2, HadGEM2-ES, and MIROC-ESM, which all vary in complexity, and therefore speed.

Earth system models of intermediate complexity (EMICs), such as UVic ESCM 2.9 and Loveclim 1.3 have also been extensively used for land-use analyses due to their ability to carry out faster simulations, making them a useful tool for experiments with longer time scales (Claussen et al., 2002; Brovkin et al., 2006; Alexander and Easterbrook, 2015). Their outputs are, however, generally coarser than those of GCMs. While IAMs can be used to determine

GHG emissions, with some including simplified DGVMs, it is common practice to instead utilise land-use outputs from IAMs as inputs into GCMs/EMICs to determine more accurate estimates of LUC emissions and corresponding climate impacts (Brovkin et al., 2015; Jia et al., 2019).

While GCM and DGVM models are useful tools for understanding global teleconnection impacts, their model resolutions are currently too coarse to guide local policy decisions. More specifically, what is considered a ‘local’ change is still at the scale of an entire climate model grid cell (typically  $\geq 10000 \text{ km}^2$ ) (Duveiller et al., 2020). Remote sensing data of much finer resolution ( $\leq 5 \text{ km}^2$ ) have recently revealed discrepancies amongst models calculating local biogeophysical effects (Duveiller, Forzieri, et al., 2018). They are therefore valuable in this instance and should be used alongside modelling techniques. Other uncertainties in modelling arise with the partitioning of energy between latent or sensible heat (De Noblet-Ducoudré et al., 2012), and model representations of land cover changes, which can vary in sign, magnitude, and geographical distribution (as already shown in Section 2.2.3.3 for integrated assessment models) (Devaraju et al., 2015; Lawrence and Vandecar, 2015; Garcia et al., 2016; Laguë and Swann, 2016; Quesada et al., 2017; Boysen et al., 2020). Even so, the ability to determine indirect effects and feedbacks makes modelling a valuable approach for providing an overall view of land-use impacts on climate across the globe and is therefore utilised in this work.

### 2.3.2.3 TCRE Methodology

As discussed, climate models (i.e., GCMs and EMICs) are required to calculate the global climate effects of anthropogenic land-use  $\text{CO}_2$  emissions (or ‘LUC emissions’ from now onwards). Additionally, sensitivity studies have demonstrated that the transient climate response to cumulative carbon emissions (or TCRE) is a linear trajectory over the 21<sup>st</sup> century, and can thus be used as a tool for identifying global biogeochemical climate impacts of LUC emissions previously estimated from the mentioned model- and observation-based methods (Matthews et al., 2009; Gillett et al., 2013; Collins et al., 2013). In other words, the slope of the linear relationship (the TCRE value) between global cumulative  $\text{CO}_2$  emissions and mean surface temperature occurring in a scenario can be multiplied by calculated cumulative changes in LUC emissions ( $\Delta \text{LCO}_2$ ), to estimate corresponding changes in global temperature ( $\Delta T$ ) (see **Equation (2.1)**).

$$\Delta T = \Delta \text{LCO}_2 \times \text{TCRE} \quad (2.1)$$

Simmons and Matthews (2016) further demonstrate the possibility of using a linear scaling factor (like the TCRE) to calculate biogeophysical climate impacts, due to the strong linear relationship between biogeophysical effects and LUC emissions, though this has not yet been applied in the literature. While the TCRE method is not the main approach used in this thesis, its application in multiple other studies (whose values will be discussed) makes it worth noting.

### 2.3.3 Global and Regional Climate Impacts of Deforestation

Biogeochemical effects from deforestation at any location (tropical, temperate, or boreal) can lead to global climate change, largely because emitted CO<sub>2</sub> has a long residence time and becomes well mixed in the atmosphere. Climate models have indicated that, globally, deforestation leads to a biogeochemical warming effect. For instance, recent findings in a multi-model CMIP6 assessment by Boysen et al. (2020) show that large-scale deforestation over a 50-year period results in carbon losses of 259±80 PgC and a global warming response to these emissions of 0.46±0.22 °C. This biogeochemical warming is also seen at the regional level in numerous studies, whereby forest loss in the tropics typically causes higher global mean warming levels (ranging between 0.19 °C and 1.06 °C) compared to temperate and boreal regions (0.10 °C to 0.40 °C) (Claussen et al., 2001; Bala et al., 2007; Devaraju et al., 2015; Jia et al., 2019).

In contrast, biogeophysical effects are much more localised to where land has been modified, though over time have significant impacts on overall global surface temperatures. Boysen et al. (2020) illustrate this, calculating a global mean biogeophysical cooling of (-)0.22 ±0.21 °C. Regionally, however, over half of the models in their study simulate an overall surface temperature increase across deforested land in the tropics and a cooling over deforested boreal land. This corroborates previous model- and observation-based estimates, which show that deforestation in the tropics leads to a regional biogeophysical warming exacerbating the biogeochemical warming associated with released CO<sub>2</sub> emissions, due to a reduction in evapotranspiration from reduced leaf area and shallower root systems (Li et al., 2015; Alkama and Cescatti, 2016; Schultz et al., 2017; Prevedello et al., 2019). Across seven studies, this warming is between (+)0.13 and (+)1.2 °C (e.g., Claussen et al. (2001); Ganopolski et al. (2001); Snyder et al. (2004)). Longobardi et al. (2016), however, calculate a regional biogeophysical cooling of (-)0.19 °C from tropical deforestation, which they attribute to drier climates (negative precipitation minus evaporation) and higher soil temperatures. There is less agreement among global impacts, with modelled estimates ranging from a biogeophysical

cooling of  $(-)$ 0.57 °C (Jones et al., 2013) to a biogeophysical warming of  $(+)$ 0.23 °C (Lawrence et al., 2018) due to variations in compensating effects.

At higher latitudes, biogeophysical cooling due to deforestation becomes more prevalent regionally and globally. In boreal regions, this cooling is significantly higher than the biogeochemical warming, reaching up to  $(-)$ 1.8 ± 1.2 °C (Bathiany et al., 2010; Devaraju et al., 2015; Longobardi et al., 2016; Jia et al., 2019). In addition, seasonal impacts show that deforestation in temperate and boreal regions results in summer warming and winter cooling (Bright et al., 2017; Ahlswede and Thomas, 2017; Strandberg and Kjellström, 2019). Summer warming occurs from decreases in turbulent fluxes and evapotranspiration, whereas winter cooling is driven by increased albedo, amplified by the snow-albedo feedback. Some models suggest that cooling is further amplified by high latitude changes in sea-ice and snow extent (polar amplification) when large-scale deforestation occurs (Boysen et al., 2020).

Almost all modelled studies on biogeophysical processes resulting from global deforestation focus on the total contribution of all biogeophysical effects to climate changes. Davin and de Noblet-Ducoudre (2010) however separate these effects, simulating a cooling of 1.36 °C due to increased albedo when forest is converted to grass, with stronger cooling occurring at higher latitudes. Reductions in evapotranspiration and roughness length in their study result in a small global warming of 0.24 °C and 0.29 °C, respectively.

### **2.3.4 Climate Impacts of Historical Land-Use Changes**

Informing local to global level policy requires understanding biogeochemical and biogeophysical impacts not only in terms of forest loss but also considering ongoing changes to the land system as a whole. Calculating climate impacts of historical land-use changes can provide a basis for assessing future impacts.

There are no direct observations of how historical land-use changes have affected atmospheric dynamics and physics at the global and regional scales. Therefore, studies surrounding historical impacts of LUC on climate focus on climate modelling experiments or estimates using TCRE values combined with observations and DGVM outputs. Recent findings from a range of DGVMs, GCMs and bookkeeping models in the Global Carbon Project indicate that land-use activities have released as high as  $870 \pm 278$  GtCO<sub>2</sub> into the atmosphere since the beginning of the pre-industrial era (between 1750–2020); accounting for roughly one third of

total anthropogenic CO<sub>2</sub> emitted throughout this period ( $2,553 \pm 296$  GtCO<sub>2</sub>) (Friedlingstein et al., 2022). Also shown is that LUC emissions were the dominant anthropogenic emissions until the mid-1900s, when fossil fuel emissions became dominant.

A wide range of estimates have been found for climate responses to biogeochemical effects, though all indicate a global net warming over the historical period. Modelled and observed findings are of similar magnitudes, with a warming of approximately 0.1–0.53 °C calculated between 1850 and 2014 (see **Figure 2.8**). Biogeophysical estimates from GCMs (global climate models) are more varied ranging from a cooling of (–)0.57 °C to a warming of (+)0.06 °C, which is attributed mainly to changes in surface albedo. Many studies have investigated the counteracting impact of these effects on surface temperatures. Simmons and Matthews (2016), for instance, show that a global biogeophysical cooling of (–)0.24 °C is dampened by a biogeochemical warming of (+)0.22 °C, resulting in a net cooling of (–)0.02 °C. Across other studies, this dampening leads to an overall net global warming (0.11 °C in Zhang et al. (2013) and 0.16 °C in Matthews et al. (2004)).

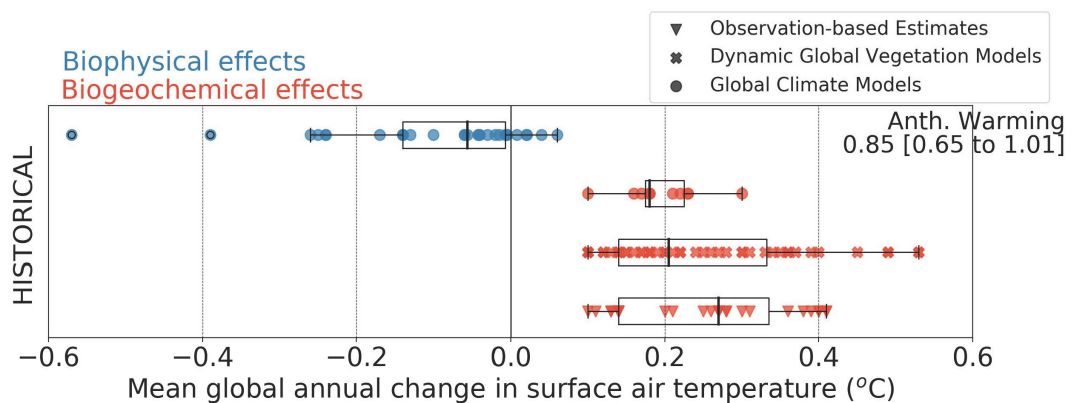


**Figure 2.8:** Changes in mean global annual surface air temperature (°C) in response to historical anthropogenic land-use changes, estimated in a range of studies using observations, DGVMs and GCMs; reproduced from Jia et al. (2019). Values are for certain years in the period 1990–2014 relative to years in 1700–1920.

Variation in findings, particularly between modelled and observed biogeochemical effects, has been discussed in depth in previous literature (Houghton et al., 2012; Gasser and Ciais, 2013; Smith et al., 2014; Pongratz et al., 2014; Hansis et al., 2015). These discrepancies can be explained by differences in methodological parameters, such as the spatial distributions of land-use change, definitions of land-use types (Tubiello et al., 2013; Tyukavina et al., 2015),

climate-carbon cycle interactions in climate models (Houghton et al., 2012), estimates of biomass and soil carbon density, and methods for tracking emissions through time (Jia et al., 2019). In addition, land-use processes such as wood harvest, peatland drainage and fires can a considerable influence on findings (Pugh et al., 2015; Jia et al., 2019; Friedlingstein et al., 2022; Nabuurs et al., 2022). Further, in comparison to observations, model-based estimates are limited in that they mostly only calculate direct impacts of LUC, excluding indirect effects (Jia et al., 2019; Nabuurs et al., 2022). On the other hand, complexities in incorporating direct, indirect and natural effects have led to wide overestimations in observed findings (Nabuurs et al., 2022).

### **2.3.5 Lessons from First-Generation Bioenergy Expansion**

As previously discussed, most mitigation scenarios rely upon second-generation bioenergy, along with afforestation and reforestation, to remove CO<sub>2</sub> from the atmosphere. However, only in recent years has the concept of large-scale second-generation bioenergy become a potentially viable option. Prior to this, spatial data production has generally been targeted towards present day first-generation bioenergy production, with the development of projected second-generation energy cropland distributions in SSP-RCP scenarios rapidly increasing (Popp et al., 2017; Rogelj, Shindell, et al., 2018). While there are significant research efforts to advance biofuel production in developed countries (mainly in the U.S and the EU), with the exception of Brazil and China, second-generation biofuel production is relatively non-existent elsewhere (Gasparatos et al., 2013). Understanding how LUC for first-generation bioenergy production currently affects climate (and other environmental and socio-economic systems) can provide important lessons with regards to transitioning to more advanced feedstock.

The topic of first-generation biofuels – and bioenergy as a whole – in providing climate change mitigation benefits is a highly controversial topic within the biofuel debate. Life cycle emission assessments have indicated a wide range of conclusions, due to the extensive variety of methodologies used. One major factor is that many of these studies fail to include emissions from land-use change, instead only accounting for the carbon benefits of using land for biofuels (e.g., carbon sequestration in energy crops). Studies that do account for these extra emissions tend to find negative results (Fargione et al., 2008; Searchinger et al., 2008; Johnston et al., 2008; Stratton et al., 2010; Lapola et al., 2010; Achten and Verchot, 2011; Gasparatos et al., 2013; Elshout et al., 2015; Daioglou, 2016). For example, Bailis and Baka (2010) show that when LUC effects are excluded, jatropha biodiesel in Brazil emits 55% less emissions than

conventional diesel. On the other hand, when included, jatropha biodiesel produces 59% more emissions than conventional diesel. Fargione et al. (2008) similarly project that the conversion of natural vegetation for first-generation bioenergy production could release 17–420 times more CO<sub>2</sub> than the annual greenhouse gas reductions biofuels provide by displacing fossil fuels.

Many studies that do incorporate LUC effects also indicate the loss of carbon from soils into the atmosphere, creating carbon debts that could take several decades to repay. These studies tend to use a metric of “ecosystem carbon payback time” (ECPT) to determine how long it takes for bioenergy carbon savings from avoided fossil fuel combustion to offset LUC emissions resulting from the conversion of different ecosystems for bioenergy production. Findings for ECPT vary widely, depending on the type of feedstock, its location and the original land use or ecosystem being replaced. Across the literature, ECPTs for the conversion of forest or woodland to first generation bioenergy feedstock have been estimated as 18 to 93 years for palm oil biodiesel, 179 to 481 years for soybean biodiesel, 15 to 39 years for sugarcane ethanol, 16 to 52 years for corn ethanol, and 10 to 966 for jatropha (Gasparatos et al., 2013; Elshout et al., 2015). Similarly large ECPTs have been found for the conversion of other carbon-rich (and nitrogen-rich) ecosystems such as peatlands and mangroves. For replacing tropical peatlands, ECPT is estimated to be 75–700 years for oil palm plantations, 750 years for sugarcane plantations and 12,000 years for soybean plantations (Johnston et al., 2008; Danielsen et al., 2009).

Indirect LUC effects are expected to result in even greater carbon emissions and debts, although there are large uncertainties in estimates (Upham et al., 2009; Lapola et al., 2010; Achten and Verchot, 2011; Taheripour and Tyner, 2013; Rajagopal and Plevin, 2013; Kim et al., 2014; Plevin et al., 2015; Valin et al., 2015; Ahlgren and Di Lucia, 2016; Zilberman, 2017). Searchinger et al (2008), for instance, display the indirect land-use effects of increasing US corn ethanol production over 30 years. They show that, instead of producing a 20% savings in emissions, corn expansion nearly doubles GHG emissions per fuel mile compared to conventional gasoline, largely due to conversion of land elsewhere in the world to maintain demands. Findings also indicate that, in the event that excess croplands in the US or Europe become available due to dramatic yield improvements or the release of agricultural reserve lands, avoiding LUC emissions would still not be possible. This is because the use of these excess lands, which could otherwise be used for forest or grassland regrowth, would sacrifice this potential carbon benefit and possibly exceed the carbon saved by using this land for biofuel production (FAO, 2006; COM, 2006).

In contrast, some studies have found more positive results for first-generation biofuels, such as previous successes of the Soy Moratorium policy in Brazil between 2004 and 2012 (Gibbs et al., 2015; Leal et al., 2017; Heilmayr et al., 2020) (see Section 2.5.1.1 for more information), and model predictions of high GHG savings due to low future deforestation from sugarcane expansion in southeast Brazil (Nassar et al., 2009). Regarding the latter, such low anticipated carbon debts and high CO<sub>2</sub> savings (consistently over 50%) meant that in 2010 the U.S Environmental Protection Agency (EPA) designated Brazilian bio-ethanol an “advanced biofuel” (EPA, 2010), largely due to the reductions in emissions from using ethanol blends over conventional gasoline. Millet et al. (2012), for instance, calculate that E85 ethanol blends could reduce NO<sub>x</sub> emissions by 14% and CO emissions by 13%, and E10 blends by 7.5% (NO<sub>x</sub>) and 6.7% (CO). There is evidence to show that the development of first-generation biofuels, such as sugarcane bioethanol, has likely driven vehicle fleet modernisation, resulting in overall lower air pollution within the transport sector (Gasparatos et al., 2012). Though life cycle assessments of pollutants from biofuel production continue to produce higher values than those of conventional transport fuel, largely due to the agricultural sector (Hewitt et al., 2009; Tsao et al., 2012; Obidzinski et al., 2012).

Temperature responses further highlight the potential implications of land use for first-generation bioenergy production, particularly at the regional and local level (Sampaio et al., 2007; Loarie et al., 2011; Georgescu et al., 2011; K. Ashworth et al., 2012; Caiazzo et al., 2014; Tölle et al., 2014; Brando et al., 2016; Wang et al., 2017; Duden et al., 2021). For example, Loarie et al. (2011) investigate the biogeophysical climate impacts of sugarcane expansion in the Brazilian Cerrado during the 2000s, calculating both a cooling (~0.93 °C) and a warming (~1.55 °C), depending on whether existing land being converted is cropland or forest, respectively. By 2030, 29% of the Centre West Cerrado is projected to experience agricultural drought because of sugarcane expansion (Duden et al., 2021). Warming effects of 0.3–2.4 °C have also been calculated from Amazonian deforestation for soy agriculture (Sampaio et al., 2007; Brando et al., 2016). Sampaio et al. (2007) further indicate that this conversion leads to significant reductions in precipitation (4.6–25.8%), evapotranspiration (5.6–31.2%), relative humidity (3.4–17.5%), net surface radiation (2.8–7%), and cloud cover (2.1–16.2%), as well as large increases in sensible heat flux (4.9–53.7%) and outgoing longwave radiation (0.3–4.9%).

Albedo-induced climate impacts from LUC can be of comparable magnitude to biogeochemical impacts (Simmons and Matthews, 2016). Caiazzo et al. (2014) illustrate this



by comparing changes in surface albedo to estimates of life cycle GHG emissions for soy, oil palm and rapeseed cropland expansion, suggesting that surface albedo can dominate overall climate impacts from these biofuels. Hence, for a complete assessment of aggregate climate impacts of biofuel production, it is necessary to include albedo effects. Further, oil palm expansion in the tropics could increase isoprene emissions, though the effects on global climate may be negligible (K. Ashworth et al., 2012).

It is evident that the expansion of first-generation bioenergy could have significant implications for land and climate. Previous literature has highlighted the importance of using alternative biofuel methods, with a particular emphasis on strategies that avoid LUC altogether, such as the use of waste products (e.g., municipal waste, crop waste, and fall grass harvests from reserve lands) (Perlack et al., 2005). One of the main issues is that emissions from LUC are likely to occur indirectly, therefore proposed environmental criteria focussing on direct LUC would have little effect (COM, 2006). Second-generation bioenergy is a potential solution to this, with a variety of studies calculating lower indirect LUC emissions than for first-generation biofuels (Chum et al., 2011; Wicke et al., 2012; Valin et al., 2015; Ahlgren and Di Lucia, 2016). In theory, the production of second-generation energy cropland on carbon-poor lands could prevent increases in emissions from LUC. Though, in practice, this remains unknown.

### **2.3.6 Climate Impacts of Second-Generation Bioenergy Within Future Pathways**

As previously mentioned, a major benefit of second-generation bioenergy cropland (“energy cropland” from here on) is its capacity to grow on pastures and marginal lands. Cultivation of energy crops, such as short rotation woody crops and perennial grasses, on marginal land typically accumulates carbon in soils due to their deep root systems (Don et al., 2012; Robertson et al., 2017). However, the extent to which marginal land is utilised for energy cropland varies widely across future pathways, resulting in different projections of potential climate impacts.

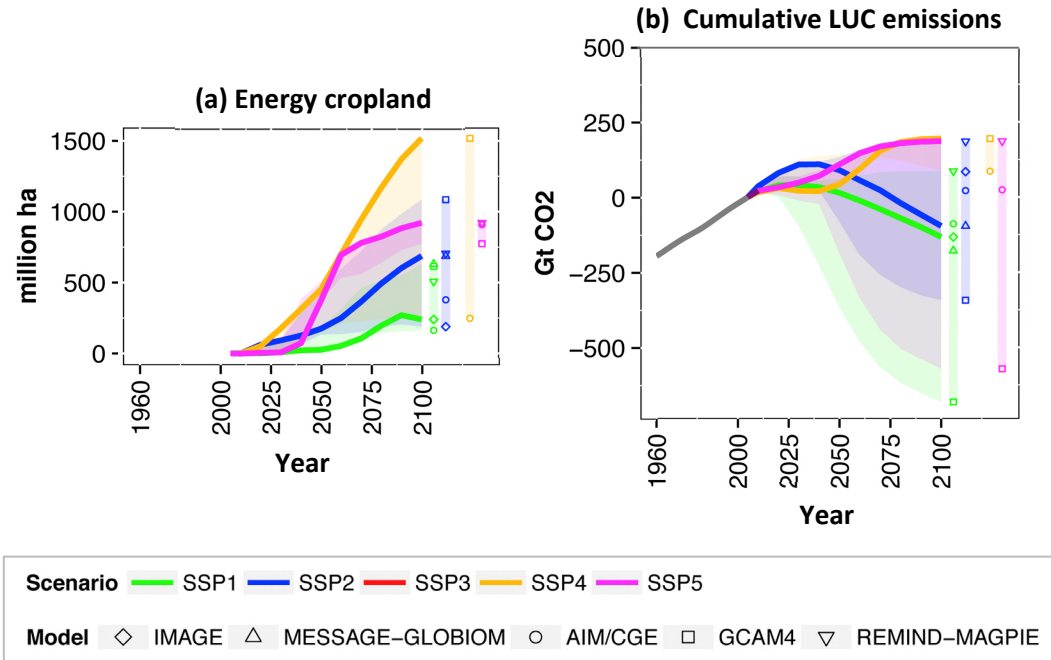


**Figure 2.9:** Changes in energy cropland area (a) and cumulative LUC emissions (b) in SSP scenarios following RCP2.6, calculated from five different integrated assessment models; reproduced from Popp et al. (2017). Coloured lines indicate marker model results for each SSP, shaded areas indicate range of data across the timeline, and the grey line in Figure (b) represents historical trends.

Numerous land-use pathways incorporating second-generation bioenergy expansion have been determined by different integrated assessment models (IAMs) (Popp et al., 2017; IIASA, 2018b). Depending on the model and pathway (SSP and RCP) used, LUC in scenarios has shown to result in both positive and negative cumulative CO<sub>2</sub> emissions to the atmosphere by 2100. In RCP2.6, positive emissions are mainly attributed to large-scale expansion of second-generation energy cropland onto natural vegetation as a result of high bioenergy demands (78–477 EJyr<sup>-1</sup> in 2100 across the SSPs) (IIASA, 2018b) (see **Figure 2.9**). Findings from IAMs show that cumulative LUC emissions in the RCP2.6 pathway could increase to up to around 207 GtCO<sub>2</sub> by 2100 following pathways SSP2 (REMIND-MAGPIE), SSP4 (GCAM), and SSP5 (REMIND-MAGPIE) (Popp et al., 2017). In addition to extensive energy cropland expansion, this is also the result of several factors i.e., medium regulation of land-use change, slow declines in the rates of deforestation (or high deforestation rates in SSP4), and low afforestation and reforestation (Popp et al., 2017). In contrast, negative emissions of up to –

680 GtCO<sub>2</sub> have been calculated following SSP1 (e.g., using the GCAM4 model), largely due to low energy cropland and food/feed cropland expansion, strong land-use regulation, high afforestation, and reforestation, as well as high improvements in agricultural productivity.

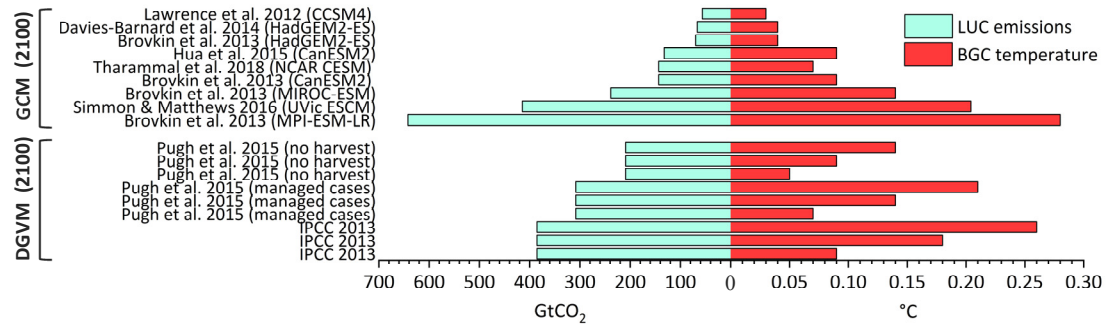


**Figure 2.10:** LUC emissions and corresponding biogeochemical effects on temperature, calculated for RCP2.6 scenarios in a range of studies using GCMs and DGVMs. Values are for the period 2099-2100 relative to 2000-2006.

So far, calculation of biogeochemical temperature responses to LUC emissions has mostly been carried out for the RCP scenarios alone (RCP 2.6, 4.5 and 8.5) without SSP analysis. In the case of RCP2.6, all GCM and DGVM models show that land acts as a carbon source to the atmosphere, resulting in a global mean biogeochemical warming response. Findings from nine GCM model experiments indicate that LUC (mostly due to second-generation bioenergy expansion) in RCP2.6 leads to a global net flux of between 57 and 648 GtCO<sub>2</sub> emissions, and biogeochemical warming of 0.03 to 0.28 °C by 2100 (Lawrence et al., 2012; Brovkin et al., 2013; Davies-Barnard et al., 2014; Hua et al., 2015; Simmons and Matthews, 2016; Tharammal et al., 2018) (see **Figure 2.10**). In addition, estimates from two DGVM models and subsequent TCRC calculations produce LUC emissions of 211 to 389 GtCO<sub>2</sub> and a biogeochemical warming response of 0.05 to 0.26 °C by 2100 (IPCC, 2013; Pugh et al., 2015). These findings suggest that LUC in RCP2.6 could potentially result in significantly higher CO<sub>2</sub> emissions compared to initial estimates from IAMs in **Figure 2.9** (up to 207 GtCO<sub>2</sub> by 2100), with values comparable to IAM predictions for RCP4.5 and baseline pathways (see Figure 6 in Popp et al. (2017)). They are also of similar magnitude to historical estimates (148 to 995 GtCO<sub>2</sub> in 1750–2014; Jia et al (2019)) and are significant compared to the overall projected mean warming for this scenario (1 °C by 2100, ranging from 0.3 °C–1.7 °C since 1986–2005).

Disparities between findings could be due to a variety of factors, outlined previously in Section 2.3.4 and Section 2.2.3.3. Brovkin et al. (2013) further suggest that the upper limit from GCM estimates is the result of an over-estimation of initial carbon stocks in the tropics and dry lands in the MPI-ESM model they use. They also state that higher terrestrial carbon losses for the MPI-ESM and MIROC-ESM models are due to the use of transition land-use matrices in these models (Hurtt et al., 2011). A transition matrix implements rotational LUC instead of only net changes, which lead to different outcomes for the carbon cycle than for the vegetation cover. Hence, the clearing and regrowth of forest results in additional CO<sub>2</sub> emissions due to transitional changes in carbon pools, although net forest cover in the grid cell remains unchanged.

GCM and DGVM estimates for RCP2.6 are generally lower than those for RCP8.5. Hence, most of the literature focuses on RCP8.5, with regards to how potential LUC will affect the highest levels of global warming (see **Figure 2.11**). Although second-generation bioenergy deployment is higher in RCP2.6, large-scale deforestation and wood harvest in RCP8.5 results in cumulative LUC emissions of 74 to 947 GtCO<sub>2</sub> across GCM models, and 559 to 633 GtCO<sub>2</sub> in DGVM models (Jia et al., 2019). Subsequently biogeochemical warming ranges from 0.04 to 0.49 °C.

Findings for RCP4.5 are more mixed, representing similar values to those calculated by IAMs (see Figure 6 in Popp et al. (2017)). Some estimates show that land, overall, acts as a sink for carbon, likely due to lower second-generation bioenergy expansion (than RCP2.6), and increased afforestation and CO<sub>2</sub> fertilisation (Tharammal et al., 2018). In these findings, carbon is stored in the land for a long period, thereby removing CO<sub>2</sub> from the atmosphere and producing negative emissions. For instance, Tharammal et al. (2018) and Davies-Barnard et al. (2014) use GCM models to calculate net CO<sub>2</sub> fluxes of –107 and –148 GtCO<sub>2</sub> between 2005 and 2100, respectively. Pugh et al. (2015) similarly calculate a removal of –67 GtCO<sub>2</sub> using a DGVM model. Positive net fluxes in RCP4.5 are, however, found across five of the studies, ranging between +59 GtCO<sub>2</sub> (Pugh et al., 2015) and +548 GtCO<sub>2</sub> (Lawrence et al., 2012) by 2100. Like the RCP4.5 scenario, more analysis of biogeochemical effects in RCP2.6 could potentially show both positive and negative global carbon fluxes, as illustrated in original IAM estimates (**Figure 2.9**). This could produce wider insight into the impacts of bioenergy expansion over the 21st century.

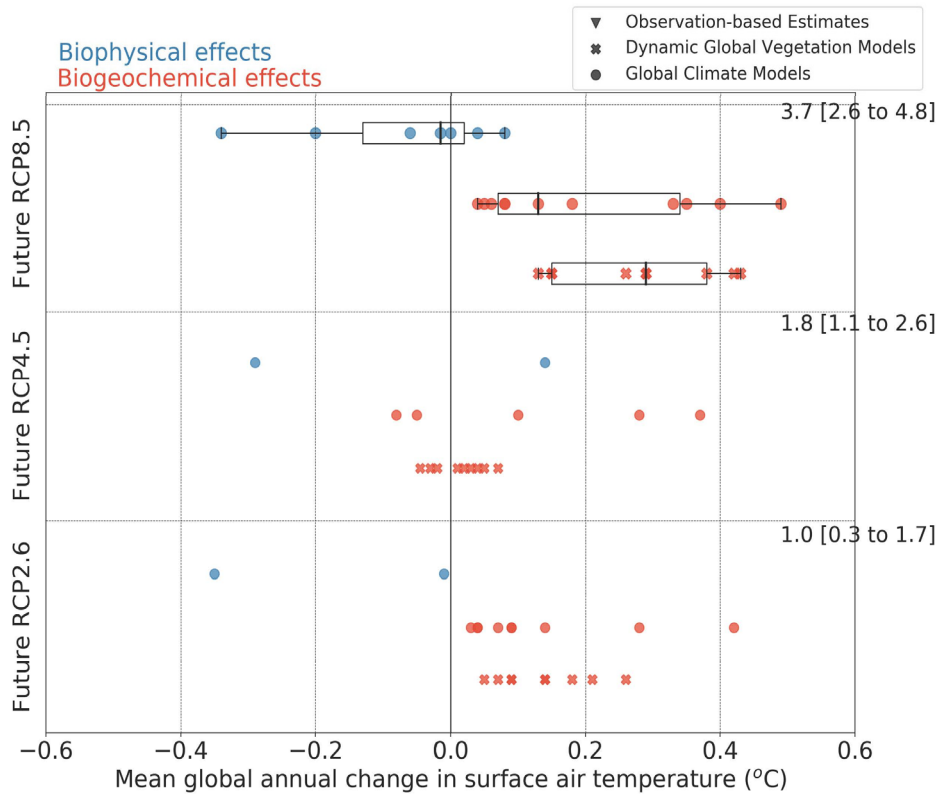


**Figure 2.11:** Changes in mean global annual surface air temperature ( $^{\circ}\text{C}$ ) in response to future anthropogenic land-use changes, estimated in a range of studies using DGVMs and GCMs; reproduced from Jia et al. (2019). Values are for the period 2099-2100 relative to 2000-2006.

Fewer studies have been carried out for future biogeophysical climate responses to LUC, particularly in the cases of the RCP2.6 and RCP4.5 scenarios, for which only two previous findings have been calculated (Jia et al., 2019). Most future estimates show a biogeophysical cooling, with values reaching  $(-)$ 0.015  $^{\circ}\text{C}$  to  $(-)$ 0.34  $^{\circ}\text{C}$  in the RCP8.5,  $(-)$ 0.29  $^{\circ}\text{C}$  in RCP4.5 and  $(-)$ 0.01  $^{\circ}\text{C}$  to  $(-)$ 0.35  $^{\circ}\text{C}$  in RCP2.6 (see **Figure 2.11**). Some findings, however, indicate biogeophysical warming (of 0.04–0.09  $^{\circ}\text{C}$  in the RCP8.5 and 0.14 in RCP4.5). These studies have attributed this warming to reductions in evapotranspiration in the tropics due to land conversion (for second-generation bioenergy and food/feed cropland) and therefore more SW radiation reaching the surface. All but one (Brovkin et al., 2013) of the future studies calculating global net impacts of both biogeophysical and biogeochemical responses estimate an overall warming effect. In these findings, warming ranges from 0.01 to 0.27  $^{\circ}\text{C}$  for RCP8.5, 0.06 to 0.08  $^{\circ}\text{C}$  for RCP4.5, and 0.03 to 0.07  $^{\circ}\text{C}$  for RCP2.6.

## 2.3.7 Isolated Impacts of Bioenergy Expansion in Future

### Mitigation Pathways

As shown in Section 2.3.6, analysis of future pathways can be used to roughly identify the potential impacts of LUC for second-generation bioenergy expansion. However, these findings also include impacts of other land-use practices, such as food/feed cropland and afforestation. Few studies attempt to isolate the effects of bioenergy expansion within these scenarios, largely due to the lack of global spatial data for projected second-generation energy cropland distributions. Hence, most literature calculating these impacts focus on a specific region or country. Examples include analyses in the US (VanLoocke et al., 2010; Georgescu et al., 2011; Anderson et al., 2013; Caiazzo et al., 2014; Harding et al., 2016), Germany (Tölle et al., 2014), Malaysia (Caiazzo et al., 2014) and Mexico (Caiazzo et al., 2014).

#### 2.3.7.1 Regional Impacts

Avoiding deforestation, most regional analyses evaluate the impacts of converting arable land or land that is currently used for agriculture (e.g., corn or soybean) to second-generation perennial crops (such as miscanthus, poplar, or switchgrass). Results have shown that this type of conversion generally leads to a local and regional biogeophysical cooling, due to increases in albedo and evapotranspiration. A study by Georgescu et al. (2011) indicates that this cooling is enough to partially offset local warming from GHGs in the short term. In their work, significant reductions in radiative forcing from increases in albedo alone are 6 times larger than annual biogeochemical effects arising from offsetting fossil fuel use. Caiazzo et al. (2014) further show that the regional cooling albedo impact of switchgrass cultivation is around 5–13 times greater than the biogeochemical life cycle effects of converting the existing first generation and marginal land. However, they also discuss the negative implications of warming from reduced albedo as a result of converting desert land in Mexico to *Salicornia* plantations for biofuel. Searchinger et al. (2008) further indicate that when converting corn fields to switchgrass for ethanol production in America, the emissions from land-use change would take approximately 52 years to pay back.

Rapid conversions of land to second-generation energy cropland can lead to considerable implications for the reservoir of stored soil water, whereby depletion of soil moisture in the summer could potentially reduce crop productivity (VanLoocke et al., 2010; Georgescu et al.,

2011; Anderson et al., 2013). Changes to the water cycle can also result in slightly higher relative humidity in spring and slightly lower relative humidity in summer, as well as increased precipitation (Anderson et al., 2013; Tölle et al., 2014; Harding et al., 2016). Overall, studies are in agreement that cultivation of energy cropland will likely have significant local effects, including both positive and negative impacts. On a regional scale, however, findings are more diverse, with results illustrating both substantial (e.g., Anderson et al. (2013)) and less substantial (e.g., Caiazzo et al. (2014)) impacts. All findings, however, demonstrate the importance of incorporating biogeophysical impacts into future analyses.

### 2.3.7.2 Global Impacts

Only a handful of studies have evaluated global climate impacts of LUC for second-generation bioenergy production. Between 2009 and 2013, scientists from the MIT Joint Program on the Science and Policy of Global Change were the first to publish such findings (Melillo, Reilly, et al., 2009; Melillo, Gurgel, et al., 2009; Kicklighter et al., 2012; Hallgren et al., 2012; Hallgren et al., 2013). Melillo, Gurgel, et al. (2009) and Melillo, Reilly, et al. (2009) initiated this research by investigating the GHG implications of global LUC for bioenergy expansion. Using an economic model coupled with a terrestrial biogeochemistry model, they create two land-use scenarios: Case (1) a “deforestation scenario”; whereby large-scale deforestation occurs directly or indirectly to meet second-generation bioenergy demands (141 EJ yr<sup>-1</sup> by 2050), and Case (2) an “intensification scenario”; in which existing managed lands are used more intensively for bioenergy production (128 EJ yr<sup>-1</sup> by 2050) to reduce deforestation. Together, their findings demonstrate a dramatic difference in carbon balances between the two scenarios. In Case (1), direct and indirect effects of LUC for energy cropland expansion results in cumulative CO<sub>2</sub> emissions of 92 GtCO<sub>2</sub> by 2100 (since 2020), with the maximum LUC emissions (164 GtCO<sub>2</sub>) occurring in 2050–2055. In Case (2), negative emissions (i.e., net land carbon accumulation) of (–)75 GtCO<sub>2</sub> occurs by 2100, as a result of enhanced carbon sequestration in soils due to nitrogen fertilisers (Melillo, Reilly, et al., 2009).

By integrating climate and biogeophysical components into the economic-biogeochemical modelling framework already mentioned, Hallgren et al. (2013) (further detailed in the work of Hallgren et al. (2012)) have determined spatial climatic effects of LUC resulting from bioenergy expansion in Cases (1) and (2). Their study projects that, even in the deforestation scenario (Case (1)), second-generation bioenergy expansion is expected to have a negligible impact on Earth’s global surface air temperature (–0.01 °C). This is, however, due to the

compensation of significant biogeochemical warming (0.11 °C) impacts with significant biogeophysical cooling impacts (0.12 °C) at both regional and global levels. They also demonstrate that incorporation of forest protection in the intensification scenario (Case (2)) reduces individual biogeochemical and biogeophysical impacts globally (to (+)0.04 °C and (–)0.10 °C respectively), however, combined this leads to more cooling ((–)0.06 °C).

Since the release of the IPCC Special Report on Global Warming of 1.5 °C (SR15), negative emission technologies like BECCS have become subject to greater scrutiny, particularly with regards to their availability, and thus contribution, in reaching the 1.5 °C goal within ambitious RCP and SSP scenarios (Vaughan and Gough, 2016). Recent studies have utilised similar scenarios to Case (1) and (2) (i.e., a deforestation scenario and intensification scenario) to determine potential impacts of BECCS within 1.5–2 °C pathways on the land and climate systems. Harper et al. (2018), for instance, determine the impacts of additional LUC from global BECCS expansion when transitioning from a 2 °C to a 1.5 °C world in scenarios created by the IMAGE IAM. Their findings show that carbon lost to the atmosphere from land is twice as strong in the 1.5 °C scenario compared to the 2 °C scenario, largely offsetting the additional carbon removed from the atmosphere through BECCS from changing to the more ambitious scenario. This is due to both the CO<sub>2</sub> fertilisation effect being larger, and the growth of more high latitude vegetation in the 2 °C scenario. They also find that ecosystem carbon payback time (ECPT; discussed in Section 2.3.5) can be around 10–100+ years in the tropics, where energy cropland replaces both agriculture and carbon-rich land. Whereas at higher latitudes, ECPTs (payback times) can be more than 100 years due to significant losses of soil carbon.

Muri (2018) further calculate, for the RCP2.6 pathway, a warming of 0.29 °C above the 1.5 °C goal (i.e., 1.79 °C), and show that the incorporation of a BECCS intensification scenario reduces this value to 0.17 °C, whereas a BECCS deforestation scenario increases it to 0.43 °C above 1.5 °C. Using an Earth system model, they show that LUC in these scenarios results in a cooling of (–)0.1 °C and a warming of 0.17 °C by 2100, respectively; largely due to changes in CO<sub>2</sub> flux from LUC (–144 GtCO<sub>2</sub> and 481 GtCO<sub>2</sub>, respectively). Humpenöder et al. (2018a) similarly estimate large CO<sub>2</sub> fluxes from pathways following RCP2.6 (SSP2), calculating that the incorporation of a forest conservation policy reduces LUC emissions to ~145 GtCO<sub>2</sub> between 2010 and 2100, compared to a scenario where deforestation is unrestricted (~350 GtCO<sub>2</sub>) (values are approximated from their Figure 2). The isolated impacts of bioenergy within these findings are, overall, larger than those found by Melillo, Reilly, et al. (2009) mentioned earlier in this section, equating to around 85 GtCO<sub>2</sub> for the forest conservation



scenario and 293 GtCO<sub>2</sub> for the unrestricted deforestation scenario (findings by Melillo, Reilly, et al. (2009) are –72 GtCO<sub>2</sub> and 95 GtCO<sub>2</sub> by 2100, respectively).

High CO<sub>2</sub> emissions from LUC have the potential to tip life cycle CO<sub>2</sub> emissions of second-generation bioenergy production out of balance. In addition, previous literature indicates that biogeophysical effects can have significant impacts on climate. However, the magnitude of these impacts strongly depends on factors such as type of feedstock, geographical location, prior land use, and land management practice. Further, energy crops themselves are sensitive to changes in climate conditions, atmospheric CO<sub>2</sub> concentrations, water availability, and heat stress, though there is potential for crops to adapt to such changes (Oliver et al., 2009; Rosenzweig et al., 2014; Arias et al., 2021; Canadell et al., 2022). The viability of large-scale energy cropland cultivation in future scenarios will thus depend on how crops respond to such conditions.

## 2.4 Impacts of Bioenergy Expansion on Biodiversity

One of the main sustainability concerns related to global-scale bioenergy production is the impacts of cropland expansion on biodiversity. In this context, biodiversity is defined as the “variability among living organisms from all sources including, inter alia, terrestrial, marine and other aquatic ecosystems and the ecological complexes of which they are part; this includes diversity within species, between species and of ecosystems”, as stated by the Convention on Biological Diversity (CBD) (CBD, 2010). The importance of biodiversity can be reflected in the different values humans place upon it. These include economic, ecological, cultural, scientific, and recreational values, as well as its intrinsic value – that is, the notion that each species has a value and a right to exist, whether or not it is known to have anthropogenic value (Morton and Hill, 2014). The Millennium Ecosystem Assessment, in 2005, was the first global effort to understand the relationship between biodiversity and human well-being, outlining the role of biodiversity in four ecosystem services: provisioning services (e.g., food, fibre and water production), regulating services (e.g., climate and disease control), supporting services (e.g., nutrient cycling and crop pollination), and cultural services (e.g., spiritual and recreational benefits) (MEA, 2005). A loss or deterioration in biodiversity can therefore compromise these services and affect human well-being (Wright et al., 2021).

Today, global biodiversity is already declining at rates ranging between several hundred to ten thousand times the natural background rates. Overall, more than 40,000 species are threatened with extinction, including 41% of amphibians, 37% of sharks and rays, 34% of conifers, 33% of reef building corals, 26% of mammals and 13% of birds (IUCN, 2022b). Changes in land use, and therefore the loss of habitats, are currently the largest threats to biodiversity, followed by overexploitation, climate change, pollution, and invasive species and disease (MEA, 2005; Fritsche et al., 2006; Butchart et al., 2010; Dornburg et al., 2010; WWF, 2012; Díaz et al., 2019; Tudge et al., 2021). The expansion of bioenergy cropland is a relatively recent cause of land-use change, however its impacts on biodiversity are already apparent. Different bioenergy systems can have varying impacts on biodiversity and ecosystem services (Meller et al., 2015). Numerous studies, worldwide, have sought to understand these impacts, displaying a wide range of findings.

### **2.4.1 Impacts of First-Generation Bioenergy Expansion**

Overall, findings are mostly negative, especially for first generation biofuels and in the tropics. A review of 53 publications carried out by Immerzeel et al (2014) shows that around 87% of studies investigating the relationship between first-generation crops and biodiversity report negative impacts. This is largely due to the conversion of forest or natural vegetation for cropland (Williams et al., 2020). Compared to natural ecosystems (e.g., primary or secondary forests, grasslands, wetlands), intensively managed monocultures such as first-generation crops support much fewer species. This is because they are structurally less complex than natural ecosystems, have a shorter life span and cause major landscape fragmentation (Flather and Bevers, 2002; Fitzherbert et al., 2008; Fahrig et al., 2011; Gasparatos et al., 2013).

Globally, at least 405 species could be threatened by oil palm expansion, of which 193 are listed as Critically Endangered, Endangered or Vulnerable (Meijaard et al., 2018). Examples of species loss due to oil palm plantations have been reported for a variety of taxa, including plants (Fitzherbert et al., 2008; Danielsen et al., 2009), mammals (Maddox et al., 2007; Freudmann et al., 2015; Wearn et al., 2016), birds (Aratrakorn et al., 2006; Peh et al., 2006; Sheldon et al., 2010), lizards (Danielsen et al., 2009) and invertebrates (Barnes et al., 2014), such as forest butterflies (Koh and Wilcove, 2008). Typically, the simple ecological structure of oil palm favours generalist species (e.g. pigs and certain mammalian carnivores), and non-forest invertebrate species (Danielsen et al., 2009), over specialist species (e.g. orangutans, gibbons, tigers and rhinos). Meijaard et al. (2018) further show that, globally, at least 405

species could be threatened by oil palm expansion, of which 193 are listed as Critically Endangered, Endangered or Vulnerable.

Brazil holds the largest areas of soy and sugarcane production, yet it is ranked the most biodiverse country on the planet (Butler, 2016). These plantations are mainly (90%) situated in the Centre-Southern region of Brazil within the São Paulo and Goiás states. Although the majority of sugarcane expansion has so far displaced pasture lands (Durán et al., 2020), significant advances towards the Cerrado savanna and Atlantic Forest biomes have been identified (Rudorff et al., 2010; Scarpore et al., 2016; Leal et al., 2017). These biomes contain substantially high concentrations of endemic and threatened species and have therefore been categorised as biodiversity hotspots (Mittermeier et al., 2005).

Historically, soybean expansion in Brazil has been concentrated in the Cerrado biome (Lima et al., 2011; Gibbs et al., 2015; Durán et al., 2020). Gibbs et al. (2015) estimate that around 21% of land in this biome has been converted for soy production. In more recent years (2002–2013), soy production has also expanded into the Amazon biome, clearing approximately 13–18% of forests, of which 6% can be attributed to biodiesel. This forest loss is located within the “arc of deforestation”, one of the most active land-use frontiers in the world with regards to total forest decline (Morton et al., 2006).

### **2.4.2 Impacts of Indirect Land-Use Change**

While most studies investigating the impacts of bioenergy production on biodiversity focus on the direct impacts of converting natural or non-natural habitats, there is growing concern regarding the potential indirect effects (iLUC) cropland expansion could have. For example, continued expansion of sugarcane plantations in Brazil is likely to further displace cattle ranchers and soybean producers onto the Amazon and Atlantic Forest biomes, resulting in extensive indirect deforestation (Casson, 2003; Martinelli and Filoso, 2008; Lapola et al., 2010). Quantification of iLUC-induced biodiversity effects is difficult and few studies have attempted it (Kessler et al., 2007; Eggers et al., 2009; Hellmann and Verburg, 2010). Kessler et al. (2007), for instance, analysed the ‘multiplier effect’ from commodity development in six countries across the tropics in 2005. This effect reflects additional land-use change as a collateral effect outside actual cropping areas and was expressed in the study in terms of loss of Natural Capital Index, an indicator for changes in biodiversity status (UNEP, 2004). They

found that the highest multiplier effects occurred for soy production in Brazil (87%) and for palm oil in Indonesia (35%).

Cropland intensification is one strategy that could help reduce the competition between food, animal feed, and biofuel production, and therefore alleviate iLUC (Dornburg et al., 2010; Wicke et al., 2012). Various studies, however, have highlighted the potential threats that biodiversity may face as a result of intensification (Sala et al., 2000; Tscharntke et al., 2012; Pereira et al., 2012; Molotoks et al., 2017; Zabel et al., 2019). These include habitat homogenisation (Benton et al., 2003; Meehan et al., 2011), irrigation (De Frutos et al., 2015), and pollution resulting from increased use of fertilisers and pesticides (Geiger et al., 2010). Additionally, there is ongoing debate as to whether cropland production and conservation should be integrated on the same land (i.e., ‘land sharing’) or separated (i.e., ‘land sparing’) (Phalan et al., 2011; Tscharntke et al., 2012; Fischer et al., 2014; von Wehrden et al., 2014). However, studies are increasingly arguing for land sharing approaches, stating that wildlife friendly farming could help sustain ecosystem services, maintain functional biodiversity and minimise environmental costs (Porter et al., 2009; Tscharntke et al., 2012). Linking agricultural intensification for biofuel production with biodiversity conservation is thus complex and requires well-informed regional and targeted solutions (Lotze-Campen et al., 2010).

## **2.4.3 Impacts of Second-Generation Bioenergy Expansion**

### **2.4.3.1 An Improvement on First-Generation Bioenergy?**

Some studies argue that impacts of second-generation crops are less negative than first generation crops (Immerzeel et al., 2014; Tudge et al., 2021). In several cases they have shown to provide benefits to biodiversity, particularly in temperate regions (Kessler et al., 2007; van Dam et al., 2009; Van Der Hilst et al., 2012). As mentioned in Section 2.2.3.1, this is largely due to their capacity to grow on marginal or degraded land, unlike first generation crops, reducing their competition with food crops and the need for land clearance (Erb et al., 2012). However, the extent of marginal land currently available or unused has been debated, with many areas considered marginal in fact harbouring rich biodiversity (Myers et al., 2000; Creutzig et al., 2015; IPBES, 2019). Other benefits of second-generation crops are their longer rotation periods, reduced chemical inputs needed and increased spatial heterogeneity (Dauber et al. 2010). Perennial grasses (e.g., miscanthus) and short rotation coppiced willow have shown potential in providing habitat and shelter for specific species, such as migratory birds,

as well as improving connectivity or supporting restoration of marginal or degraded lands (Dauber et al., 2010; Meehan et al., 2011; Robertson et al., 2011; Haughton et al., 2016). Most studies, however, state that such benefits are dependent on several factors, including the different species responses, the spatial scale and geographical location studied, and characteristics of the plantation being studied i.e., management practices used, age, size, and heterogeneity. Some findings conversely show that perennial bioenergy cropland can be a driver of changes in biodiversity due to invasive traits, though the extent of this is largely unknown and dependent on the type of crop planted (Hartman et al., 2011; Barney, 2012; Barney, 2014).

Until recently, most work investigating impacts of second-generation bioenergy on biodiversity have been carried out at present day, at the field level, in temperate regions, and for only a small number of species/taxa, with few studies calculating future global impacts (Immerzeel et al., 2014). This is largely due to the lack of data available for global present day and future projections of spatial energy cropland distributions. Overall, it is clear that global scale cultivation of second-generation crops will have significant environmental impacts due to the amount of land, water and nutrients that would be needed, which could in turn affect biodiversity (Bonsch et al., 2016; Heck et al., 2018; Stoy et al., 2018; Williams et al., 2020; Ai et al., 2021). However, this is highly dependent on the location, the previous land use in this location, and the magnitude of energy cropland cultivation needed (Smith et al., 2019). If BECCS continues to remain a major component of climate change mitigation strategies, it is important to fully understand how, and to what extent, it could affect biodiversity.

### **2.4.3.2 Measuring Impacts of Second-Generation Bioenergy Production on Biodiversity**

As demonstrated previously in Section 2.3, climate modelling is generally considered to be a well-established field, spanning several decades of development. Biodiversity modelling, however, is still relatively new, hindered by factors such as limitations in observational data and accounting for scale dependencies, each of which can influence the accuracy and applicability of a model. Additionally, the overall inherent complexity of biodiversity, with its numerous interacting factors, intricate ecological processes, and wide range of taxonomic groups, habitats, and ecosystem types, has made it challenging to develop comprehensive models that capture all the elements of biodiversity patterns and dynamics. This has led to

difficulties in defining biodiversity metrics, choosing appropriate modelling techniques, and selecting relevant predictors.

Despite this, over the last decade increasing numbers of studies have tried to determine the global impacts of second-generation bioenergy production on biodiversity (Powell and Lenton, 2013; Hof et al., 2018; Heck et al., 2018; Tudge et al., 2021; Hanssen et al., 2022). The advancement of data on present day and projected energy cropland distributions has further enabled research into biodiversity responses and the use of various well-established methods and indicators typically applied in biodiversity literature.

#### **2.4.3.2.1 Land-Use Impacts**

Due to the complexity of biodiversity, a wide range of approaches have been used to calculate impacts of global LUC across the biodiversity literature. These approaches are based on indicators which define certain aspects of biodiversity, such as their variety or richness (the number of different types), vulnerability (how vulnerable each type is), abundance (how much there is of each type), and/or distribution (where biodiversity is located) (BIP, 2010) (see **Table 2.1**). Each of these indicators is as important as the other in understanding how biodiverse a region is. Equally, identification of one indicator is not a guarantee that the others are also present in that ecosystem. Several studies, including life cycle assessments, have identified and compared these indicators, with many highlighting the importance of incorporating multiple dimensions of biodiversity in impact assessments (Grenyer et al., 2006; Davies and Cadotte, 2011; Souza et al., 2015; Gabel et al., 2016; Marquardt et al., 2019; Molotoks et al., 2020).

**Table 2.1:** Literature findings for biodiversity impacts of global land conversion for second-generation energy cropland using different biodiversity indicators; based off findings in Immerzeel et al (2014) and example studies provided in the table.

Indicator	Example Methods and Data (in addition to LUC data)	Positive (+) or negative (-) impacts related to second-generation (2 <sup>nd</sup> gen) energy crops	Example studies
Habitat quality	Calculating change or loss of habitat/ecosystem	+/-	Studies generally show a loss of habitat and ecosystems, although benefits occur in some scenarios. Beringer et al. (2011); Buchanan et al. (2008); Hansen et al. (2013); Hellmann and Verburg (2010)
	Calculating changes to High Nature Value areas	+	Small impacts in scenarios, with conversion to perennial crops having a much lower impact than first-generation energy crops. Hellmann and Verburg (2010); Van Der Hilst et al. (2012)
Species richness	Species-area and Endemics-area relationship modelling (SAR/EAR). <i>Data:</i> IUCN species ranges	-	No study specifically isolates impacts of 2 <sup>nd</sup> gen crops. However, overall LUC scenarios that include bioenergy expansion indicate negative impacts of increased LUC. Chaudhary and Mooers (2017); Hanssen et al. (2022); Jantz et al. (2015)
	Spatial analysis <i>Data:</i> field surveys and databases e.g., PREDICTS, BirdLife International, GBIF	+/-	Studies indicate a loss of species richness due to 1 <sup>st</sup> and 2 <sup>nd</sup> gen bioenergy crops, though effects can be positive in the case of 2 <sup>nd</sup> gen crops. Bird species are the most studied taxonomic group. Barlow et al. (2007); Loyn et al. (2007); Newbold et al. (2015); Schulz et al. (2009); Tudge et al. (2021); Volpato et al. (2010)
Species abundance	Calculating Mean Species Abundance (MSA) relative to undisturbed state. <i>Data:</i> field surveys, PREDICTS data, GLOBIO model	+	Unlike 1 <sup>st</sup> gen crops, positive MSA values are calculated for 2 <sup>nd</sup> gen crops. Kessler et al. (2007); Schipper et al. (2020); Van Dam et al. (2010); Van Der Hilst et al. (2012)
	Spatial analysis of species abundance and composition. <i>Data:</i> field surveys, PREDICTS data, GLOBIO model	+/-	Abundance and composition quality decreases with increased 1 <sup>st</sup> and 2 <sup>nd</sup> gen cropland. Studies show an increase of general species and decrease of species with restricted ranges. Barlow et al. (2007); Codesido et al. (2011); Hsu et al. (2010); Tudge et al. (2021); Volpato et al. (2010)
	Spatial analysis using Biodiversity Intactness Index (BII)	-	All studies indicate a reduction in BII due to 2 <sup>nd</sup> gen bioenergy expansion as increases in natural land are used, suggesting the necessity of marginal land use. Fritz et al. (2013); Heck et al. (2018); Noone et al. (2013)
Species distribution and vulnerability	Species distribution modelling to calculate habitat suitability and species sensitivity <i>Data:</i> IUCN species ranges and Digital Elevation Models	+/-	Species distribution impacts are understudied. However, habitat suitability for endemic species has been calculated using distributional ranges showing mainly negative impacts, though less so for 2 <sup>nd</sup> gen crops. Bellard et al. (2014); Buchanan et al. (2008); Eggers et al. (2009); Louette et al. (2010); Stoms et al. (2012)

Many studies use habitat quality as a proxy for the state of biodiversity. The loss or fragmentation of a habitat can thus be associated with the loss of biodiversity within the habitat (Buchanan et al., 2008; Hellmann and Verburg, 2010; Hansen et al., 2013). Most assessments, however, also incorporate ‘species richness’ as an indicator, and use a form of the Species-Area Relationship (SAR) ecological model, combined with species richness databases, to calculate species loss due to land use. The SAR is an empirical relationship between the number of species and the land area of a region, often used to estimate extinction risk (Arrhenius, 1921; Rosenzweig, 2001; Brooks et al., 2002; Thomas et al., 2004). Species extinctions are calculated as the direct function of habitat loss contraction based on the observation that extinction risk increases with decreasing range and population size.

Species richness is often derived from global, spatially explicit maps showing species distribution ranges (e.g., BirdLife International (2022) and IUCN Red List (2022a)) or areas of suitable habitat in which individual species are located (e.g., the Biodiversity Hotspots; Mittermeier et al. (2005)). Jantz et al. (2015) and Chaudhary and Mooers (2017), for example, use variations of the SAR model to project future land use-driven species extinctions resulting from different climate pathways (RCPs) and climate plus socio-economic pathways (RCP-SSPs), respectively. Both studies estimate that, even in the best-case scenarios (i.e., RCP 2.6 IMAGE and RCP2.6 SSP-1, respectively), up to 1,030 and 1,230 vertebrate species are committed to extinction globally by 2100, respectively, largely due to the expansion of second-generation energy cropland across key habitats. Only one study has been found by the author that isolates second-generation bioenergy impacts using the SAR method (Hanssen et al., 2022). Hanssen et al. (2022) use conversion factors based on SARs, derived by Chaudhary and Brooks (2018), and similarly calculate a global loss of around 1500 vertebrate species by 2100, due solely to energy cropland expansion for BECCS following a 1.5 °C pathway.

Site-level species richness and abundance can be quantified across the globe using the PREDICTS database (Projecting Responses of Ecological Diversity In Changing Terrestrial Systems). This database contains information about biodiversity on different croplands across the world, and can be used to project biodiversity responses to different land uses and related pressures (Hudson et al., 2017). Tudge et al. (2021) use the PREDICTS database to show that species richness and abundance are 19% and 25% lower in sites planted with second-generation biomass crops than in sites with natural vegetation; smaller, but still significant, findings in comparison to their estimates for first-generation biofuel effects (37% and 49% respectively). Newbold et al. (2015) corroborate these findings and use the PREDICTS database to further



illustrate the major negative effects of global scale second-generation bioenergy implementation in ambitious mitigation scenarios.

Some studies use the Scholes and Biggs (2005) Biodiversity Intactness Index (BII) indicator to explore the trade-offs between LUC for bioenergy and biodiversity-related planetary boundaries (PBs) (Fritz et al., 2013; Noone et al., 2013). Heck et al. (2018), for instance, calculate that large-scale second-generation bioenergy could result in a +7% loss of biodiversity intactness due to transgressions of the PBs for land-system change and biosphere integrity. Their work further demonstrates the impossibility of converting natural land for bioenergy and states the importance of limiting biomass production to marginal land and existing cropland (Núñez-Regueiro et al., 2021). Even in the latter case, this has shown to cause negative impacts on biodiversity (Powell and Lenton, 2013).

Relatively positive impacts have also been calculated using six out of the eight indicator methods mentioned (see **Table 2.1**). Hellmann and Verburg (2010), for instance, demonstrate that LUC projections of the European Union biofuel directive for 2030 have minor direct impacts on semi-natural vegetation, forest and High Nature Value farmland, however that indirect impacts are more substantial. Van Der Hilst et al. (2012) and van Dam et al. (2009) further identify potential positive effects of land conversion to second-generation biofuels. Both works illustrate significant improvements in Mean Species Abundance (MSA) values from using second-generation crops (e.g., switchgrass and miscanthus) compared to first-generation crops (e.g., soybean and sugar beet), with environmental benefits particularly seen when converting abandoned land in temperate regions. It is, however, noted that no areas studied contain only positive impacts from cropland conversion, whereby small negative impacts tend to occur on natural vegetation or wet pasture. Other, less used, indicators include species vulnerability and distribution, which show mixed findings resulting from both changes to land and climate (Eggers et al., 2009; Louette et al., 2010; Stoms et al., 2012; Bellard et al., 2014).

#### **2.4.3.2.2 Climate Impacts**

In addition to LUC, climate change is expected to be one of, if not the, greatest threats to biodiversity over the next few decades (Leadley et al., 2010). This has motivated widespread research into potential responses of biodiversity to climate change, including studies on the fossil records (Lorenzen et al., 2011), recently observed trends (Parmesan, 2006), and projected

impacts (Bellard et al., 2012). Climate variables play a large role in determining the geographical distribution ranges of species (Guisan and Zimmermann, 2000; Pearson and Dawson, 2003; Gilman et al., 2010; Dawson et al., 2011; Beaumont et al., 2011; Warren et al., 2013; Nunez et al., 2019). Species either shift their geographical ranges or become extinct when the climate conditions in their habitat are no longer adequate. This is largely dependent on their dispersal capacities and their ability to track preferred climate space across what is often an increasingly fragmented landscape (Settele, 2014; Smith et al., 2018). Other biodiversity components affected by climate change include species physiology, phenology, community structures and ecosystem functions (Bellard et al., 2012).

As in the case of LUC, a wide range of modelling techniques can be used to determine future impacts of climate change on biodiversity (Bellard et al., 2012). Bellard et al. (2014) use the standardized Euclidian distance (SED) method, developed by Williams et al. (2007), to quantify the climatic dissimilarity between current and future climate within biodiversity hotspots. They estimate that a warming of 3.5–5 °C above pre-industrial levels will negatively impact 25% of endemic species across the hotspots. A meta-analysis similarly estimates that 20–30% of plant and vertebrate species could be at risk of extinction if global mean temperatures increase beyond 2–3 °C above pre-industrial levels (Fischlin et al., 2007). Thomas et al (2004) predict that even a warming of 1.8–2 °C could lead to a loss of 15–37% endemic species globally. Their work demonstrates the potential severity of even moderate levels of climate change and the importance of rapid implementation of mitigation strategies.

Some of the studies analysing the impacts of LUC from second-generation bioenergy on biodiversity also explore the potential positive effects that may occur from climate change mitigation (Melillo, Gurgel, et al., 2009; Powell and Lenton, 2013; Heck et al., 2018; Hof et al., 2018; Hanssen et al., 2022). Climate-explicit species distribution modelling has shown that reduced species richness from LUC for bioenergy is not compensated by lower climate change impacts; however this excludes negative emissions from CCS implementation (Hof et al., 2018). When incorporating negative emissions, species-area relationship (SAR) modelling produces mixed findings. Powell and Lenton (2013) show that reduced species richness still offsets the benefits of prevented climate change on inclusion of negative emissions. Hanssen et al. (2022), on the other hand, show that over a longer period (80 years) the positive effects of climate change may outweigh the negative effects of LUC on species richness, particularly if large-scale second-generation bioenergy is deployed as early as possible to allow maximum

sequestration before future climate targets. However, they further state that these interactions are highly uncertain and require more research.

It is evident that both land-use change and climate change contribute to biodiversity loss in different ways, whereby the two effects can often interact and have synergistic impacts on biodiversity. It is therefore crucial that policies surrounding second-generation bioenergy expansion address both factors, incorporating conservation strategies that aim to not only mitigate greenhouse gas emissions but reduce habitat destruction, promote sustainable land-use practices, and enhance ecosystem resilience to ensure the long-term survival of biodiversity. That said, some studies suggest that land-use change currently poses a more immediate threat to biodiversity due to its direct and localised nature, particularly in areas with high rates of deforestation and habitat conversion (Gibson et al., 2011; Laurance et al., 2012). Climate change, on the other hand, is increasingly considered a significant long-term driver of biodiversity loss, as its effects intensify over time and interact with other stressors (Bellard et al., 2012; Bellard et al., 2014). As discussed, exploration of these two factors requires complex analyses and resources, and while the author recognises the equal importance of both, only land-use impacts from bioenergy expansion will be considered in the main body of biodiversity assessments from here on.

### **2.4.3.2.3 Critical Analysis of Biodiversity Modelling Techniques**

Choosing a suitable approach for calculating impacts on biodiversity ultimately depends on the context in which it is used. All indicators and models discussed in this section have previously been determined as viable options for biodiversity modelling associated with land-use change (and climate change) impacts due to the fact that they cover a wide set of criteria: they are a function of land-use change, are high resolution (at least 10km by 10km), spatially explicit, globally applicable, peer reviewed, and readily available (Molotoks et al., 2020).

However, each of these approaches has methodological, spatial and temporal limitations that constrain their predictive power (McMahon et al., 2011). Even in the most ambitious studies, the range of species used generally represents a small percentage of known biodiversity. As mentioned previously, approaches using species richness (e.g., the SAR or PREDICTS models; see **Table 2.1**) as an indicator are currently more widely used, because it is thought to influence the resilience and resistance of ecosystems to environmental change. It also acts as a broad parameter for providing information about the biodiversity of an entire eco-region (whereas

abundance, for instance, tends to provide a more nuanced information on individual species within a specific community or ecosystem). However, species richness only considers the number of species present in a given area, without considering the identity or composition of those species. It treats all species as equal, regardless of their ecological importance, rarity, or functional role. It can also be influenced by taxonomic biases, where certain taxonomic groups are better studied, documented, or recognised than others, so may be over- or under-represented (Thuiller et al., 2011).

The SAR model is a valuable tool for understanding patterns of species richness, however it is widely criticised in the literature. Though many studies have utilised the SAR model for extinction estimates (e.g. Brooks et al. (2002), Malcolm et al. (2006) and Jantz et al. (2015), several studies have shown that estimates generated using the model are frequently greater than observed extinctions (May et al., 1995; Pimm and Askins, 1995; Rosenzweig, 1995). One explanation for this could be it implies that species are immediately removed and are committed to extinction after habitat loss. In reality, extinctions will tend to occur over an unspecified length of time (May et al., 1995), depicted as the “relaxation time” in Diamond (1972).

Further, the area required for species extinctions is normally larger than the sample area needed to encounter the species, hence the SAR does not accurately represent species losses as habitat area is reduced (He and Hubbell, 2011). Extinction estimates should depend more on the number of species confined to the cleared habitat area rather than to the total number of species in the original habitat area (Pimm and Askins, 1995; Pimm et al., 1995). To overcome this discrepancy, Harte and Kinzig (1997) have used the SAR model to derive the endemics-area relationship (EAR) model, where “endemic” refers to species located *only* within a cleared patch of larger habitat and nowhere else.

Most studies using the SAR or EAR models assume unrealistically that non-natural habitats harbour no biodiversity (Jantz et al., 2015; Molotoks et al., 2020). These models also do not consider the specific ecological context or environmental conditions of different areas, instead assuming that a habitat is uniform. In reality, factors such as habitat quality, heterogeneity, fragmentation, and connectivity can significantly influence species richness. In addition, individual responses of species to land-use change may vary as some species are more sensitive than others. Thus, ignoring these contextual factors could result in inaccurate predictions or interpretations of species richness patterns. The SAR model also assumes that species have unlimited dispersal abilities, whereby species can freely colonise all available habitats within

an area. However, dispersal barriers, such as distance decay effects or specific habitat requirements, can restrict movements of species. A handful of studies have tried to account for these influences. For instance, De Baan et al. (2013) developed the Matrix SAR model, which accounts for habitat heterogeneity to assess patterns of species richness in multi-habitat landscapes. Although, their model assumes 100% species loss after habitat loss, and does not incorporate species vulnerability. Chaudhary et al. (2015) further improved on this model by implementing a larger range of land-use types and varying use of habitats by species, acknowledging that some species can live in habitats that have undergone conversion. However, their model depends on characterisation factors (CFs) that can be based on relatively outdated land cover datasets.

The calculation of ‘extinction’ within the mentioned approaches also has its limitations. Though extinction is a potential immediate impact of land-use change, it is only the last step of a decline in abundance of a species. This fact has led to the development of models such as GLOBIO and PREDICTS. They calculate mean species abundance (MSA) (Alkemade et al., 2009) and Biodiversity Intactness Index (BII) (Scholes and Biggs, 2005), which depict the impact of human activities on species abundance (see **Table 2.1**). There are, however, several limitations to these models. They require quality input data (of which more is needed than in most other models), which may be lacking or incomplete, particularly in regions with limited monitoring or data collection efforts. In addition, mean species abundance methods can be strongly influenced by a few dominant species that have high abundances and may not adequately capture the presence or importance of rare species (which may have low abundances or occur sporadically). In the case of BII, setting thresholds to determine what constitutes “intact” or “degraded” biodiversity can be challenging. Further, BII calculations are influenced by the spatial and temporal scale, thus aggregating data at larger scales may mask local or fine-scale variations in biodiversity patterns and responses, and potentially miss important temporal dynamics and lagged effects. Finally, translating BII values into meaningful conservation actions or policy decisions can be difficult and requires careful consideration of local context and stakeholder involvement.

While indicators and models play a major role in biodiversity modelling, successful implementation requires (often complex) biodiversity data. This data is generally based on ‘seminal’ datasets, such as the IUCN data, which are widely accepted throughout the conservation science community, however it can lead to considerable overlap across data

sources. In addition, the difficulties involved in producing and updating such large global datasets often means that the information provided can be years, or even decades out of date.

#### **2.4.3.2.4 Accounting for Species Vulnerability and Irreplaceability**

One way to address these data limitations is by focussing on ‘important’ habitat locations. The ‘importance’ of a habitat can be assigned using the framework of vulnerability and irreplaceability (Margules and Pressey, 2000). Vulnerability measures the risk of a habitat being transformed, in which species are highly threatened but not protected. Irreplaceability is the extent to which the loss of an area will compromise regional conservation targets. These targets are built on several factors i.e. presence of a species in a region, minimum area of e.g. a vegetation type in that region, or predicted probabilities of occurrence of a species (Ferrier et al., 2000). The most common measure of irreplaceability is species endemism. The greater the number of endemic species in a region, the more biodiversity is lost if that region is lost. More strictly, any location with even one endemic species is irreplaceable. Other aspects of irreplaceability include taxonomic uniqueness, unusual phenomena, and global rarity of major habitat types (Brooks et al., 2006).

Areas of habitat with high values for both vulnerability and irreplaceability are considered the highest priority for conservation action. They have the largest risk of being lost and will have the most serious impact on achievement of conservation targets. Biodiversity conservation organisations have proposed nine templates of global priorities, including for instance the “crisis ecoregions”, “endemic bird areas” and “centers of plant diversity”, to name a few (Brooks et al., 2006). Conceptually they all fit within the framework of “irreplaceability versus vulnerability”, however they map onto different proportions of the framework, with most prioritising high irreplaceability. Out of all the templates, the “biodiversity hotspots” are the only template that maps onto both high irreplaceability and high vulnerability, defined as biogeographic regions with significant concentrations of endemic species and exceptional loss of habitat. Major efforts and resources have thus been allocated for their study and preservation, with possibly over \$1 billion of funding already provided (Schmitt, 2012). Despite this, future impacts of LUC within the biodiversity hotspots have received considerably little attention so far.

In addition to important habitats, the principles of irreplaceability and vulnerability are also used to highlight specific species at threat. The Alliance for Zero Extinction (AZE) database has increasingly been used for its up-to-date identification of species classified as endangered or critically endangered under the IUCN criteria. These species face extinction due to their remaining habitat being degraded locally or because their small global range makes them vulnerable to external threats (AZE, 2010).

## **2.5 Sustainability Measures and Conservation Schemes**

Environmental protection measures will be required to avoid sustainability trade-offs occurring from land-use changes associated with second-generation bioenergy expansion. In the context of bioenergy, literature addressing these trade-offs and potential conservation schemes is mostly limited to impacts on natural land and freshwater due to the indispensability of these natural resources in climate regulation, ecosystem protection and human-wellbeing (Popp, Dietrich, et al., 2011; Kraxner et al., 2013; Calvin et al., 2014; Bonsch, 2015; Bonsch et al., 2016). Other sustainability measures, such as improved soil nitrogen uptake efficiency, increased crop yields, and higher livestock productivity have only recently been incorporated into bioenergy impact assessments (Humpeöder et al., 2018a). While research on land and freshwater conservation is well established within the literature, few studies have determined how incorporating these measures into future pathways could influence land-use interactions with climate and biodiversity. The work in this thesis therefore focuses on these two conservation areas in terms of their implementation with future bioenergy scenarios.

### **2.5.1 Land Conservation**

#### **2.5.1.1 Existing Land Conservation Schemes**

Government policies and certification schemes can play a key role in counteracting the impacts of agricultural expansion on forest and other natural land, though combined forest-energy policies are lacking in most countries (Roos, 2002; Ladanai and Vinterbäck, 2010). International treaties and initiatives, such as the New York Declaration on Forests (NYDF) (FDP, 2023), Glasgow Leaders' Declaration on Forests (GLDF) (Abdenur, 2022), Nationally Determined Contributions (NDCs) (UNFCCC, 2023), and National Biodiversity Strategies and Action Plans (NBSAPs) (CBD, 2023), have been devised to encourage and monitor forest

conservation and restoration, support sustainable supply chains, and promote nature-based solutions within individual countries. Interventions such as these can serve as frameworks and catalysts for conservation and certification schemes.

While certification schemes have been developed for some first-generation energy crops, such as soy, palm oil and sugarcane (e.g., Roundtable for Sustainable Palm Oil (RSPO), Roundtable on Responsible Soy Oil (RRSO), Better Sugarcane Initiative (BSI)), specific certification systems or initiatives for other more advanced energy crops are in their infancy (e.g., Roundtable on Sustainable Biofuel (RSB), International Sustainability and Carbon Certification (ISCC), Green Gold Label (GGL), Sustainable Biomass Program (SBP)) (Biomass Technology Group, 2008). Forestry- and agricultural-related schemes also further incorporate bioenergy production (e.g., Sustainable Forestry initiative (SFI), Forest Stewardship Council (FSC), Sustainable Agriculture Network (SAN) Rainforest Alliance) (Fehrenbach, 2011).

Europe is the largest importer of palm oil, and recently amended regulations to limit future imports for biofuels (Rulli et al., 2016). However, there remains concern regarding rising demands within Indonesia, Malaysia and China, which could make up for this market shift and lead to continued palm oil production in these regions (Coca, 2020). In contrast, Brazil has been considered a global exception in terms of forest conservation, with a significant policy-driven reduction in Amazon Basin deforestation. Observations indicate that, while Brazilian gross forest loss is the second highest globally, other countries, such as Malaysia, Cambodia, Tanzania, Cote d'Ivoire, Paraguay and Argentina, have experienced a higher percentage of loss in forest cover (Hansen et al., 2013).

In Brazil, the main legislation that protects the native vegetation and regulates the use of land is the Forest Code, initiated in 1965 and updated in 2012. This law mandated that private landowners set aside between 20 and 80 percent of native forests and savannas on their rural properties as 'legal reserves', though this percentage has since been reduced (Azevedo et al., 2017; Asher, 2019). Leal et al. (2017) further show that sugarcane expansion in Brazil has, since 2009, been successfully controlled by the Sugarcane Agroecological Zoning (AEZ) law, a policy which indicates new areas where sugarcane can be cultivated. They suggest that only minor impacts on native vegetation have occurred, with most of the sugarcane expansion happening on land which has already been largely deforested. Similarly, Brazil's Soy Moratorium (SoyM) was introduced in 2006, preventing major soybean traders from



purchasing soy grown on lands deforested in the Amazon (Heilmayr et al., 2020). While these policies led to a successful 84% decline in rate of deforestation between 2004 and 2012, rates doubled between 2012 and 2019 due to violations of agreements (Gibbs et al., 2015; Heilmayr et al., 2020). It is therefore important that such policies continue to develop. Ongoing debates regarding this continuation and recent political changes in Brazil highlight how challenging this could be, as well as the overall tenuous nature of all forest conservation policies.

Tropical deforestation and forest degradation represent the second largest source of global greenhouse gas emissions, accounting for 12–20% of anthropogenic carbon emissions (Houghton and Hackler, 2008; Ghazoul et al., 2010). To prevent deforestation, the expansion of second-generation bioenergy will likely require the development of similar policies and certification schemes to those mentioned, as well as financial incentives to reduce climate impacts. The REDD+ (reducing emissions from deforestation and forest degradation) initiative is the most well-known mechanism for creating such incentives, and can be incorporated into conservation schemes. First negotiated at the Conference of the Parties (COP) of the UN Framework Convention on Climate Change (UNFCCC) in 2005, it aims to incentivise developing countries to reduce emissions from deforestation and forest degradation, providing them with compensation from developed nations who need to meet their emissions reduction targets (Ghazoul et al., 2010).

However, until recently, few countries were operating REDD+ on a national level, due to a range of political and technical challenges (Minang et al., 2014; Sunderlin et al., 2015). These can be categorised under three umbrellas: ‘leakage’; the movement of economic destructive activities to other locations due to REDD+ implementation, ‘permanence’; the risk that carbon is just temporarily stored in the forests, and ‘additionality’; the possibility that reduced carbon emissions may occur even without REDD+ payments (Ghazoul et al., 2010; Atmadja and Verchot, 2012). In addition, there are huge concerns regarding the negative impacts of REDD+ on forest-dependent communities, such as unequal benefit sharing, illegal land acquisition, food insecurity, and agricultural changes (Bayrak and Marafa, 2016). The UNFCCC framework for REDD+ therefore includes a set of environmental and social safeguards to ensure projects are consistent with forest and biodiversity conservation, as well as respect the knowledge and rights of indigenous peoples and local communities. To date, 65 countries in Africa, Asia and the Pacific, and Latin America have signed up to the UN-REDD Programme, which provides a platform for REDD+ implementation. As of January 2020, nine countries

reported 8.82 billion tonnes of emissions reductions due to reduced rates of deforestation and forest degradation (FAO and UNEP, 2020).

Uncertainties around REDD+ are largely attributed to the disconnect between policy and operational capabilities. Country-level observational data can be a useful tool for understanding forest extent and change, with Brazil still being the main country that produces and shares spatially explicit information. The use of Landsat data has been one of the key reasons for Brazil's past success in policy formulation and implementation. Ongoing development of current forest distribution maps, such as those produced by Hansen et al (2013), can assist countries lacking such data, inform national monitoring methods, as well as provide continually updated baseline information for future global land modelling. As shown in this thesis, global impact assessments can provide useful findings for international policy and highlight regions most at risk. However, real-world implementation of REDD+ and other forest conservation policies can only occur with ground-level information.

### **2.5.1.2 Land Conservation in Future Impact Assessments**

Land-use regulation is a key component of ambitious future mitigation pathways implementing second-generation bioenergy expansion (Popp et al., 2012; Popp et al., 2017). However, few studies have isolated the potential sustainability implications of land conservation schemes within these pathways, with little focus on climate and biodiversity implications (Kraxner et al., 2013; Calvin et al., 2014; Bonsch et al., 2016; Humpenöder et al., 2018a).

Studies that do investigate these interactions tend to incorporate a REDD+ policy into the scenarios by restraining expansion of agriculture (particularly bioenergy cropland) into forests and putting a price on CO<sub>2</sub> emissions from LUC. Humpenöder et al. (2018a) and A. Popp, Humpenöder, et al. (2014), for instance, show that forest loss is significantly reduced with global REDD+ implementation. However, they also demonstrate potential ramifications, including carbon leakage from the displacement of cropland onto both forested and non-forested areas (Yanai et al., 2012; A. Popp, Humpenöder, et al., 2014), and increased food prices (Humpenöder et al., 2018a).

Literature on climate impacts show mostly positive results. As discussed in Section 2.3.7, restricted use of forests and agricultural intensification within bioenergy scenarios could substantially reduce LUC emissions resulting from energy cropland expansion. Findings by Melillo et al. (2009) and Humpenöder et al. (2018a) suggest potential CO<sub>2</sub> reductions of 167

GtCO<sub>2</sub> and 208 GtCO<sub>2</sub> respectively by 2100 from incorporating a global forest conservation policy with second-generation bioenergy expansion. Hallgren et al. (2013) further demonstrate positive climate impacts, estimating both a reduction in global biogeochemical warming (0.7 °C) and global biogeophysical cooling (0.02 °C) by 2050 when implementing forest protection. The studies mentioned additionally indicate the need for more research into climate impacts of land conservation within future bioenergy scenarios, as well as other sustainability concerns such as biodiversity.

While literature exists on impacts of land conservation schemes and biodiversity conservation schemes within mitigation pathways, there is little evidence of research on the interaction between these two sustainability measures. Previous studies incorporating land conservation policies in future bioenergy scenarios suggest the need for more research into biodiversity implications (Hallgren et al., 2013; Humpenöder et al., 2018a). On the other hand, studies incorporating biodiversity conservation targets in scenarios point out the simplicity of implementing these targets in current models, with most using an additional constraint for land allocation (e.g., excluding protected areas from bioenergy or food production) (Beringer et al., 2011; Erb et al., 2012; Meller et al., 2015; Heck et al., 2018; Leclère et al., 2018; IPBES, 2019). Regarding the latter, estimates by Beringer et al. (2011) and Erb et al. (2012) indicate global bioenergy potentials of 26–270 EJ yr<sup>-1</sup> depending on how much biodiversity conservation is incorporated in the scenario. Uncertainty within this estimate implies the need for more research into biodiversity impacts within future mitigation pathways. Spatial analysis comparing biodiversity data and land conservation schemes in bioenergy scenarios could aid the development of more sustainable pathways.

## **2.5.2 Water Conservation**

### **2.5.2.1 Current Water Requirements and Conservation Schemes**

Around 70% of global freshwater withdrawals are used for irrigating agricultural systems, of which a large portion is lost due to bad management and faults in conveyance systems (Postel et al., 2008; Gleick and Cooley, 2009; Molden et al., 2010; Foley et al., 2011; Gerbens-Leenes, 2017). Irrigated areas have almost doubled over the last 50 years, and currently constitute around 20% of global cultivated land (Foley et al., 2011; Meier et al., 2018). Cultivation of

dedicated bioenergy crops is very water intensive; thus, irrigation application could play a crucial role in achieving high yields (Berndes, 2002; Gerbens-leenes et al., 2009; Bonsch, 2015; Bonsch et al., 2016). Previous work has shown that irrigation could increase bioenergy yields by more than 100% compared to rainfed production systems (Beringer et al., 2011). However, such large withdrawals can put additional pressure on freshwater ecosystems (SDG 14) (Berndes, 2002; Bonsch et al., 2016; Heck et al., 2018; Stoy et al., 2018; Fajardy et al., 2019).

Water is heterogeneously distributed around the globe, hence there exist highly water stressed areas, particularly in China, South Asia, and the United States (Oki and Kanae, 2006). Estimates have shown that over 1 billion people live in areas exposed to high water stress, and that over 700 million people lack access to safe drinking water (Oki and Kanae, 2006; WHO/UNICEF, 2014). Further, freshwater biodiversity trends indicate declines averaging 54% among freshwater vertebrates due to global water usage (Groombridge and Jenkins, 2000; Loh, 2000). Humpenöder et al. (2018a) calculate that second-generation bioenergy expansion could lead to a +142% global increase in water use above environmental flow (EF) requirements, i.e., water required to maintain the ecosystem functions of rivers and lakes, compared to a scenario without bioenergy. With many regions already facing water scarcity and ecosystem degradation, this increase would be fatal.

Policies protecting freshwater ecosystems from destruction due to bioenergy production need to be designed, addressing potential trade-offs between ecosystems and economic incentives opposing sustainable water use. Current certification schemes, including those mentioned for land conservation in addition to the Alliance for water Stewardship (AWS), incorporate water conservation to varying degrees (Fehrenbach, 2011; Bonsch et al., 2016). Most of these schemes cover three key areas: excessive water consumption, water scarcity and protection of water quality. Water quality is reasonably accounted for with legal threshold values largely in place, though difficulties arise in agricultural activities such as the application of fertilisers and pesticides. Tracing of pollutants from these applications to surface or ground water bodies is complex and generally delayed. Monitoring and auditing of these application processes can identify more efficient options and areas for improvement. The ISCC (International Sustainability and Carbon Certification), for instance, incorporate an extensive list of criteria and requirements regarding fertiliser, chemical use, washing and storage etc to help prevent water contamination. Avoidance of excessive water consumption is further addressed in most schemes through water management plans, efficient use and re-use, and optimisation of irrigation. However, a case-by-case approach is needed as even efficient and sparing use of

water can be excessive if the consumer is larger than the available water supply. Water scarcity is harder to evaluate and standardise and is highly dependent on physical factors such as the regional resolution of the data used, and economic aspects of the region being studied.

For a biomass project to be certified, each of the above areas will need to be considered. Schemes such as RSB (The Roundtable on Sustainable Biofuel), SAN (Sustainable Agriculture Network) and GGL (Green Gold Label) are prepared to cover these. However, even with the best intentions, the overall water policy of a country can counteract aims outlined in small projects. The AWS is an initiative that could potentially tackle this as it connects bioenergy production with all other water-relevant sectors. Overall, the certification of bioenergy-related water impacts will be a challenge, with periodic monitoring of regional, national, and international policies, and stakeholder engagement, needed for successful implementation.

### **2.5.2.2 Water Conservation in Future Impact Assessments**

Research into sustainability implications of water conservation regarding bioenergy production is growing though still in great need of further work. One method for incorporating certification schemes is by incentivising rainfed bioenergy production e.g., irrigating only food and feed cropland and leaving energy cropland to be rainfed (Bonsch et al., 2016; Humpenöder et al., 2018a). This could allow consumers to make an informed choice and thus generate a market incentive for less water intensive production. Additionally, governments could further create direct incentives for rainfed bioenergy production through taxes and subsidies. For example, South Africa has already ceased the support of bioenergy crops under irrigation (Moraes et al., 2011). While incentivising rainfed bioenergy production could be beneficial for protecting water resources, it neglects trade-offs with land resources. To overcome threats to both land and freshwater resources, human water withdrawals can be limited to sustainable levels. This would require site specific understanding of how much water is required for a functioning ecosystem. Estimates of such water requirements — or Environmental Flows (EF) — are already available, though more research is needed to improve the accuracy of these (Smakhtin et al., 2004; Poff et al., 2010; Gerten et al., 2013; Pastor et al., 2014; Bonsch et al., 2015; Humpenöder et al., 2018a).

Previous work in this field has shown that without dedicated water protection policies, large-scale bioenergy production from second-generation energy crops may lead to severe degradation of freshwater ecosystems (Bonsch et al., 2016). However, prohibiting irrigated

energy crop production could also lead to increased food prices (de Fraiture and Wichelns, 2010; Bonsch et al., 2015) and loss of natural land that contain important terrestrial ecosystems and high carbon stocks (Bonsch et al., 2016; Humpenöder et al., 2018a). Humpenöder et al. (2018a), for instance, calculate that implementation of a water protection policy with bioenergy expansion results in higher global LUC emissions (425 GtCO<sub>2</sub>) than for a bioenergy scenario without water protection (349 GtCO<sub>2</sub>). Measures for increasing irrigation efficiency, such as improvements in water storage and transport, and better land management practices (e.g., mulching and tillage), can help reduce these negative impacts (Humpenöder et al., 2018a). Establishing a balance between use of water protection policies, increasing irrigation efficiency, and sustainable use of land will be required for the development of large-scale bioenergy. Though previous work has indicated potential adverse impacts on the land system as a whole, more research into specific interactions with biodiversity and climate could contribute to knowledge within this field.

## 2.6 Conclusions from the Literature

Global second-generation bioenergy production remains a key option for achieving negative emissions in mitigation pathways. However, the subject of bioenergy is controversial, with many studies highlighting significant trade-offs with the land system. This concern has been a major driver for model and scenario intercomparison studies aiming to determine the potential for bioenergy deployment within our developing society. Previous work on sustainability implications of land use for bioenergy tends to focus on food security, energy security, and life cycle GHG emissions, aspects that can be directly calculated by integrated assessment models (IAMs). Climate regulation and biodiversity are two other major environmental concerns that will be affected yet are relatively understudied, largely due to a lack of suitable data resources and the overall complexity involved in calculating these impacts.

Most literature on land-use impacts of bioenergy focus on present day first-generation bioenergy cropland and/or tend to be at the regional or local scale. This is largely due to a lack of data on spatial projections of more advanced energy cropland within future pathways. As second-generation bioenergy production becomes a more viable option, developments in such data has progressed, enabling ongoing research into potential global impacts of second-generation bioenergy expansion within SSP and RCP pathways. This data can further be used within climate and biodiversity modelling, alongside other spatial climate data and biodiversity

indicators (e.g., the Red List Index) that are often utilised in climate and biodiversity research however are less represented in the bioenergy literature (Dornburg et al., 2008; Beringer et al., 2011; Hallgren et al., 2013; Immerzeel et al., 2014; Heck et al., 2018; Harper et al., 2018; Muri, 2018; Tudge et al., 2021; Hanssen et al., 2022). For this study, land-use data has been created using the MAgPIE (Model of Agricultural Production and its Impact on the Environment) land-use optimisation model, obtained from researchers at the Potsdam Institute for Climate Impact Research (PIK) (Humpenöder et al., 2018a).

As discussed in this chapter, a variety of methods can be used to understand the interactions between bioenergy deployment, land-use changes, and corresponding climate and biodiversity impacts. Regarding climate impacts, findings in Section 2.3.2.2.2. indicate the efficiency and accuracy of implementing the LUCID-CMIP5 simulation method within an Earth system model of intermediate complexity (EMIC) using land-use projections from a well-established IAM (in this case, the MAgPIE model). Hence, the University of Victoria (UVic) ESCM v.29 has been chosen for this analysis, provided by Concordia University, Montreal (Weaver et al., 2001; Matthews, 2004; Simmons and Matthews, 2016).

An assessment of biodiversity modelling approaches in Section 2.4.3.2.1 further indicates that, while it has its limitations, the species richness indicator can be used to broadly demonstrate information about an entire eco-region, so is a suitable choice for understanding global impacts of bioenergy expansion on biodiversity. By applying a form of the species-area modelling to the mentioned MAgPIE land-use projections, alongside species ranges, projected habit and species loss can be calculated. However, due to high criticism of the species-area relationship (SAR) model and its tendency to overestimate, the endemics-area relationship (EAR) model will be used in this work (Kinzig and Harte, 2000). High priority areas, namely the biodiversity hotspots and Alliance for Zero Extinction (AZE) sites, will be used to explore loss of habitat as well as potential impacts on endangered and critically endangered species. Literature findings further indicate the importance of both climate and land-use impacts in biodiversity assessments (Powell and Lenton, 2013; Bellard et al., 2014; Jantz et al., 2015; Chaudhary and Mooers, 2017; S. V Hanssen et al., 2020; Tudge et al., 2021). However, due to time limitations and resource availability, only land-use impacts will be calculated in this assessment.

Previous work has further demonstrated the importance of incorporating sustainability measures alongside large-scale bioenergy deployment (Bonsch et al., 2016; Humpenöder et al., 2018a). Without dedicated forest and water protection policies, as well as other measures such

as improved agricultural productivity, second-generation bioenergy expansion could lead to severe degradation of freshwater and terrestrial ecosystems, higher LUC emissions, nitrogen losses, and increases in food prices. While a number of land and water conservation schemes do currently exist, attention to land for bioenergy is still in its infancy. Such schemes also face ongoing challenges, such as counteractions with country-level policies, violations in implementation, and cropland ‘leakage’ onto other important ecosystems. Understanding the impacts of these regulations within the context of global bioenergy deployment is a crucial component of future climate and biodiversity impact assessments and will thus be included in this work.



## **Chapter 3 Methods: The MAgPIE Land-Use Model and Scenarios**

### **3.1 Overview**

This chapter describes the four land-use scenarios used in this thesis to represent mitigation pathways with and without bioenergy expansion. These scenarios have been generated using the global multi-regional land-use optimisation model MAgPIE (Model of Agricultural Production and its Impacts on the Environment) and have been provided by the creators (Humpenöder et al., 2018a) for the purpose of this work. This chapter explores some of the key features within the MAgPIE scenarios and provides a comparison to other land-use pathways used in the current literature.

### **3.2 Introduction to the MAgPIE Scenarios**

#### **3.2.1 MAgPIE Land-Use Optimisation Model**

As discussed in *Chapter 2*, a variety of integrated assessment models (IAMs) can be used to determine potential socio-economic (SSP) and climate (RCP) pathways. Each of these models contain land-use modules which explicitly model land-use change, depending on biogeochemical, biogeophysical and socio-economic inputs. At the time this work was carried out, the isolation of bioenergy cropland expansion within spatial land-use change was in the development stage for many IAM research groups. Obtaining adequate scenario data — i.e., including spatial energy cropland distributions in the correct format — for determining bioenergy impacts was therefore the first challenge. Through personal communication with creators of leading IAMs (i.e., GCAM, IMAGE, and REMIND-MAgPIE), it was decided by the author that four land-use scenarios (see Section 3.2.2) created by the MAgPIE land-use

optimisation model would be most suited for the purpose of this work, due to their readily available format type and usefulness in understanding bioenergy impacts.

The MAgPIE model has been developed by the Potsdam Institute for Climate Impact Research (PIK). It consists of a spatially explicit global land and water-use allocation model which simulates land-use dynamics at a spatial resolution of  $0.5^\circ \times 0.5^\circ$ . The goal of MAgPIE is to minimise total costs of production whilst fulfilling food, feed, material, and bioenergy demand, under socio-economic and biophysical constraints. Cost minimisation is solved through endogenous changes in land conversion (at the simulation unit level), technological change (at the regional level), and spatial rainfed and irrigated production patterns (subject to regional trade constraints).

Socio-economic constraints include, for instance, demand for agricultural commodities, technological development, and production costs, and are defined for 10 world regions. Biophysical constraints comprise land availability (Erb et al., 2007; Krause et al., 2013), as well as crop yields, carbon density and water availability, derived from the global hydrology and vegetation model LPJmL (Lund-Potsdam-Jena model for managed Land) (Bondeau et al., 2007; Rost et al., 2008; Müller and Robertson, 2014). The LPJmL model combines process-based, large-scale representations of terrestrial vegetation dynamics and land-atmosphere carbon and water exchanges into a modular framework. Over decades, this model has been developed as a DGVM of intermediate complexity, based on the well-established BIOME family of models (Prentice et al., 1992; Haxeltine and Prentice, 1996; Haxeltine et al., 1996; Kaplan, 2001). The MAgPIE model is particularly equipped for modelling irrigation and rainfed cropland. Unlike many other IAMs (e.g., IMAGE and GCAM), MAgPIE can shift all types of cropland production from being irrigated to rainfed, and vice versa, in response to economic or climatic drivers (see Section 3.2.2.4) (A. Popp, Rose, et al., 2014). Based on all considered conditions, the model determines specific land-use patterns, yields and total costs of agricultural production for each grid cell for different scenarios.

A variety of studies have been carried out previously using MAgPIE. Land-based assessments cover a wide range of topics, such as diet shifts, bioenergy, afforestation, trade liberalisation, technological changes in agriculture, as well as associated impacts on GHG emissions and water and land availability (Lotze-Campen et al., 2008; Popp et al., 2010; Schmitz et al., 2012; Dietrich et al., 2014; Bonsch, 2015; Bonsch et al., 2016; Wang et al., 2016; Humpenöder et al., 2018a). As previously discussed, MAgPIE is also commonly used in connection with the

integrated assessment model REMIND (REgional Model of Investment and Development), also developed by PIK. REMIND is a global multi-regional model that can be used to assess future climate change mitigation policies, while integrating interactions between the economy, the energy sector, and climate change (Leimbach, Bauer and Baumstark, 2010; Leimbach, Bauer, Baumstark, et al., 2010; Bauer et al., 2012; Luderer et al., 2013). Together, these models have therefore been used to produce outputs for the RCP and SSP pathways, which incorporate changes of land use, economy, energy, and climate.

### 3.2.2 MAgPIE Land-Use Scenarios

The four MAgPIE land-use scenarios have been created by researchers at PIK, and comprise a control scenario without second-generation bioenergy ('NoBio'), a bioenergy scenario incorporating large-scale second-generation bioenergy ('Bio'), a bioenergy scenario which further includes a global REDD+ policy ('Bio-REDD'), and a bioenergy scenario including a global water protection policy ('Bio-WaterProt') (Humpeöder et al., 2018a) (see **Figure 3.1**). All four scenarios are based on the SSP2 'middle-of-the-road' storyline, which depicts a continuation of current economic, social, and technological trends into the future (though SSP1 and SSP5 have been used for a sensitivity analysis to determine food demand). This pathway has been chosen as it provides a basis for determining potential implications of implementing global bioenergy production (and REDD+/water conservation policies) into society as it stands today.

Land-use types within the scenarios include energy cropland, food/feed cropland, pasture, forest, and other natural land (such as non-forest natural vegetation, abandoned agricultural land and desert) (Humpeöder et al., 2018a). For the purpose of this thesis, all land-use types apart from other natural land have been utilised by the author. First-generation bioenergy follows the same trajectory in each scenario, increasing to 7 EJ globally by 2020 and remaining constant from then onwards. First-generation bioenergy crops consist of conventional food crops such as maize and sugarcane, thus is included in the land-use type 'food/feed cropland'. The forestry sector (i.e., forestry plantations and modified natural forest) in MAgPIE is currently not executed dynamically and is therefore kept fixed over the century. This accounts for around 30% of initial global forest area in the scenarios. In addition, 12.5% of this initial forest area is undisturbed natural forest within protected forest areas, also kept fixed throughout the scenarios.

### 3.2.2.1 NoBio

The absence of second-generation bioenergy expansion in the NoBio scenario means that this scenario can be used as a control to compare bioenergy scenarios to. It can also be used to represent the impacts of expanding food/feed cropland on global land-use change over the century. As outlined in the work of Humpenöder et al. (2018a), food demand for 10 world regions is determined based on population and income projections following the SSP1, SSP2, and SSP5 pathways. The methodology for calculating food demand has been taken from Bodirsky (2015) and is a regression analysis based on calorie demand and income. Food and feed are produced in MAgPIE by 20 cropping activities and 3 livestock activities, whereby feed for livestock is a mixture of crops, crop residues, processing by products and pasture (PIK, 2022).

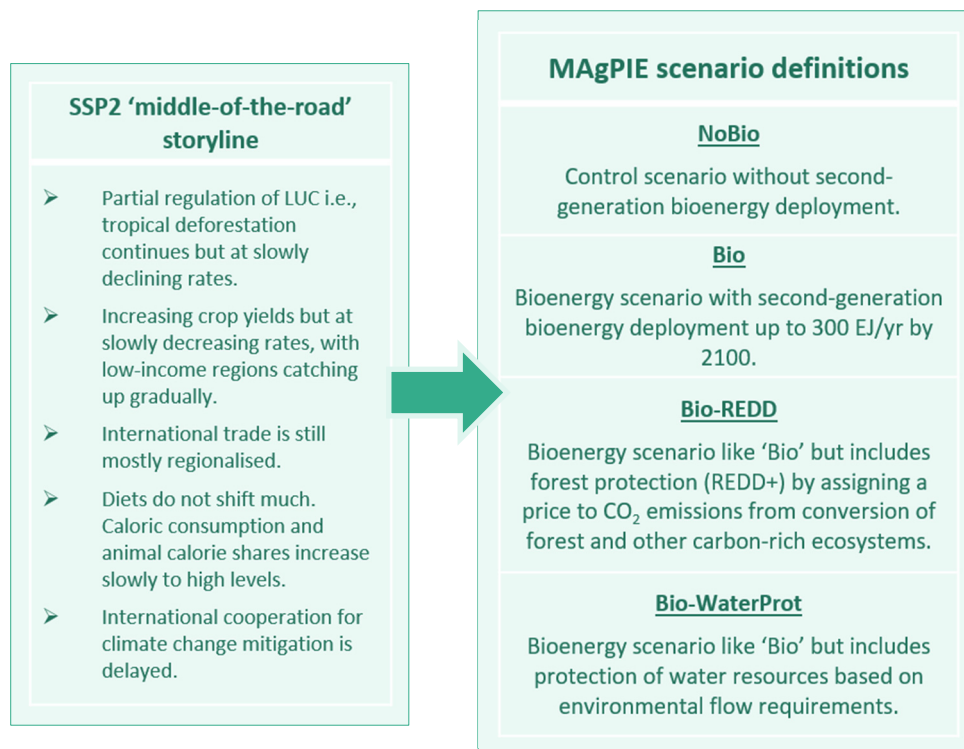


**Figure 3.1:** Summary of the MAgPIE scenarios. These scenarios have been created by authors Humpenöder et al. (2018a), and generally follow the SSP2 'middle-of-the-road' pathway, detailed by Popp et al (2017).

### 3.2.2.2 Bio

In the aim of avoiding competition with food production whilst reaching ambitious climate mitigation targets, the Bio scenario incorporates the increasing use of second-generation bioenergy production across the globe (Humpenöder et al., 2018a). This includes high-yielding dedicated crops such as grasses (e.g., miscanthus) and fast-growing trees (e.g., eucalyptus, poplar). While first-generation bioenergy is implemented based on current biofuel policies, second-generation bioenergy production is based on upper end projections of bioenergy deployment in 1.5 °C to 2 °C pathways determined by integrated assessment models (IAMs). Hence, the scenario creators have implemented a linear increase of second-generation bioenergy demand from 0 EJ to 300 EJ between 2010 and 2100 in the model. As shown in **Figure 3.2**, this demand trajectory is roughly midway between all other IAM projections for the SSP2 pathway.

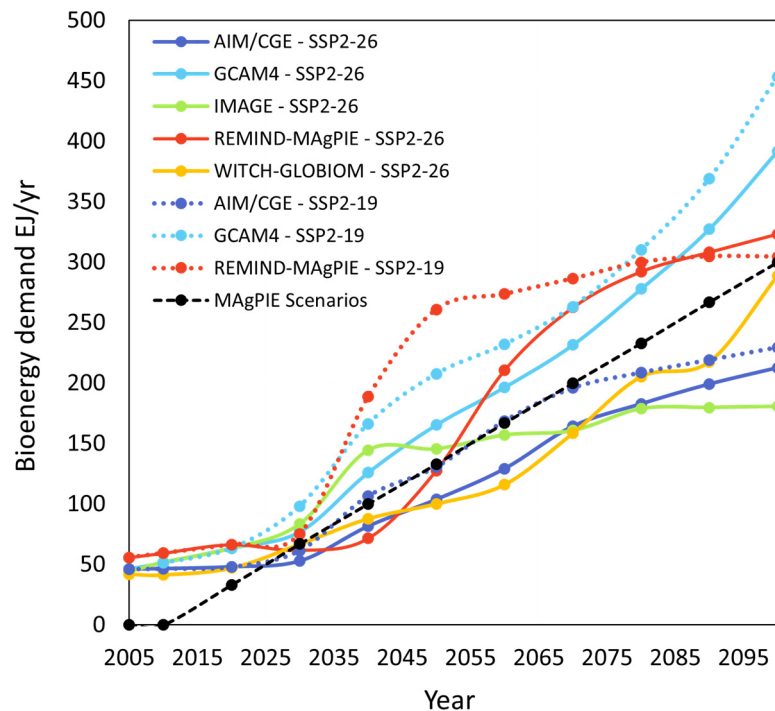


**Figure 3.2:** Second-generation bioenergy demand in the MAgPIE scenarios between 2005 and 2100. Bioenergy demand is also provided for other SSP2 scenarios following RCP2.6 and RCP1.9 pathways. Values for the SSP-RCP pathways have been taken from the online SSP database (IIASA, 2018b).

Energy cropland for second-generation bioenergy expands into all other land-use types (i.e., forest, pasture, food/feed cropland and other natural land). Cropland expansion into forests is limited by intra-regional transport costs and travel times to major cities (Narayanan and Walmsley, 2008; Nelson, 2008), as well as the fact that 42.5% of initial global forest area is unavailable due to wood harvest and forest protection (Humpenöder et al., 2018b). Food/feed cropland can be displaced either nearby or to another region due to energy cropland expansion, though at the global level food/feed cropland is kept constant.

Other factors influencing bioenergy expansion in the MAgPIE scenarios are changes in yields of both energy and food/feed crops. These result from technological change and irrigation, whereby irrigation of cropland leads to higher yields than rainfed cropland. The LPJmL model is used to determine potential crop yields, derived for seven different intensity management levels (Dietrich et al., 2012) which are in line with observed country level yields from (FAO, 2015). These are then calibrated to maximise agreement between MAgPIE and FAO cropland in the starting year for each of the modelled 10 world regions. Both bioenergy and food/feed cropland yields are calibrated using the same land-use intensity assumptions, because there is currently no robust information on 2<sup>nd</sup> generation bioenergy available in FAO. For future predictions, it is assumed that bioenergy yields in Europe and USA align with yields produced under highest present day observed land-use intensification. In all other regions, bioenergy yields are downscaled proportional to the land-use intensity of Europe. Large yield gaps regarding management practices are represented by low calibration factors for Sub-Saharan Africa and Latin America.

### **3.2.2.3 Bio-REDD**

Reduced Emissions from Deforestation (REDD+) schemes can be implemented to help prevent the loss of carbon-rich forest and, in turn, reduce negative impacts on climate and biodiversity. The Bio-REDD scenario incorporates forest protection through a global REDD+ scheme (Humpenöder et al., 2018a). This scheme is deployed by pricing CO<sub>2</sub> emissions from the conversion of forests and other natural ecosystems. Consequently, costly conversion of carbon-rich ecosystems for cropland is avoided where possible, displacing this cropland onto other land types, such as pasture. In the Bio-REDD scenario, CO<sub>2</sub> price trajectory increases nonlinearly at a rate of 5% per year, starting from 0 US\$ in 2010, up to 155 US\$ in 2100 (A. Popp, Humpenöder, et al., 2014; Humpenöder et al., 2018a). For scenarios without forest protection (NoBio, Bio and Bio-WaterProt), the CO<sub>2</sub> price remains at 0 US\$ over the century.

#### 3.2.2.4 Bio-WaterProt

In the MAgPIE model, water used for domestic, industrial, and agricultural purposes is provided by renewable blue water resources only. These include precipitation that enters rivers, lakes and aquifers (Rost et al., 2008). However, cultivation of bioenergy and food/feed crops is very water intensive (Berndes, 2002; Gerbens-leenes et al., 2009). Therefore, to avoid degradation of freshwater ecosystems due to bioenergy expansion, human water withdrawals can be limited to an amount compatible with local environmental flow (EF) requirements i.e., water required to maintain the ecosystem functions of rivers and lakes (Gerten et al., 2013; Bonsch et al., 2015; Humpenöder et al., 2018a). As indicated by the scenario creators (Humpenöder et al., 2018a), the Bio-WaterProt scenario incorporates water protection based on environmental flow protection (EFP) as described by Bonsch et al. (2015), whereby annual volumes of water are saved for EFP from 2015 onwards. In contrast, no water is reserved for environmental purposes in all other scenarios (NoBio, Bio and Bio-REDD), in which all renewable freshwater is made available for human use.

### 3.3 Land-Use Changes Within the MAgPIE Scenarios

#### 3.3.1 Global Land-Use Change

Trajectories of land-use changes in the MAgPIE scenarios indicate the potential impacts of bioenergy expansion on different land-use types. An analysis of the scenarios by the author indicates that, to fulfil bioenergy demands of 300 EJ/yr by 2100, global second-generation energy cropland increases steadily over the century, reaching  $6.36\text{--}6.67 \times 10^6 \text{ km}^2$  by 2100 across all scenarios (relative to  $0 \times 10^6 \text{ km}^2$  in 2005) (see **Figure 3.3**). Increased food demand due to bioenergy incorporation leads to more land needed for food/feed cropland over the century ( $4.42 \times 10^6 \text{ km}^2$  or 29% by 2100 relative to 2005 in Bio), compared to the scenario excluding bioenergy expansion ( $3.51 \times 10^6 \text{ km}^2$  or 23% by 2100 in NoBio). Both energy and food/feed cropland mainly expand into pasture and forest land, by varying amounts depending on the scenario.

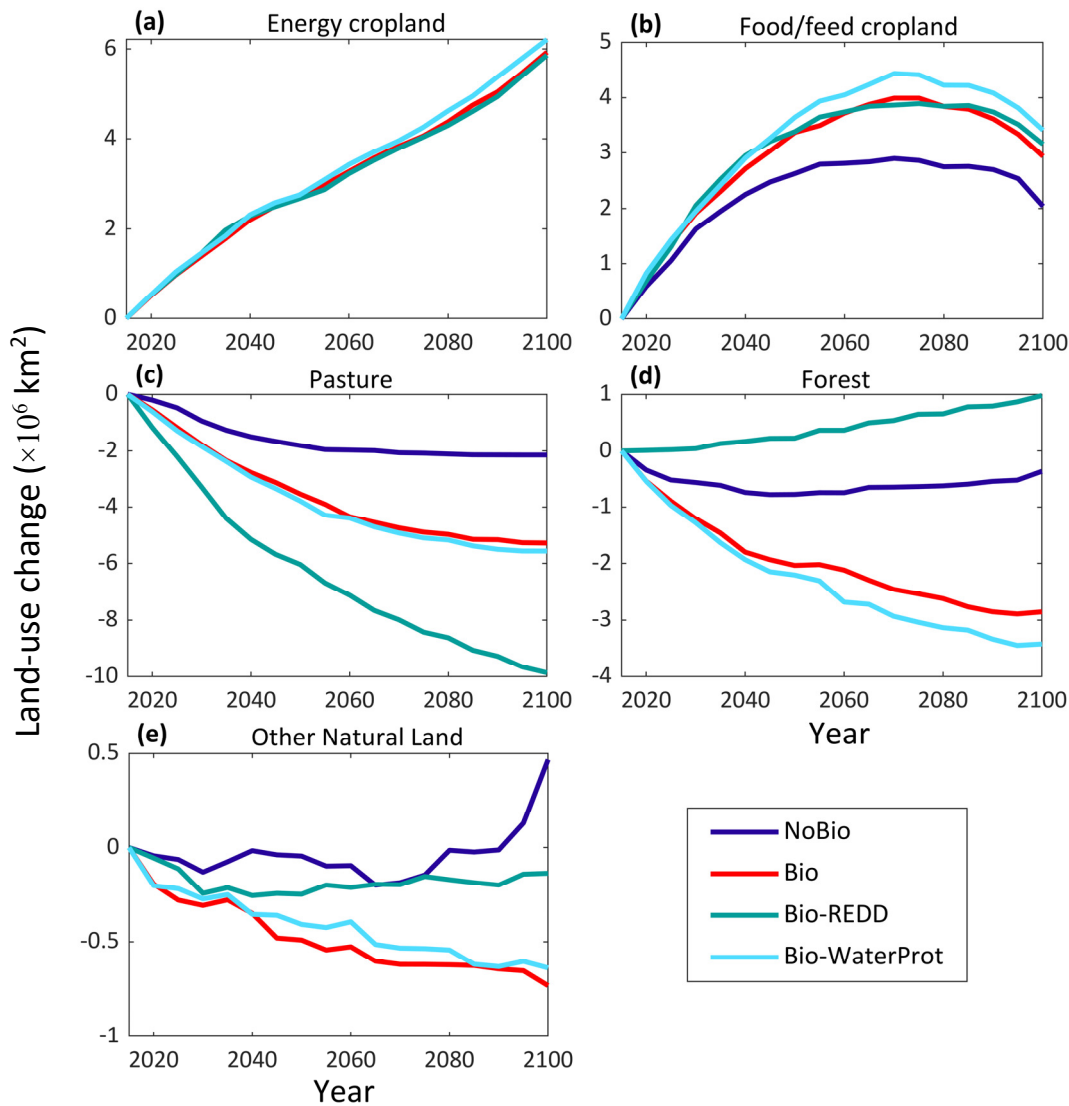


**Figure 3.3:** Global land-use changes for each land type in the MAGPIE scenarios, between 2005 and 2100.

In the absence of a global REDD+ policy (in Bio/ Bio-WaterProt), forest declines to  $(- )3.27/(- )3.95 \times 10^6 \text{ km}^2$  ( $(- )7.9/(- )9.5\%$ ) by 2100 relative to 2005. When REDD+ is incorporated, this eliminates the use of forest for cropland, whereby a global increase in forest occurs instead ( $0.915 \times 10^6 \text{ km}^2$  or 2.2% by 2100). Pasture is used to a large extent in all scenarios, however, is largest in Bio-REDD to compensate for the lack of forest used. As a result, almost double the amount of pasture is used in Bio-REDD ( $11.5 \times 10^6 \text{ km}^2/38\%$  by 2100) compared to Bio and



Bio-WaterProt ((-) $6.24 \times 10^6$  km<sup>2</sup>/(-)21% and (-) $6.90 \times 10^6$  km<sup>2</sup>/(-)23% by 2100 respectively) for cropland expansion. Other natural land declines by only a small amount across the Bio/Bio-WaterProt scenarios ((-) $1.26/(-)1.29 \times 10^6$  km<sup>2</sup> or (-)3.1/(-)3.2% by 2100), with REDD+ incorporation reducing these impacts significantly (to (-) $0.38 \times 10^6$  km<sup>2</sup> or (-)0.93% by 2100).

The overall impact of a global water protection policy is a small further increase in pasture and forest used for food/feed and energy cropland (compared to the Bio scenario). This is because the global water protection policy prohibits irrigation of bioenergy production, leaving energy cropland to be rainfed. Irrigated cropland leads to substantially higher yields per unit area compared to rainfed cropland. Thus, in the absence of irrigation, more land is needed to utilise rainwater and fulfil energy cropland demands.

### 3.3.2 Regional Land-Use Change

As illustrated in **Figure 3.4**, bioenergy expansion in the MAgPIE scenarios mainly occurs in the tropics, with Sub-Saharan Africa and Latin America together accounting for half of production. Significant expansion also takes place in Southeast Asia and Eastern parts of North America. This expansion occurs at the expense of both pasture and forest, whereby deforestation is particularly high in the Democratic Republic of Congo. Food/feed cropland is also affected globally, with significant displacement occurring due to bioenergy expansion. According to Humpenöder et al. (2018a), this leads to increases in food prices among all regions, however Latin America is impacted the most.

Implementing REDD+ in the Bio-REDD scenario significantly reduces forest lost from bioenergy production, with increases in forest cover occurring across parts of Latin America, Europe, and Asia (compared to the NoBio scenario). However, shifts in food/feed cropland yield further increases in food prices, particularly in developing and emerging economies such as Southern Asia, Latin America, and Sub-Saharan Africa (Humpenöder et al., 2018a). Incorporation of water protection leads to food/feed and energy cropland expanding further into nearby forests and pasture. Implications due to the absence of irrigation are strongest in regions that have less water availability (e.g., Sub-Saharan Africa). In these regions, more area is needed for food/feed cropland, leaving less area for energy cropland. This results in a shift of cropland to other regions which may contain carbon- and biodiverse-rich forest or pasture.

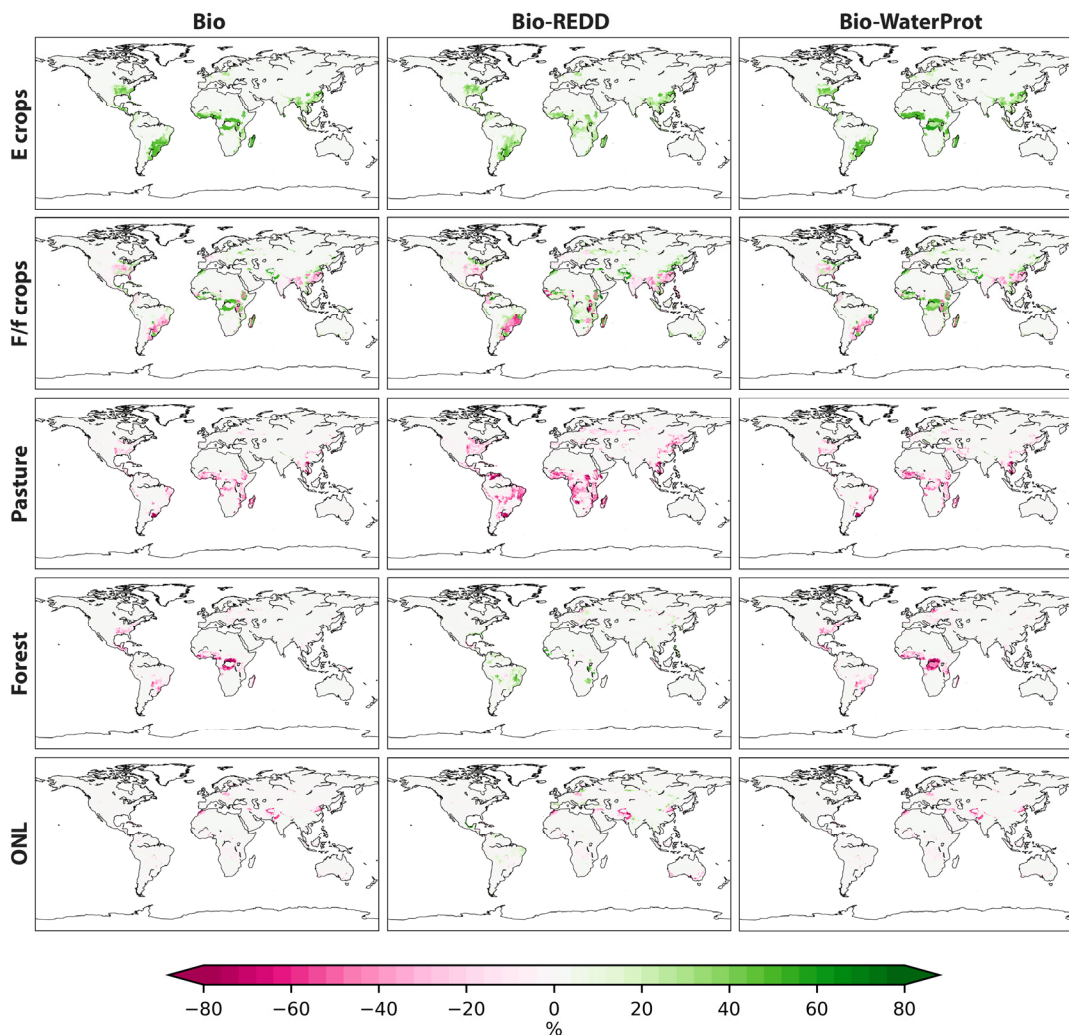


**Figure 3.4:** Regional bioenergy-induced land-use changes within the bioenergy scenarios (Bio, Bio-REDD and Bio-WaterProt compared to NoBio), in 2100 relative to 2005. Values are percentages of grid cells undergoing land cover changes.

### 3.3.3 Comparison to Other Pathways

A comparison of the MAGPIE scenarios to other SSPs and RCPs calculated from different IAMs (by Popp et al., (2017)), can help identify the overall structural features of these IAMs; in particular, how land is used within these models for climate mitigation and changing socio-economic patterns (see **Figure 3.5**).

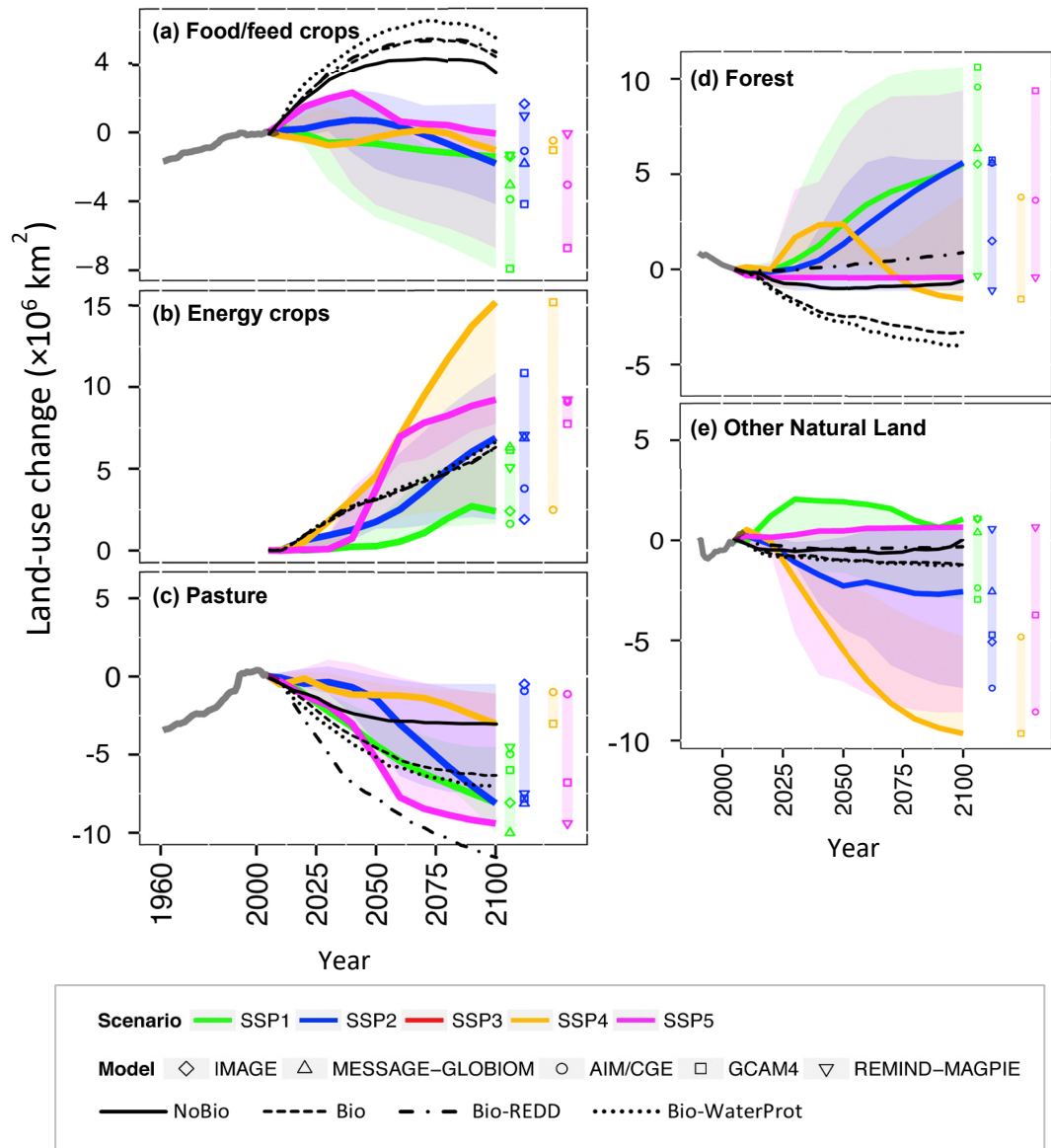


**Figure 3.5:** Global land-use changes in the MAGPIE scenarios. These have been overlaid by the author onto trajectories previously calculated by Popp et al. (2017) for each SSP following RCP2.6 using different integrated assessment models. Values are presented for the period 2005 to 2100.

All models use bioenergy as a land-based mitigation option to some degree. In comparison to other projections in **Figure 3.5**, the energy cropland trajectories for the MAGPIE scenarios are mostly in line with those from the REMIND-MAGPIE model for SSP2 RCP2.6, as expected. Similarly to the bioenergy demands seen in **Figure 3.2**, values for energy cropland expansion in the MAGPIE scenarios are situated roughly midway between all SSP trajectories for the

RCP2.6 pathway. This illustrates that bioenergy is a strong land-based CDR mitigation measure within the MAgPIE scenarios, making them ideal for the purpose of this work.

Other land-based mitigation options used within the models are avoided deforestation and afforestation. In the MAgPIE (and REMIND-MAgPIE) scenarios, avoided use of forest or other natural land is implemented as the main mechanism for land-based mitigation (alongside bioenergy) (A. Popp, Rose, et al., 2014; Popp et al., 2017). Afforestation, in addition to avoided deforestation, is also incorporated with higher land regulation (i.e., in the Bio-REDD scenario). Hence, values for Bio-REDD closely align with those of other SSP2 pathways, which have similarly strict forest regulations. In some of these other models, afforestation is used partly to compensate for less bioenergy production as a CDR measure (e.g., IMAGE, AIM/CGE).

Overall, conservation of forest and other natural land in the MAgPIE scenarios results in significant use of pasture for energy and food/feed cropland. This is reflective of other SSP2 pathways, though the incorporation of REDD+ leads to losses of similar magnitude to high findings for the SSP1 (MESSAGE-GLOBIOM) and SSP5 (REMIND-MAgPIE) pathways, which also impose strong regulations on forest conversion. For the SSP1 scenario, this is due to overall large sustainability goals, whereas for SSP5 avoided deforestation (and afforestation) is used to help compensate for high fossil fuel emissions.

In contrast to energy cropland, increases in food/feed cropland expansion in the MAgPIE scenarios are significant compared to other modelled findings for the SSP2 RCP2.6 pathway, partly due to the use of SSP1, SSP2 and SSP5 population and income projections to derive the food demand scenarios (Humpeñöder et al., 2018a). This is also due to model assumptions regarding sensitivities of food demand to increased food prices from mitigation pressure on land (Popp et al., 2017). For the MAgPIE model (and REMIND-MAgPIE and IMAGE), this sensitivity is low compared to models such as GCAM and MESSAGE-GLOBIOM, thus more food/feed cropland growth occurs. Additionally, energy cropland expands onto land previously used for food/feed cropland, therefore displacing this food/feed cropland onto other land.

Competition for land between energy and food/feed cropland is one of the main causes of increased forest loss in the MAgPIE scenarios. This is particularly displayed in scenarios Bio and Bio-WaterProt, whereby values are close to high estimates in the RCP4.5 pathway (SSP3 AIM/CGE and SSP2 IMAGE; see Figure 4 in Popp et al. (2017)). Another reason for this forest loss could be the avoided use of ‘other natural land’ in MAgPIE, land that is used significantly in other modelled SSP2 pathways. Thus, if more other natural land was used in MAgPIE, this

could imply that less forest loss may occur. On the other hand, this other natural land may also contain high carbon stocks and biodiversity so its preservation could be equally as important. As illustrated by the Bio-REDD scenario, with increased avoided deforestation, afforestation, and more use of pasture, this forest loss is significantly reduced. The wide variation between Bio and Bio-REDD scenarios highlights the substantial impact of forest conservation within models and thus further provides ground for using these scenarios in this work.

### **3.4 Uncertainties in Land-Use Modelling**

Differences in land-use projections across the various pathways in Section 3.3.3 demonstrate large uncertainties in the global agricultural system and its dynamics. These variations are due to differences in model architectures and philosophies, uncertainties in modelled processes (e.g., irrigation of cropland, forest conservation), and differences in parameterising these processes with regards to the SSP storylines. Gross domestic product (GDP) and population trends tend to be explicitly prescribed depending on the pathways, whereas other drivers (e.g., agricultural production, trade, land use, and food prices) are prescribed in more qualitative terms from the scenario creators (Popp et al., 2017). Such factors lead to even more range between the model outputs.

One of the largest areas of uncertainty across models is in assumed increase in crop yields. Most models, including MAgPIE, calculate a doubling of current food/feed levels, which is in agreement with FAO projections until 2050 (Alexandratos and Bruinsma, 2012). However, researchers are continually questioning whether it is possible to reach such high yields in the future, as some important sources of yield improvements, like increasing the harvested index, might have reached their limits. Alternatively, improvements in regions such as Sub-Saharan Africa to help reach currently attainable yields would be a very achievable way to help close yield gaps (Mueller et al., 2012; Smith et al., 2014).

Bioenergy implementation itself is a major uncertainty in all mitigation pathways. As discussed in Section 3.3.3, a large range of land-use changes can occur around increasing bioenergy potential. Successful implementation will rely on huge innovations, such as substantial yield increases, and large-scale implementation of BECCS technology, all whilst carrying out measures to preserve natural land. Uncertainties also occur within other mechanisms for mitigation. For instance, reductions of non-CO<sub>2</sub> emissions in the agricultural sector will depend

on high adoption rates worldwide. Additionally, some land-based mitigation options such as soil carbon management are not included in these pathways, including the MAgPIE scenarios, yet will be equally as important (Smith et al., 2013; Smith et al., 2014). Furthermore, mitigation within scenarios is determined based on emissions and carbon balances, rather than land cover and land management (Luyssaert et al., 2014). IAMs therefore tend to neglect the biogeophysical consequences of land-based mitigation, discussed previously in *Chapter 2*, Section 2.3.6.

### **3.5 Advantages of Using the MAgPIE Land-Use Scenarios**

While the MAgPIE scenarios have their limitations, one major benefit they have compared to the mentioned SSP pathways (in Section 3.3.3; Popp et al., (2017)) is that they provide information at a finer spatial resolution ( $0.5^\circ \times 0.5^\circ$ ). At present, the SSP land-use information (including energy cropland expansion) is mostly refined to the level of 5 world regions and is not widely available in a spatial format. This strongly limits research into areas such as climate modelling (of projections, impacts, vulnerability, and adaptation), biodiversity assessments using local level species information, as well as the overall assessment of sustainable development.

Plans to generate such spatial data are ongoing, and have consequently led to the creation of innovative data such as the MAgPIE scenarios. Previous work by the scenario creators implements the MAgPIE scenarios in a multi-criteria sustainability assessment of large-scale bioenergy crop production, focussing on sustainability indicators: deforestation, LUC emissions, water withdrawals, nitrogen losses, and food prices (Humpenöder et al., 2018a). Access to these scenarios thus provides opportunities for further research into areas such as climate and biodiversity impact modelling, as shown throughout this thesis.

## Chapter 4 Impacts of Bioenergy Expansion on Climate

### 4.1 Overview

Land-use transformations resulting from large-scale second-generation bioenergy deployment can have consequences for Earth's Climate System. As discussed in *Chapter 1*, alterations to global and regional climate can occur through increased greenhouse gas (GHG) emissions from land conversion (biogeochemical effects) or through reflective and energy exchange characteristics of land ecosystems (biogeophysical effects).

A review of the current literature highlights only a handful of studies researching these impacts with regards to bioenergy expansion. In addition, most work focusses on land-carbon fluxes, excluding potential biogeophysical effects. Climate modelling experiments, in general, tend to neglect the effects of changes in land management and sustainability measures with most studies only calculating impacts of anthropogenic land cover changes.

Using the MAgPIE scenarios presented in *Chapter 2*, this work aims to build on the multi-criteria sustainability analysis carried out by Humpenöder et al. (2018a). By implementing the MAgPIE scenarios in the UVic Earth System Climate Model (version 2.9), this chapter explores the potential impacts of bioenergy-induced land-use changes on global and regional climate over the 21<sup>st</sup> century, and the effects of incorporating water protection and REDD+ sustainability measures. Through understanding these impacts, this work aims to contribute to knowledge of bioenergy's role within sustainable development goal (SDG) 13: "Climate Action".

## 4.2 Method

### 4.2.1 Model Description

The following work carries out climate simulations using the University of Victoria's UVic Earth system climate model (ESCM) version 2.9. This is an intermediate complexity climate model that is particularly well suited for determining the role of external climate influences and internal climate feedbacks that occur over times scales of decades to centuries. The model operates on a resolution of 1.8° latitude by 3.6° longitude and consists of three main components: ocean, atmosphere, and terrestrial biosphere components. These features are displayed in **Figure 4.1**. The ocean model is a 3D general circulation model with 19 vertical layers. It incorporates biogeochemical subcomponents such as inorganic carbon (Ewen et al., 2004), organic carbon and nutrient cycling, and is coupled to an ocean sediment component (Eby et al., 2009) and a dynamic-thermodynamic sea ice module. The atmosphere is represented by a one-layer (2D), vertically integrated energy-moisture balance model which calculates the atmospheric surface air temperature and humidity, with prescribed winds controlling atmospheric advection and wind stress on the ocean surface. The atmospheric component is coupled to the ocean model and the terrestrial biosphere component.

The terrestrial biosphere of the UVic ESCM is represented by the top-down representation of interactive foliage and flora including dynamics (TRIFFID) model (Cox, 2001), coupled to the one-layer Met Office Surface Exchange Scheme (MOSES) model (Cox et al., 1999), in which vegetation litter is stored and respired (Meissner et al., 2003; Matthews, 2007; Pinsonneault et al., 2011). Similarly to the LPJmL model, the TRIFFID and MOSES coupled models have been established over decades, developed at the Hadley Centre for use in coupled climate-carbon cycle simulations (Cox et al. 2000). The MOSES land surface scheme further improves on the simple land surface “bucket” model developed by Manabe (1969) and used in Matthews et al. (2003), by incorporating a better representation of evapotranspiration, surface albedo, and runoff. The models define five different plant functional types (PFTs): broadleaf trees, needleleaf trees, C3 grasses, C4 grasses, and shrubs. These vegetation types are represented as a fractional coverage of each grid cell, and compete with each other for dominance as a function of the simulated climate. The different PFTs have varying impacts on roughness and land surface albedo, as well as the uptake of carbon from the atmosphere and its transfer to the soil layer (Matthews, 2004). Terrestrial sequestration is enhanced by higher CO<sub>2</sub> concentrations in



the atmosphere. The nitrogen cycle is not a dynamic component, thus coupling of nitrogen and carbon cycles is not represented in the model.

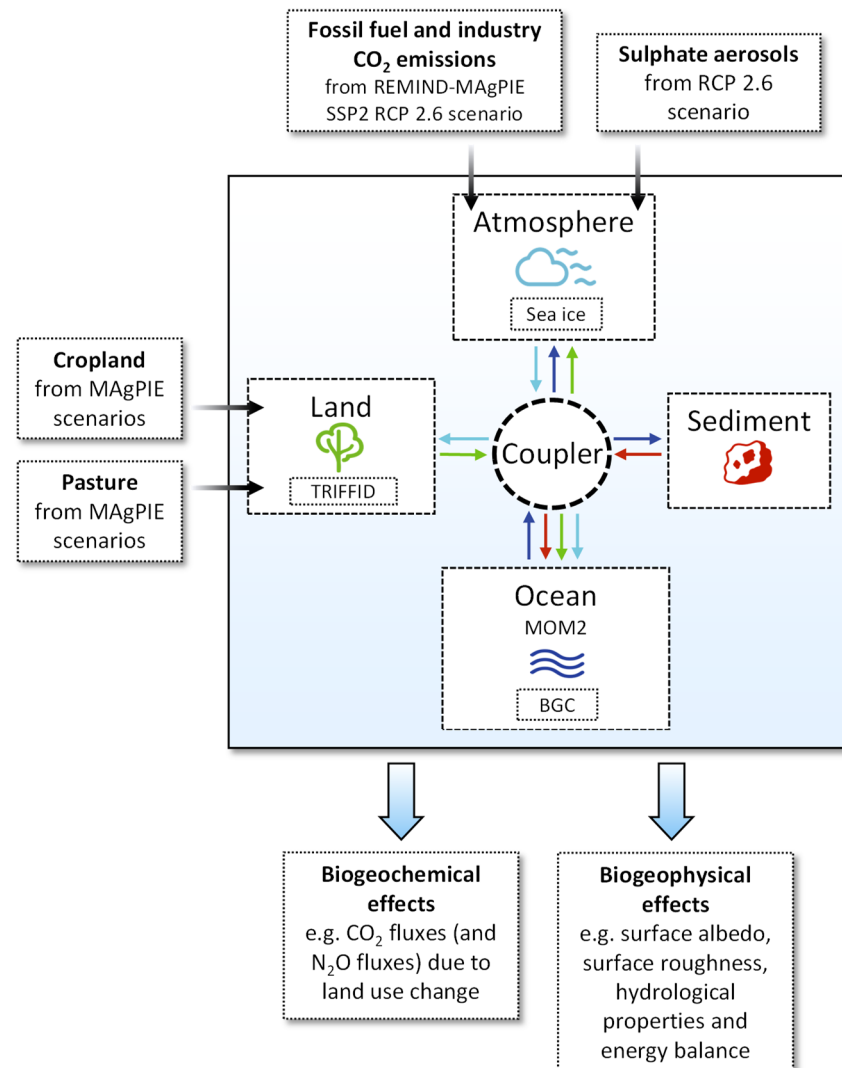


**Figure 4.1:** Architecture diagram of the UVic ESCM v2.9 and inputs and outputs. The model consists of 4 components: Atmosphere, land, ocean, and ocean sediment. Arrows inside the model diagram represent the coupling of these components- the colour of each arrow matches the colour of the symbol on the component being coupled. Inputs include cropland and pasture land-use fractions, CO<sub>2</sub> emissions, and sulphate aerosol forcing. Cropland here is a combination of food/feed cropland (including first-generation energy cropland), and second-generation energy cropland. Outputs include various biogeochemical and biogeophysical effects.

## 4.2.2 Experimental Setup

### 4.2.2.1 Land-Use Data Input

The experiments in this chapter are used to explore the biogeochemical and biogeophysical climate impacts of the spatially explicit MAgPIE land-use scenarios. As shown in *Chapter 3*, these scenarios consist of five main land-use types: Forest, energy cropland, food/feed cropland, pasture and other natural land. Land-use data can be inputted into the UVic model via its cropland and pasture components. The pasture input is a direct representation of ‘pasture’ in the MAgPIE scenarios (shown previously in *Chapter 3*, Section 3.3). On the other hand, the cropland input is a combination of all cropland types in the MAgPIE scenarios i.e., food/feed cropland (which includes first-generation energy cropland) and second-generation energy cropland. Cropland and pasture are then inputted as a ‘disturbed fraction’ of vegetation and are partitioned between C3 and C4 grasses in the TRIFFID model. Therefore bioenergy, particularly second-generation bioenergy, is not distinguished through this variable. Instead, bioenergy impacts are isolated further on in the experiment (see Section 4.2.3), as the difference between simulations with and without bioenergy implementation, whereby simulations with bioenergy implementation include more changes in C3 and C4 grasses in relation to the additional energy cropland within the cropland input.

The UVic model does not currently have an input component for forest and other natural land. Changes in the distribution of broad leaf trees, needle leaf trees and shrubland are therefore dependent on interactive processes in the TRIFFID model, not the forest changes displayed in the original MAgPIE scenarios (shown in *Chapter 3*). Hence, agricultural expansion in the model results in the complete removal of tree and shrub PFTs in the land-use fraction of each grid cell and the growth of C3 and C4 grasses in their place. In grid cells that are designated as pasture, 50% of the existing tree or shrub cover is removed for replacement by grasses. For grid cells that are already dominated by C3 and C4 grasses, LUC leads to no change in PFT biomass or fractional coverage. After LUC occurs, removed vegetation carbon is distributed between soil carbon in the form of litter-fall (30%), CO<sub>2</sub> emissions to the atmosphere (30%), and two wood carbon pools which have different residence times (40%), i.e., a fast-respiring pool with a 2-year residence time and a slow-respiring pool with a 20-year residence time (Simmons and Matthews, 2016).

Cropland and pasture data from the MAgPIE scenarios have been interpolated to the UVic model resolution (downscaled to the UVic model's  $1.8^\circ \times 3.6^\circ$  resolution from the original  $0.5^\circ \times 0.5^\circ$  MAgPIE resolution), whereby any resulting land-use fractions over the model's ocean grid cells were removed (set to zero) rather than redistributed to nearby land grid cells. To create an accurate representation of initial (or current) land use, the data was interpolated for years 1991–2010 using the year 1991 from an historical dataset and 2010 from the future MAgPIE scenarios. This produces a smooth transition from historical land use to the land use in the scenarios, as shown in **Figure 4.2**. This historical data covers the period 1750 to 2005 and is based on the HYDE 3.1 dataset (Goldewijk et al., 2011). It has been obtained from data produced in the CMIP5 study (CMIP5, 2009) and interpolated to the UVic model resolution.

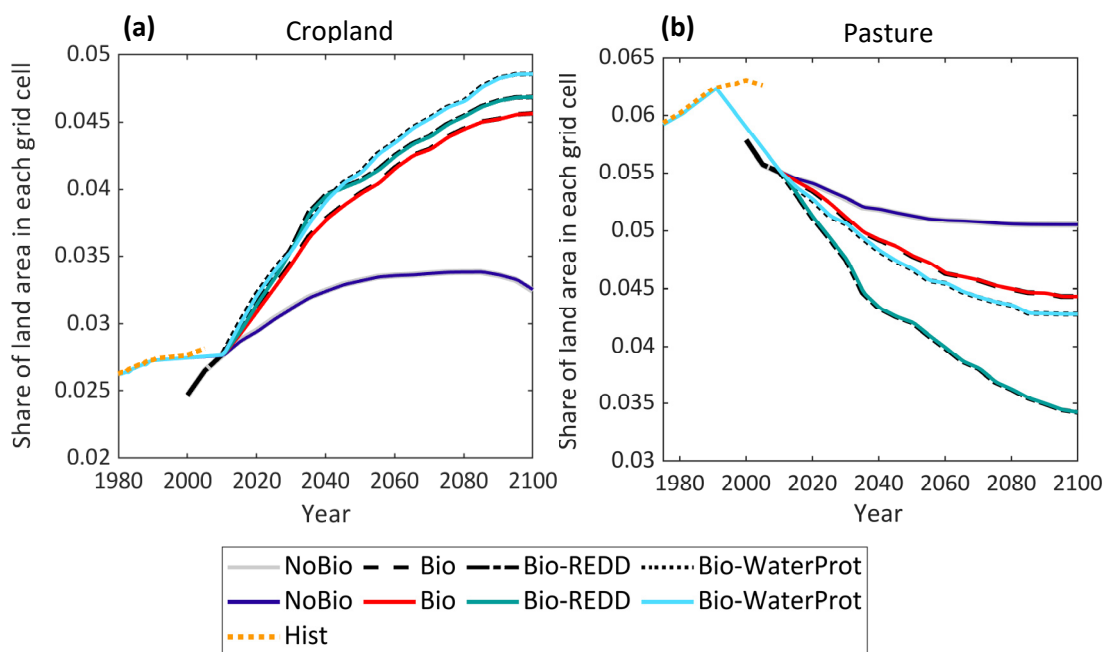


**Figure 4.2:** Global mean grid cell fraction trajectories of cropland (a) and pasture (b) inputs for the UVic ESCM, taken from the cropland and pasture variables in the MAgPIE scenarios (shown previously in Chapter 3, Section 3.3). Cropland here encompasses food/feed cropland (including first-generation energy cropland) and second-generation energy cropland. Values have been calculated as average fractions of the whole globe (including land and ocean grid cells), to indicate global interpolation between historical data ('Hist'), taken from the HYDE 3.1 dataset (Goldewijk et al., 2011), and future data, taken from the MAgPIE scenarios. Scenario trajectories in black and grey represent non-interpolated data, whereas coloured trajectories are the newly interpolated scenarios used as input for the UVic simulations.

### 4.2.2.2 Fossil Fuel Data Input

Annual fossil fuel emission data for the historical period (1750–2005) were taken from the Carbon Dioxide Information Analysis Centre (Marland et al., 2013). Future fossil fuel emissions for the scenarios were obtained from the SSP2 ‘middle of the road’ scenario produced by the REMIND-MAGPIE model for the RCP2.6 target, given in the Shared Socioeconomic Pathways (SSP) database (IIASA, 2018b) (see **Table 4.1**). This future scenario data assumes the nearly complete replacement of fossil fuel-powered energy with renewable energy by 2100 (i.e., bioenergy, solar, wind, geothermal and hydro power).

**Table 4.1:** CO<sub>2</sub> emission and removal values taken from the SSP database for the REMIND-MAGPIE SSP2 RCP2.6 scenario for years 2005 to 2100. Fossil fuel and industry emissions (‘FF’) are highlighted in green alongside LUC emissions and CCS removals in this scenario (IIASA, 2018b). Additional CO<sub>2</sub> emissions (‘BE’) have been calculated and added to FF for the NoBioBE scenario (represented as ‘FF + BE’) and are highlighted in blue. Positive values represent emissions, whereas negative values represent removal of emissions.

Year	REMIND-MAGPIE SSP2 RCP 2.6 (MtCO <sub>2</sub> /yr) (3 s.f.)						NoBioBE (MtCO <sub>2</sub> /yr) (3 s.f.)	
	Total			CCS portion of ‘Fossil fuel and industry emissions’			Extra fossil fuel CO <sub>2</sub> emissions from no bioenergy	Fossil fuel and industry emissions + CO <sub>2</sub> from no bioenergy
	Total net CO <sub>2</sub> emissions	LUC emissions	Fossil fuel and industry emissions	Total net CCS removals	Biomass CCS removals	Fossil fuel CCS removals		
	TotCO <sub>2</sub> <sup>a</sup>	LUC <sup>a</sup>	FF <sup>c</sup>	TotCCS <sup>a,b</sup>	BCCS <sup>a</sup>	FFCCS <sup>a</sup>	BE	FF + BE
2005	35,100	5,520	29,600	0	0	0	0	29,600
2010	35,600	3,470	32,100	0	0	0	0	32,100
2020	43,300	4,910	38,400	-2	0	-2	2,360	40,700
2030	36,000	1,600	34,400	-163	-99	-65	4,790	39,200
2040	27,600	1,770	25,900	-1,490	-1,050	-440	7,140	33,100
2050	19,400	3,280	16,100	-5,080	-4,240	-840	9,500	25,600
2060	7,550	2,470	5,080	-9,310	-8,460	-850	11,900	17,000
2070	-1,440	1,410	-2,850	-12,100	-11,400	-700	14,300	11,400
2080	-6,850	860	-7,710	-14,000	-13,700	-300	16,600	8,940
2090	-10,500	353	-10,800	-15,100	-15,100	0	19,100	8,230
2100	-12,100	116	-12,200	-15,600	-15,600	0	21,400	9,250

<sup>a</sup> Values taken from the online SSP database (IIASA, 2018b)

<sup>b</sup> TotCCS = BioCCS + FFCCS

<sup>c</sup> FF = TotCO<sub>2</sub> – LUC

As shown in **Table 4.1**, the total amount of CO<sub>2</sub> emissions produced in the REMIND-MAGPIE SSP2 RCP2.6 scenario over the 21<sup>st</sup> century is made up of ‘Fossil fuel and industry emissions’ and ‘LUC emissions’. Fossil fuel and industry emissions encompass fossil fuel emissions, as well as emissions eliminated through carbon capture and storage in both energy production and industry using biomass and fossil fuel sources. ‘LUC emissions’ from the SSP database were not used in this study and were instead calculated using the UVic model.

As discussed in *Chapter 3*, the ‘NoBio’ scenario does not include 2<sup>nd</sup> generation bioenergy demand expansion over the 21<sup>st</sup> century. This would most likely result in higher emissions from fossil fuel production to compensate for the lack of bioenergy production. To account for these emissions, additional fossil fuel emissions due to this absence of bioenergy have been calculated (‘BE’) and added to the fossil fuel and industry emissions values (‘FF + BE’) (see the last two columns of **Table 4.1**). The new version of the ‘NoBio’ scenario, including these newly calculated emissions, is called ‘NoBioBE’ and is discussed further on in this chapter.

To calculate these extra emissions, a weighted average amount of CO<sub>2</sub> emissions per Exajoule (EJ) of total fossil fuel energy production ( $7.14 \times 10^{10}$  kgCO<sub>2</sub>EJ<sup>-1</sup>) was determined and multiplied by the bioenergy demand used in the scenarios that do incorporate bioenergy production (0–300EJ per year between 2010 and 2100) using **Equation (4.1)**. The amount of CO<sub>2</sub> emissions was calculated in kgCO<sub>2</sub> per second as this is the input required for the UVic model, however they are provided in MtCO<sub>2</sub> per year in **Table 4.1**.

$$\text{Kg of fossil fuel CO}_2 \text{ per sec (kgCO}_2\text{s}^{-1}) = \quad (4.1)$$

$$\text{Bioenergy demand (EJyr}^{-1}) \times \frac{\text{Weighted av. CO}_2 \text{ per EJ FF energy production (kgCO}_2\text{EJ}^{-1})}{31536000 \text{ (s)}}$$

Calculating this weighted average required multiple steps (shown in **Table 4.2**). Firstly, the amount of CO<sub>2</sub> produced from burning different types of fossil fuels was obtained from open source data provided by the U.S. Energy Information Administration (E.I.A, 2019). Using this data, an average of CO<sub>2</sub> emissions per EJ of energy for each fossil fuel type (coal, oil, and natural gas) was calculated. The results were then multiplied to the total primary energy supply percentages of each of these fuel types in 2014 (obtained from I.E.A (2016)) to produce the weighted average amount of CO<sub>2</sub> emissions per EJ of fossil fuel energy production (see **Equation (4.2)**).

$$\begin{aligned} \text{Weighted average CO}_2 \text{ per EJ fossil fuel energy production} = & \quad (4.2) \\ & \text{Average kg of CO}_2 \text{ per EJ of energy for each fossil fuel type} \\ & \times \text{Percentage fuel share in 2014 in comparison to only fossil fuels} \end{aligned}$$

**Table 4.2:** Procedure for calculating the weighted average amount of CO<sub>2</sub> emissions per EJ of fossil fuel energy production.

Fossil fuel type	Fossil fuel	kg of CO <sub>2</sub> per EJ of energy (x 10 <sup>10</sup> kgCO <sub>2</sub> EJ <sup>-1</sup> )	Average kg of CO <sub>2</sub> per EJ of energy for each fossil fuel type (x10 <sup>10</sup> kgCO <sub>2</sub> EJ <sup>-1</sup> )	Percentage fuel share in 2014 compared to other energy fuels (%)	Percentage fuel share in 2014 in comparison to only fossil fuels (%)	Weighted average of CO <sub>2</sub> per EJ of fossil fuel energy production (x10 <sup>10</sup> kgCO <sub>2</sub> EJ <sup>-1</sup> )
<b>Coal</b>	Coal (anthracite)	9.84				
	Coal (bituminous)	8.85	9.29	29	35.8	3.33
	Coal (lignite)	9.27				
	Coal (subbituminous)	9.22				
<b>Oil</b>	Diesel fuel and heating oil	6.94	6.56	31	38.3	2.51
	Gasoline	6.76				
	Propane	5.98				
<b>Natural gas</b>	Natural gas	5.03	5.03	21	25.9	1.31
	<b>Total</b>			<b>81</b>	<b>100</b>	<b>7.14</b>

### 4.2.2.3 Other Inputs and Forcings

Transient spatial data for sulphate aerosols has been taken from the RCP 2.6 scenario. In previous work (e.g. Matthews (2004) and Johns et al. (2003)), sulphate aerosols (produced from fossil fuel combustion and greenhouse gases) were shown to have a negative radiative forcing. This is because sulphate aerosols back-scatter incoming solar radiation and have even shown to offset greenhouse-gas induced warming.

Volcanic and solar forcings were not included in the model simulations due to their average being around zero from 1998 onwards. These two forcings are generally used to closely align

historical temperature with observations, an outcome that is not needed in this study as it focuses on future predictions.

### 4.2.3 Simulations

The simulations were performed based on the methodology of Simmons and Matthews (2016), which follows the LUCID-CMIP5 protocol discussed previously in *Chapter 2*, Section 2.3.2.2.2. This approach is well-established, having been used in a variety of studies investigating historical and future land-use effects on climate (MPI, 2009; Shevliakova et al., 2009; Pitman et al., 2009; Hurtt et al., 2009; Pongratz et al., 2009; Brovkin et al., 2013; Boysen et al., 2014). By calculating differences between simulations with and without land-use changes, this allows isolation of climatic effects due to LUC at global and regional scales.

**Table 4.3** summarises the components of each simulation carried out in this study. To determine the biogeochemical and biogeophysical effects of LUC in the MAgPIE scenarios, four types of simulations were used to calculate changes in terrestrial carbon content and surface air temperature. These include a historical simulation ('Historical'), a simulation with fixed land and prescribed fossil fuel emissions ('PF'), a simulation with transient land and prescribed fossil fuel emissions ('TL'), and a simulation with fixed land and prescribed CO<sub>2</sub> concentrations determined in the TL simulation ('PC').

In more detail, the model was firstly run for the historical 'H' scenario, between 1750 and 1991, whereby initial CO<sub>2</sub> concentration in 1750 was set to 279 ppm and spatial land cover data was taken from the CMIP5 study (CMIP5, 2009). The results produced for 1991 were then used as the initial conditions for the future time-evolving simulations (1991 to 2100). Next, 'PF' simulations were performed using only prescribed fossil fuel emissions forcing with (FF + BE) and without (FF) fossil fuel emissions from the absence of bioenergy production (as shown in **Table 4.3**).

'TL' simulations were then run using land cover changes outlined in the MAgPIE land-use scenarios with corresponding fossil fuel and industry emissions from **Table 4.1**. For the NoBio scenario, two types of simulations were run using the 'NoBio' cropland and pasture input data, alongside two different prescribed fossil fuel emissions forcings: 'LUC + FF + BE' and 'LUC + FF'. This was to determine whether including prescribed fossil fuel emissions from the absence of bioenergy production (+BE) made an impact on the final LUC emissions and

climate outputs of the simulations. Lastly, ‘PC’ simulations were carried out in which prescribed CO<sub>2</sub> concentrations, calculated in the ‘TL’ runs, were used as forcing mechanisms and land-use was kept fixed at 1991: ‘PC(LUC + FF + BE)’ and ‘PC(LUC + FF)’. Terrestrial carbon storage and surface air temperature outputs from the simulations ‘PF’, ‘TL’ and ‘PC’ were then used to calculate climate responses to LUC emissions and other biogeophysical effects of LUC.

**Table 4.3:** A summary of the simulations used for each scenario in this study. ‘Spatial land use’ refers to land-use data used for historical (HYDE 3.1 dataset) and future (MAGPIE scenarios) simulations. Prescribed CO<sub>2</sub> emissions are the input fossil fuel and industry CO<sub>2</sub> emissions (with added emissions for absence of bioenergy in NoBioBE), released directly to the atmosphere from a yearly emissions data file. Prescribed CO<sub>2</sub> concentration refers to simulations in which atmospheric CO<sub>2</sub> is forced to follow a specified CO<sub>2</sub> concentration trend. The method in this table has been adapted from that in Simmons and Matthews (2016). Emissions forcings in column 3 are linked to identifying abbreviations provided previously in Table 4.1.

Simulation	Scenario	Emissions forcing	Simulated years	Spatial land use	Prescribed CO <sub>2</sub> emissions	Prescribed CO <sub>2</sub> concentrations
<b>Historical</b>	H	LUC + FF	1750-1991	Historical	Fossil fuels	None
	<b>PF</b>	PF	FF	1991-2100	Fixed at 1991	Fossil fuels
PFBE		FF + BE	1991-2100	Fixed at 1991	Fossil fuels + Biofuels	None
<b>TL</b>	NoBioBE	LUC + FF + BE	1991-2100	Dependent on NoBio scenario	Fossil fuels + Biofuels	None
	NoBio	LUC + FF	1991-2100	Dependent on NoBio scenario	Fossil fuels	None
	Bio, Bio-REDD & Bio-WP	LUC + FF	1991-2100	Dependent on Bio-scenarios	Fossil fuels	None
<b>PC</b>	NoBioBEPC	PC(LUC + FF + BE)	1991-2100	Fixed at 1991	None	From TL (LUC + FF + BE) simulation
	NoBioPC	PC(LUC + FF)	1991-2100	Fixed at 1991	None	From TL (LUC + FF) simulation
	BioPC, Bio-REDDPC & Bio-WPPC	PC(LUC + FF)	1991-2100	Fixed at 1991	None	From TL (LUC + FF) simulation



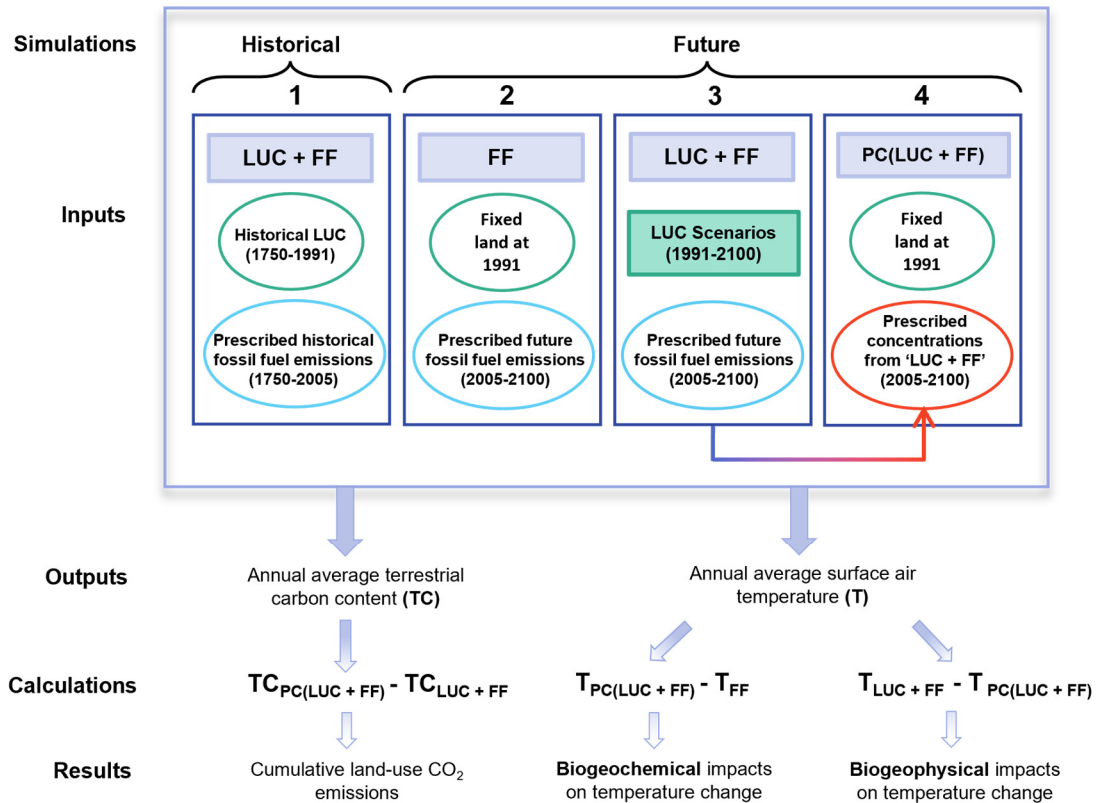


**Figure 4.3:** Architecture diagram of the four types of simulations used for each scenario in this study. This figure is linked to **Figure 4.1** and illustrates the inputs (i.e., land-use data and prescribed fossil fuel emissions) and outputs (i.e., annual average global terrestrial carbon TC and surface air temperature T) for the historical and future simulations, as well how the outputs have been used to calculate LUC emissions and biogeochemical and biogeophysical climate impacts of LUC within the scenarios. Abbreviations in these calculations are linked to those provided in **Table 4.1**, **Table 4.3**, and **Table 4.4**. The method here has been adapted from that in Simmons and Matthews (2016).

Cumulative LUC emissions were calculated as the differences in total terrestrial carbon storage between the PC simulations and their corresponding TL simulations with spatially-varying LUC (e.g. PC(LUC + FF) and (LUC + FF)) (see **Table 4.3** and **Figure 4.3**). Because both simulations have the same atmospheric CO<sub>2</sub> concentrations, the difference in the terrestrial carbon storage between them shows the net effect of spatially-explicit land use on terrestrial carbon storage, and thus, net terrestrial emissions. These net terrestrial emissions are made up of three different processes which alter carbon fluxes from land to the atmosphere:

- 1) As forest is converted to cropland or pasture in the TL scenarios, less carbon is stored in the land, and therefore stays in the atmosphere as CO<sub>2</sub>. These emissions are known

as ‘direct CO<sub>2</sub> emissions from LUC’ and they increase over time as more deforestation occurs. They also encompass the ‘lost additional sink capacity’ (LASC) i.e., the carbon uptake due to environmental effects on forests (such as CO<sub>2</sub> fertilisation) that does not happen once the forests are removed (see *Chapter 2*, Section 2.2.3.5) (Sitch et al., 2005; Pongratz et al., 2010; Ciais et al., 2013; Friedlingstein et al., 2022). Because land use is fixed at 1991 in the PC simulations, CO<sub>2</sub> emissions from LUC do not occur within these simulations. The overall effect is an increase in  $TC_{PC(LUC + FF)} - TC_{LUC + FF}$ .

- 2) By keeping land use fixed at 1991 in the PC simulations, global potential natural vegetation distribution alters in response to the prescribed CO<sub>2</sub> concentrations taken from the respective TL simulations. This occurs particularly in regions that would have been affected by LUC in the TL simulations. The resulting effect is more CO<sub>2</sub> sequestered in the PC simulations than the TL simulations over time, and thus an increase in  $TC_{PC(LUC + FF)} - TC_{LUC + FF}$ .
- 3) As stated in previous work (Friedlingstein et al., 2006; Arora et al., 2011; Arora et al., 2020), higher temperatures and precipitation promote a flux of carbon from the land into the atmosphere, therefore resulting in a loss of terrestrial carbon stored. Such changes in climate conditions can also lead to absorption of CO<sub>2</sub> emissions from land (CO<sub>2</sub> fertilisation), though the more CO<sub>2</sub> is emitted the less efficient the land sinks become. The differences between these carbon fluxes in TL and PC simulations is therefore reflected in the net terrestrial emissions (see *Chapter 2*, Section 2.2.3.5) (Arias et al., 2021).

**Table 4.4:** Calculations of global net cumulative LUC emissions, biogeochemical temperature change, and biogeophysical temperature change. In the formulae,  $TC$  denotes the annual-average global terrestrial carbon content and  $T$  the annual-average surface air temperature. Subscripts indicate identifying abbreviations from the source simulation emissions forcings in **Table 4.3**, also shown in **Table 4.3** and **Figure 4.3**. The method in this table has been adapted from that in Simmons and Matthews (2016).

Scenario	Cumulative LUC emissions (GtCO <sub>2</sub> )	Biogeochemical effect (°C)	Biogeophysical effect (°C)
NoBioBE	$TC_{PC(LUC + FF + BE)} - TC_{LUC + FF + BE}$	$T_{PC(LUC + FF + BE)} - T_{FF + BE}$	$T_{LUC + FF + BE} - T_{PC(LUC + FF + BE)}$
NoBio, Bio, Bio-REDD, & Bio-WP	$TC_{PC(LUC + FF)} - TC_{LUC + FF}$	$T_{PC(LUC + FF)} - T_{FF}$	$T_{LUC + FF} - T_{PC(LUC + FF)}$

The climate response to biogeochemical effects of terrestrial emissions was calculated as the temperature difference between the PC simulations and the corresponding simulations without any land-use change i.e., the corresponding PF (FF or FF + BE) simulations. The biogeophysical effect of LUC was calculated as the temperature difference between TL and corresponding PC simulations (e.g., PC(LUC + FF) and (LUC + FF)). These analyses assume that the climate response to LUC emissions is equivalent to that of fossil fuels under the assumption that, once in the atmosphere, the origin of the CO<sub>2</sub> emissions is irrelevant.

## 4.3 Results

### 4.3.1 Land-Use Dynamics

#### 4.3.1.1 Land Impacts in Relation to Climate-Carbon Cycle Feedbacks

As detailed in the previous section, two main types of simulations were used in this analysis: TL simulations, whereby land scenario inputs (cropland and pasture) change over time, and PC simulations, in which land inputs are kept fixed at the year 1991. In both simulations, vegetation in the TRIFFID model alters dynamically in response to these land-use changes, as well as changes in CO<sub>2</sub> concentrations and temperature. In the PC simulations, while agricultural input is kept fixed, natural loss and increase of each plant type still occurs.

As discussed in *Chapter 2* Section 2.2.3.5, increases in atmospheric CO<sub>2</sub> concentrations generally lead to CO<sub>2</sub> fertilisation and therefore more land carbon accumulation and vegetation growth across the globe, particularly in tropical regions. In contrast, higher surface temperatures reduce carbon uptake in most regions apart from high latitudes in the northern hemisphere. Assuming carbon uptake as a proxy for vegetation growth, findings for the PC simulations corroborate these phenomena. For instance, in the BioPC scenario, significant natural loss of broad and needle leaf forest occurs in the tropics due to changes in climate (see **Figure 4.4**). Lower net primary productivity (NPP) values in these areas confirm reductions in carbon uptake.

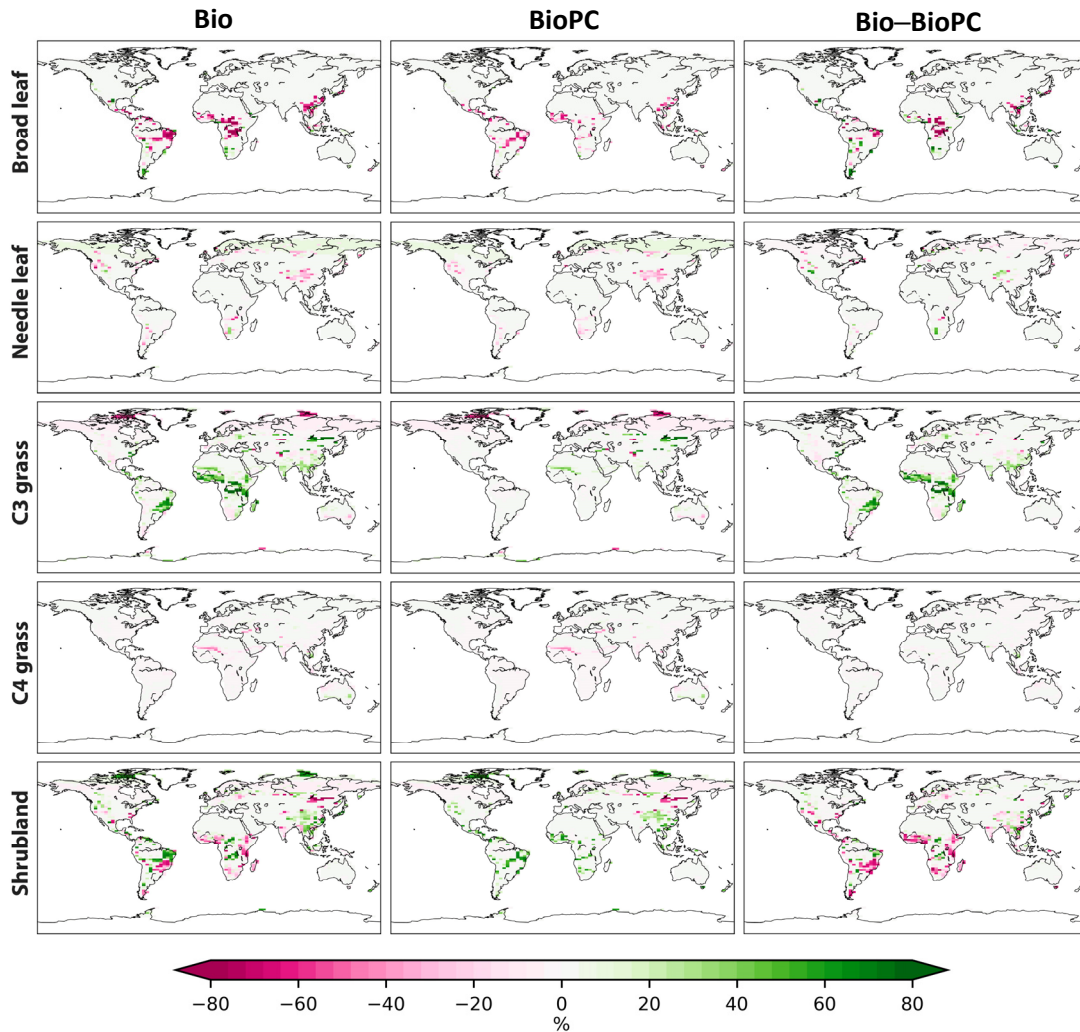


**Figure 4.4:** Regional land-use changes in Bio, BioPC and BioPC minus Bio (BioPC–Bio) simulations, in 2100 relative to 2005. BioPC indicates values are percentages of grid cells undergoing land cover changes.

Small increases in broad leaf forest also occur at the start of the century, particularly over the Democratic Republic of Congo and the Amazon rainforest. This suggests that increased carbon uptake responses to increases in prescribed CO<sub>2</sub> levels (from the TL simulations) are initially higher than reduced carbon uptake responses to climate change in these regions (see **Figure 2.5** in *Chapter 2* for more information; Arias et al. (2021)). However, towards the end of the century this effect is dampened as climate impacts become more prevalent. Similarly, increased CO<sub>2</sub> fertilisation and NPP leads to small natural increases in C3 grasses across the globe (shown in the PC simulations), which are reduced in the tropics towards the end of the century due to increased surface temperatures. This indicates that bioenergy cropland growth (and thus crop

yield) in the TL simulations (C3 grasses) is somewhat enhanced by increases in CO<sub>2</sub> concentration at both high and low latitudes, however, becomes more affected by changes in climate in the tropics. Shrubland, increases across the globe as it fills newly unallocated spaces made by forest loss, and decreases where it is converted to new cropland.

### 4.3.1.2 Land-Use Changes in TL and PC Simulations

The natural loss of forest in the UVic PC simulations reaches up to approximately  $(-3.5 \times 10^6)$  km<sup>2</sup> in all scenarios ( $-18\%$ ) by 2100 (see **Figure 4.5**). In comparison to other studies, this forest loss is significantly high. Brovkin et al. (2013), for instance, calculate an increase, rather than a loss, in tree cover for most of their modelled simulations, which they attribute to changes in climate and CO<sub>2</sub> concentration. In the TL simulations, these natural patterns of LUC occur in addition to impacts of agricultural expansion. As discussed in Section 4.2.2.1, cropland and pasture are inputted into the UVic model as a ‘disturbed fraction’ of vegetation and are partitioned between C3 and C4 grasses. This leads to a further removal of broad leaf forest and needle leaf forest, as well as shrubland across the globe.

**Table 4.5:** Global land use for the five scenarios in years 2050 and 2100 relative to 2005, in their original form taken from the MAgPIE model (represented by five land-use types) and in their new form in the UVic ESCM (represented by the UVic ESCM’s five plant functional types). Values from the UVic simulations are calculated as the difference between TL and PC simulations.

Scenario Form	2050						2100				
	NoBio-BE	NoBio	Bio	Bio-REDD	Bio-WP	NoBio-BE	NoBio	Bio	Bio-REDD	Bio-WP	
Original MAgPIE ( $\times 10^6$ km <sup>2</sup> )	Energy Crops	–	–	3.12	3.13	3.22	–	–	6.36	6.32	6.67
	Food/Feed	4.10	4.10	4.85	4.88	5.71	3.52	3.52	4.42	4.66	5.48
	Crops	–	–	–	–	–	–	–	–	–	–
	Pasture	-2.60	-2.60	-4.50	-7.70	-5.12	-2.93	-2.93	-6.24	-11.5	-6.90
	Forest ONL	-0.98	-0.98	-2.45	0.17	-2.74	-0.56	-0.56	-3.27	0.92	-3.95
UVic ( $\times 10^6$ km <sup>2</sup> )	Broad leaf	-1.25	-1.25	-1.46	-1.29	-1.59	-0.46	-0.54	-1.44	-0.56	-1.90
	Needle leaf	-0.03	-0.04	-0.05	-0.04	-0.07	0.08	0.09	0.04	0.07	0.02
	C3 grass	2.27	2.27	3.79	3.05	4.19	2.35	2.33	5.79	4.04	6.67
	C4 grass	-0.24	-0.24	-0.16	-0.26	-0.14	-0.24	-0.22	-0.05	-0.18	-0.05
	Shrubs	-0.77	-0.77	-2.17	-1.49	-2.42	-1.74	-1.69	-4.37	-3.41	-4.76

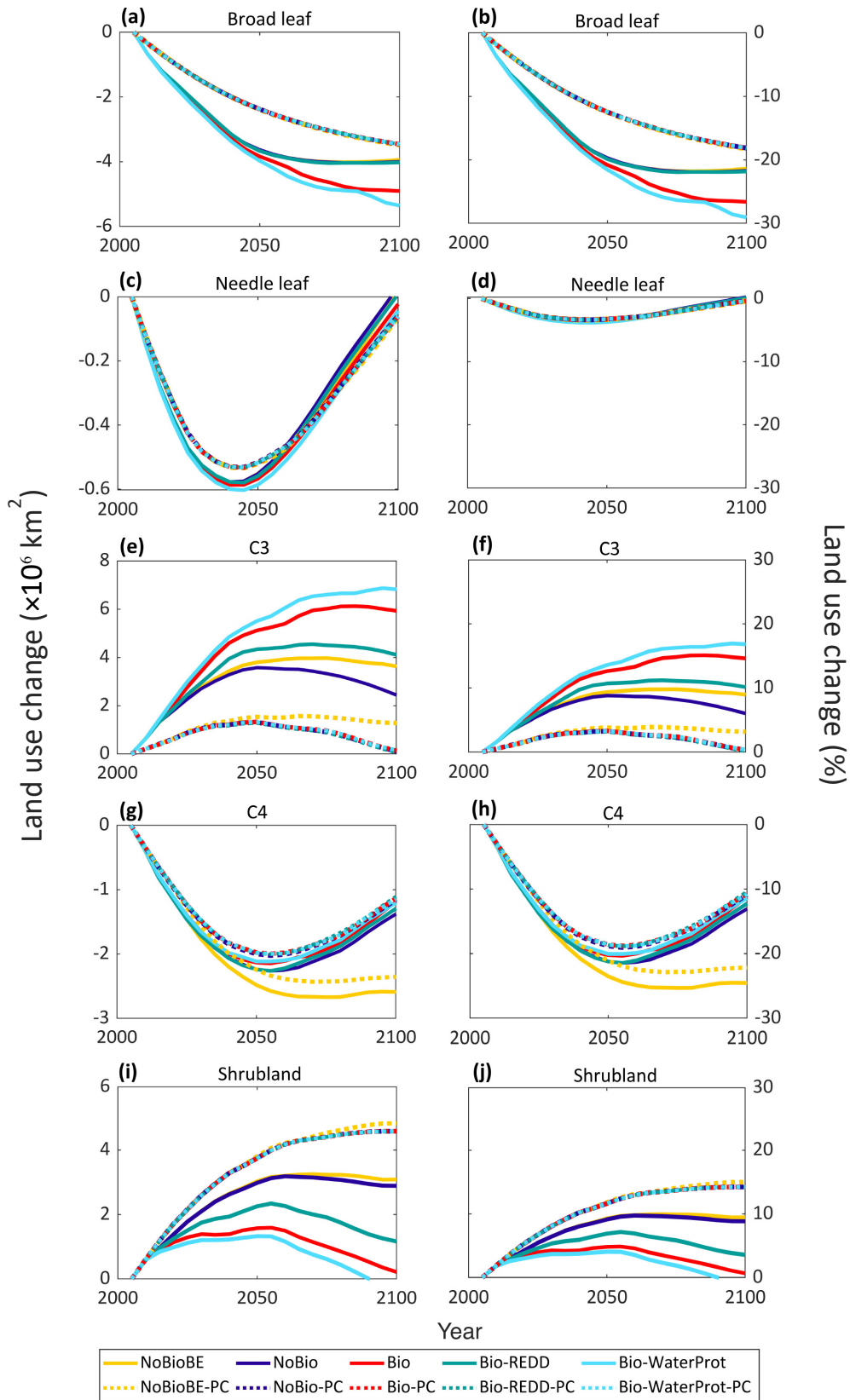


**Figure 4.5:** Trajectories of land-use change for five different plant functional types in the UVic ESCM simulations. Values are in area and percentage units relative to 2005.

The differences between land-use changes in the TL and PC simulations indicate the influence of changes in cropland and pasture inputs as outlined in the MAgPIE scenarios (see **Figure 4.5**). By 2100, such changes result in a  $2.33\text{--}6.67 \times 10^6 \text{ km}^2$  (5.75 – 16.44%) increase in global C3 grasses across the scenarios, leading to a total forest loss of  $(-)\text{0.39--}(-)\text{1.88} \times 10^6 \text{ km}^2$  ( $(-)\text{2.68--}(-)\text{10.82\%}$ ) by 2100. In comparison to land-use changes calculated for the original MAgPIE scenarios, these values are relatively low (see **Table 4.5**). As mentioned, this is partly because large areas of shrubland are used for cropland expansion (in addition to pasture) in the UVic model, contrasting with the original MAgPIE scenarios, in which the loss of ‘other natural land’ (containing shrubland) is significantly lower (see *Chapter 3*). Previous work, comparing projections of other natural land (ONL) for different IAMs, similarly show that estimates of ONL from the MAgPIE model are at the low end of the spectrum due to the use of pasture and forest for cropland conversion instead (Popp et al., 2017).

### 4.3.1.3 Isolated Impacts of Bioenergy and Conservation

#### Schemes

Modest forest loss is further reflected in the differences between scenario outputs. Results for the control NoBioBE/NoBio (e.g., NoBioBE–NoBioBEPC) scenarios show that, alone, food/feed cropland expansion leads to a loss of around  $0.46/0.5 \times 10^6 \text{ km}^2$  (3.17/3.55%) (for NoBioBE/NoBio) of forest by 2100, relative to 2005. The incorporation of bioenergy, and thus an additional increase of  $3.44/0.18 \times 10^6 \text{ km}^2$  (8.5/1.8%) of C3/C4 grasses, results in further forest loss of  $(-)\text{1.02} \times 10^6 \text{ km}^2$  ( $(-)\text{5.6\%}$ ) by the end of the century. These values are calculated as the difference between Bio (e.g., Bio–BioPC) and NoBioBE (NoBioBE–NoBioBEPC) scenarios (see **Table 4.5** and **Figure 4.6**). The original MAgPIE scenarios, however, indicate a much stronger influence of bioenergy on forest loss, suggesting a loss of  $2.71 \times 10^6 \text{ km}^2$  (6.5%) by 2100, relative to 2005.

Similarly, implementation of REDD+ to the Bio scenario results in the prevention of  $4.19 \times 10^6 \text{ km}^2$  of forest loss in the MAgPIE scenarios, but when simulated in UVic this decreases to  $0.88 \times 10^6 \text{ km}^2$  (5%). Even so, the UVic model manages to depict the significant reduction of cropland expansion into forest, whereby shrubland is used instead. The model also portrays additional forest loss due to incorporation of a global water protection scheme ( $0.47 \times 10^6 \text{ km}^2$ ; 2.6%), with large increases concentrated in the Congo region, as similarly depicted in the MAgPIE Bio-WaterProt scenario (See *Chapter 3*, **Figure 3.4**). However, it fails to capture

additional forest loss in Eastern US, Southern Brazil, and eastern Europe, instead showing more forest loss in Asia. As discussed in *Chapter 3*, this loss is due to the absence of irrigation for energy cropland, and thus the need for more land for rainfed cropland.

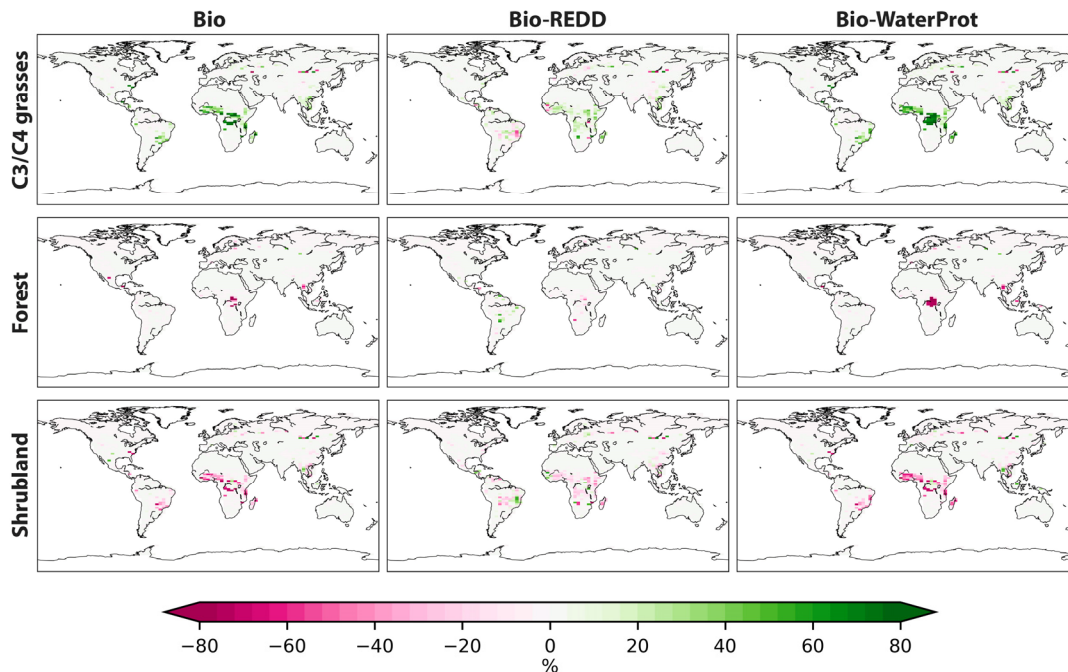


**Figure 4.6:** Spatial land-use changes for C3/C4 grasses, forest and shrubland in the UVic model as a result of bioenergy expansion; for 2100 relative to 2005. Values are calculated as the difference between Bio (e.g., Bio-BioPC) and NoBioBE (NoBioBE-NoBioBEPC) simulations and are percentages of grid cells undergoing land cover changes.

### 4.3.2 Surface Air Temperature and Atmospheric CO<sub>2</sub> Dynamics

**Figure 4.7** illustrates the evolution of global CO<sub>2</sub> emissions (c and d) in the scenarios, and the corresponding atmospheric CO<sub>2</sub> concentrations (b) and surface air temperatures (a) over the 21<sup>st</sup> century. Between 2005 and 2100, CO<sub>2</sub> emissions increase by 1,201–1,234 GtCO<sub>2</sub> across the scenarios. As a result, SAT and CO<sub>2</sub> concentration reach approximately 1.82–1.83 °C and 434–437 ppm, respectively, by 2100. Excluding the NoBioBE scenario, these trajectories are mostly reflective of those shown in the RCP2.6 pathways, in which SAT and CO<sub>2</sub> concentration values in 2100 range between 1.73 °C and 1.82 °C, and 397 ppm and 439 ppm, respectively. In contrast, the NoBioBE projections are closer to an average of RCP3.4 and RCP4.5 trajectories.



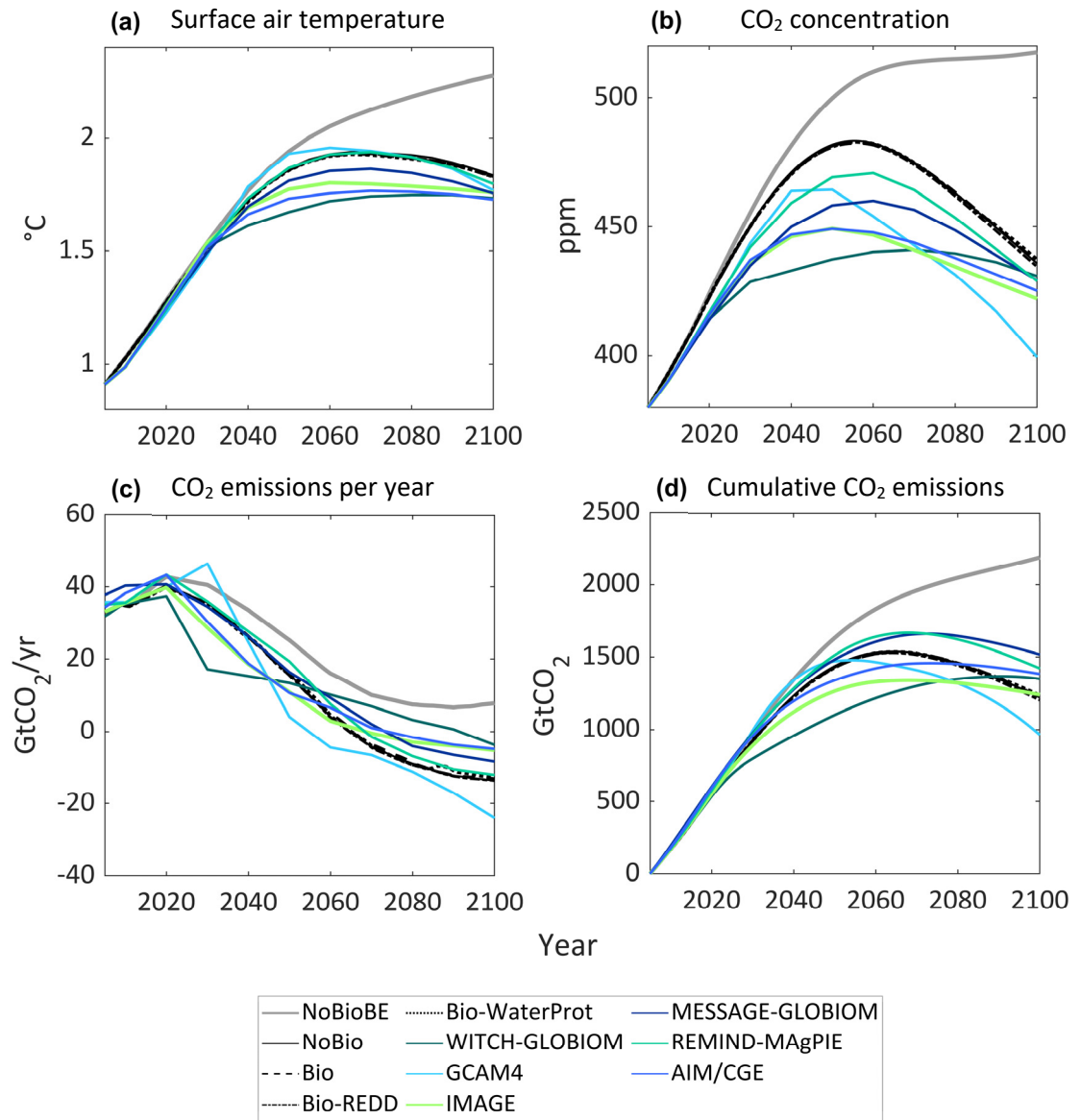


**Figure 4.7:** Global annual mean projections for surface air temperature (a), CO<sub>2</sub> concentration (b), yearly CO<sub>2</sub> emissions (c) and cumulative CO<sub>2</sub> emissions (d), for the UVic simulations between years 2005 and 2100. Additionally, findings for SSP2 RCP2.6 scenarios are included, taken from the online SSP database (IIASA, 2018b). Values in (a) and (c) have been calculated relative to the pre-industrial base period 1850–1900, as demonstrated in the work of Rogelj, Shindell, et al. (2018). Cumulative and yearly CO<sub>2</sub> emissions are made up of LUC emissions calculated from this study and input fossil fuel emissions shown in **Table 4.1**.

Findings further show that at the global scale, the incorporation of a bioenergy expansion program reduces atmospheric CO<sub>2</sub> concentration by 81 ppm, resulting in a cooling effect of –0.44 °C by 2100 (relative to the pre-industrial base period 1850–1900), but only when the reduction in FF emissions associated with the energy obtained from biofuels (by adding FF emissions to the NoBioBE scenario) is included in the analysis. When excluded, bioenergy incorporation (with or without REDD+ or water protection policies) results in only a small (almost negligible) reduction in atmospheric CO<sub>2</sub> and SAT. This implies that the cooling effect of substituting FF emissions in the scenarios is significantly more dominant compared to the climate impacts of LUC emissions that are produced due to bioenergy incorporation.

Incorporation of REDD+ or water protection policies have little impact on global values, however, result in regional differences due to changes in land use, as discussed later in this chapter. As shown in **Figure 4.7**, findings in this study align well with findings for other SSP2 scenarios, closely matching results for the REMIND-MAgPIE SSP2 scenario. This is due to the use of the same ‘Fossil fuel and industry’ emissions as the REMIND-MAgPIE SSP2 scenario, as discussed in Section 4.2.2.2.

### 4.3.3 Transient Climate Response to Cumulative Carbon Emissions (TCRE)

The overall temperature response to cumulative CO<sub>2</sub> emissions (both fossil fuel and LUC emissions) in the UVic model is a linear relationship. Across the scenarios, constant TCRE is 0.6–0.7 °C per 1000 GtCO<sub>2</sub> (or 2.16–2.52 °C/TtC). As shown in **Figure 4.8**, these values align with TCRE values calculated for SSP and RCP scenarios (in the range of 0.6–0.8 °C per 1000 GtCO<sub>2</sub> or 2.16–2.88 °C/TtC; Jia et al. (2019)). In comparison to studies investigating future biogeochemical and biogeophysical impacts of LUC, TCRE values for the UVic model are at the higher end of the spectrum (0.88–2.52 °C/TtC; Jia et al. (2019)). The curve in the results for the MAgPIE and SSP2 scenarios represents the drop in SAT due to yearly CO<sub>2</sub> (GtCO<sub>2</sub>/yr) emissions becoming negative towards the end of the century. As discussed in *Chapter 2* (Section 2.3.2.3), the TCRE metric can be used as a tool for identifying biogeochemical climate impacts of LUC emissions, however this chapter uses a similar method to the LUCID-CMIP5 protocol, as described in Section 4.2.3.

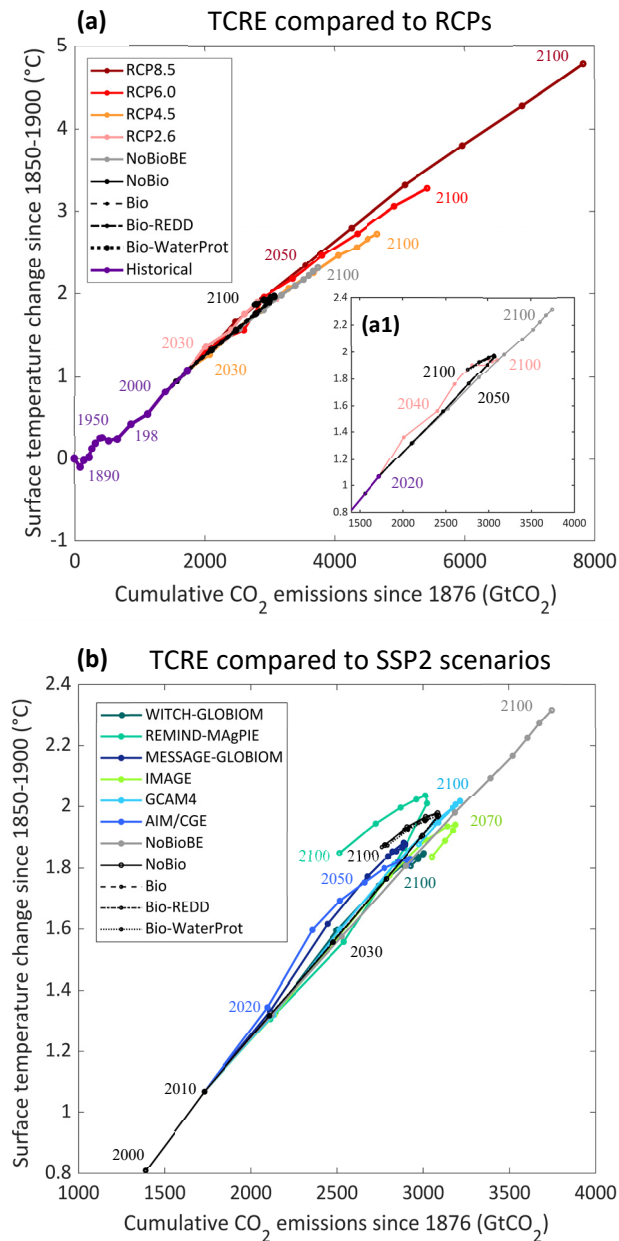


**Figure 4.8:** Transient climate response for MAGPIE scenarios compared to the RCP scenarios (a) and the SSP2 scenarios (b). Annual-average surface air temperatures from 1850-1990 are plotted against cumulative CO<sub>2</sub> emissions since 1976. Graph (a1) shows a close-up of the MAGPIE TCRE results compared to the RCP 2.6 TCRE results. Results for the SSP scenarios have been taken from the SSP database (IIASA, 2018b). Results for the RCP scenarios in (a) have been extracted from Figure SPM.10 in Gray (2007) using software by GetData (2019). Historical values are extracted from Figure 2.3 in Rogelj et al (2018).

## 4.3.4 Impacts of Land-Use Changes on Surface Climate

### 4.3.4.1 Global Impacts

The contribution of LUC to net global warming in each of the scenarios is displayed in **Figure 4.9**. Overall, there is little variation between scenario findings, mainly due to the small differences in forest loss discussed previously in Section 4.3.1. Across the scenarios, a combined net warming of between 0.010 °C and 0.019 °C occurs by 2050 (compared to 2005) due to biogeochemical (BGC) effects, which is then dampened by cooling from biogeophysical (BGP) effects towards the end of the century ((-)0.01 °C to (+)0.005 °C in 2100). Individually, the global mean biogeochemical and biogeophysical effects are also small throughout the period, whereby in 2050 and 2100 biogeochemical impacts are (+)0.026–(+0.027 °C and (-)0.0058–(+0.0091 °C across all scenarios, and biogeophysical effects are (-)0.016–(-)0.0073 °C and (-)0.015–(+0.0064 °C, respectively. Rapid declines in biogeochemical warming towards the end of the century can also be explained by global increases in soil carbon uptake post-deforestation (see Section 4.4.3.3 for more detail).

Expansion of food/feed cropland alone results in a small combined global warming of 0.0092 °C by 2075–2100, relative to 2005 (in the NoBioBE scenario). The combined global impact of a bioenergy expansion scheme (in the Bio scenario) is an overall cooling effect of (-)0.0067 °C by 2075–2100 (since 2005), in comparison to the NoBioBE scenario. Both biogeochemical warming and biogeophysical cooling increase, however biogeophysical effects are higher (BGC = (+)0.0087°C, BGP = (-)0.015°C). These values are relatively low due to the use of more shrubland than forest for cropland expansion in the UVic model (see Section 4.3.1).

The incorporation of a water protection scheme has very little global impact. In comparison to the NoBioBE scenario, bioenergy expansion with water protection leads to a combined cooling of (-)0.01 °C by 2075–2100 (BGC effects = (+)0.0078 °C, BGP effects = (-)0.018 °C), an increase in cooling of (-)0.0033 °C compared to the Bio scenario. The prevention of forest loss implemented through a global REDD+ policy (in Bio-REDD) dampens both biogeochemical warming and biogeophysical cooling slightly, resulting in values almost resembling findings for the NoBio and NoBioBE scenarios. Compared to the NoBioBE scenario, a cooling of (-)0.0012 °C by 2075–2100 (BGC = (+)0.0074 °C, BGP = (-)0.0086 °C) occurs in Bio-REDD.

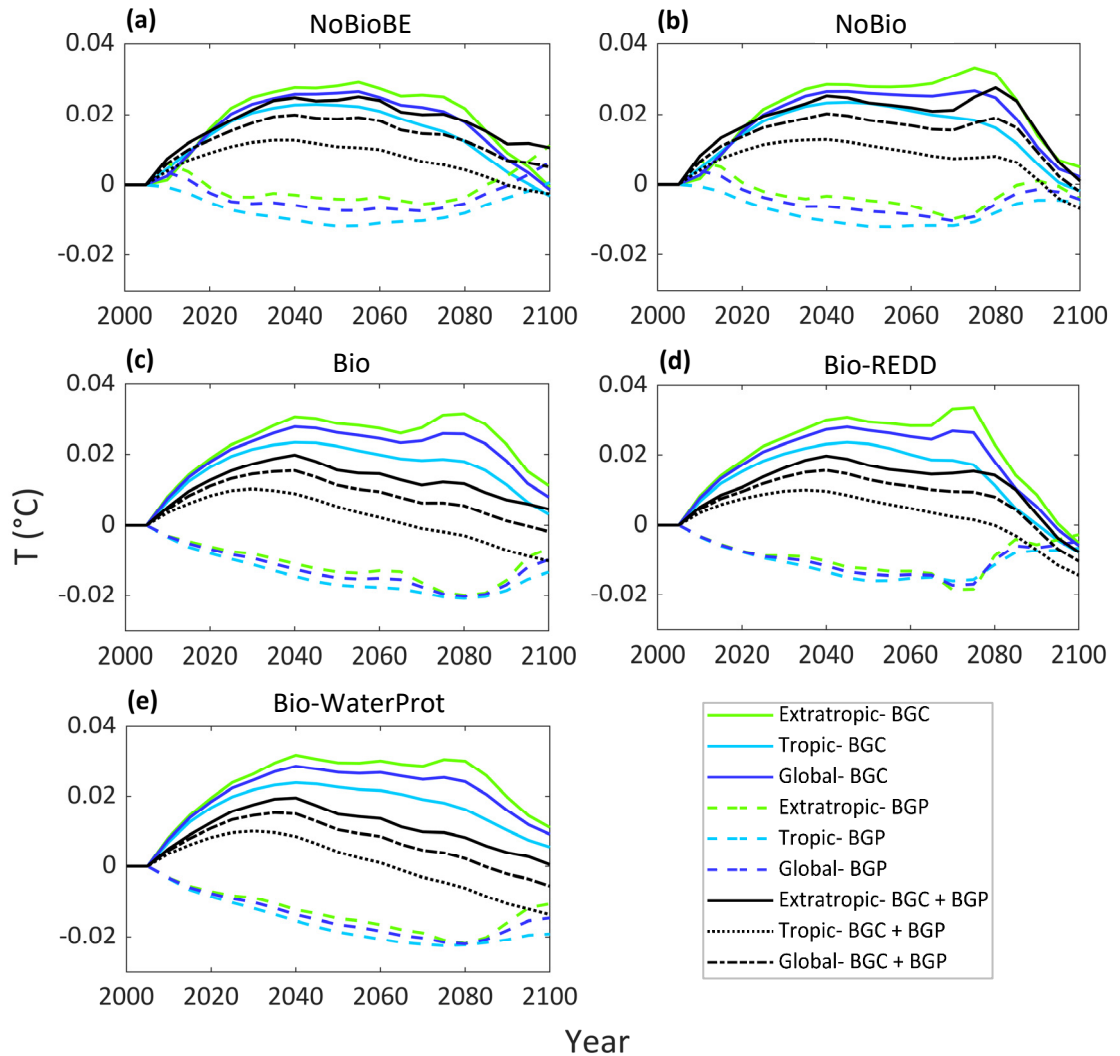


**Figure 4.9:** Annual-average global biogeophysical (BGP) and biogeochemical (BGC) impacts of LUC on surface temperature for all 5 scenarios between 2005 and 2100. Light blue lines represent impacts in the tropical ( $25^{\circ}\text{S}$  to  $25^{\circ}\text{N}$ ) region, light green lines represent results for the extratropical (lower= $65^{\circ}\text{S}$  to  $25^{\circ}\text{S}$  and upper= $25^{\circ}\text{N}$  to  $65^{\circ}\text{N}$ ) regions, and dark blue lines show the global impacts. Tropical values are calculated as yearly averages over the tropics. Extratropical values are calculated as yearly averages of the lower and upper regions together. Black lines denote the combined (BGC + BGP) impacts of LUC on surface temperature. BGP and BGC temperature changes were obtained using the calculations:  $T_{PC(LUC+FF)} - T_{FF}$  and  $T_{LUC+FF} - T_{PC(LUC+FF)}$  respectively, as shown previously in **Table 4.4**.

#### 4.3.4.2 Regional Impacts

Compared to global findings, regional impacts of LUC are projected to be more significant (see **Figure 4.10**). In addition, warming/cooling is not only limited to areas experiencing land-use conversion but has a global impact. This is particularly the case for biogeochemical warming which is generally higher in the extratropics than in the tropics. In the carbon cycle component of the UVic model, CO<sub>2</sub> emissions are assumed to be instantaneously well mixed in the atmosphere (Matthews, 2004). As a result, biogeochemical warming from cropland expansion is transported via the atmosphere (and extensive ocean) towards the poles through polar amplification (Holland and Bitz, 2003). Across the scenarios, a mean warming of 0.013–0.029 °C occurs in the extratropics by 2075–2100 relative to 2005, despite being largely due to altered CO<sub>2</sub> fluxes from LUC in the mid latitudes (see **Figure 4.10**). This warming reaches up to 0.034–0.051 °C (by 2075–2100) in certain grid cells in the extratropics. The impact of bioenergy on regional biogeochemical warming is of similar magnitude, whereby mean warming equates to 0.016 °C/0.005 °C/0.015 °C in the extratropics in the Bio/Bio-REDD/Bio-WaterProt scenarios compared to the NoBioBE scenario. In certain regions warming reaches up to 0.10 °C in the Bio scenario, 0.083 °C in Bio-REDD, and 0.097 °C (by 2075–2100) in Bio-WaterProt, compared to the NoBioBE scenario.

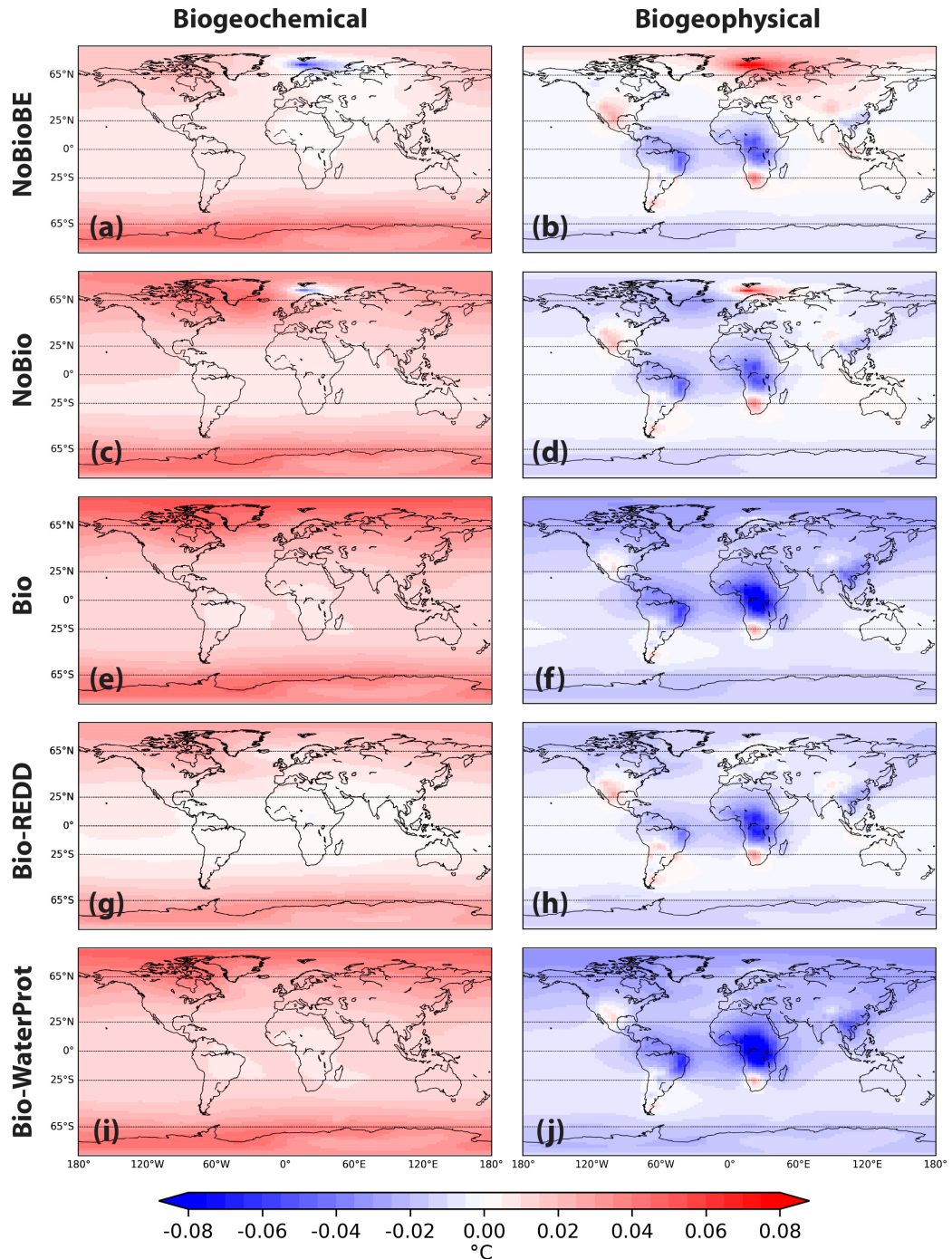


**Figure 4.10:** The spatial distribution of biogeophysical and biogeochemical impacts on surface temperature for the MAGPIE scenarios. Results have been plotted for the 25-year average of the period 2075–2100 compared to the 15-year average of the period 1995–2010. Biogeochemical and biogeophysical temperature changes were obtained using the calculations:  $T_{PC(LUC+FF)} - T_{FF}$  and  $T_{LUC+FF} - T_{PC(LUC+FF)}$  respectively, as shown previously in **Table 4.4**. Tropical and extratropical regions are illustrated by dotted lines at latitudes: 65°S, 25°S, 25°N and 65°N.

In contrast, biogeophysical cooling is higher in the tropics than in the extratropics in all scenarios, with stronger patterns occurring locally near to their source. In the tropics a mean biogeophysical cooling of  $(-0.0047-(-0.021) \text{ }^\circ\text{C}$  occurs by 2075–2100 relative to 2005 across all scenarios. This cooling is the result of effects such as increased surface albedo, reduced sensible heat, increased evaporation, and higher soil temperatures (see Section 4.4.4 detailing these effects). The most impacted regions are those that undergo large-scale energy and food/feed cropland expansion, namely Latin America, Sub-Saharan Africa, and Southeast Asia. In these regions, cropland expansion into forest and shrubland leads to a cooling of up to  $(-0.054-(-0.12) \text{ }^\circ\text{C}$  across the scenarios. Incorporation of bioenergy (in the Bio scenario) leads to a mean cooling of  $(-0.013) \text{ }^\circ\text{C}$  by 2075–2100 in the tropics, compared to the NoBioBE scenario. Implementation of REDD+ reduces this mean cooling (to  $(-0.0047) \text{ }^\circ\text{C}$  in Bio-REDD), whereas a slight increase in mean cooling occurs from adding water protection (to  $(-0.016) \text{ }^\circ\text{C}$  in Bio-WP). For certain regions, this cooling reaches up to  $(-0.090) \text{ }^\circ\text{C}$  in the Bio scenario,  $(-0.079) \text{ }^\circ\text{C}$  in Bio-REDD, and  $(-0.093) \text{ }^\circ\text{C}$  in Bio-WaterProt (compared to the NoBioBE scenario). Though the impact of incorporating water protection is only a small increase in regional biogeophysical cooling ( $(-0.003) \text{ }^\circ\text{C}$ ), cooling in this scenario occurs over a wider area compared to the Bio scenario, due to more forest land needed for rainfed cropland expansion. The opposite occurs for the incorporation of a REDD+ policy ( $(+0.0088) \text{ }^\circ\text{C}$ ), whereby less forest is lost.

Small patches of biogeophysical warming occur in Southern Africa, North America, and lower South America (see **Figure 4.10**). In these regions, increases in broad leaf forest implemented by the dynamic TRIFFID model result in lower surface albedo, increased sensible heat, reduced evaporation, and lower soil temperature. In the NoBioBE and NoBio scenarios, biogeophysical warming also occurs in the mid to high latitudes as high GHG-induced warming reduces snowpack and sea ice, further lowering surface albedo. This ice-albedo feedback is likely to account for much of polar amplification, though the strength of the feedback has shown to differ considerably among climate models (Holland and Bitz, 2003).



## 4.3.5 Climate Impacts from Land-Use Change Explained

### 4.3.5.1 Carbon Fluxes from Land-Use Change

Biogeochemical climate impacts determined in this study are due to altered fluxes of CO<sub>2</sub> from land-use change. In all PC and TL simulations, global terrestrial carbon stocks increase up to 41–59 GtC and 29–60 GtC respectively between 2005 and 2100, declining towards the end of the century for all scenarios apart from NoBioBE (see **Figure 4.11 (c)**). This trajectory is largely attributed to increases in soil carbon storage up to around 2060–2075, which then decline and are further dampened by loss of vegetation carbon over the century (see **Figure 4.11 (a) and (b)**). This increase in soil carbon mainly occurs over non-deforested areas and where shrubland has been converted to cropland (see Section 4.4.1.2 for more detail). The difference between land carbon storage for PC and TL simulations ( $TC_{PC(LUC+FF)} - TC_{LUC+FF}$ ; see Section 4.2.3), multiplied by the carbon-CO<sub>2</sub> conversion factor 3.67, provides the net LUC emissions (see **Figure 4.11 (d)**).

Globally, increases in soil carbon occur in both TL and PC simulations over the century, however more carbon is stored in TL simulations (up to ~54–65 GtC relative to 2005 in bioenergy scenarios) than in PC simulations (up to ~50 GtC) (See **Figure 4.11 (b)**). As a result, negative emissions occur for soil carbon (see **Figure 4.12 (f)**). Although this increase is relatively large, at the start of the century it is not enough to compensate for the loss of carbon from land-use changes (**Figure 4.11 (a)**), hence the net positive LUC emissions. Towards the end of the century, however, increased uptake of carbon from soil, and to a lesser extent C3 grasses and natural needle leaf vegetation growth, counteract the loss of carbon. This leads to a rapid reduction in LUC emissions, and for some scenarios (Bio-REDD and NoBioBE) net negative LUC emissions, thus reduced biogeochemical warming regionally and globally (see **Figure 4.11 (b)**).

In total, LUC emissions from the scenarios increase up to (+)53.7–(+63.4 GtCO<sub>2</sub> over the 21<sup>st</sup> century (in 2045), declining to (–)17.2–(+15.6 GtCO<sub>2</sub> by 2100. This occurs particularly in the tropics over deforested broad leaf areas (see **Figure 4.12**). Additionally, conversion of shrubland to C3 and C4 grasses (cropland and pasture) also has a significant influence, accounting for roughly 20% of overall LUC emissions in 2100, relative to 2005. C3 and C4 grasses take in CO<sub>2</sub> emissions through photosynthesis, enhanced by CO<sub>2</sub> fertilisation, however the magnitude of this is almost ten times smaller than the amount emitted from deforestation.

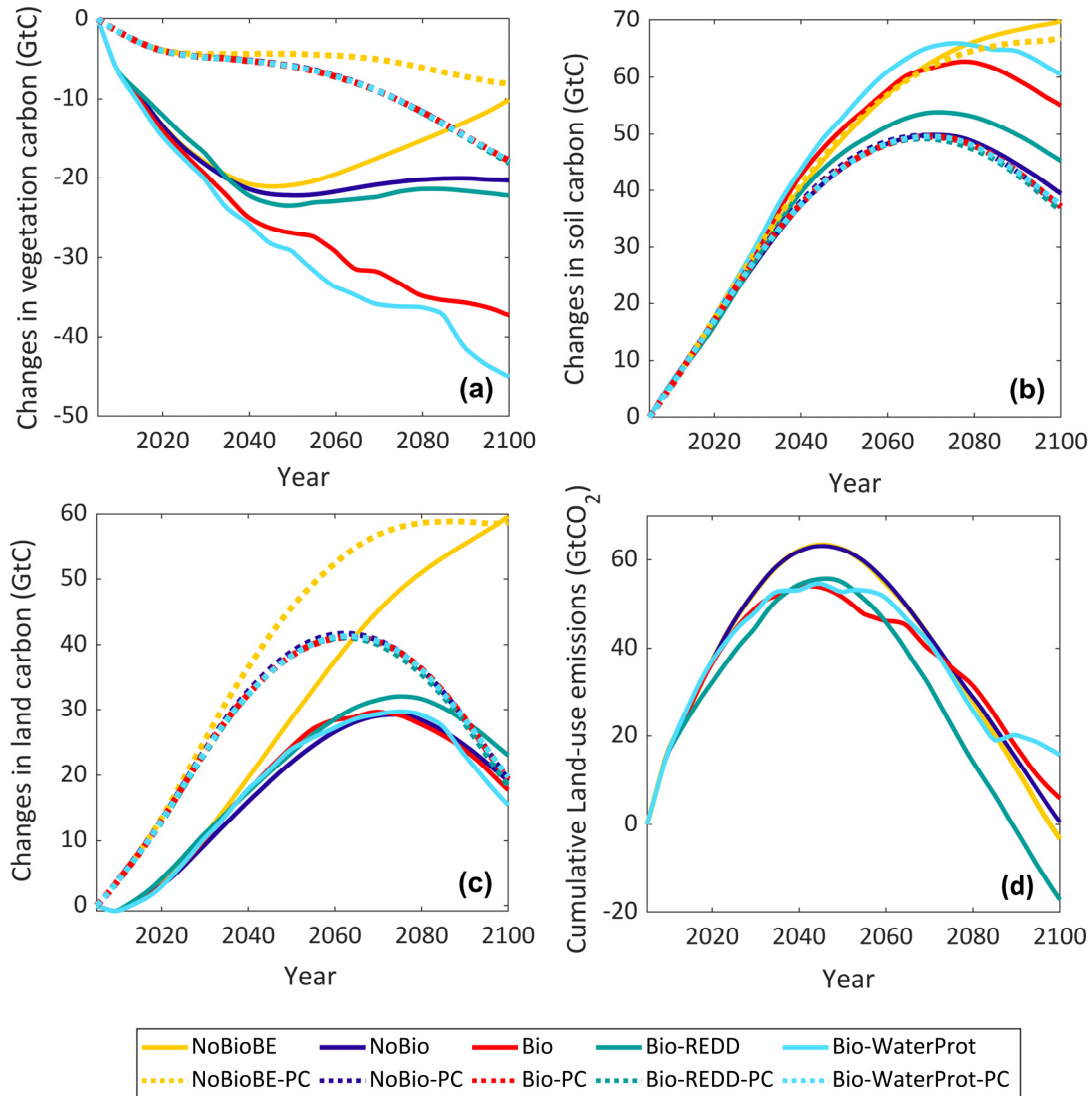


**Figure 4.11:** Projections of changes in vegetation carbon (a), soil carbon (b), land carbon (c) and cumulative LUC emissions (d) for the UVic simulations, between years 2005 and 2100. Plain lines represent TL simulations, and dotted lines represent PC simulations. LUC emissions in (d) are calculated as the difference between terrestrial carbon storage for PC and TL simulations ( $TC_{PC(LUC + FF)} - TC_{LUC + FF}$ ), multiplied by the carbon-CO<sub>2</sub> conversion factor 3.67.

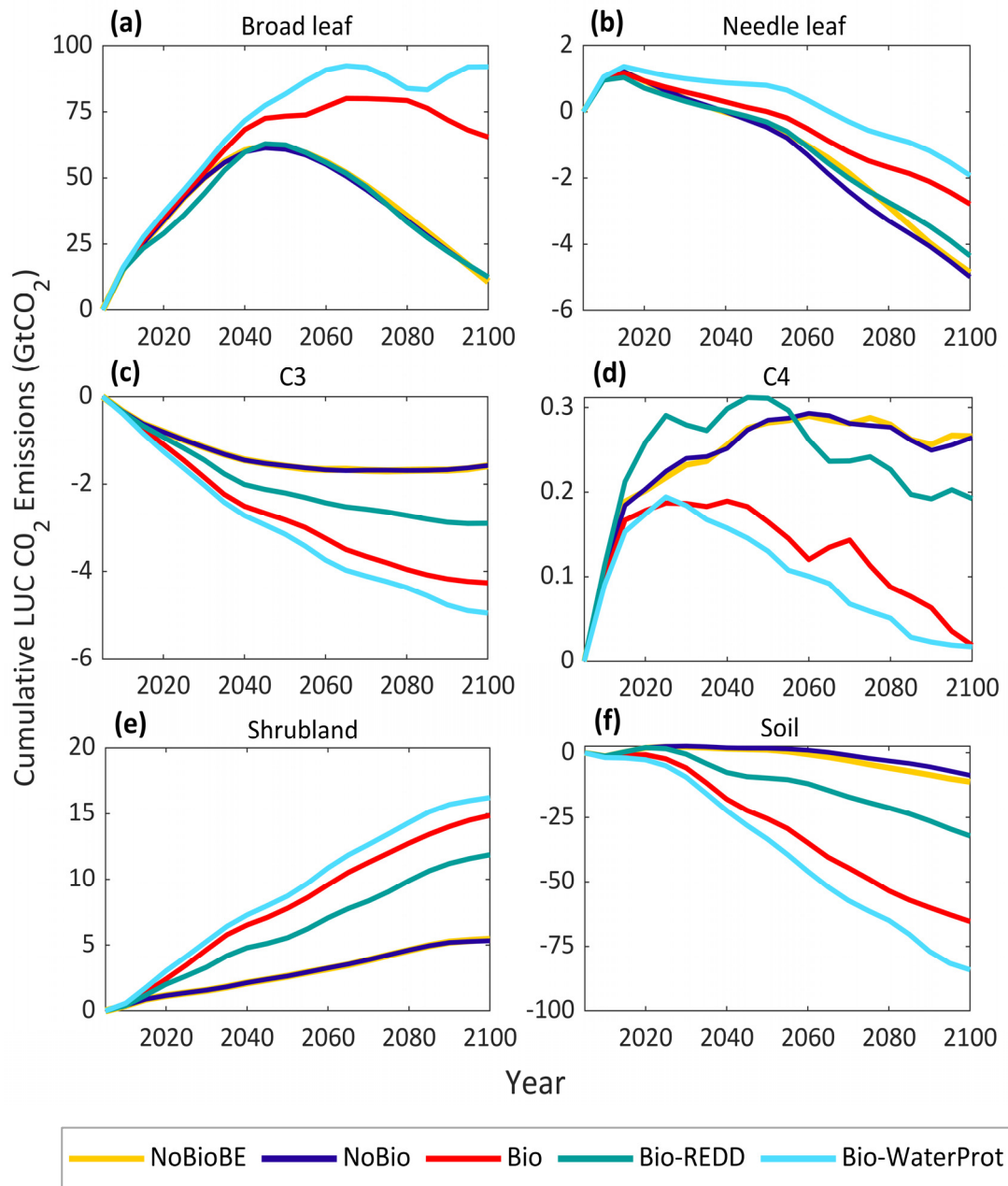


**Figure 4.12:** Projections of cumulative LUC emissions in the UVic simulations, for the five plant functional types (broad leaf trees, needle leaf trees, C3 grasses, C4 grasses and shrubland) and soil.

Findings further illustrate the relationship between soil carbon and the extent of shrubland converted to cropland/pasture, whereby increases in soil carbon (reductions in soil carbon emissions) are proportional to the area of shrubland lost to C3 grasses. For instance, in scenarios that have larger scales of shrubland conversion (Bio and Bio-WaterProt), soil CO<sub>2</sub> emissions reduce (and soil carbon increases) more significantly than in scenarios with less shrubland loss (NoBio, NoBioBE and Bio-REDD). The result is LUC emissions of magnitude 10 GtCO<sub>2</sub> lower in the Bio and Bio-WaterProt scenarios compared to the NoBio and NoBioBE scenarios at the start of the century (by 2050) (see **Figure 4.11** (d)). In addition to the small overall area of forest loss between TL and PC simulations (see Section 4.3.1), these interactions further explain the lack of variation in total LUC emissions and corresponding climate impacts between the scenarios. By 2075–2100 (compared to 2005), the impact of bioenergy (Bio-NoBioBE) is a small, almost negligible, increase in LUC emissions of 5 GtCO<sub>2</sub>, as forest clearing for energy cropland increases.

The incorporation of a water protection policy, in Bio-WaterProt (compared to NoBioBE) somewhat exacerbates this increase to 5.7 GtCO<sub>2</sub> by 2075–2100, as a result of larger areas of forest needed for cropland. As mentioned previously, the water protection policy used in the creation of the original MAgPIE scenario (Humpenöder et al., 2018a) implements the irrigation of only food/feed crops. In regions that have less water available for irrigation, more area is needed for these crops to make full use of rainwater. The resulting effect is less land area available for energy cropland which leads to a relocation of cropland to other regions that contain forest and shrubland. In contrast, reduced deforestation in the Bio-REDD scenario (compared to the NoBioBE scenario) lowers LUC emissions to (–)14 GtCO<sub>2</sub> by 2075–2100, indicating the importance of including REDD+ policies in future bioenergy expansion schemes. Forest management strategies, such as reduced clear cutting of managed forests and reforestation have been proposed for sequestering soil carbon and hence mitigating CO<sub>2</sub> emissions. However, their impacts on soil carbon accumulation remain uncertain, showing both positive and negative effects (Vesterdal et al., 2002; Lemma et al., 2006; Diocion et al., 2009; Yang et al., 2011; Li et al., 2012; Deng et al., 2014; Zhang et al., 2015; Bashkin and Binkley, 2017).

### 4.3.5.2 Biogeophysical Effects from Land-Use Change

Overall, the scenarios in this study induce a global biogeophysical cooling over the 21st century, as shown previously in Section 4.3.4. This can mainly be attributed to increased global surface albedo due to the biogeophysical effects of LUC i.e., conversion of less-reflective forest (broad leaf trees), to more-reflective cropland/pasture (C3 grasses) (see **Figure 4.13** (b) for the Bio scenario). This especially occurs in the tropics, where total surface albedo reaches up to 8–11% in grid cells (**Figure 4.14** (a)), and surface albedo due to LUC only ('Biogeophysical') reaches up to 6.10–6.15%, by 2075–2100, depending on the scenario (**Figure 4.14** (b)). As shown in **Figure 4.13** (a) and **Figure 4.14** (a), total surface albedo decreases over the century due to the overall reduction in snow and ice cover caused by increased CO<sub>2</sub> emissions and the polar amplification effect. This reduction is similarly shown in the biogeophysical contribution to albedo changes (**Figure 4.13** (b)) and largely accounts for the reduction in global biogeophysical cooling towards the end of the century in all scenarios.

Further analysis also shows evidence of the snow-vegetation albedo feedback (otherwise known as the tundra-taiga feedback) occurring in the scenarios. This process arises due to the increase in surface albedo as snow covers newly created open surfaces, which results in a cooling. Cooling at mid (20–40°N) and high (40°N and above) latitude regions favours expansion of Arctic sea ice, which in turn increases albedo, thereby exacerbating the overall cooling (Bonan et al., 1992; Claussen et al., 2001; Hallgren et al., 2012; Simmons and Matthews, 2016). This can be seen previously in **Figure 4.10** Section 4.3.4.2, whereby increased cooling in the higher latitudes occurs when bioenergy is incorporated. The cooling increases further when a water protection policy is included, due to more forest clearing occurring, and reduces when a REDD+ policy is implemented, due to prevented forest clearing.

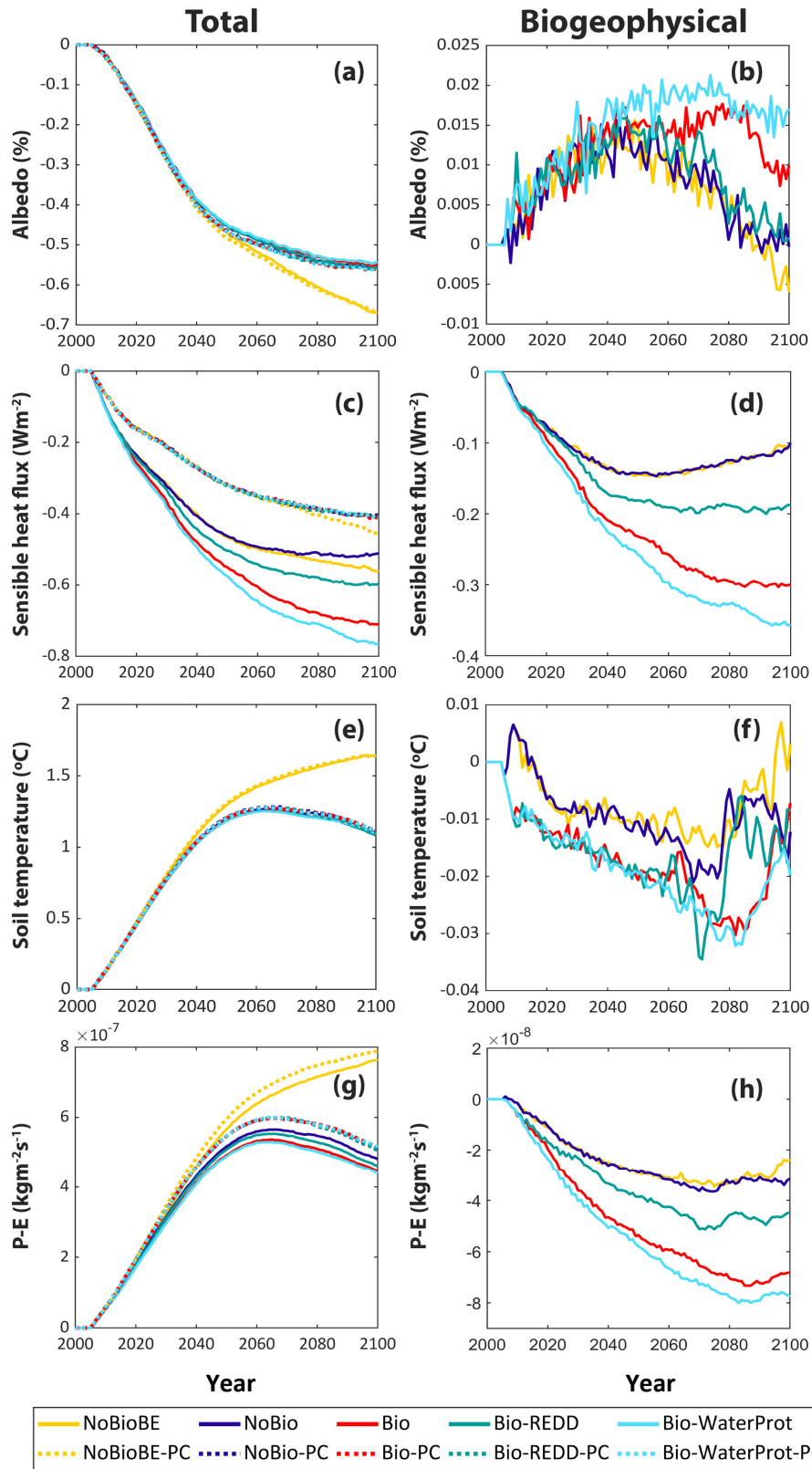


**Figure 4.13:** Projections of changes in soil temperature, sensible heat flux and P-E. Findings are shown for TL and PC simulations ((a), (c), (e), (g)) and the differences between them (LUC + FF – PC(LUC + FF)) indicating their relative contributions to biogeophysical effects leading to surface cooling or warming ((b), (d), (f), (h)).

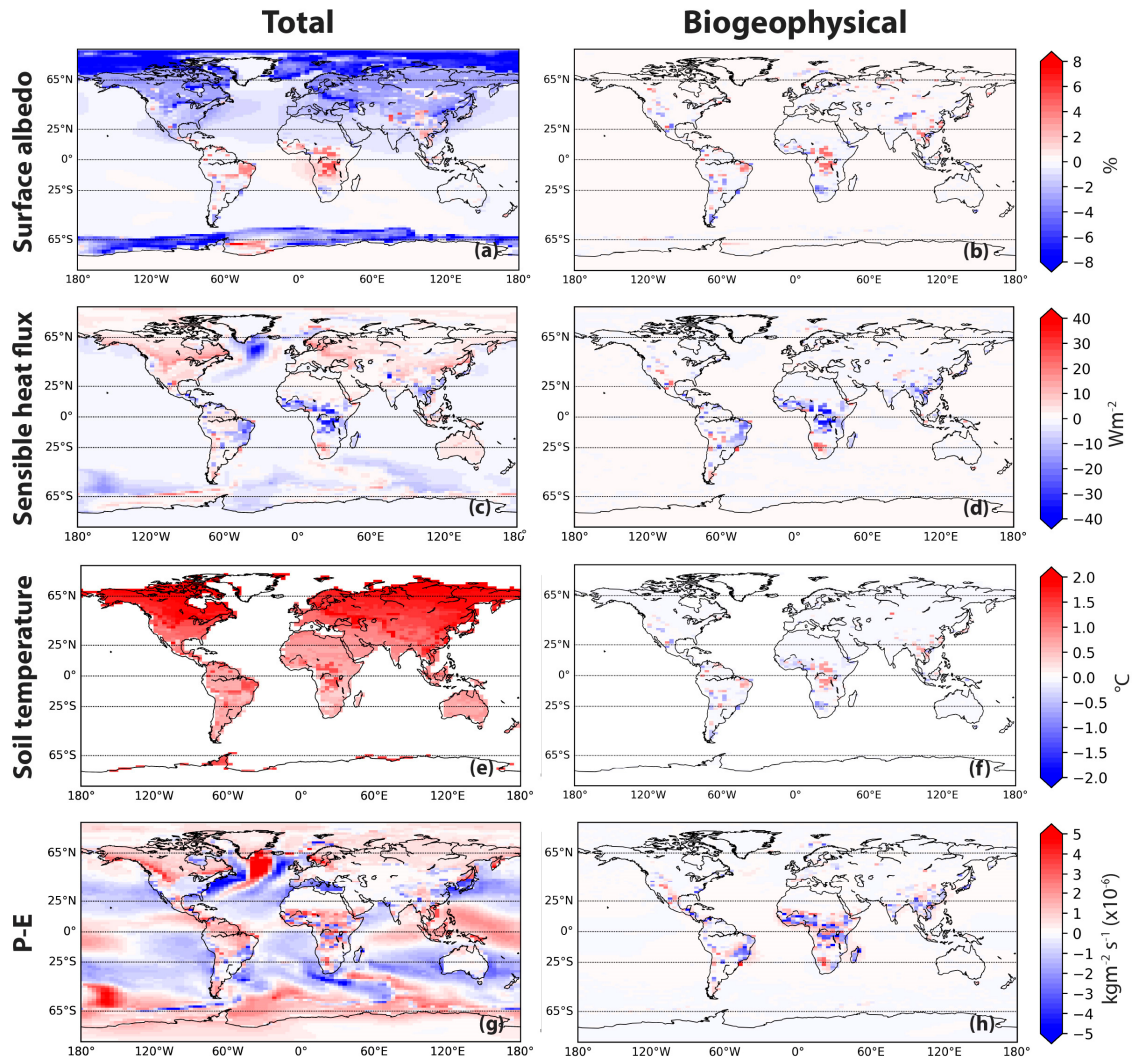


**Figure 4.14:** Spatial projections of changes in soil temperature, sensible heat flux and P-E in the Bio scenario. Findings are shown for TL and PC simulations ((a), (c), (e), (g)) and the differences between them ( $LUC + FF - PC(LUC + FF)$ ) indicating their relative contributions to biogeophysical effects leading to surface cooling or warming ((b), (d), (f), (h)). Results are for the 25-year average of the period 2075-2100 compared to the 15-year average of the period 1995-2010.

As roughness length over deforested areas lessens, the surface's ability to lose sensible heat (SH) reduces. Depending on the scenario, global SH flux due to LUC only falls to around  $(-0.15 - (-)0.36 \text{ Wm}^{-2})$  by 2100 (see Figure 4.13 (d)). Regionally, this shows a decline of up to  $(-31.9 - (-)41.9 \text{ Wm}^{-2})$  in certain grid cells by 2075-2100 across the scenarios **Figure 4.14** (d).

This phenomenon is depicted in the UVic ESCM by the sensible heat flux equation (Matthews et al., 2004):

$$SH = \rho C_D U (T_s - T_a) \quad (4.3)$$

where SH is sensible heat,  $\rho$  is the density of air, U is the wind speed,  $T_s$  is the soil temperature,  $T_a$  is the SAT and  $C_D$  is the Dalton number. The Dalton number is calculated from a specified surface roughness length ( $z_0$ ) according to the methodology of Brutsaert (1982):

$$C_D = k^2 \left( \ln \frac{z}{z_0} \right)^{-1} \left( \ln \frac{z}{z_{0q}} \right)^{-1} \quad (4.4)$$

where k is the Von Karman constant ( $k = 0.4$ ) and z is a reference height ( $z = 10\text{m}$ ). The roughness lengths for moisture ( $z_{0q}$ ) and heat ( $z_{0h}$ ) are calculated as  $z_{0q} = z_{0h} = e^{-2} z_0$  (Brutsaert, 1982). Deforestation reduces  $C_D$  because the grassland  $z_0$  is smaller than the forest  $z_0$ . This reduction is the driving component of SH reduction as all other terms in the **Equation (4.3)** lead towards increasing SH.

**Equations (4.5)** and **(4.6)** shows how the surface energy budget is balanced:

$$S \downarrow (1 - \alpha) + L \downarrow - L \uparrow + SH + LE + G = 0 \quad (4.5)$$

$$NR + SH + LE + G = 0 \quad (4.6)$$

Where NR is the net surface radiation,  $S \downarrow$  is global radiation,  $\alpha$  is albedo,  $L \downarrow$  is atmospheric counter-radiation,  $L \uparrow$  is terrestrial radiation, LE is latent heat, SH is sensible heat, and G is the ground heat flux. The reduction in outgoing SH over deforested regions surpasses the increase in outgoing net radiative and latent heat fluxes. This leads to a local cooling over deforested areas in the tropics.

Global soil temperatures increase in all PC and TL scenarios, declining towards the end of the century due to changes in the surface energy balance; a similar trend occurs for the SAT response shown in Section 4.3.2, **Figure 4.7**. These increases occur despite the added cooling from increased latent heat and surface albedo, primarily because roughness length decreases following deforestation. The reduction in SH over deforested areas is one cause of the biogeophysical increase in soil temperatures (of up to  $(+1.19 - +1.27)^\circ\text{C}$ ) in these regions (see **Figure 4.14** (f)). This warming then induces a small increase in local evaporation (E). Precipitation (P) also increases in these deforested bins, however in most areas less than



evaporation, leading to localised drying of up to  $(-5.68 \times 10^{-6} - (-7.73 \times 10^{-6}) \text{ kgm}^{-2}\text{s}^{-1}$  by 2100 across scenarios (see **Figure 4.14** (h)). Areas that become wetter (positive P–E) also experience an increase in both precipitation and evaporation, however the increase in precipitation is larger. The overall impact is a global mean increase in drying (reduction in biogeophysical P–E) over the century (**Figure 4.13** (h)).

#### 4.3.5.2.1 Impacts of Bioenergy on Biogeophysical Effects

**Figure 4.15** shows the biogeophysical impacts of the three bioenergy scenarios (Bio, Bio-REDD and Bio-WaterProt) in comparison to the NoBioBE scenario. The incorporation of bioenergy accounts for a considerable proportion of the biogeophysical effects shown previously in **Figure 4.13** and **Figure 4.14**.

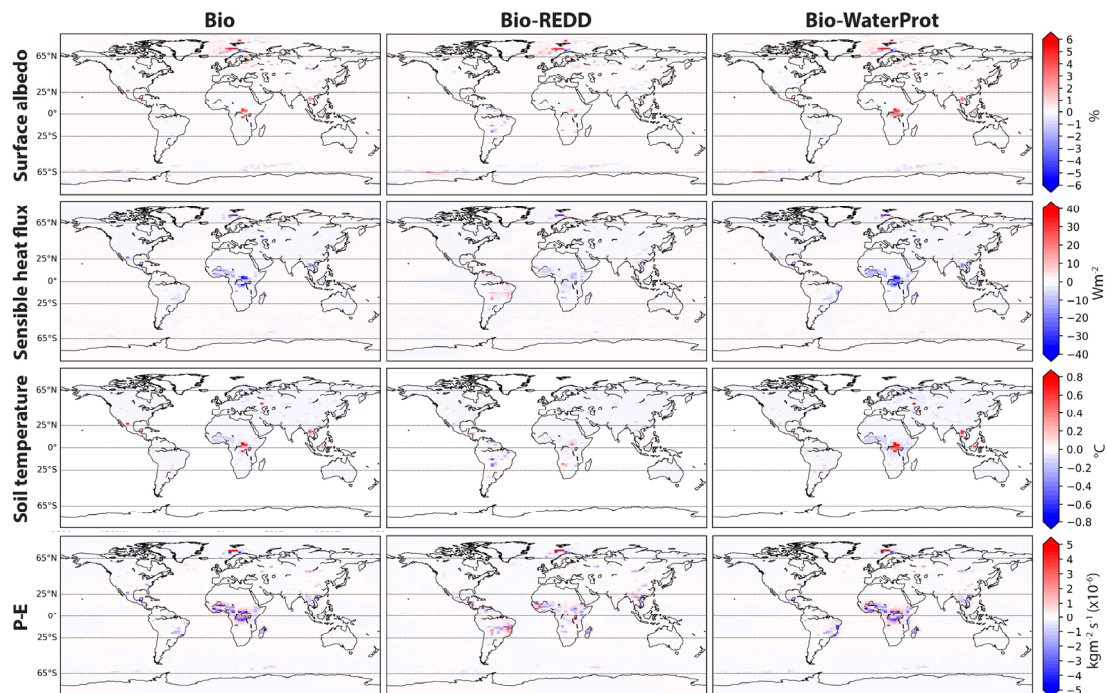


**Figure 4.15:** Impacts of bioenergy (alone and with REDD+ and water protection policies included) on biogeophysical effects. Results have been calculated as the differences between the three scenarios Bio, Bio-REDD and Bio-WaterProt, and the NoBioBE scenario. They have been plotted for the 25-year average of the period 2075-2100 compared to the 15-year average of the period 1995-2010.

This impact mainly occurs in Latin America, Sub-Saharan Africa, and Southeast Asia regions, where most conversion of forest for cropland (energy or food/feed) occurs due to bioenergy expansion. Across these regions, surface albedo reaches +13.4% in certain grid cells, SH flux reaches  $-45.6 \text{ Wm}^{-2}$ , soil temperature reaches  $-45.6 \text{ Wm}^{-2}$ , and P–E reaches up to  $-8.53 \times 10^{-6} \text{ kgm}^{-2}\text{s}^{-1}$  by 2075–2100 (compared to 1995–2010), as a result of bioenergy expansion. The incorporation of water protection does not increase these values significantly, however, causes them to occur over a wider area of land, due to more land needed for rainfed cropland expansion. The opposite effect occurs when REDD+ is incorporated due to less cropland expansion into forests. Lack of previous research into biogeophysical effects in the bioenergy literature (see *Chapter 2*), in addition to the potentially significant regional impacts discussed in this chapter, indicate that this field requires further work.

## 4.4 Discussion

### 4.4.1 Importance of Land Representations

#### 4.4.1.1 Model Representations of Land-Use Changes

As mentioned in Section 4.3, total forest loss in the UVic simulations is relatively low compared to forest loss in the original MAgPIE scenarios. This is partly because agricultural expansion in the TL simulations occurs at the expense of shrubland rather than forest. Another factor is the significant natural loss of forest in the UVic PC simulations resulting from changes in climate, particularly in the tropics. Consequently, the difference in forest loss between TL and PC simulations (PC simulation – TL simulation) is low.

Previous work indicates a mix of findings for change in forest within PC simulations. In contrast to this study, Brovkin et al. (2013) simulate an increase in tree cover in response to climate and CO<sub>2</sub> changes for most of their PC simulations, particularly for models with dynamic vegetation (HadGEM2-ES, MIROC-ESM and MPI-ESM-LR). Hence, estimations of overall forest loss, i.e., the difference between TL and PC simulations, are generally higher in their work than in this study. The spread in tree cover outputs shown in their work demonstrates the wide range of possible outcomes, dependant on the model used. These uncertainties emerge from differences in implementation of land-use data, inclusion or exclusion of specific land-use processes such as wood harvest, and varying climate-carbon cycle representations within

the models. Consequently, differences occur not only in the way land-use change is interpreted in terms of land-cover changes, but also in translating these land-cover changes into biogeophysical and biogeochemical characteristics of the land surface.

For the purpose of this work, the UVic ESCM v2.9 model was employed because of its flexibility and fast simulations. While its incorporation of dynamic vegetation arguably makes it more sophisticated than many other models with prescribed land cover, the use of only one model of intermediate complexity in this work has its limitations. As illustrated in the work of Brovkin et al. (2013), future assessment using an ensemble of multiple climate models with varying complexities could provide a broader understanding of potential climate impacts from land-use within the MAgPIE scenarios. Further work could assess other possible land-use pathways (e.g., SSPs and RCPs) constructed from different integrated assessment models.

#### **4.4.1.2 Effects of Present-Day Land Distributions**

Another reason for low forest loss in the UVic model is that the expansion of cropland, and therefore C3/C4 grasses, occurs in grid cells where C3/C4 grasses already exists, rather than over forest land, as exhibited in the MAgPIE scenarios. As shown in **Figure 4.16** for the Bio scenario, this effect is particularly prevalent in parts of Eastern US, Southern Brazil, Eastern Africa, and Madagascar, whereby forest cover exists at present day in the MAgPIE scenarios but not in the UVic model. Previous work corroborates the existence of forest in regions such as these. For instance, Hansen et al. (2013) use Earth observation satellite data to map forest loss between 2000 and 2012. In the mentioned regions, their findings indicate tree cover of up to 80% or more in the year 2000, and a loss of approximately 1-40% of forest extent by 2012. As indicated by the MAgPIE model, this loss could increase up to 80% or more by 2100 (when following the Bio scenario trajectory). Thus, the exclusion of this forest loss in the UVic model could have significant consequences on overall climate impacts.

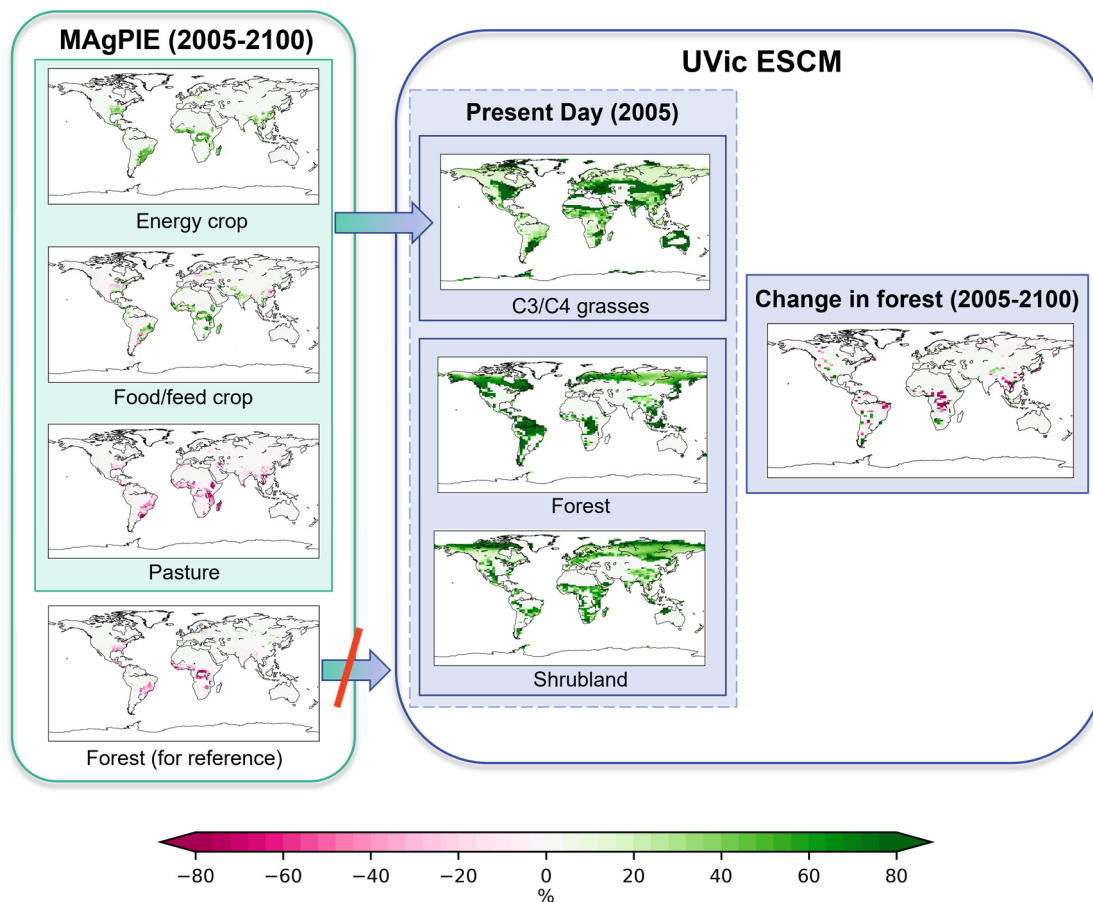


**Figure 4.16:** Spatial land-use changes occurring in the UVic model simulations, resulting from inputs (cropland and pasture) for the Bio MAGPIE scenario; calculated for 2100 relative to 2005. Corresponding changes in UVic forest cover are provided alongside changes in forest in the original MAGPIE scenario. Values are percentages of grid cells undergoing land cover changes.

On the other hand, observations also show forest gain within the mentioned regions (Hansen et al., 2013). Together, co-location of forest loss and gain is likely indicative of intensive forestry practices. In general, forestry in the temperate climatic region has a relatively low ratio of loss to gain, though extensively high losses have occurred, for instance in the intermountain West of North America, as well as in Europe across Estonia, Latvia, and Portugal. In these regions, tree mortality is largely due to fire, logging, and disease. Fire is the most significant cause of forest loss in boreal forests and has led to huge overall depletions, particularly in Siberia, Russia. Other countries that have lost forest without any gain are mainly located across tropical regions (e.g., Brazil, Malaysia, Cambodia, Paraguay, Mongolia, Zambia, Tanzania, and Argentina).

Overall, quantification of global forest dynamics is complex and depends on a variety of different factors. Changes in conservation policies can further add to this complexity, with some strategies being more successful than others. For instance, Brazil's policy intervention is considered to have helped reverse decades of previous widespread deforestation, whereas international initiatives such as the UN REDD program can be less effective due to lack of operational capabilities (see Section 2.5.1). The use of up-to-date observations within the initialisation process in land-use modelling could therefore help improve the robustness of results.

In terms of present-day forest representations, it is evident that MAgPIE outputs are more closely aligned to observations than UVic outputs, largely due to the differences in resolutions between the models (whereby UVic's resolution is lower). However, both models indicate uncertainties when depicting future changes in forest cover over time. In addition to those previously discussed for the UVic model, dissimilarities between observed and MAgPIE data can be seen in regions such as Western North America, North-Eastern Brazil, South-Eastern Asia, Siberia, and Australia, in which zero or very little forest loss occurs in MAgPIE scenarios. In observations, extensive forest loss is seen in these regions between years 2000 and 2012, suggesting that they could be expected to undergo further reductions over the 21<sup>st</sup> century (Hansen et al., 2013).

Disparities between modelled outputs further highlight the differences in land dynamics occurring within the two DGVMs used: LPJmL in the MAgPIE model, and TRIFFID in the UVic model. The evolution of these models spans over many decades, with each containing features based on different models and observation datasets. As mentioned in Section 4.2.1, the land surface scheme within TRIFFID is a simplified version of 'MOSES' (The Met Office Surface Exchange Scheme), described in Cox et al. (1999). This land surface scheme improves on the simple land surface "bucket" model used in Matthews et al. (2003), which is based on land classifications and land-atmosphere forcings derived from calculations using the Normalized Difference Vegetation Index (NDVI) observational data (Defries and Townshend, 1994; Sellers et al., 1996). On the other hand, the LPJmL model has adopted many of its land surface features from the BIOME family of models (Prentice et al., 1992; Foley et al., 1996; Haxeltine and Prentice, 1996; Haxeltine et al., 1996; Kaplan, 2001). Within these DGVMs, the area coverage, leaf area index and canopy height of each plant functional type are calculated based on bioclimatic limits and a 'carbon balance approach', in which vegetation change is

driven by climate conditions and net carbon fluxes (Foley et al., 1996; Sitch et al., 2003; Meissner et al., 2003).

Each of these models has been rigorously tested and outputs compared to various observation and cartographically derived biome datasets (Olsen and Watts, 1982; Dunderdale et al., 1999; Sitch et al., 2003; Schaphoff et al., 2018). However, findings in this section indicate opportunities for further comparison assessments using more recent observational data, such as the high-resolution forest maps produced by Hansen et al. (2013). In addition, a sensitivity analysis could be carried out, comparing the impacts of different forest distributions in the UVic model. While it is not currently possible to prescribe forest in the UVic model, future work could determine the viability and usefulness of creating such an input. This could be carried out in two ways: through input of present-day forest, while turning on the dynamic vegetation component of the model, or input of transient changes in forest distribution over the study period, while turning off the dynamic vegetation module. By inputting projected forest representations calculated in the MAgPIE scenarios using the LPJmL model, outputs can be compared to those in this study (determined by the TRIFFID model) to provide an understanding of the differences between land surface schemes within the two DGVMs and corresponding climate impacts. Creation of a forest input for the UVic model could further provide opportunities for more consistent and transparent land-use representation, as well as the simulation of important influencers such as wood harvest and fires.

## 4.4.2 Biogeochemical and Biogeophysical Climate Impacts

### 4.4.2.1 Climate Impacts of Total Land-Use Change

Previous literature, like this study, has shown that LUC has a small overall impact on global climate, however, individual biogeophysical and biogeochemical impacts vary widely across studies. **Figure 4.17** displays findings for biogeophysical and biogeochemical impacts, produced in this chapter, alongside values produced in other studies for the historical (1990–2005 to 1700–1850) and future (2005–2006 to 2070–2100) periods, taken from the work of Jia et al. (2019) and discussed previously in *Chapter 2* Section 2.3.6. Results shown for this work are the mean values for the period 2075–2100 and the maximum values of the whole time period (2005–2100). This representation has been chosen because, unlike findings in some of the literature, values for 2100 in this study were not necessarily the highest values in the 2005–2100 period.

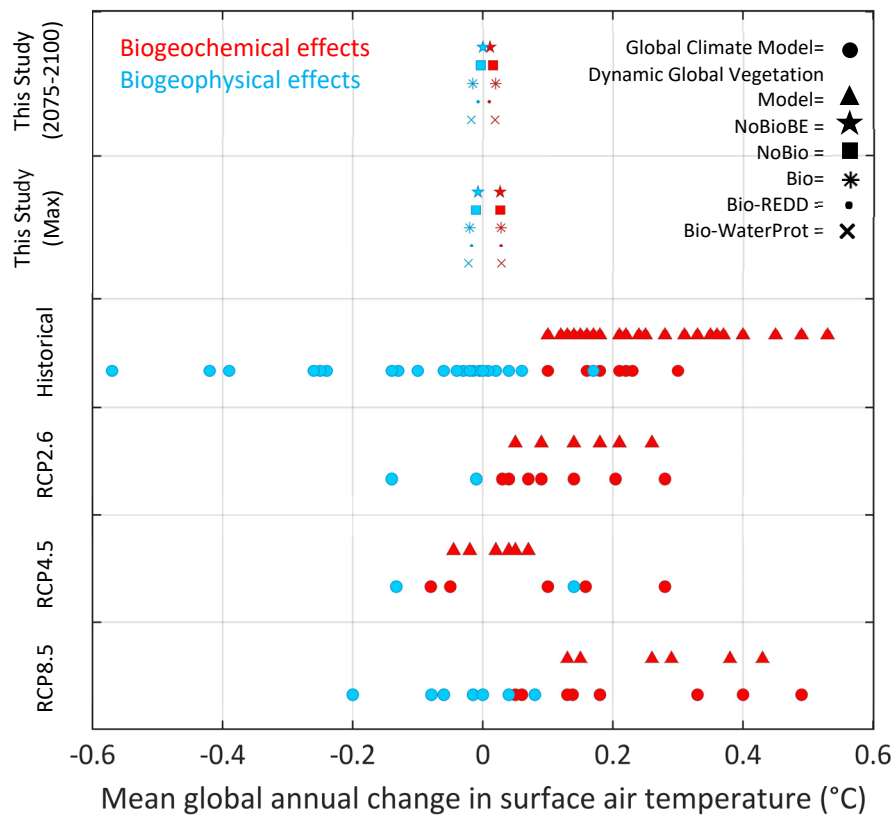


**Figure 4.17:** A comparison of global annual biogeochemical and biogeophysical changes in surface air temperature ( $^{\circ}\text{C}$ ) in response to land-use changes between this study and previous work. Results for this study are for the five MAGPIE land-use scenarios, and are shown as the average for the period 2075-2100 compared to 2005, and the maximum absolute values (within the period 2005-2100) compared to 2005. They are indicated by five different symbols (a star, square, asterisk, dot, and cross). For comparison, previous findings assessed in the work of Jia *et al.* (2019) (see **Figure 2.11** in Chapter 2) have been included. These comprise of historical absolute values (taken from years within the period 1990-2014 compared to years in the period 1700-1920) and future values (either for 2099 or 2100 compared to years in the period 2000-2006) (Chase *et al.*, 2000; Betts, 2001; Chase *et al.*, 2001; Zhao and Pitman, 2002; Gibbard *et al.*, 2005; Feddema, 2005; Brovkin *et al.*, 2006; Betts *et al.*, 2007; Findell *et al.*, 2009; Arora and Boer, 2010; Kvalevåg *et al.*, 2012; Lawrence *et al.*, 2012; De Noblet-Ducoudré *et al.*, 2012; Houghton *et al.*, 2012; IPCC, 2013; Zhang *et al.*, 2013; Jones *et al.*, 2013; Boysen *et al.*, 2014; Davies-Barnard *et al.*, 2014; Carvalhais *et al.*, 2014; Pugh *et al.*, 2015; Devaraju *et al.*, 2015; Hansis *et al.*, 2015; Hua *et al.*, 2015; Avitabile *et al.*, 2016; Simmons and Matthews, 2016; Li *et al.*, 2017; Tharammal *et al.*, 2018; Lawrence *et al.*, 2018). Note: Results from the work of Simmons and Matthews (2016) have been recalculated by the author, and included in this plot, since the work of Jia *et al.* (2019) was published.

In comparison to all future RCP estimates in **Figure 4.17**, findings in this work are at the low end of the spectrum, ranging between +0.027 °C and +0.029 °C ('Max'), and +0.0089 °C and +0.019 °C (2075–2100). Other studies which calculate similarly low values for the most comparable pathway RCP2.6 are Lawrence et al. (2012) (+0.03 °C), Davies-Barnard et al. (2014) (+0.04 °C), Brovkin et al. (2013) (+0.04 °C), and Pugh et al. (2015) (+0.05°C). Biogeophysical cooling is estimated to range between (–)0.0075 °C and (–)0.022 °C, and (–)0.00089 °C to (–)0.019°C across the scenarios in this work. In comparison to the two other studies which calculate biogeophysical cooling from LUC, findings corroborate values determined by Davies-Barnard et al. (2014), who calculate a low cooling of (–)0.01 °C using the HadGEM2-ES climate model. However, they are relatively small compared to the (–)0.14 °C cooling calculated by Simmons and Matthews (2016), who use the same UVic ESCM for their analysis. Although the results in this study are low, they are noteworthy in comparison to the projected global mean warming for the RCP2.6 pathway (0.3–1.7 °C by 2100 compared to 1986–2005, depending on the model and scenario) (Jia et al., 2019).

#### 4.4.2.2 Isolated Climate Impacts of Bioenergy

As discussed in *Chapter 2*, only a small number of studies have isolated the influence of bioenergy in future impacts of LUC on climate. The most comparable work to this study is that of Hallgren et al. (2013) (further detailed in the work of Hallgren et al. (2012)) who use an integrated global climate model to determine impacts of bioenergy expansion for two scenarios: 1) a “deforestation scenario”; whereby large-scale deforestation occurs directly or indirectly to meet bioenergy demands (141 EJ yr<sup>-1</sup> by 2050), and 2) an “intensification scenario”; in which existing managed lands are used more intensively for bioenergy production (128 EJ yr<sup>-1</sup> by 2050) to reduce deforestation.

Although similar bioenergy potentials are applied in their work to this study (around 150 EJ in 2050), findings from Hallgren et al. (2013) are generally at least ten times greater than results in this study. For instance, they show that global biogeochemical warming due to bioenergy expansion increases to 0.04–0.11 °C and that global biogeophysical cooling increases to (–)0.1–(–)0.12 °C by 2050, relative to 2000. Whereas in this study, biogeochemical warming only rises to 0.004, and biogeophysical cooling only declines to (–)0.008–(–)0.011 °C by 2050 as a result of bioenergy incorporation. This is largely due to a much higher area of forest utilised for cropland expansion in their scenarios compared to more shrubland used in the UVic model in this study (see **Table 4.6**). Combined impacts are more in line with this work, whereby



biogeochemical and biogeophysical effects cancel each other out to form overall negligible impacts on climate. In contrast, recent work by Muri (2018) shows that LUC due to bioenergy expansion has a non-negligible impact on global climate in RCP2.6 pathways aiming to reach the 1.5 °C target. Their work uses the Norwegian ESM (NorESM1-ME) and demonstrates that cultivating energy cropland on abandoned land in the extratropics could result in a combined global cooling of (–)0.1 °C, thus having a beneficial impact on global temperature. They also, however, calculate that replacing tropical forests could lead to a warming of (+)0.17 °C, largely due to increases in LUC emissions. Both findings from Muri (2018) and Hallgren et al. (2013), overall, emphasize the importance of incorporating forest conservation in future pathways with large-scale bioenergy production, also illustrated in this work.

**Table 4.6:** Bioenergy-induced LUC and climate impacts calculated in this study for the original MAgPIE scenarios and UVic simulations, in addition to findings from Hallgren et al. (2013), for the year 2050 relative to 2000. Values are calculated by subtracting results for NoBioBE from results for the bioenergy scenarios.

		<u>This study</u>			<u>Hallgren et al 2013</u>	
		Bio	Bio-REDD	Bio- WaterProt	Case 1	Case 2
<b>Global land use in original MAgPIE scenarios (2050-2000)</b>	Energy					
	Crops	3.12	3.14	3.22	15.25	14.07
	Food/Feed					
	Crops	0.75	0.78	1.6	-3.03	-1.63
	Forest	-1.48	1.14	-1.76	-1.27	-0.81
<b>Global land use in climate model (UVic) outputs (2050-2000)</b>	ONL	-1.9	-5.1	-2.5	-10.30	11.26
	Pasture	-0.49	0.04	-0.53	-0.65	-0.37
	Broad leaf forest	-0.199	-0.03	-0.33	-	-
	Needle leaf forest	-0.015	-0.006	-0.034	-	-
	C3 grass	1.32	0.54	1.7	-	-
<b>Biogeochemistry</b>	C4 grass	0.35	0.24	0.37	-	-
	Shrubland	-1.46	-0.78	-1.7	-	-
	Tropics	-0.001	+0.002	+0.001	+0.06	+0.03
	Extratropics	+0.006	+0.007	+0.007	+0.16	+0.05
	Global	+0.004	+0.004	+0.004	+0.11	+0.04
<b>Biogeophysics</b>	Tropics	-0.005	-0.004	-0.006	-0.05	-0.08
	Extratropics	-0.012	-0.011	-0.013	-0.18	-0.12
	Global	-0.009	-0.008	-0.011	-0.12	-0.10
<b>Combined</b>	Tropics	-0.006	-0.002	-0.005	-0.02	-0.06
	Extratropics	-0.006	-0.004	-0.006	0.002	-0.07
	Global	-0.005	-0.004	-0.007	-0.01	-0.06

There is consensus among the literature that regional climate impacts of LUC from bioenergy expansion may be felt more significantly than global impacts, and that these impacts vary widely depending on location. For instance, mean biogeochemical warming and biogeophysical cooling estimates are projected to be larger for the extratropics than for the tropics or the globe in both this study and the work of Hallgren et al. (2013) (see **Table 4.6**). Muri (2018) also demonstrate fluctuations in regional cooling and warming in their scenarios. The significance of regional and local climate impacts has been confirmed in various regional modelling studies for countries such as the US (VanLoocke et al., 2010; Georgescu et al., 2011; Anderson et al., 2013; Caiazzo et al., 2014; Harding et al., 2016), Germany (Tölle et al., 2014), Malaysia (Caiazzo et al., 2014) and Mexico (Caiazzo et al., 2014). This literature has demonstrated both positive and negative impacts of converting existing cropland or marginal land to second-generation bioenergy, particularly highlighting the cooling and warming effects of changes in surface albedo, and the potential implications for the water cycle (see *Chapter 2*, Section 2.3.7). Overall, variations between regional and global studies indicate the importance of understanding impacts at both levels in future work.

### 4.4.3 Biogeochemical Impacts in More Detail

#### 4.4.3.1 A Comparison to Integrated Assessment Model Studies

In general, all scenarios show a move towards negative yearly LUC emissions in the second half of the century, as deforestation of broad leaf tropical forest slows down in the mid latitudes and afforestation of needle leaf forest starts to increase in the high latitudes (see previously in **Figure 4.4**). This corroborates findings produced by the original creators of the MAgPIE scenarios, and results for other SSP2 RCP 2.6 scenarios calculated by integrated assessment models (IAMs) (Riahi et al., 2017; Popp et al., 2017; IIASA, 2018b). However, LUC emissions in this work are low and do not fluctuate much throughout the century, resembling the time series calculated by the AIM/CGE model, rather than trends from the MAgPIE or REMIND-MAgPIE models.

As a result, the impact of bioenergy on LUC emissions is significantly lower in this work (5 GtCO<sub>2</sub> by 2075–2100 relative to 2005) than for the original scenarios calculated by Humpenöder *et al.* (2018a) (293 GtCO<sub>2</sub> by 2100 compared to 2010). In their work, LUC emissions increase steadily over the century, peaking in 2100 in all scenarios apart from NoBio (see **Figure 4.18**). Melillo, Reilly, et al. (2009) similarly show a peak in LUC emissions in

2100, calculating additional LUC emissions of 164 GtCO<sub>2</sub> relative to 2000 due to bioenergy incorporation, as discussed in *Chapter 1* Section 2.3.7. In contrast to these studies, LUC emissions in the UVic simulations peak at around 2040–2050 due to differences in land carbon between PC and TL simulations being highest at this point.

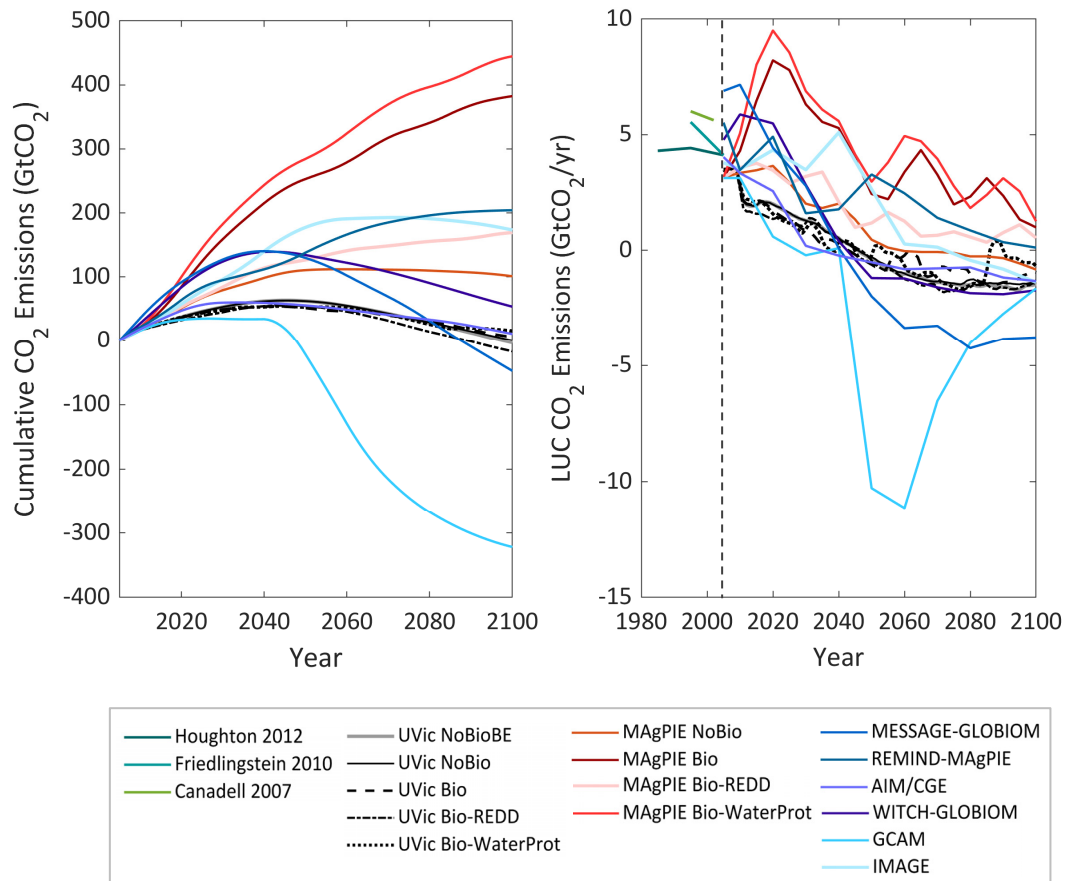


**Figure 4.18:** Projections of cumulative and yearly LUC emissions in the UVic simulations, in addition to findings for the original MAgPIE scenarios (as shown in Humpenöder et al. (2018a)), SSP2 data from the online SSP database (Riahi et al., 2017; IIASA, 2018), and historical data from the works of Houghton et al. (2012), Friedlingstein et al. (2010), and Canadell et al. (2007).

Further, by comparing cumulative LUC emissions to overall cumulative CO<sub>2</sub> emissions (shown previously in **Figure 4.7**) over the century, this can indicate the time it takes for bioenergy carbon savings from avoided fossil fuel combustion to offset LUC emissions (or ecosystem carbon payback times (ECPTs). Overall, it takes approximately 11 years (between 2005 and 2016) for CO<sub>2</sub> savings from incorporating bioenergy to compensate the 5 GtCO<sub>2</sub> of LUC

emissions produced by 2075–2100. This payback period is relatively low compared to findings from Harper et al. (2018), who predict periods of 10–100+ years for scenarios with global warming targets of 1.5 °C.

As discussed, disparities between findings can be attributed to factors such as differences in initial carbon stocks, forest change distributions and potential soil carbon uptakes between the models. In addition, the use of climate model simulations in this study incorporates the interaction between land and the atmosphere, which is not captured in results produced by IAMs. LUC emissions in IAMs are instead only calculated as changes in terrestrial carbon stocks between two time-steps. Overall, the LUC emissions determined in this study are situated almost midway between projections for other SSP2 RCP2.6 scenarios, which corresponds well with projected bioenergy demand associated with these scenarios (see **Figure 3.2** in *Chapter 3*).

#### **4.4.3.2 A Comparison to Climate Model Studies**

**Figure 4.19** displays findings in this chapter for LUC emissions and corresponding biogeochemical effects produced in the UVic simulations. Alongside these are results from previous work investigating RCP2.6 using GCMs and DGVMs (shown previously in *Chapter 1*). The most comparable results to this study are those produced by the models CCSM4 and HadGEM2-ES in the works of Lawrence et al. (2012), Brovkin et al. (2013), Davies-Barnard et al. (2012), and Davies-Barnard et al. (2014). These studies calculate LUC emissions of between 56.5 GtCO<sub>2</sub> and 68.7 GtCO<sub>2</sub>, and corresponding biogeochemical impacts of between (+)0.03 °C and (+)0.04 °C, by 2100. With regards to findings from Brovkin et al. (2013) and Davies-Barnard et al. (2014), this is most likely due to similarities between the UVic and HadGEM2-ES models in terms of their implementation of LUC, physical model components and land-carbon cycles (Alexander and Easterbrook, 2015). Low values produced in the work of Lawrence et al. (2012) are the result of low wood harvest flux and net ecosystem exchange (NEE) in the RCP2.6 scenario and CCSM4 model.

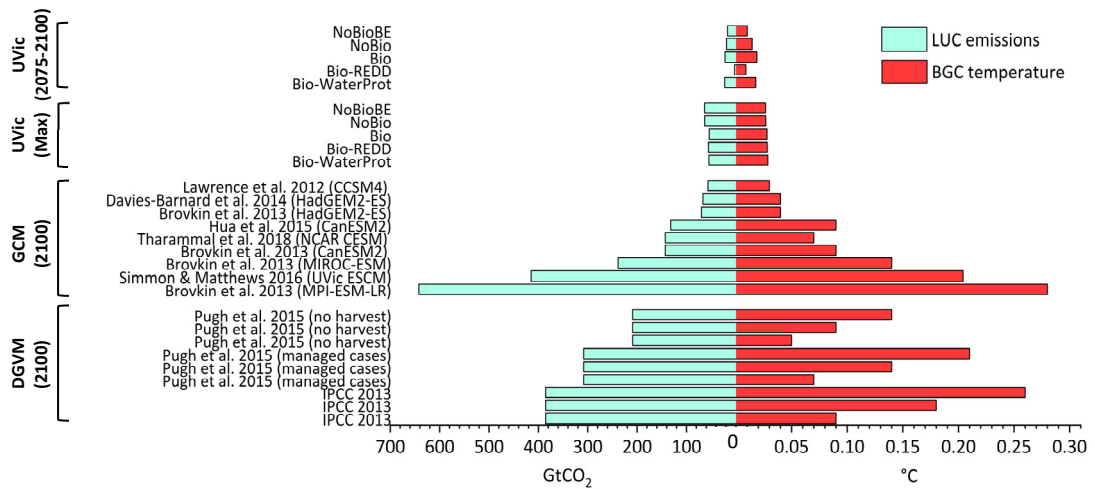


**Figure 4.19:** LUC emissions and corresponding biogeochemical effects on temperature, calculated in this study and for RCP2.6 scenarios in a range of studies using GCMs and DGVMs. Results in this study are shown as the average for the period 2075–2100, and maximum values (between 2005 and 2100, relative to 2005). Literature findings are for the period 2099–2100 relative to 2000–2006.

Disparities with other findings in **Figure 4.19** are likely due to spatial differences in LUC in the simulations, differences in climate-carbon cycle interactions (Houghton et al., 2012), and the incorporation of specific land-use processes (e.g., wood harvest). As discussed in the *Chapter 2* Section 2.3.6, the high LUC emissions projected by the MPI-ESM model, in the work of (Brovkin et al. (2013)), are attributed to an over-estimation of initial carbon stocks in the tropics and dry lands. Transition land-use matrices used in the MPI-ESM and MIROC-ESM models also lead to high terrestrial carbon losses, due to additional CO<sub>2</sub> emissions from clearing and regrowth of forest (Hurtt et al., 2011). These additional emissions are not included in results for the UVic model in this work or other studies presented in **Figure 4.19**, which only represent LUC emissions from net changes in crop, pasture, and forest area. For results produced using DGVMs, biogeochemical temperature differences for the same LUC emissions are due to different TCRE values used. It is difficult to determine why such large differences exist between this work and findings from Simmons and Matthews (2016) (who also use the UVic ESCM v2.9), without knowledge of changes in land-use areas in their RCP2.6 scenario. However, it is likely due to differing forest change distributions within PC simulations and the impact this has on natural carbon uptake from land.

### 4.4.3.3 Soil Carbon Dynamics

As displayed in Section 4.3.5.1, land-use change can greatly impact soil carbon dynamics by altering carbon inputs, decomposition, and turnover, thus impacting carbon sequestration and loss (Post W. M. and Kwon K. C., 2000; Guo and Gifford, 2002; Lal, 2004; Elmore and Asner, 2006; Lemma et al., 2006; Zhang et al., 2013). Alterations in soil carbon are dependent on multiple factors, such as the location and scale of land-use change, changes in climate, and changes in net primary production (or NPP, i.e., how much CO<sub>2</sub> is taken in via photosynthesis vs how much is released during respiration). In the UVic simulations, increases in soil carbon occur largely over non-deforested areas and where shrubland has been converted to cropland, particularly in regions such as South Brazil, Sub-Saharan Africa, and Northeast Asia (see **Figure 4.20**). This is due to changes in climate, enhanced NPP caused by increased atmospheric CO<sub>2</sub>, as well as drier conditions after shrubland conversion (dryness equals precipitation minus evaporation, explained more in Section 4.4.4).

Deforestation and dieback lead to an almost immediate loss in soil carbon which continues over the century, as shown in both TL and PC simulations across Central and Eastern Brazil, Central Africa, Central America, and Southeast Asia and Japan. After deforestation, leaf litter-fall carbon is transferred to the soil carbon pool; however, this supply is finite with a lack of input to soil carbon occurring in subsequent years. In the tropics, most of this leaf litter input is lost through the slash-and-burn removal method (Nair et al., 2009). Over time, warmer soil temperatures and wetter conditions lead to more respiration and therefore a reduction in soil carbon over deforested areas. In some regions, particularly the tropics (e.g., Central Africa), conditions become drier and cooler, causing reduced respiration, therefore larger drawdown of atmospheric CO<sub>2</sub> and an increase in soil carbon.

Previous work corroborate these findings, with most indicating significant loss of soil carbon after deforestation (Diochon et al., 2009; Bathiany et al., 2010; Nave et al., 2010; Zhang et al., 2015). For instance, Harper et al. (2018) demonstrate that the loss of soil carbon from large-scale conversion of forest to bioenergy cropland results in carbon recovery times of around 10–100+ years. A meta-analysis reviewing 74 publications found that the conversion of native forests to croplands reduces soil carbon stocks by approximately 42%, whereas stocks increase by 8% following conversion from forest to pasture (Guo and Gifford, 2002). Longobardi et al. (2016), who also use the UVic model, similarly demonstrate mixed findings at low and mid

latitudes, indicating mainly a soil carbon gain as a result of drier conditions overcoming the opposing warmer temperature impacts.

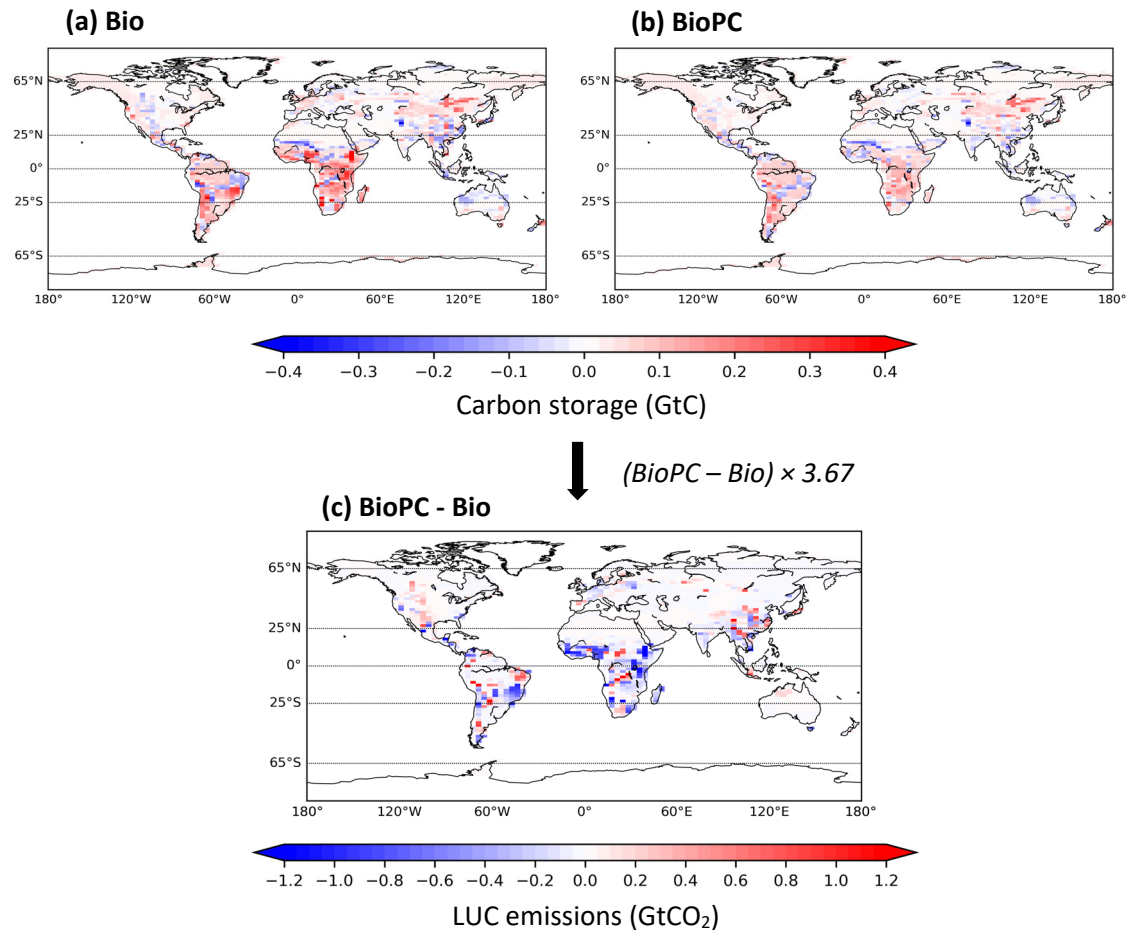


**Figure 4.20:** Spatial representations of soil carbon storage in the BioPC (a) and Bio (b) simulations, and corresponding soil CO<sub>2</sub> emissions (c). Soil CO<sub>2</sub> emissions have been calculated as the difference between terrestrial carbon storage in the Bio and BioPC simulations ( $TC_{PC(LUC + FF)} - TC_{LUC + FF}$ ), multiplied by the carbon-CO<sub>2</sub> conversion factor 3.67.

#### 4.4.3.4 Impacts of Nitrogen and Phosphorous Cycling

The terrestrial nitrogen (N) and phosphorous (P) cycles are not included as dynamic components of the UVic model (Matthews, 2004), hence the coupling of N and P cycling is not represented. In reality, CO<sub>2</sub>, N, P, and surface temperature all interact to alter plant growth and decomposition. Thus, a limitation in N and P (and therefore nutrient) availability for land ecosystems could reduce carbon uptake from reforestation, as well as carbon emissions from

deforestation, as shown in previous work (Sokolov et al., 2008; Thornton et al., 2009; Zaehle et al., 2010; Goll et al., 2012; Wang et al., 2015). This suggests that findings for LUC emissions from the UVic model (and other models included in **Figure 4.19**) could be somewhat overestimated, though they are low already.

The exclusion of dynamic N and P cycles from the analysis also omits the effects of pollution from fertiliser use and manure application, processes that would likely increase with bioenergy expansion. Such operations have led to the conversion of some 120 million tonnes of atmospheric nitrogen into reactive forms, and the mining of around 20 million tonnes of phosphorous every year (Noone et al., 2013). As a result, agriculture has become the largest source of anthropogenic N<sub>2</sub>O emissions, as well as the release of excess nutrients to waterways and coastal zones, which has led to poor water quality, eutrophication, and dead zones (Carpenter et al., 1998; Bennett et al., 2001; Townsend et al., 2003; Foley et al., 2005).

The representation of N<sub>2</sub>O emissions in climate assessments is important as it increases radiative forcing. In addition to direct emissions from fertiliser and manure applications, N<sub>2</sub>O emissions can also be released indirectly from other agricultural processes. These include, deposition of crop residues, cultivation of organic soils, and inorganic nitrogen inputs through biological nitrogen fixation (direct effects), as well as increased warming, enrichment of downstream water bodies from runoff, and downwind nitrogen deposition on soils (indirect effects) (Jia et al., 2019). The loss of nitrogen from agriculture can mainly be attributed to the lack of synchronisation between crop nitrogen demand and soil nitrogen supply. At the global scale, only around 50% of the nitrogen applied to soils is taken up by crops, while the remainder is lost to the environment and atmosphere (Bouwman et al., 2009; Bodirsky et al., 2014).

Previous literature investigating the effects of bioenergy expansion on N<sub>2</sub>O emissions demonstrate mixed findings. Melillo, Reilly et al. (2009) for example, suggest an increase that would overwhelm the abatement benefits of avoiding fossil fuels over the next 30 to 50 years. However, on further analysis, these emissions are expected to be much lower, due to reductions in N<sub>2</sub>O emissions normally released from healthy natural ecosystems (which are now deforested), and reduced application of fertiliser for food production within the scenarios used (Kicklighter et al., 2012). In addition, Humpenöder et al. (2018a) use the MAgPIE model to show that bioenergy expansion could cause a rise in nitrogen losses of 34% by 2100 due to increased fertiliser use, though improvements in fertilisation efficiency could reduce this by half.



It is evident that nitrogen and phosphorous cycles are important processes that, if included, could strengthen analyses provided in this work. However, large uncertainty remains in this field, particularly with regards to their influence on the carbon flux associated with land-use changes. Hence there is large scope for future assessments in this area. Specifically, future work could aim to quantify impacts of land-use in the MAgPIE scenarios on N<sub>2</sub>O emissions and corresponding climate changes. Furthermore, the effects of improvements in fertilisation efficiency (as shown in Humpenöder et al. (2018a)) on emissions and environmental pollution could be assessed with regards to bioenergy expansion.

#### **4.4.4 Biogeophysical Impacts in More Detail**

##### **4.4.4.1 A Comparison to Climate Model Studies**

Previous studies have shown similar biogeophysical effects to this work, particularly Longobardi et al. (2016) who have used the UVic ESCM 2.9 to determine the biogeophysical and biogeochemical effects of forest removal (5–100%) over high, mid and low latitudes. Their work similarly indicates that large-scale deforestation in the tropics leads to drier climates, higher soil temperatures, increased outgoing latent heat, and reduced sensible heat flux, which together generate more biogeophysical cooling than at higher latitudes. In contrast, other studies show a reduction in evaporation over deforested regions in the tropics, due to reduced leaf area and shallower root systems (Bala et al., 2007; Bathiany et al., 2010; Hallgren et al., 2013). This tends to lead to increased sensible heat flux which results in a biophysical surface air warming, as opposed to the cooling seen in this study. Most studies, however, unanimously show that increases in surface albedo due to deforestation have a significant impact on biogeophysical cooling. Studies in which sensible heat flux increases generally show the resulting biogeophysical warming to be offset by the increases in albedo, resulting in an overall cooling effect (Potter et al., 1975; Sagan et al., 1979; Potter et al., 1981; Claussen et al., 2001; Ganopolski et al., 2001; Devaraju et al., 2015; Brovkin et al., 2015).

As mentioned in Section 4.3.4.2, small amounts of biogeophysical warming occur in Southern Africa, North America and lower Latin America, due to increased natural forest cover. Warming due to afforestation has similarly been found in previous literature (Brovkin et al., 1999; Claussen et al., 2001; Bala et al., 2007). For example, Claussen et al. (2001) show that the biogeophysical processes in mid (20–40°N and 20–40°S) and high (40°N and above) northern latitudes dominated over biogeochemical processes, resulting in a global

biogeophysical cooling in the case of deforestation and a global biogeophysical warming in the case of afforestation.

#### **4.4.4.2 Impacts of Excluding Cloud Dynamics**

Some previous studies show decreasing atmospheric albedo from reduced cloud cover (due to reduced evaporation), both of which lead to increased temperatures (Bala et al., 2007). The UVic ESCM does not model clouds explicitly, whereby clouds are prescribed rather than calculated dynamically by the model. Thus, in the simulations, surface albedo increase due to deforestation is not compensated for by a decrease in atmospheric albedo due to reduction in cloud cover over deforested regions, as shown in other modelling studies (Bala et al., 2007; Bathiany et al., 2010). This further explains the local biogeophysical cooling that occurs over the tropics in all scenarios. Bala et al. (2007) found that the net albedo change over deforested regions is negligible as the decrease in atmospheric albedo counteracts the increase in surface albedo. On the other hand, some satellite-based literature show that, depending on the scale of deforestation, cloud cover may not change and could actually increase over deforested bins (Durieux et al., 2003; Chagnon et al., 2004; Montenegro et al., 2009). Uncertainty in previous findings further emphasises the importance of incorporating a cloud cover component when modelling temperature response to LUC and highlights a key area for further improvements in climate modelling.

#### **4.4.4.3 A Key Missing Component in Climate Assessments and Policies**

It is evident that biogeophysical effects can be significant at the local level, demonstrated both in the literature and in this work. While these effects have shown to become negligible when averaged globally, they can both magnify or dampen biogeochemical effects, depending on the location and type of land or land conversion. For instance, in the tropics, where carbon benefits of forest carbon stocks and sequestration rates are highest, the biogeophysical effects of these forests can amplify the carbon benefits. Additionally, where forests are converted for agricultural expansion, biogeochemical warming can both be exacerbated or reduced by various biogeophysical effects. Even so, biogeophysical effects tend to be neglected from many climate impact assessments. To the authors knowledge, the biogeophysical analysis covered in this chapter is one of only three studies that investigate biogeophysical impacts of land-use

change following the RCP2.6 pathway (the others being Simmons & Matthews (2016) and Davies-Barnard et al. (2014)), and one of three studies isolating global land-climate impacts associated with second-generation bioenergy expansion (the others being Hallgren (2013) and Muri (2018)). Even for the more studied RCP8.5 pathway, only a handful of assessments calculate biogeophysical impacts from land-use change (Lawrence et al., 2012; Brovkin et al., 2013; Davies-Barnard et al., 2014; Boysen et al., 2014).

This is further reflected in climate policies for land-based mitigation and adaptation, which rely heavily on GHG emissions reductions. Following the Paris Agreement (PA) goal of constraining global warming to “well below 2 °C”, countries are expected to report national contributions to GHG inventories, as a requirement from the United Nations Framework Convention on Climate Change (UNFCCC). In other words, the UNFCCC implicitly assumes that reducing GHG emissions, and hence biogeochemical effects, is the only approach for countries to mitigate climate change. Within this, the Nationally Determined Contributions (NDCs) require forests to supply up to a quarter of planned emission reductions by 2030 (Grassi et al., 2017). They further play a key role in mitigation pathways which also rely on other land-based mitigation solutions such as bioenergy expansion (Griscom et al., 2017; Rockström et al., 2017; Popp et al., 2017; Jia et al., 2019), yet as previously stated these pathways are under-researched in terms of their biogeophysical impacts.

This exclusion of biogeophysical impacts is largely due to the complexities involved in calculation methods (Perugini et al., 2017). For example, model resolutions are currently too coarse to provide clear advice for local policy decisions. On the other hand, more *in situ* methods can only provide local information, thus lack key information about global teleconnections. That said, neglecting these land-use effects will result in inaccurate quantification of contributions to climate change, and may lead to counterproductive actions. It is therefore paramount that both biogeochemical and biogeophysical effects are considered when evaluating land-use change in climate policies, at both the local and global scale.

Research is currently in its infancy with regards to tackling this problem. While many studies have advocated a more complete approach (Pielke et al., 2002; Marland et al., 2003; West et al., 2011; Gotangco Castillo et al., 2012), most do not provide any metric for this, and those that do are generally at the local scale (Bright, 2015). Recent developments in techniques using high resolution remote sensing data show significant promise for understanding local biogeophysical effects on the global scale (Li et al., 2015; Alkama and Cescatti, 2016; Bright

et al., 2017; Duveiller, Hooker, et al., 2018; Prevedello et al., 2019; Duveiller et al., 2020). However, non-local biogeophysical effects and teleconnections, which can indicate indirect effects, are still an important missing factor here. The link between global and regional processes remains a huge challenge due to multiple feedbacks between the two scales. Global outputs can serve as explicit boundary conditions for smaller scale assessments, highlighting areas most vulnerable to climate impacts and thus in need of further investigation.

The incorporation of land-based mitigation in UNFCCC targets has been a long process with complex negotiations (UNFCCC, 2011a; UNFCCC, 2011b; United Nations, 2015; Grassi et al., 2018). Small and highly uncertain estimates in global biogeophysical effects, as well the lack of a simple metric for calculating these effects, has deterred efforts to include them within policies. Significant political changes would also be required to enable country reporting of biogeophysical effects under UNFCCC, which is currently entirely based on biogeochemical effects. However, this action will become increasingly hard to ignore, given the growing body of scientific literature on biogeophysical climate impacts and their policy relevance. Accounting for these effects will be a crucial component of mitigation and adaptation policy development around bioenergy production, particularly with regards to the incentivisation of tropical forest protection through REDD+.

## 4.5 Summary and Conclusions

This chapter explores the role of BECCS as a climate mitigation solution, with a particular focus on land-climate interactions. At the global level, findings suggest major benefits in large-scale BECCS production, whereby substitution of fossil fuel emissions via BECCS leads to a cooling effect (of  $-0.44$  °C by 2100) which is significantly dominant over the biogeochemical warming effect from land conversion ( $+0.0087$  °C by 2075–2100). Consequently, estimates show that within 11 years (between 2005 and 2016), CO<sub>2</sub> savings from implementing bioenergy will pay back the LUC emissions produced due to agricultural expansion. In addition, the overall climate impact of LUC from second-generation bioenergy expansion is negligible, with the combined impact of biogeochemical and biogeophysical effects equating to a cooling of only  $-0.0063$  °C by 2075–2100. This is largely due to the conversion of shrubland, instead of forest, for cropland expansion in the UVic model, resulting in reduced biogeophysical effects and increased soil carbon uptake which significantly dampens the CO<sub>2</sub> lost from deforestation.

---

Regionally, climate impacts are more significant and vary widely across the globe. Biogeochemical warming is expected to be largest in the extratropics (reaching 0.1°C), with greater signs of polar amplification occurring due to bioenergy implementation. Biogeophysical cooling due to bioenergy expansion is higher in the tropics (reaching up to (-)0.090 °C), with stronger patterns occurring locally as a result of forest conversion and corresponding increases in surface albedo, drier conditions, higher soil temperatures and reduced sensible heat fluxes. These patterns occur mainly across parts of Sub-Saharan Africa and Latin America, where most energy cropland is planted. Hence, these regions are where REDD+ and water protection policies cause most changes in biogeophysical effects. In the case of REDD+ implementation, prevention of cropland expansion into forest leads to a small reduction in biogeophysical cooling. On the other hand, more land needed for rainfed cropland expansion in the water protection scenario results in a small increase in biogeophysical cooling over a wider area. Biogeochemical effects are impacted more at the global level, whereby incorporation of REDD+ reduces global biogeochemical warming effects. Water protection, on the other hand, has little global or regional impact on biogeochemical effects.

The use of the UVic model in this work provides a mechanism for understanding potential global teleconnection impacts of large-scale bioenergy expansion. However, it also brings to light uncertainties within certain aspects of climate modelling, such as determining local scale effects, interpretations of land-cover changes, climate-carbon cycle interactions, nitrogen and phosphorous cycles, soil carbon dynamics, and cloud dynamics. This work also highlights a key missing component within land-based climate policies. In addition to effects on atmospheric CO<sub>2</sub>, biogeophysical impacts of LUC need to be included within NDCs over the coming years. This will more accurately capture the complete ecological functions of forests (and other natural land), and therefore the significance of land conversion for agricultural practices such as bioenergy.



## Chapter 5 Impacts of Bioenergy Expansion on Biodiversity

### 5.1 Overview

One of the major concerns regarding large-scale bioenergy deployment is the impacts it could have on biodiversity. Potentially significant land requirements could lead to the destruction of priority habitat across the globe and thus the loss of many endemic and endangered species. In addition, subsequent loss of ecosystem function and different ecosystem services will likely impact human health and well-being.

*Chapter 2* highlighted the main gaps in this field, indicating that most previous work is at the regional and field level, or focuses on first-generation bioenergy production at the present day. Increasing development of projected spatial energy cropland data has led to more recent research into the relationship between second-generation bioenergy expansion and biodiversity loss (Heck et al., 2018; Tudge et al., 2021; Hanssen et al., 2022). However, a detailed spatial analysis of projected land-use pathways is yet to be carried out.

This chapter implements the MAgPIE scenarios, discussed in *Chapter 2*, in a two-part intercomparison analysis. The first part uses a new approach to the Endemics-Area Relationship model to examine potential impacts of habitat loss within the scenarios on endemic species loss in biodiversity hotspots. The second part assesses the impacts of cropland expansion in the scenarios on endangered and critically endangered species across the Alliance for Zero Extinction sites. Further, the effects of incorporating water protection and REDD+ sustainability measures will be determined. Through understanding these impacts, this work aims to contribute to knowledge of bioenergy's role within sustainable development goal (SDG) 15: "Life on Land".

## 5.2 Materials and Methods

### 5.2.1 Data

#### 5.2.1.1 Land-Use Change

To estimate the effects of land-use change on habitat area, this study incorporated the forest and cropland variables from the original MAgPIE scenarios. As discussed in *Chapters 3 and 4*, these scenarios follow the SSP2 ‘middle of the road’ pathway and lead to global warming of around 1.8 °C by 2100, relative to pre-industrial levels.

Food/feed cropland and energy cropland were used as shown in the MAgPIE scenarios in *Chapter 3*. Although not indicated in *Chapter 3*, ‘forest’ depicted in the MAgPIE scenarios contains both ‘secondary’ and ‘primary’ forest. These two types of forest will both be utilised in this chapter. Secondary forest is forest previously disturbed by human activities and recovering, while primary forest refers to undisturbed natural forest, both since the beginning of the historical simulation. A portion of undisturbed natural forest is within protected forest areas, which cover about 12.5% of the initial global forest area. As discussed in *Chapter 3*, unlike the agricultural and livestock sectors, the forestry sector is not executed dynamically in the MAgPIE model. The forestry sector consists of forest plantations and modified natural forest (e.g., timberland for wood production), and accounts for around 30% of current global forest area. Any loss of primary or secondary forest in the MAgPIE scenarios is therefore due to conversion to cropland.

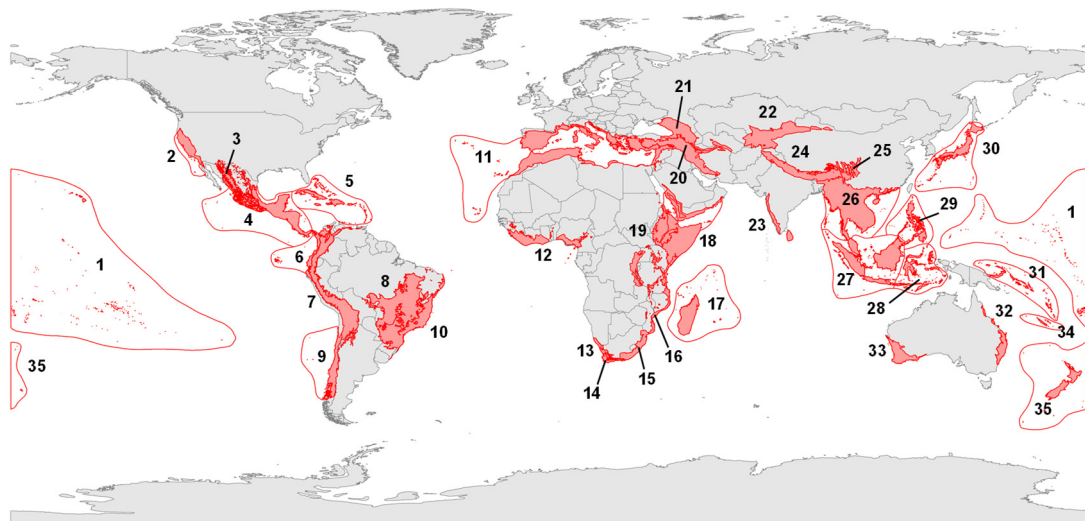
#### 5.2.1.2 Biodiversity

To determine the impacts of land-use change on biodiversity, this work focused on habitat areas of high priority i.e., areas with high values for both vulnerability and irreplaceability (discussed previously in *Chapter 2*, Section 2.4.3.2.4). Two publicly available datasets were therefore used which account for this: biodiversity hotspots, outlined in the work of Mittermeier et al. (2011), and the Alliance for Zero Extinction (AZE) database (AZE, 2010).



### 5.2.1.2.1 Biodiversity Hotspots

Biodiversity hotspots were originally identified in the effort to conserve high priority areas. They depict biogeographic regions with significant concentrations of endemic species and exceptional loss of habitat. 35 hotspots have been identified, each of which contains at least 1500 (0.5%) of the world's endemic plant species and has lost at least 70% of its original habitat extent (Myers et al., 2000; Mittermeier et al., 2005; Mittermeier et al., 2011). Around 27,298 vertebrate species have been found, consisting of 4,809 mammals (Nowak, 1999), 9,881 birds (Sibley and Monroe, 1990), 7,828 reptiles (Uetz and Etzold, 1996) and 4,780 amphibians (Glaw and Köhler, 1998). The other vertebrate group, fishes, is excluded due to poor data, though approximately 5,000 species are predicted to inhabit these regions 25 (Eschmeyer, 1998; Myers et al., 2000).



#### **Biodiversity Hotspots**

**1** Polynesia-Micronesia; **2** California Floristic Province; **3** Madrean Pine-Oak Woodlands; **4** Mesoamerica; **5** Caribbean Islands; **6** Tumbes-Chóco-Magdalena; **7** Tropical Andes; **8** Cerrado; **9** Chilean Winter Rainfall and Valdivian Forests; **10** Atlantic Forest; **11** Mediterranean Basin; **12** Guinean Forests of West Africa; **13** Succulent Karoo; **14** Cape Floristic Region; **15** Maputaland-Pondoland-Albany; **16** Coastal Forests of Eastern Africa; **17** Madagascar and the Indian Ocean Islands; **18** Horn of Africa; **19** Eastern Afromontane; **20** Irano-Anatolian; **21** Caucasus; **22** Mountains of Central Asia; **23** Western Ghats and Sri Lanka; **24** Himalaya; **25** Mountains of Southwest China; **26** Indo-Burma; **27** Sundaland; **28** Wallacea; **29** Philippines; **30** Japan; **31** East Melanesian Islands; **32** Eastern Australia; **33** Southwest Australia; **34** New Caledonia; **35** New Zealand.

*Figure 5.1: Biodiversity hotspots and their outer limits, as defined in the works of Mittermeier et al. (2005) and Conservation International (2011).*

Combined, the 35 hotspots originally covered  $23.7 \times 10^6$  km<sup>2</sup>, or 15.9% of the Earth's land surface (Mittermeier et al., 2011). Now, only  $3.4 \times 10^6$  km<sup>2</sup> (2.3%) of this natural land remains, because of extreme habitat destruction over the past century. The hotspots are located to a large extent in the tropics, where most of future land-use change is expected to occur (Sala et al., 2000) (see **Figure 5.1**).

#### 5.2.1.2.2 Alliance for Zero Extinction (AZE) Sites

In addition to large-scale conservation initiatives, finely tuned conservation will be essential in small regions of remnant habitat which have equally high irreplaceability and threat (Brooks et al., 2006). The AZE database identifies such regions, where species have been classified as Endangered (EN) or Critically Endangered (CR) under the IUCN-World Conservation Union criteria (IUCN, 2018) (see **Figure 5.2**). The AZE itself is formed of 93 biodiversity conservation institutions from 37 countries, all working to prevent species extinctions (AZE, 2010). An AZE site is designated if it is the sole area where an EN or CR species occurs and contains more than 95% of the global population of that species. These areas have definable boundaries within which the character of habitats, biological communities, and/or management issues have more in common with each other than they do with those in adjacent areas (Ricketts et al., 2005).

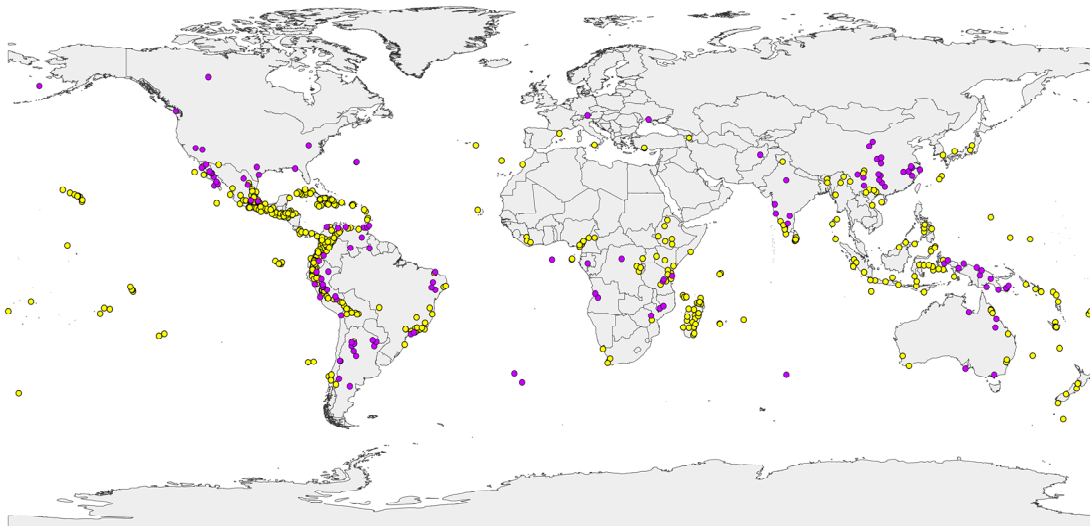


**Figure 5.2:** Sites of critically endangered and endangered species provided in the Alliance for Zero Extinction (AZE) database (AZE, 2010). Coloured dots represent AZE sites inside (yellow) and outside (purple) the biodiversity hotspots shown in **Figure 5.1**.

This study used the number of AZE sites and species count from the year 2018. The AZE dataset comprises 585 sites for 918 species of mammals, birds, reptiles, amphibians and conifers, of which 81% of the sites are located within biodiversity hotspots (AZE, 2010). Each site contains small populations of rare and endemic species. With limited protection and extreme vulnerability to habitat destruction, these sites face imminent extinction in the absence of conservation action (McDonald et al., 2008). This can either be due to local causes or as a result of their restricted global range, making them susceptible to external threats.

## 5.2.2 Experiments

### 5.2.2.1 Biodiversity Hotspot Analysis

Vulnerability of species within biodiversity hotspots was determined by calculating the potential number of species extinctions resulting from LUC in the MAGPIE scenarios. Extinction estimates were determined for 5 species groups: plants, mammals, reptiles, amphibians, and birds, using the endemics-area relationship (EAR) model. The following sections discuss the origins of the EAR model, calculations of habitat loss in the MAGPIE scenarios, and application of the EAR model for calculating species loss in biodiversity hotspots.

#### 5.2.2.1.1 Origins of the Endemics-Area Relationship Model

##### The Species-Area Relationship (SAR) Model

The EAR model was originally derived from the species-area relationship (SAR) model, one of the longest-researched empirical laws of ecology (Arrhenius, 1921). The SAR model consists of a power function that relates the accumulation of species to increasing area, and takes the form:

$$S = cA^z \quad (5.1)$$

where  $S$  is the number of species and  $A$  is habitat area.  $c$  and  $z$  are constants which vary depending on the type, location, and sample-size of the species, and can be determined using the logarithmic representation of the SAR model:

$$\log(S) = \log(c) + z\log(A) \quad (5.2)$$

where  $z$  describes the slope of the log-log relationship and  $\log(c)$  describes its intercept. Using this representation, studies have determined values of  $z$  for different forms of habitat locations. For habitat accumulation within a biological region (or province),  $z$  values depend on different-size samples, and area of habitat, and tend to approximate 0.1-0.2 (Rosenzweig, 2001). Island system values range between 0.25 and 0.55, depending on sample sizes and distances between archipelagic islands (Rosenzweig, 1995; Rosenzweig, 2001). Unlike island species, biogeographical provinces generally contain species which have evolved within them, rather than immigrating from somewhere else. This is particularly true for different continents or well-separated periods in the history of life. However, it is expected that every region contains a few species that have arrived as immigrants. The  $z$ -values of interprovincial SARs account for these occurrences, and mostly range between 0.8 and 1 (Rosenzweig, 2003a; Rosenzweig, 2003b). Lastly, habitat fragmentation can have an impact on  $z$  values in SARs. This is a process whereby large and contiguous habitats are divided into smaller, isolated patches of habitat, resulting from changes in geological processes in the environment, or more destructive human activity, such as land conversion. Across studies, the value for habitat fragmentation has been empirically shown to be 0.25 (Rosenzweig, 1995; Crawley and Harral, 2001; Brooks et al., 2002).

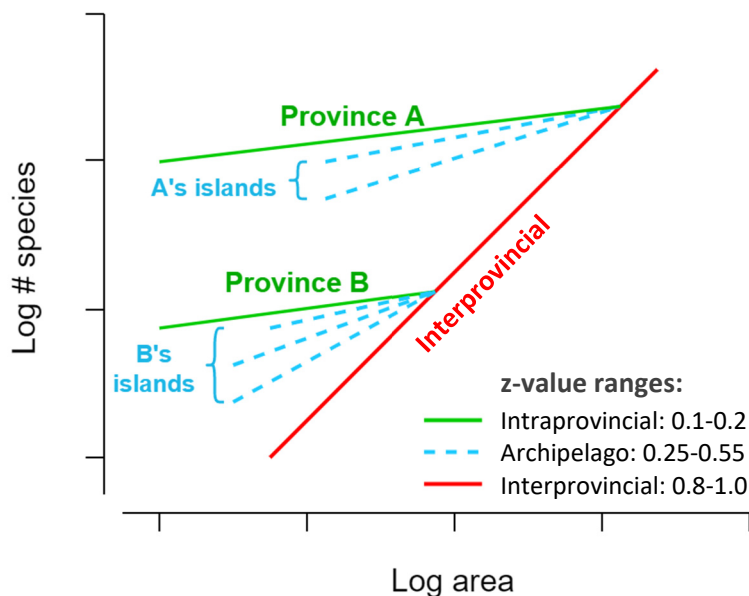


**Figure 5.3:** The three scales of species-area curve, recreated using findings in Rosenzweig (2001) and Rosenzweig (2003a). Island SARs are bounded by the intraprovincial SAR of their province and the interprovincial SAR on which their province lies.

The original SAR can be modified to predict the number of species extinctions that could occur from habitat loss. **Equations (5.3)–(5.9)** describe this transformation, whereby **Equation (5.1)** is first adjusted for species count  $S_O$  and area  $A_O$  for the original habitat:

$$S_O = cA_O^z \quad (5.3)$$

As well as species count  $S_N$  and area  $A_N$  for the remaining patch of habitat after habitat loss:

$$S_N = cA_N^z. \quad (5.4)$$

Dividing **Equation (5.4)** by **Equation (5.3)** thus yields the fraction of original species remaining in a sub-patch of habitat:

$$S_N/S_O = (A_N/A_O)^z. \quad (5.5)$$

Multiplying **Equation (5.5)** through by  $S_O$  yields

$$S_N = S_O(A_N/A_O)^z. \quad (5.6)$$

Lastly, subtracting from the original  $S_O$  estimates the number of potential extinctions occurring:

$$S_O - S_N = S_O - S_O(A_N/A_O)^z \quad (5.7)$$

The fraction of original species  $S_O$  lost is therefore:

$$f_{lost-SAR} = 1 - (A_N/A_O)^z. \quad (5.8)$$

In some literature this is written as

$$f_{lost-SAR} = 1 - [1 - \phi_{Alost}]^z, \quad (5.9)$$

where  $\phi_{Alost}$  is the fraction of the habitat being cleared.

### Discrepancies Using the SAR Model

While numerous studies have implemented the SAR model for extinction estimates (Brooks et al., 2002; Malcolm et al., 2006; Jantz et al., 2015; Chaudhary and Mooers, 2017), it has been highly criticised across literature for over-estimating species extinction risk (May et al., 1995; Pimm and Askins, 1995; Rosenzweig, 1995). This is largely because it doesn't account for the fact that the area required for species extinctions is normally larger than the sample area needed to encounter the species (He and Hubbell, 2011). It also fails to indicate a time frame in which

extinctions are likely to occur because extinction debt is not accounted for (Chevin et al., 2010; Pereira et al., 2010) (see *Chapter 2*, Section 2.4.3.2.3 for more detail).

### The Endemics-Area Relationship (EAR) model

Harte and Kinzig (1997) overcome this discrepancy by using the SAR model to derive the endemics-area relationship (EAR) model, where “endemic” refers to species located *only* within a cleared patch of larger habitat and nowhere else. Using the EAR, the fraction of species lost can be calculated as

$$f_{lost-EAR} = \phi_{Alost}^{z'} = (A_{lost}/A_0)^{z'}. \quad (5.10)$$

where, as in the case for **Equation (5.9)**,  $A_{lost}$  and  $\phi_{Alost}$  are the area and fraction of the habitat being cleared, respectively.  $z'$  is a constant, related to the SAR exponent  $z$  by the formula

$$z' = -\ln(1 - 1/2^z)/\ln(2). \quad (5.11)$$

As stated previously,  $z$  values can vary depending on habitat location. This study used three different values of  $z$  to calculate  $z'$ : a typical value for island systems and fragmented habitats ( $z = 0.25$ ; Rosenzweig (2001), Brooks (2002)), a conservative value more representative of continental situations ( $z = 0.15$ ; Malcolm et al. (2006); and an intermediate value ( $z = 0.2$ ; Bergl et al. (2007)).

#### **5.2.2.1.2 Habitat Loss in Biodiversity Hotspots**

Calculating the fraction of habitat being cleared ( $\phi_{Alost}$ ) requires defining what “habitat” is suitable for the 5 species groups (plants, amphibians, birds, mammals, and reptiles) being considered. In this study, forest was considered as the best quality habitat. In other words, a transition from forest to any other land-use state was counted as a complete loss of habitat, as assumed in previous similar work (Malcolm et al., 2006; Jantz et al., 2015). Other land-use types such as energy cropland, food/feed cropland, pasture, other natural land and built-up area were treated as low-quality habitat or uninhabitable (i.e. not a habitat) (Wiens et al., 2011).

Primary (or ‘old-growth’) forest is considered to be more favourable habitat than secondary forest (IPBES, 2019; FAO and UNEP, 2020), however secondary forest regrowth could help prevent mass extinctions in the long term (Wright and Muller-Landau, 2006). Thus, for the purpose of this study, both primary forest and secondary forest were treated as habitat. Previous

literature has demonstrated that a proportion of species occurring in primary forests can be found in nearby secondary forests, depending on the age of the secondary forest (Dunn, 2004; Barlow et al., 2007; Chazdon et al., 2009; Xu et al., 2015). The work of Chazdon et al. (2009), for instance, provides such proportions, collected from 26 different studies and covering a variety of plant and vertebrate species in 14 countries. **Figure 5.4** displays relationships between proportions taken from Chazdon et al. (2009) and age of secondary forest, categorised into the five main species classes: plants, amphibians, birds, mammals and reptiles.

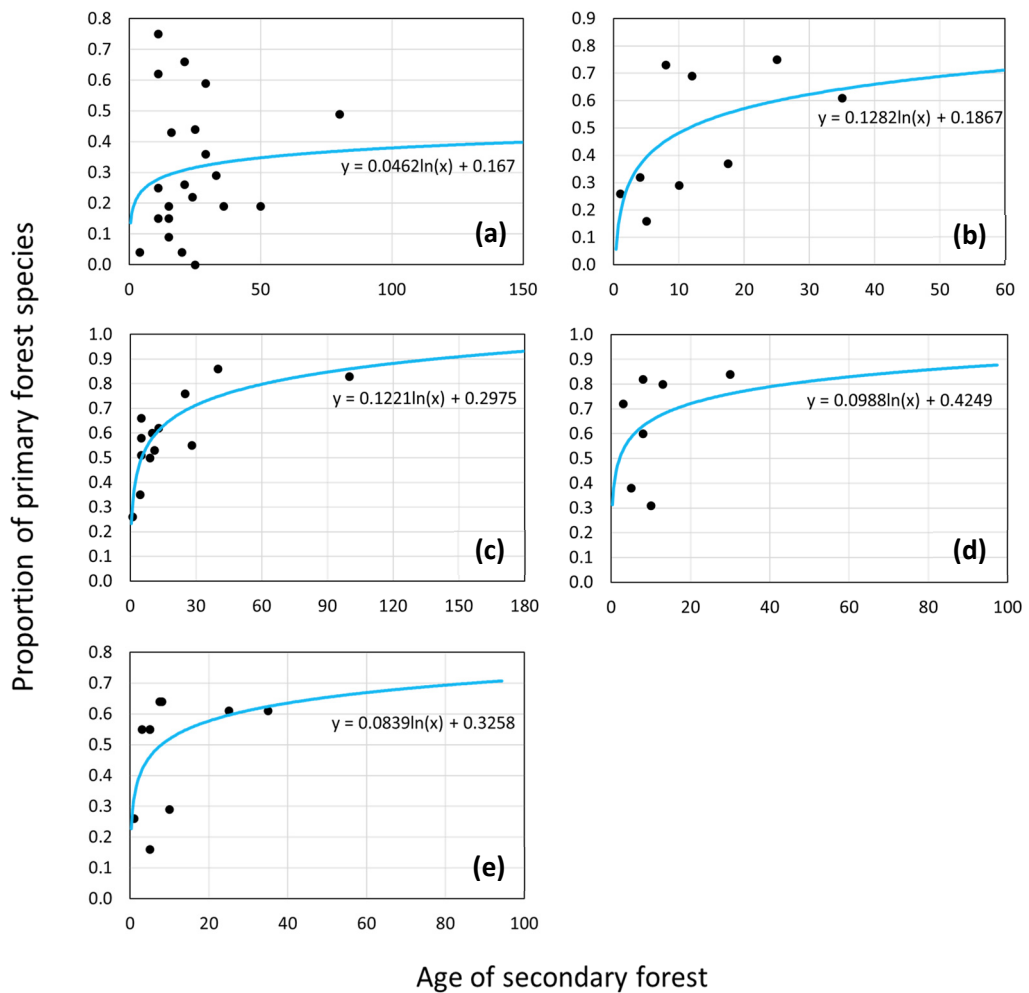


**Figure 5.4:** Relationships between proportions of primary forest species found in secondary forests and different ages of secondary forest. Proportions have been taken from the work of Chazdon et al. (2009) for (a) plants, (b) amphibians, (c) birds, (d) mammals and (e) reptiles.

Using these relationships, proportions were determined for three potential scenarios: a ‘Baseline’ case, whereby secondary forest is 20 years old in 2005, a ‘Low’ case in which secondary forest is 10 years old in 2005, and a ‘High’ case which assumes secondary forest is 40 years old in 2005. **Table 5.1** provides proportions of species occurring in both primary and secondary forests (‘Mixed’), alongside remaining species occurring *only* in primary forests (‘Only Primary’), for each scenario and species class. These values were then factored into the EAR equation to calculate species extinctions for each biodiversity hotspot.

**Table 5.1:** Proportions of species from primary forests that can occur in nearby secondary forests (‘Mixed’), and remaining proportions of species only found in primary forests (‘Primary’), depending on the age of the secondary forest (10, 20 or 40 years old).

	<b>Baseline</b> 20 years		<b>Low</b> 10 years		<b>High</b> 40 years	
	Mixed	Only Primary	Mixed	Only Primary	Mixed	Only Primary
<b>Plants</b>	0.31	0.69	0.27	0.73	0.34	0.66
<b>Mammals</b>	0.72	0.28	0.65	0.35	0.79	0.21
<b>Birds</b>	0.66	0.34	0.58	0.42	0.75	0.25
<b>Reptiles</b>	0.58	0.42	0.52	0.48	0.64	0.36
<b>Amphibians</b>	0.57	0.43	0.48	0.52	0.66	0.34

### 5.2.2.1.3 Species Extinctions in Biodiversity Hotspots

The EAR model in **Equation (5.10)** can be modified to encompass species that can exist in both primary and secondary forests. For species which *only* occur within primary forest, the fraction of species lost by 2100 due to primary forest clearing is:

$$f_{L-prim} = \Phi_P^{z'} = (PA_L/PA_O)^{z'}, \quad (5.12)$$

whereby  $PA_O$  is the original primary forest area.  $PA_L$  and  $\Phi_P$  are the area and fraction of primary forest being cleared, respectively. For species which occur within *both* primary and secondary forest, the fraction of species lost (by 2100) due to primary and secondary forest clearing is thus:

$$f_{L-mix} = \Phi_P^{z'} \Phi_S^{z'} = (PA_L/PA_O)^{z'} (SA_L/SA_O)^{z'}, \quad (5.13)$$



whereby  $SA_O$  is the original secondary forest area.  $SA_L$  and  $\phi_S$  are the area and fraction of secondary forest being cleared, respectively. To calculate areas of primary and secondary forest loss within biodiversity hotspots, land-use data for the MAGPIE scenarios is overlaid with hotspot extents, taken from the Conservation International (2011) database.

Multiplying **Equations (5.12)** and **(5.13)** through by the original number of species *only* in primary forest  $PS_O$ , and in *both* primary and secondary forest (mixed)  $MS_O$  respectively, gives the number of species lost due to primary and secondary forest loss:

$$PS_L = PS_O \phi_P^{z'} = PS_O (PA_L/PA_O)^{z'} \quad (5.14)$$

$$MS_L = MS_O \phi_P^{z'} \phi_S^{z'} = MS_O (PA_L/PA_O)^{z'} (SA_L/SA_O)^{z'}. \quad (5.15)$$

Here,  $PS_O$  and  $MS_O$  are calculated as

$$PS_O = f_{o-prim} TS_O \quad (5.16)$$

$$MS_O = f_{o-mix} TS_O, \quad (5.17)$$

whereby  $f_{o-prim}$  and  $f_{o-mix}$  are the original fractions of species occurring in *only* primary forest and in *both* primary and secondary forests, respectively, displayed in **Table 5.1**.  $TS_O$  is the total number of species found within each hotspot in 2005, taken from Mittermeier et al. (2005).

Lastly, the total number of species lost due to habitat loss in the biodiversity hotspots can be calculated as

$$TS_L = PS_L + MS_L. \quad (5.18)$$

### 5.2.2.2 AZE Analysis

To understand impacts on endangered and critically endangered species, this study used spatial overlay to quantify infringement of energy and food/feed cropland expansion on AZE sites. To do this, the number of AZE sites directly impacted by cropland in the MAGPIE scenarios was calculated, whereby sites which contained grid cell fractions higher than zero as a result of cropland expansion were counted as ‘impacted’ sites. Next, the sum of species per site was estimated, and the results used to predict the total species impacted by future cropland expansion.

## 5.3 Results

### 5.3.1 Biodiversity Hotspot Analysis

#### 5.3.1.1 Habitat Extent at Present Day

In 2005, the biodiversity hotspots contain  $1.12 \times 10^6$  km<sup>2</sup> of primary forest and  $6.25 \times 10^6$  km<sup>2</sup> of secondary forest (around 0.75% and 4.2% of the Earth's surface respectively). Together this equates to  $7.37 \times 10^6$  km<sup>2</sup> (4.9%) of total global forest that exists across the hotspots. Previous studies show varying but comparable findings. Jantz et al. (2015) use primary forest only as a proxy for habitat. They report area of primary forest in hotspots to be  $6.79 \times 10^6$  km<sup>2</sup> (4.6%) in 2005, around six times the area of primary forest found in this study. This discrepancy is due to the exclusion of wood harvest from data used in this study (Humpenöder et al., 2018b). Wood harvest accounts for approximately 30% of current global forest area, and is incorporated as primary forest in the work of (Jantz et al., 2015). Mittermeier et al. (2005) estimate total habitat area to be  $3.38 \times 10^6$  km<sup>2</sup> (2.3%), whereby habitat covers a variety of biomes situated in primary forests, secondary forests, grasslands and shrublands. This value is somewhat closer to the  $7.37 \times 10^6$  km<sup>2</sup> habitat area used in this study, assuming that only a portion of species are expected to occur in the  $6.25 \times 10^6$  km<sup>2</sup> of secondary forest.

Discrepancies between studies could also be caused by variation in spatial distributions of land use across biodiversity hotspots. Differences are mainly evident in Indo-Burma, Sundaland, and Cerrado, accounting for  $0.35 \times 10^6$  km<sup>2</sup> (32%) of primary forest. This could be due to a lack of data for these hotspots, which should demonstrate rapid increases in deforestation rates that have occurred over recent decades (Sodhi et al., 2004).

#### 5.3.1.2 Future Global Habitat Loss

Across the four MAgPIE scenarios, total changes in forest (primary and secondary) in the biodiversity hotspots is projected to be from  $(-1.37 \times 10^6$  km<sup>2</sup> to  $(+0.216 \times 10^6$  km<sup>2</sup> between 2005 and 2100, equivalent to around  $(-18.6\%$  –  $(+2.9\%$  of forest present in 2005. As shown in **Figure 5.5**, the loss of forest is due to the expansion of food/feed and energy cropland worldwide.

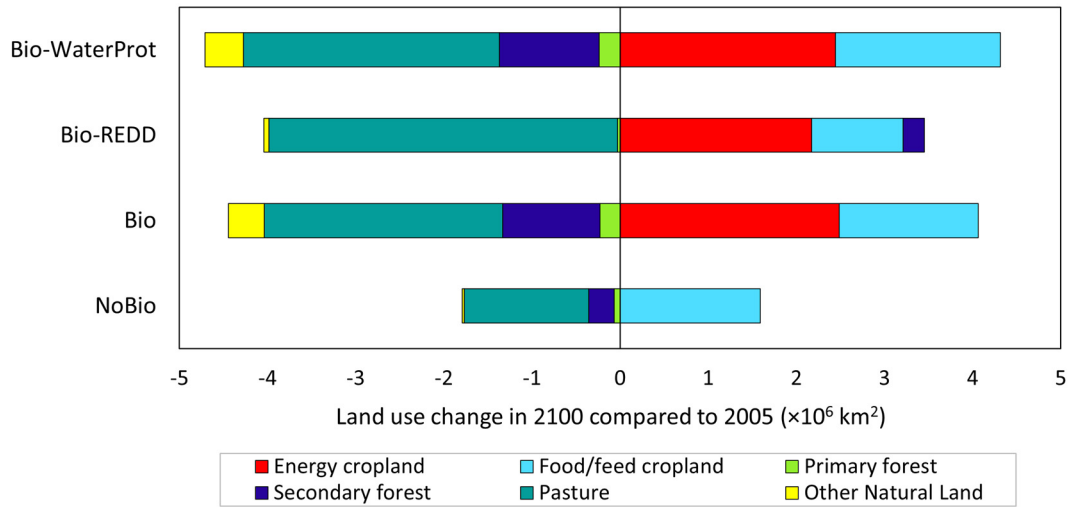


**Figure 5.5:** Total land-use change in the MAGPIE scenarios across 35 biodiversity hotspots in 2100, relative to 2005.

In the scenario without bioenergy (NoBio), a 44% increase in food/feed cropland leads to a loss of  $0.0694 \times 10^6$  km<sup>2</sup> (6%) of primary forest and  $0.287 \times 10^6$  km<sup>2</sup> (5%) of secondary forest. The incorporation of large-scale second-generation bioenergy production results in an additional increase in energy cropland of  $2.49 \times 10^6$  km<sup>2</sup> by 2100, instigating a further loss of around  $0.157 \times 10^6$  km<sup>2</sup> (14%) of primary forest and  $0.819 \times 10^6$  km<sup>2</sup> (13%) of secondary forest (a total of  $0.977 \times 10^6$  km<sup>2</sup> of forest loss) compared to the NoBio scenario. This is further exacerbated by the inclusion of a water protection policy, resulting in an additional loss of  $0.04 \times 10^6$  km<sup>2</sup> of total forest compared to the Bio scenario. In contrast, the effect of a REDD+ scheme, alongside bioenergy production, is an overall total gain in forest ( $0.216 \times 10^6$  km<sup>2</sup>; 2.9%) relative to forest extent in 2005, whereby land currently used for pasture and food/feed cropland is instead used for energy cropland expansion.

### 5.3.1.3 Regional Habitat Loss

Regional analysis of the scenarios shows that habitat loss due to cropland expansion mainly occurs across biodiversity hotspots located in the tropics. The impact of both food/feed and energy cropland expansion is evident in results for the Bio scenario (see **Figure 5.6**). In this scenario, condensed but highly concentrated loss of primary forest occurs in five main regions: the Philippines, East Africa (in the Eastern Afromontane and Madagascar hotspots), West Africa (in the Guinean Forests), Brazil (in the Atlantic Forest), and Central America and the

western edge of the Amazon basin (in the hotspots Mesoamerica and the Tropical Andes) (see **Figure 5.6**, (a)–(e)). Large patches of dense secondary forest loss often occur adjacent to primary forest loss in most of these regions. Such high concentrations are mainly attributed to energy cropland expansion. As shown in **Figure 5.7**, considerably lower percentages of primary and secondary forest loss occur in most of these regions for the scenario excluding bioenergy (NoBio).

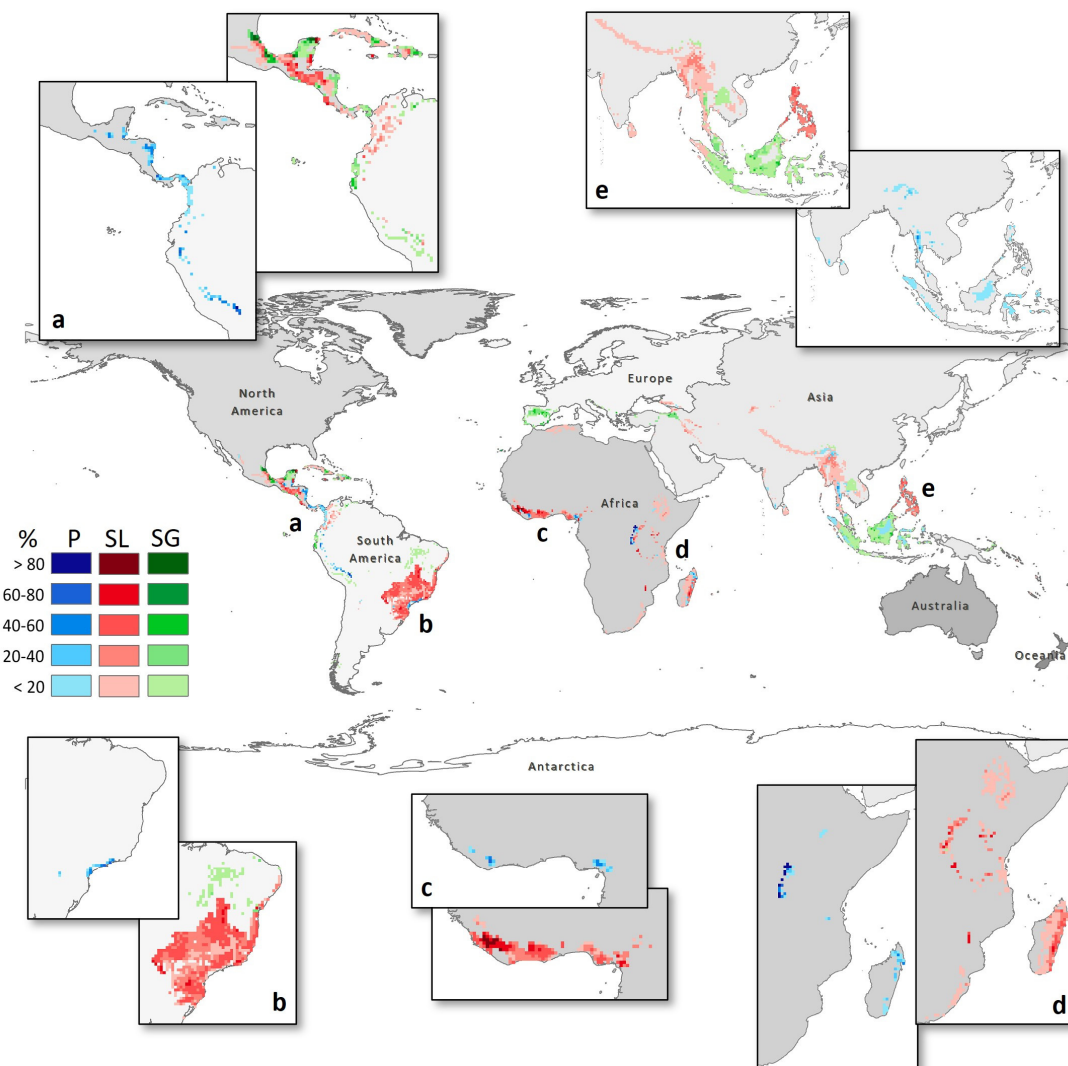


**Figure 5.6:** Percentage of primary forest loss (P-blue) and secondary forest loss (SL-red) and gain (SG-green) in the MAGPIE Bio scenario, for 2100 relative to 2005.

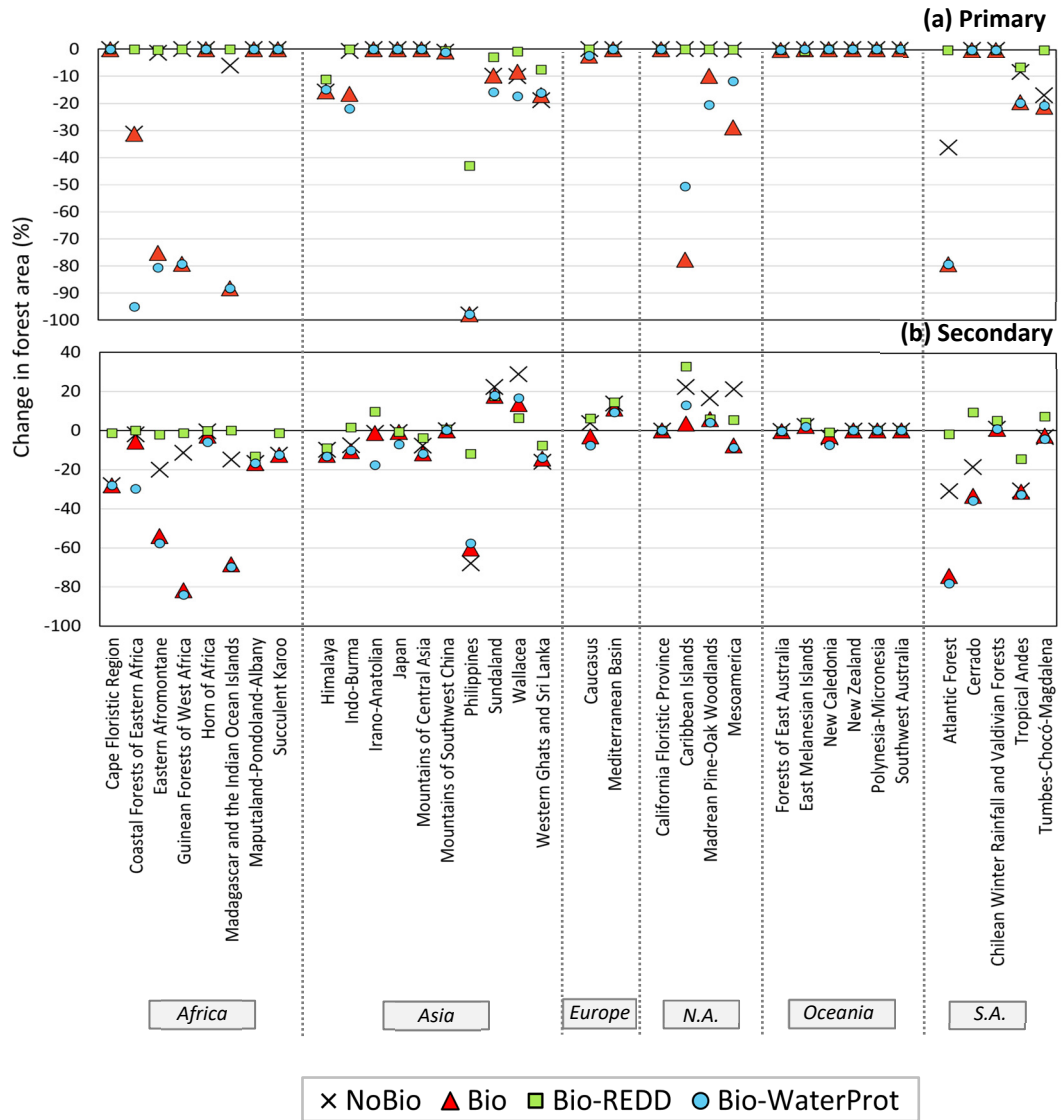


**Figure 5.7:** Percentage change in primary and secondary forest in the MAGPIE scenarios for each biodiversity hotspot, by 2100 relative to 2005.

Implementation of REDD+ in Bio-REDD reduces the overall impact of cropland expansion on forest. In some hotspots, this leads to lower forest loss than that found in the NoBio scenario. The REDD+ scheme is least effective in Asia, where total secondary and primary forest loss reaches up to 6% ( $(-)\times 3.54 \times 10^6 \text{ km}^2$ ) and 2% ( $(-)\times 0.636 \times 10^6 \text{ km}^2$ ), respectively — across Japan, Mountains of Central Asia, Western Ghats and Sri Lanka, Himalaya, and the Philippines — by 2100 (relative to forest 2005), whereby the highest percentage occurs in the Philippines. The overall impact of a water protection policy alongside bioenergy production (in Bio-WaterProt) is an increase in forest loss in many hotspots. For most affected hotspots this is a small increase,

though larger impacts are seen in the Coastal Forests of Eastern Africa, Madrean-Pine Oak Woodlands, Irano-Anatolian and South-East Asian hotspots: Sundaland, Wallacea and Indo-Burma.

In some areas, dispersed low percentages of habitat loss occur because of cropland expansion. This is particularly noticeable in Southeast Asia, where low-density primary and secondary forest loss occurs across almost the entire Himalaya and Wallacea hotspots, as well as large patches of Indo Burma (most of Myanmar) and Sundaland (see **Figure 5.6** (e)). In these hotspots, though percentages of forest loss are relatively low across the scenarios, total areas of primary forest loss lie within the tenth highest findings of all 35 hotspots, as displayed in **Figure 5.8**.

Overall, 20 hotspots show signs of primary forest loss, whereby significant losses occur in 13 of these hotspots. Reductions in secondary forest appear in most of these hotspots, in addition to several others. In Cerrado, a loss of around 800,000 km<sup>2</sup> of secondary forest occurs across the scenarios — the highest out of all 35 hotspots — however there is zero primary forest loss. The highest area of primary forest loss occurs in the Tropical Andes, estimating at around 44,000 km<sup>2</sup> for the Bio scenario, and 45,000 km<sup>2</sup> and 1,900 km<sup>2</sup> for the Bio-WaterProt and Bio-REDD scenarios, respectively.

In some hotspots, secondary forest increases (see **Figure 5.6** (b)). This mainly occurs in South-East Asia, Europe, and Central America, and is more prevalent in the NoBio and Bio-REDD scenarios. As discussed in *Chapter 3*, changes in forestry do not occur in the MAgPIE scenarios. Increases in secondary forest are therefore mainly due to natural regeneration after disturbance and tend to occur near regions of primary and secondary forest loss. Species loss is calculated using forest *loss* extent; hence, increases in secondary forest are not mentioned further in this study.

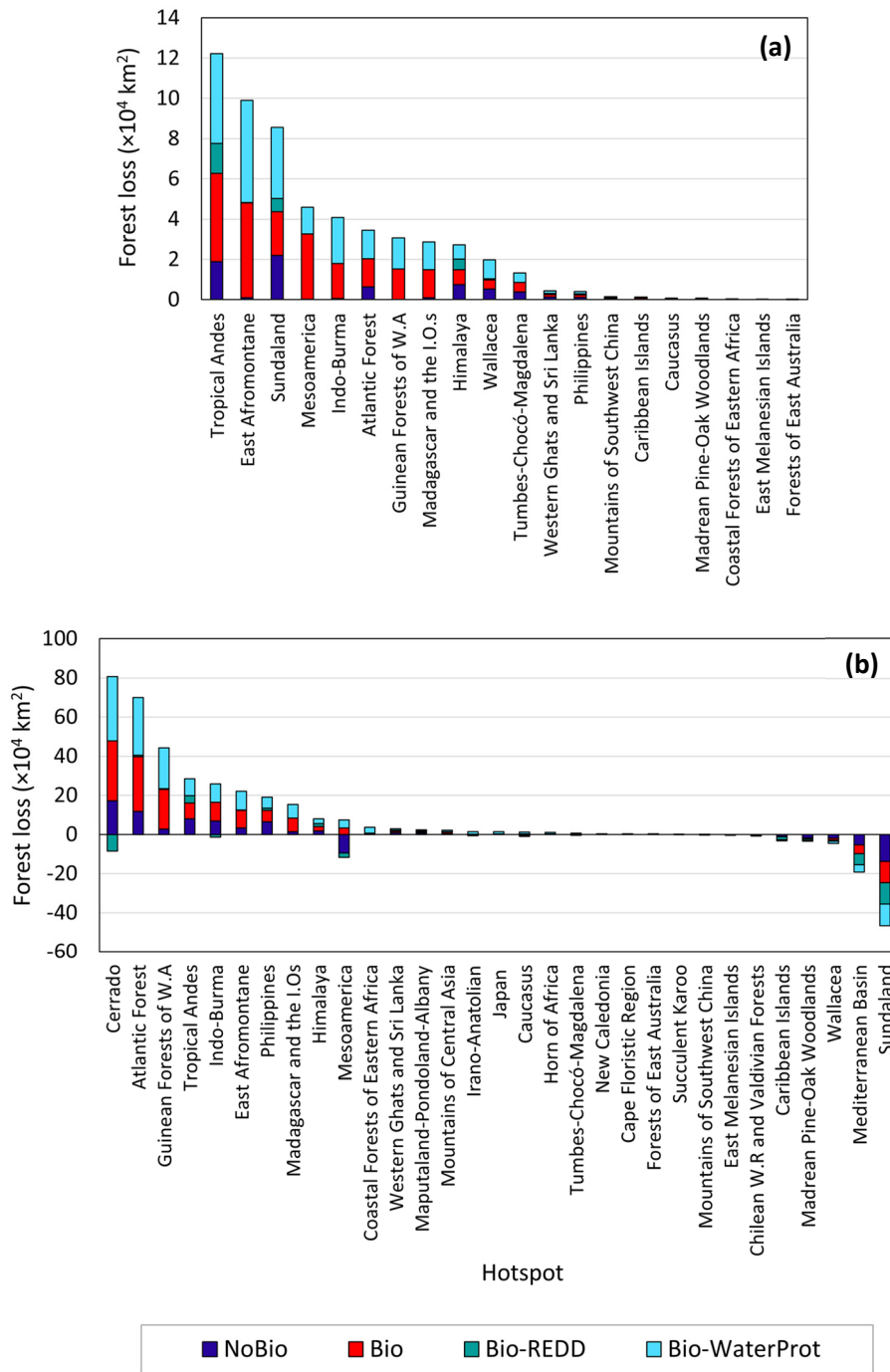


**Figure 5.8:** Primary (a) and secondary (b) forest loss in the MAgPIE scenarios, for each biodiversity hotspot, by 2100 relative to 2005. 'I.O.s' stand for Indian Ocean islands, and 'W.A' stands for West Africa.

### 5.3.1.4 Endemic Species Extinctions Due to Habitat Loss

#### 5.3.1.4.1 Global Species Loss

Using the EAR model, estimates of endemic plant and vertebrate (mammal, bird, reptile, and amphibian) species extinctions have been calculated as a result of habitat loss occurring in each hotspot between 2005 and 2100. As discussed in Section 5.2.2.1.2, this study assumes that all species considered occur primarily in primary forests, whereby a portion of these species also occur in secondary forests. Therefore, hotspots that show zero primary forest loss result in zero extinctions, even if loss of secondary forest occurs in the hotspot.

In total, 16 biodiversity hotspots contain species loss due to habitat loss. **Figure 5.9** displays potential global numbers of extinctions, for each MAgPIE scenario; calculated using  $z$  values: 0.15, 0.2 and 0.25, to represent varying habitat locations, and secondary forest ages: 10, 20 and 40 years old.

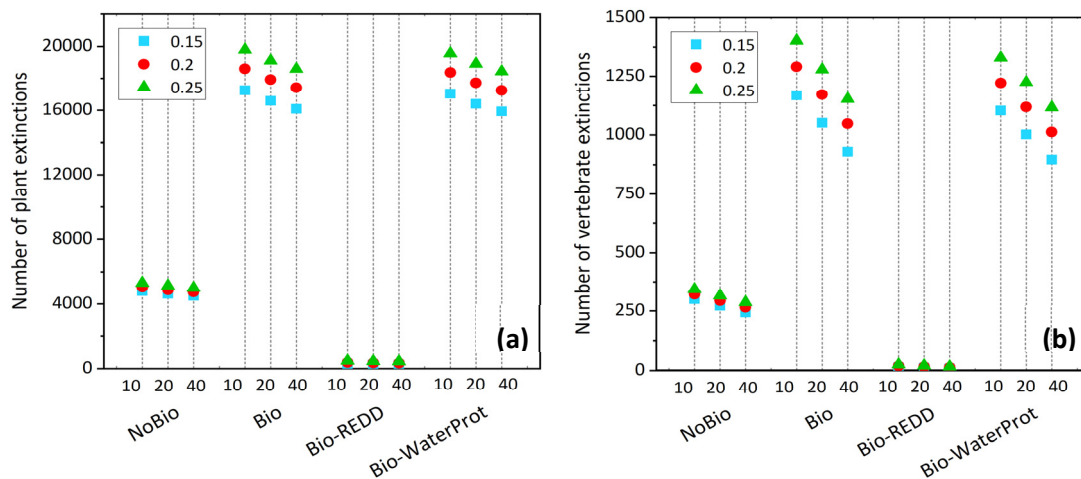


**Figure 5.9:** Global numbers of plant (a) and vertebrate (b) extinctions in the MAgPIE scenarios, calculated using  $z$  values: 0.15, 0.2 and 0.25, and secondary forest ages: 10, 20 and 40 years old.

Habitat loss due to conversion to food/feed cropland in the scenario excluding bioenergy, NoBio, results in a potential loss of approximately 4,500–5,330 (3–3.5%) plant species and 243–343 (2.3–3.3%) vertebrate species. In comparison to the NoBio scenario, energy cropland expansion in the Bio scenario leads to an additional loss of around 11,600–14,500 (10.5–13%



in total) plant species and 686–1060 vertebrate species (8.8–13% in total). Although the implementation of a water protection policy alongside bioenergy expansion leads to a small increase in global forest loss (as discussed in Section 5.3.1.2), the distribution of this deforestation across the biodiversity hotspots results in a slightly lower number of overall plant and vertebrate extinctions than in the Bio scenario. In comparison to the NoBio scenario, the Bio-WaterProt scenario leads to an additional loss of around 11,400–14,500 plant species (10.4–12.8%) and 653–987 (8.5–12.6%) vertebrate species, thus reducing impacts of bioenergy by around 200 plant species and 33–73 vertebrate extinctions.

Implementation of a REDD+ scheme in the Bio-REDD scenario significantly reduces the impact of bioenergy on biodiversity, whereby species loss is even smaller than the loss from excluding bioenergy altogether (in the NoBio scenario). The resulting impact from Bio-REDD is a total of 242–491 (0.16–0.32%) plant species and 9–25 vertebrate (0.09–0.24%) species lost by 2100. This equates to 15,858–19,339 plant and 920–1,378 vertebrate species prevented from being lost compared to the bioenergy scenario without REDD+ (Bio). Thus, together the REDD+ and water protection policies could considerably reduce the loss of terrestrial species, and aquatic species (Bonsch et al., 2015).

Further demonstrated in **Figure 5.9** is the impact of  $z$  values and secondary forest ages used to quantify species extinctions. The higher the  $z$  value, the larger the number of extinctions found for a particular hotspot. In addition, the more extinctions calculated for a scenario, the more impact  $z$  has; for example, a wider range of extinctions is found for the Bio scenario than for the NoBio scenario. Secondary forest age has a negative correlation with species extinctions across all scenarios. In other words, as the age of secondary forest increases, more species are found in these forests (in addition to primary forests), therefore the number of species lost decreases.

#### 5.3.1.4.2 Species Loss Within Hotspots

**Table 5.2** displays values of endemic species lost in each of the 16 hotspots between 2005 and 2100. Results are provided for each MAGPIE scenario; whereby secondary forest age and  $z$  value are assumed to be 20 years and 0.2 respectively. For the Bio and Bio-WaterProt scenarios, the majority of species lost occurs in roughly half of the hotspots, whereby the highest number of extinctions occurs in Madagascar and the Indian Ocean Islands. In relative terms, the highest percentage of extinctions occurs in the Philippines, despite the area of primary forest loss in

this hotspot ranking thirteenth out of all findings (see **Figure 5.8** (a)). This is due to its high level of biodiversity in 2005 (see **Table 5.2**), in addition to large percentages of primary and secondary forest loss by 2100 (as shown in **Figure 5.7**). Other hotspots with significantly high species loss in these scenarios are the Atlantic Forest, the Caribbean Islands, East Afromontane and the Guinean Forests of West Africa, reaching values of 654–3,613 (9–42%).

**Table 5.2:** Numbers (and percentages) of species lost in 16 biodiversity hotspots, for each MAgPIE scenario, in 2100 compared to 2005. Species counts in 2005 have been taken from the work of Mittermeier et al (2005). Values are calculated using parameters:  $z = 0.2$  and secondary forest age = 20 years.

Hotspot	Number of species in 2005	Number (and percentage) of species lost by 2100							
		NoBio		Bio		Bio-REDD		Bio-WaterProt	
Tropical Andes	16,598	7	(0.05)	91	(0.6)	4	(0.02)	96	(0.6)
Sundaland	15,735	11	(0.07)	11	(0.07)	0	(0)	46	(0.3)
Madagascar and the Indian Ocean Islands	12,520	2	(0.02)	6,701	(54)	0	(0)	6,757	(54)
Atlantic Forest	8,599	292	(3)	3,518	(41)	0	(0)	3,613	(42)
Indo-Burma	7,489	0	(0)	25	(0.3)	0	(0)	57	(1)
Caribbean Islands	7,390	0	(0)	2,310	(31)	0	(0)	654	(9)
Philippines	6,612	4,791	(72)	4,589	(69)	363	(6)	4,532	(69)
Madrean Pine-Oak Woodlands	4,091	0	(0)	3	(0.07)	0	(0)	26	(0.7)
Himalaya	3,277	9	(0.3)	9	(0.3)	3	(0.1)	8	(0.2)
Western Ghats and Sri Lanka	3,416	16	(0.5)	12	(0.35)	1	(0.03)	10	(0.3)
Mesoamerica	3,813	0	(0)	61	(1.6)	0	(0)	4	(0.1)
Tumbes-Chocó-Magdalena	2,999	11	(0.4)	20	(0.7)	0	(0)	20	(0.7)
Eastern Afromontane	2,742	0	(0)	831	(30)	0	(0)	1,035	(38)
Guinean Forests of West Africa	2,077	0	(0)	878	(42)	0	(0)	896	(43)
Coastal Forests of Eastern Africa	1,835	40	(2)	40	(2)	0	(0)	1,083	(59)
Wallacea	2,023	1	(0.07)	1	(0.04)	0	(0)	7	(0.35)
<b>Total</b>	<b>101,216</b>	<b>5,182</b>	<b>(5)</b>	<b>19,100</b>	<b>(19)</b>	<b>372</b>	<b>(0.4)</b>	<b>18,845</b>	<b>(19)</b>

As shown in Section 5.3.1.4.1, the overall impact of implementing a water protection policy in the biodiversity hotspots, is a reduction in species loss. Five out of the sixteen hotspots in **Table 5.2** show less species extinctions in the Bio-WaterProt scenario compared to the Bio scenario, however the largest reduction occurs in the Caribbean Islands, whereby 1,656 fewer species are impacted. This is due to a reduction of 30% of primary forest and 10% of secondary forest from implementation of water protection in this hotspot. For the five most populated hotspots, the addition of a water protection policy, in Bio-WaterProt, leads to a slight increase in number of endemic species extinctions. Increases are also seen in the three African hotspots, Eastern Afromontane, Guinean Forests of West Africa and Coastal Forests of Eastern Africa. The latter of these is the strongest affected out of all hotspots, whereby an additional 1,043 species are lost due a further loss of around 60% of primary forest and 20% of secondary forest compared to the Bio scenario.

Incorporation of REDD+ in the Bio-REDD scenario results in dramatic reductions of extinctions across all hotspots, whereby nearly zero species loss occurs in all hotspots apart from the Philippines. In the Philippines, around 360 (6%) species are still lost in the Bio-REDD scenario by 2100. This is due the conversion of approximately 40% of primary forest and 10% of secondary forest to cropland.

Eliminating bioenergy altogether in the NoBio scenario similarly reduces extinctions in all hotspots, though the expansion of food/feed cropland still induces high species loss in the Atlantic Forest and Philippines. For the latter, this cropland expansion is higher than in any other MAgPIE scenario, leading to greater species loss (e.g., 3% more extinctions than in the Bio scenario).

## **5.3.2 AZE analysis**

### **5.3.2.1 Impacts of Cropland Expansion on AZE sites**

Cropland expansion in the MAgPIE scenarios is expected to have significant impacts on endangered and critically endangered species occurring in the Alliance for Zero Extinction (AZE) sites. In the NoBio scenario, around 27% (247) of all 920 species are affected by conversion of habitat to food/feed cropland (see **Table 5.3**). High increases in energy cropland in the bioenergy scenarios (Bio, Bio-REDD and Bio-WaterProt), in addition to food/feed cropland expansion, lead to around two thirds of all species experiencing loss of habitat in these

scenarios. For the Bio scenario, 601 (out of 894) vertebrate species and 18 (out of 26) conifer species are affected. Thus, 372 (40%) out of 920 AZE species are impacted by bioenergy incorporation alone. The impact of a water protection scenario is a slight increase of 4 conifer and 3 vertebrate species being affected. Unlike in the hotspot analysis, the incorporation of REDD+ has an overall negative impact on AZE species, whereby an extra 9 species are affected by corresponding changes in cropland distribution.

In the NoBio scenario, South America is projected to have the largest number of species affected by food/feed cropland expansion, reaching 79 species by 2100; all of which are vertebrates. For the scenarios including energy cropland expansion, the highest impacts occur in North America, whereby habitats of 219-222 species are affected. As shown in **Figure 5.10** for the Bio scenario, most impacted AZE sites occur in concentrated regions across Mexico and countries in Central America, as well as in South American countries Colombia, Ecuador, Peru and Brazil. Simultaneously, these sites are located near or within hotspots Mesoamerica, Tumbes Chocó-Magdalena, Tropical Andes, and Atlantic Forest; areas which, as shown in Section 5.3.1, are particularly affected by potential primary and secondary forest loss, and therefore species loss.

**Table 5.3:** Numbers of endangered and critically endangered AZE species impacted by energy and food/feed cropland expansion by 2100 in the MAgPIE scenarios.

Type of Cropland	Scenario	Conifer	Vertebrate	Total
Energy cropland	Bio	10	547	557
	Bio-REDD	12	569	581
	Bio-WaterProt	15	553	568
Food/feed cropland	NoBio	8	239	247
	Bio	11	270	281
	Bio-REDD	9	293	302
	Bio-WaterProt	14	272	286
Either energy or food/feed cropland	NoBio	8	239	247
	Bio	18	601	619
	Bio-REDD	17	611	628
	Bio-WaterProt	22	605	627

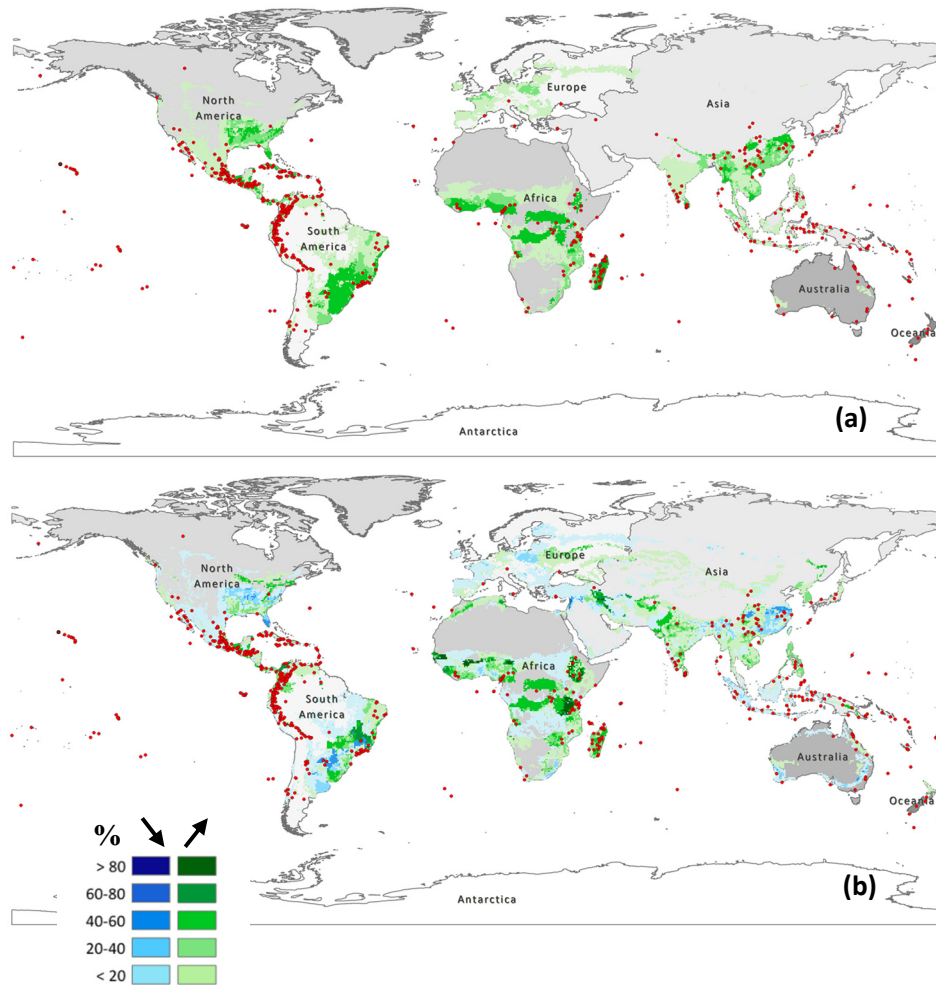


**Figure 5.10:** Alliance for zero extinction (AZE) sites of endangered and critically endangered species (red dots), overlaid onto changes in energy (a) and food/feed (b) cropland, in the MAGPIE Bio scenario, between 2005 and 2100. In the figure key, upward and downward arrows represent increase and loss in cropland.

Asia and Africa have similarly high impacts, with 107-109 and 85-87 species respectively being infringed upon across the bioenergy scenarios. For Asia, this is widespread across Southern, East and South-East Asia, and contains the highest number of affected plant species compared to other regions. For Africa, affected AZE sites mostly occur in eastern regions, though are spread out across the continent, as well as being located within biodiversity hotspots. The lowest numbers of species loss are seen in regions with fewer AZE sites, i.e., Oceania and Europe, with only 1-2 species being affected in Europe across the scenarios.

**Table 5.4:** Regional numbers of endangered and critically endangered AZE species impacted by cropland expansion in the MAGPIE scenarios.

Region and Species	Scenario				
	Total in 2010	NoBio	Bio	Bio-REDD	Bio-WaterProt
<b>Africa</b>	<b>140</b>	<b>41</b>	<b>107</b>	<b>109</b>	<b>107</b>
Conifer	3	1	3	3	3
Vertebrate	137	40	104	106	104
<b>Asia</b>	<b>141</b>	<b>54</b>	<b>87</b>	<b>87</b>	<b>85</b>
Conifer	9	2	9	8	7
Vertebrate	132	52	78	79	78
<b>Europe</b>	<b>11</b>	<b>1</b>	<b>2</b>	<b>2</b>	<b>3</b>
Conifer	1	0	0	0	1
Vertebrate	10	1	2	2	2
<b>North America</b>	<b>298</b>	<b>56</b>	<b>219</b>	<b>222</b>	<b>220</b>
Conifer	5	1	4	4	4
Vertebrate	293	55	215	218	216
<b>Oceania</b>	<b>80</b>	<b>16</b>	<b>14</b>	<b>10</b>	<b>20</b>
Conifer	8	4	2	2	7
Vertebrate	72	12	12	8	13
<b>South America</b>	<b>250</b>	<b>79</b>	<b>190</b>	<b>198</b>	<b>192</b>
Conifer	0	0	0	0	0
Vertebrate	250	79	190	198	192
<b>World</b>	<b>920</b>	<b>247</b>	<b>619</b>	<b>628</b>	<b>627</b>
Conifer	26	8	18	17	22
Vertebrate	894	239	601	611	605

## 5.4 Discussion

### 5.4.1 Impacts on Species Classes

Expansion of cropland in the MAgPIE scenarios leads to significant impacts across all species classes, whereby the largest numbers of extinctions occur for plants (see **Figure 5.11**). The biodiversity hotspots collectively hold over 150,000 endemic plant species, accounting for 50% of all endemic plant species worldwide (Mittermeier et al., 2011). Of these, around 11–13% (~11,600–14,500 species) are projected to become extinct following habitat loss in the bioenergy scenarios, though this is significantly reduced with REDD+ implementation (as shown in Section 5.3.1.4.1). In addition, 54% (14) of endangered and critically endangered AZE conifer species are threatened by cropland expansion. Out of all species classes, plants are most at risk of extinction, with 7,925 endangered species and 4,819 critically endangered species being identified globally in 2021. Plants are particularly vulnerable during habitat destruction due to their inability to disperse to new habitat patches. In many cases, even plants that appear dominant (i.e. are abundant in undisturbed fragments remaining after destruction), disappear over time, otherwise known as “extinction debt” (Tilman et al., 1994; Noh et al., 2019).

Among the vertebrate species, amphibians are the most heavily impacted species in the AZE analysis. By 2100, food/feed cropland expansion in the NoBio scenario is projected to affect 170 (33%) amphibian species. The incorporation of second-generation bioenergy has a significant impact on amphibians, whereby a loss of 246 species is projected by 2100, relative to the NoBio scenario. This is equivalent to 48% of total amphibian species present in 2010. Amphibians are currently undergoing severe global decline, and many are on the brink of extinction (Stuart et al., 2004). The IUCN Red List indicates that amphibian species are notably more at risk than any other vertebrate species, with 2,444 species being globally threatened and 663 species listed as Critically Endangered (IUCN, 2022b).

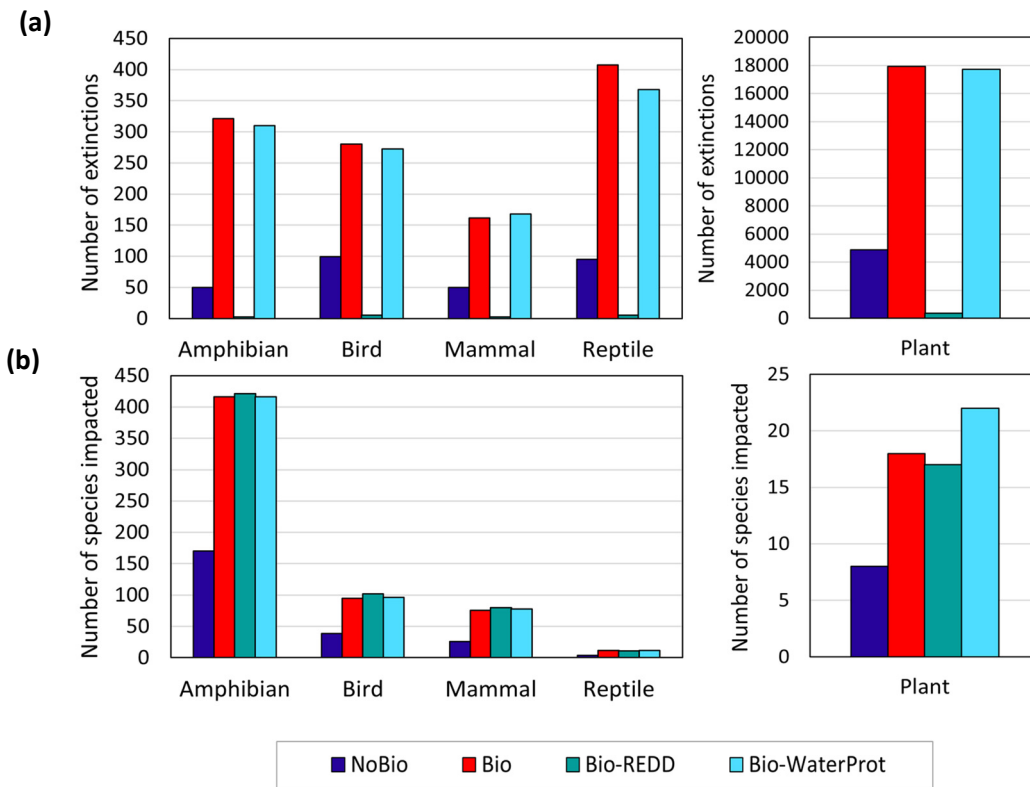


**Figure 5.11:** Numbers of threatened species, per class, in both the hotspot (a) and AZE (b) analyses. Values for the hotspots were calculated using parameters:  $z = 0.2$  and secondary forest age = 20 years old. In the hotspot analysis values represent extinctions by 2100 relative to 2005, whereas in the AZE analysis, values represent number of impacted species by 2100 relative to 2010.

The number of critically endangered reptiles is also rapidly increasing, with 368 species listed in 2021, more than six times the number in 2000 (Gibbons et al., 2000; IUCN, 2022b). In the hotspot analysis, reptiles are projected to undergo the greatest number of extinctions followed closely by amphibians. By 2100, loss of reptiles due to bioenergy expansion equates to around 313/273 species by 2100 in the Bio/Bio-WaterProt scenarios (whereby  $z=0.2$  and secondary forest is 20 years old). This is significantly reduced when incorporating the REDD+ scheme, with around 307/267 species prevented from being lost. The combination of water protection and REDD+ policies therefore has the most beneficial impact for these species, particularly those that live both in water and on land (Bonsch et al., 2015; Dudgeon et al., 2015).

In terms of percentages, all species classes are committed to similarly large impacts, whereby up to 12% of mammals, 12% of reptiles, 11% amphibia and 10% of birds are projected to become extinct in the Bio and Bio-WaterProt scenarios by 2100. Birds experience the lowest



percentage of extinctions, which could be explained by their ability to disperse more readily than other species. However, numbers of bird extinctions are still relatively high, reaching similar levels to amphibian losses in the Bio and Bio-WaterProt scenarios. In fact, the impact of food/feed cropland expansion alone (in the NoBio scenario) is projected to be highest on birds compared to other vertebrate classes. Jetz et al. (2007) similarly calculate high threats for birds over the next century, estimating a potential loss of 900 bird species by 2100 as a result of both climate and land-use change.

In addition to habitat loss and fragmentation, factors such as climate change, water and air pollution, invasive species, and diseases are expected to have increasingly significant impacts on all species (van Vuuren et al., 2006; Bellard et al., 2014; Bonsch, 2015), with amphibians being particularly effected (Pounds et al., 2006; Cushman, 2006; Gascon et al., 2007; Fisher et al., 2009; Mittermeier et al., 2011).

### 5.4.2 Regional Threats

Most of the biodiversity hotspots and AZE sites are located within the tropics. Consequently, larger numbers of species loss occur across tropical regions of Africa, Asia, and Latin America. These regions contain some of the highest and poorest populations and are, in most cases, already undergoing significant land-use changes, threats to biodiversity, and impacts from climate change (Cincotta et al., 2000; Mittermeier et al., 2011; Turner et al., 2012).

#### 5.4.2.1 Africa

The largest numbers of endemic species extinctions occur in Sub-Saharan Africa, in the Bio and Bio-WaterProt scenarios (see **Figure 5.12** (a)). By 2100, approximately 8,450–9770 out of a total 32,738 endemic species in Africa are projected to be lost. Around 70–80% of these extinctions occur in Madagascar, one of the most biodiverse hotspots with high percentages of primary and secondary forest loss. Madagascar has some of the highest levels of endemism out of all the hotspots, partly because it is an island system. Around 90% of Madagascar's 13,000+ plant species and 50–100% of its 1000+ vertebrate species are listed as endemic (Barthlott et al., 1996; Phillipson et al., 2006). It is also home to many endangered and critically endangered species; hence, around one quarter of all impacted AZE species in Africa occur in Madagascar. Remote sensing of Madagascar has shown that around half the forest cover present in 1950 was lost by c.2000 (Allnutt et al., 2008; McConnell and Kull, 2014), due to several causes. These

include slash-and-burn for agricultural cultivation, collection of firewood for cooking in rural areas, illegal logging of timber for the international market, and mining. Such activities have been the cause of forest loss in many other low-income countries located in Africa, South-East Asia, South America and Southern North America, where populations are rapidly increasing. In mainland Africa, this has led to widespread deforestation, particularly in central parts, with the Democratic Republic of Congo experiencing substantial losses (Hansen et al., 2013).

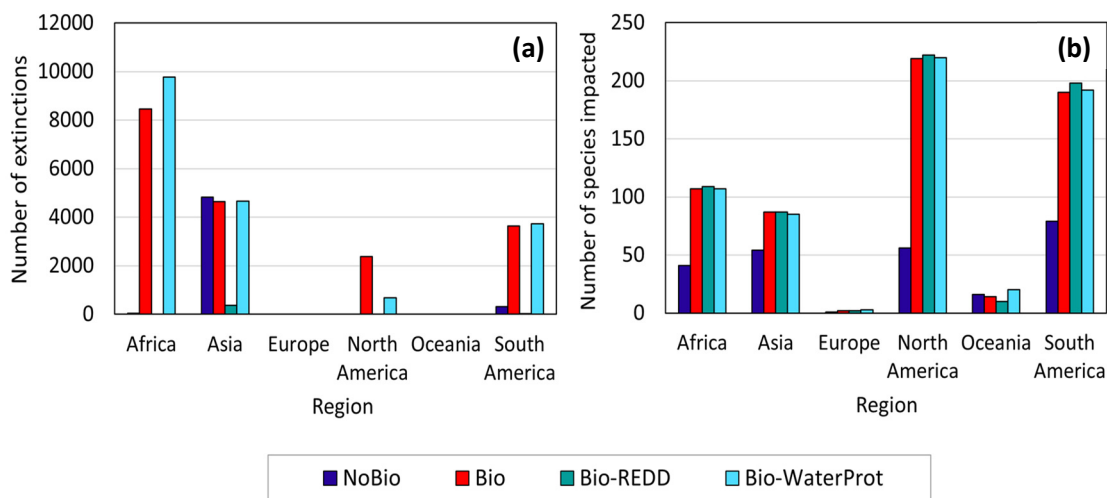


**Figure 5.12:** Regional numbers of threatened species, in both the hotspot (a) and AZE (b) analyses. Values for the hotspots were calculated using parameters:  $z = 0.2$  and secondary forest age = 20 years old.

In the MAgPIE scenarios, pasture and secondary forest are primarily used for the continuation of food/feed cultivation across the African hotspots, as shown in the NoBio scenario. However, unless REDD+ is implemented, incorporation of second-generation bioenergy expansion could lead to extensive losses of primary forest. In addition to Madagascar, significant primary and secondary forest loss also occurs in Eastern Afrotropical, Guinean Forests of West Africa and Coastal Forests of Eastern Africa in the Bio and Bio-WaterProt scenarios. Combined, these changes contribute to the remaining 20–30% of endemic species extinctions occurring in Africa.

### 5.4.2.2 Asia

The Philippines hotspot is projected to have the highest percentages of extinctions across the MAgPIE scenarios, with up to 6–72% of endemic species being lost by 2100, depending on the scenario (see **Table 5.2**). It is also home to eight endangered or critically endangered species, three of which are impacted by cropland expansion in the MAgPIE scenarios. Over the last two decades, the human population in the Philippines has increased by around 32 million (World Bank, 2021), ranking it the second highest populated hotspot in 2010 (Mittermeier et al., 2011). This, along with economic pressures for the country, has led to large-scale conversion of forests, as well as overexploitation of coastal resources (Shi et al., 2005; Fisher and Christopher, 2007). It is therefore one of the hotspots most at-risk of destruction and has been debated as to whether its diversity is salvageable (Terborgh, 1999; Posa et al., 2008).

Species loss in the Philippines accounts for around 97–99% of all extinctions calculated in Asia, most of which occur in Tropical Asia (Stibig et al., 2014). Tropical Asia occupies nearly 15% of the world’s tropical forests; however, is also one of the world’s major deforestation hotspots (Sodhi et al., 2010), with rates comparable only to that of Latin America (Hansen et al., 2013). Studies have further shown that intact and protected forests are being degraded and cleared, and that most of this forest conversion is attributed to agriculture as well as logging for fuelwood (Sodhi et al., 2004; DeFries et al., 2005; Sodhi et al., 2010; Wilcove et al., 2013; Stibig et al., 2014). Though the Philippines holds the largest percentages of extinctions, due to its highly concentrated biodiversity, total (primary and secondary) forest loss in Asia is highest in the Indo-Burma hotspot. Indo-Burma contains some of the largest areas of cropland conversion, with energy cropland exceeding values calculated for all other hotspots (486,000–498,000 km<sup>2</sup> by 2100; see **Figure 5.13**). Other studies equivalently show extensive land-use change across Indo-Burma. Molotoks et al (2018) similarly use a “middle of the road” scenario produced by the IMAGE 3.0 model and find that 178,677 km<sup>2</sup> of land will be converted to cropland in Indo-Burma by 2050, making it the most threatened hotspot. Jantz et al. (2015) further project that, for a range of RCP scenarios, Indo-Burma will lose an additional 20% of its primary forest by 2100, the most among the hotspots in their analysis.

Large areas of cropland expansion are also spread out in other parts of Asia, such as Sundaland, Western Ghats and Sri Lanka, and southern parts of China. As a result, 85–87 endangered and critically endangered species are impacted across Asia in the bioenergy scenarios, which is reduced to 54 species with the exclusion of energy cropland (in the NoBio scenario). In

comparison to other regions, this makes Asia one of the lowest threatened regions in the AZE analysis (see **Figure 5.13 (b)**), likely due to most of the AZE sites being located in the Americas. These sites are mainly situated in Mexico, Central America and western parts of South America.

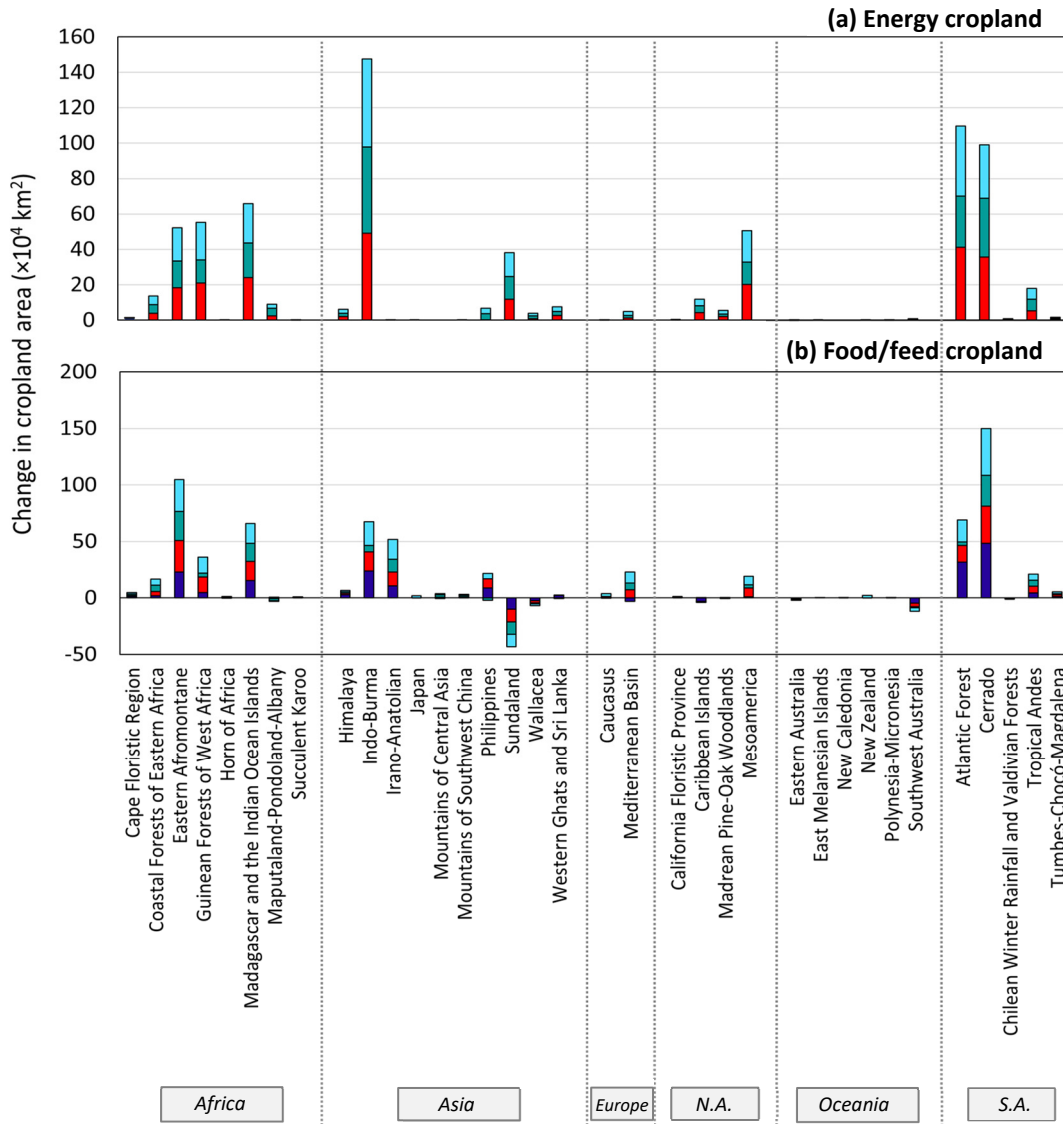


**Figure 5.13:** Changes in energy and food/feed cropland area in each biodiversity hotspot, for each MAGPIE scenario, between 2005 and 2100.

### 5.4.2.3 Latin America

Mexico contains the highest number of threatened AZE sites in comparison to all other countries, with 132 species affected in the bioenergy scenarios and 45 species affected in the NoBio scenario by 2100. This is more than half of the total species impacted in North America (56–220 species). With around 30,000 plant species and 5,700 vertebrate species, Mexico is one of the most biodiverse countries globally, recently ranking sixth after Brazil, Indonesia and Colombia, China, and Peru in terms of species diversity (Mayani-Parás et al., 2021), and 4<sup>th</sup> in terms of vertebrate diversity (Cantú et al., 2004; Butler, 2016). Its suitable climate conditions and fertile soils make Mexico a prime location for agricultural expansion (Delzeit et al., 2017). This, alongside a lack of species protection in the region (Ricketts et al., 2005; Botello et al., 2015), makes it one of the highest countries at risk of habitat loss from land conversion (Visconti et al., 2011; Mayani-Parás et al., 2021). Results for the Mesoamerica hotspot (where Mexico is located) in this study reflect such losses, in which approximately 32,400km<sup>2</sup> (29%) of primary forest is projected to be lost in the Bio scenario by 2100, ranking it second highest amongst all 35 hotspots (see **Figure 5.8**). Molotoks et al (2018) calculate similar threats in Mexico, estimating a total of 111 endangered and critically endangered species impacted by 2050; around 75% of all AZE species affected in North America, and the highest count in the world.

South America has the second highest number of threatened AZE species. Most of these occur within the Tropical Andes hotspot situated across Colombia, Ecuador, Peru, and Bolivia, where almost half of all AZE species in South America are located (163 out of 250). As shown in Section 5.3.1.3, across the MAgPIE scenarios the Tropical Andes undergoes some of the largest areas of primary forest loss in comparison to all other hotspots. Consequently, up to 96 endemic species (1%) are committed to extinction by 2100, relative to 2005. Though this value is low compared to other findings in this study (see **Table 5.2**), results from the AZE analysis indicate that the likelihood of these species being endangered or critically endangered is high.

Brazil, on the other hand, experiences some of the largest numbers of species extinctions, yet low numbers of impacted AZE species. In total, Brazil contains 28 AZE sites, 23–24 of which are impacted by cropland expansion in the bioenergy scenarios. These sites are located across six major biomes: the Amazonia rainforest, the Caatinga xeric shrublands, the Pantanal wetlands, the Cerrado savanna and the Atlantic Forest (Fernandes et al., 2017). Together these biomes host about 15–20% of all species worldwide (Duden et al., 2020), however only the

Cerrado and the Atlantic Forest are considered biodiversity hotspots. This is because they are home to large numbers of endemic species and have lost extensive areas of original habitat land (Mittermeier et al., 2005). At present, around 12% of original vegetation cover is left in the Atlantic Forest, in which remaining tropical and semi-deciduous forest areas are largely fragmented (Beca et al., 2017; Bovo et al., 2018). In 2005, the Atlantic Forest inhabited approximately 8599 endemic species (Mittermeier et al., 2005). Around 292 of these species are projected to become extinct following loss of primary and secondary forest in the MAgPIE scenarios, increasing to approximately 3,518 species lost with bioenergy implementation (see **Table 5.2**).

The Cerrado hotspot is the biggest savanna region in South America, containing a rich diversity of different vegetation types, such as tree and scrub savanna, grasslands with scattered trees, and patches of dry, closed-canopy forests. Located in the Cerrado are approximately 4,400 (2%) plant species and 89 (0.4%) vertebrate species. Only 1.5–2% of it is protected, making it the least protected ecosystem in Brazil (Casson, 2003; Klink and Machado, 2005; Carvalho et al., 2009). This has resulted in over 40% (60,000km<sup>2</sup>; Rocha et al. (2011)) of its original extent being converted to cropland. Projections calculated in the hotspot analysis for the Cerrado show that large percentages of secondary forest loss occur, however, zero primary forest loss is predicted. The method used in this study only accounts for species that occur in primary forests, assuming a portion of these species also occur in secondary forests. Hence, zero primary forest loss in the Cerrado leads to zero extinctions calculated. As shown in **Figure 5.13**, between approximately 300,000–360,000 km<sup>2</sup> of energy cropland and 270,000–490,000 km<sup>2</sup> of food/feed cropland is planted in the Cerrado across the MAgPIE scenarios. It is therefore likely that such large-scale changes to the land will have substantial impacts on the species located here, as illustrated in other studies (Malcolm et al., 2006; Jantz et al., 2015; Molotoks et al., 2018).

### 5.4.3 Impacts of Bioenergy on Biodiversity

#### 5.4.3.1 Isolated Impacts of Bioenergy Expansion

As discussed in *Chapter 2*, only a handful of studies have investigated isolated impacts of large-scale second-generation bioenergy deployment on global biodiversity. However, recent advancement of spatial energy cropland data has instigated further research into this field, as well as the use of various well-established methods and indicators typically applied in the biodiversity literature. Hanssen et al. (2022), for example, use characterisation factors (potential species loss per m<sup>2</sup>) based on SARs, derived by Chaudhary and Brooks (2018), to determine loss of endemic and non-endemic vertebrate species richness across 804 ecoregions when following an ambitious 1.5 °C SSP2 pathway incorporating large scale BECCS. They predict that bioenergy expansion leads to a loss of approximately 1500 vertebrate species by 2100, an amount 40–120% times greater than findings in this work (686–1,060 endemic vertebrate species extinctions), due to the incorporation of different study regions and non-endemic species. Tudge et al. (2021) instead use the PREDICTS database to show that species richness and abundance for plant, vertebrate and invertebrate species are 19% and 25% lower in sites planted with second-generation bioenergy crops than in sites with natural vegetation. This 19% reduction in species richness corroborates findings in this chapter, whereby in total up to 13% endemic plant and vertebrate species are lost due to the conversion of forest to cropland for bioenergy expansion.

Overall, there is consensus among previous literature that it is impossible to convert additional natural land for bioenergy expansion without further transgressing the planetary boundaries for land-system change and biosphere integrity. Heck et al. (2018), for instance, calculate that large-scale bioenergy could result in a 7% loss of biodiversity intactness. Even the conversion of existing managed cropland for energy cropland has shown negative implications for biodiversity (Powell and Lenton, 2013). On the other hand, several studies have demonstrated that, if implemented carefully, conversion of marginal or abandoned land for energy cropland can provide significant benefits (Shi et al., 2005; Dauber et al., 2010; Meehan et al., 2010; Robertson et al., 2011; Immerzeel et al., 2014; Haughton et al., 2016). These benefits include providing habitat and shelter for specific species (such as migratory birds), as well as improving connectivity or supporting restoration of marginal or degraded lands, with particular benefits seen in temperate regions.

### 5.4.3.2 Impacts of Bioenergy in Future Mitigation Pathways

Impacts of bioenergy expansion can also be deduced from assessments of overall LUC impacts in future mitigation pathways. Malcolm et al (2006) calculate endemic species loss resulting from climate-induced habitat change across the biodiversity hotspots, following a pathway with global warming target of  $\sim 2.5$  °C above pre-industrial temperatures. Using both the SAR and EAR models with  $z$  value of 0.15, they estimate a loss of approximately 231 to 56,000 plant species, and 17 to 3,700 vertebrate species by 2100, dependant on factors such as biome type, species migration capabilities, and global vegetation model used. Reaching a 2.5 °C warming target will require achieving negative emissions by 2100, thus implies the use of CDR methods such as BECCS. Findings for the Bio and Bio-WaterProt scenarios in this work reflect mid-range estimates calculated by Malcolm et al. (2006), whereby around 15,900–19,830 plant species and 896–1,403 vertebrate species are projected to be lost globally by 2100 (see Section 5.3.1.4.1). In contrast, the 242–491 plant and 9–25 vertebrate species lost in the Bio-REDD scenario are more in line with their lowest estimates, calculated for species with perfect migration, within tropical broad leaf forest biomes.

The impact of bioenergy expansion within future mitigation pathways can be further assessed by comparing calculated species extinctions for different pathways with bioenergy deployment potentials used in these pathways. **Figure 5.14** displays such findings for this work and two other studies by Jantz et al. (2015) and Chaudhary and Mooers (2017). Jantz et al. (2015) calculate a loss of 200–20,000 plant species and 20–1,500 vertebrate species by 2100 (relative to 2005) for all RCPs using the SAR model with  $z$  values 0.1, 0.33, and 0.55. Chaudhary and Mooers (2017) also utilise the SAR model, with  $z$  values 0.23, 0.44, and 0.48 and calculate an average loss of around 1,230–1,841 vertebrate species for a collection of hybrid RCP-SSP scenarios, excluding reptiles from analysis. The 242–19,830 plant and 9–1,403 vertebrate extinctions found in this study therefore lie within findings from these studies, and are particularly comparable to the RCP 2.6 projection.



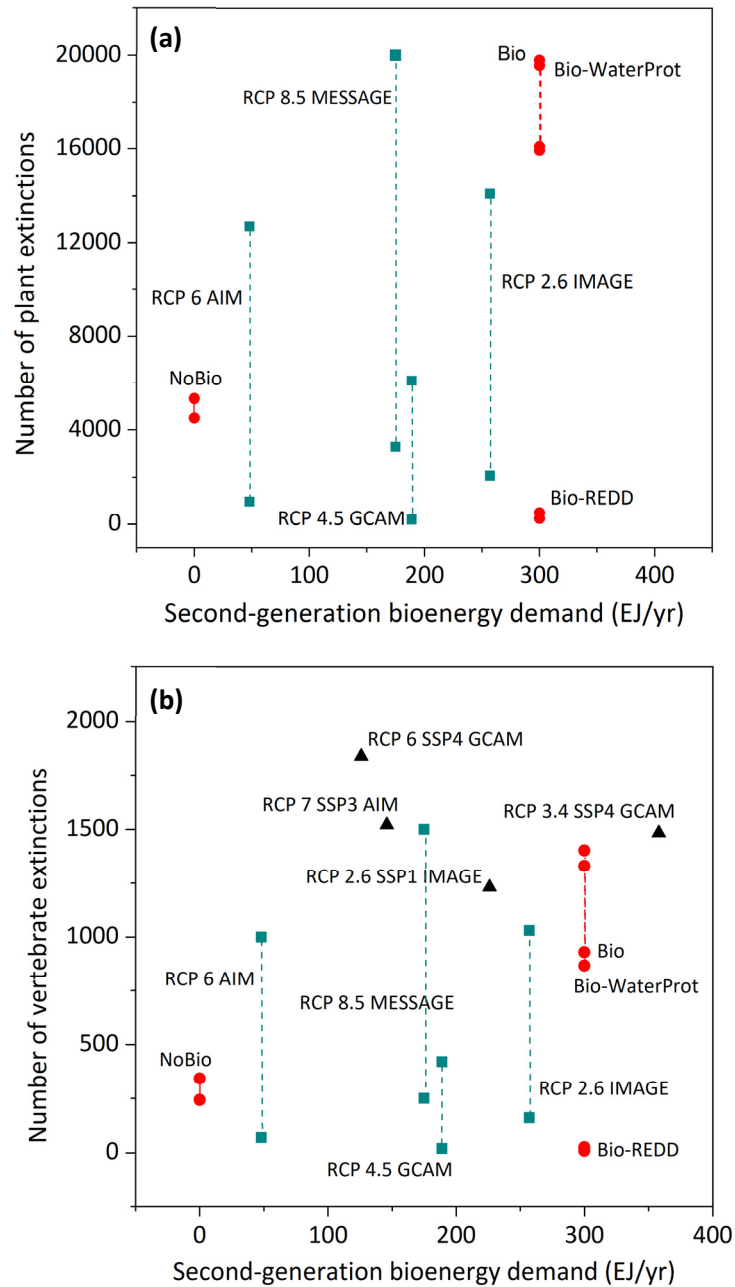


**Figure 5.14:** Number of plant (a) and tetrapod (b) extinctions versus second-generation bioenergy demand in 2100 compared to 2005. Graph (a) shows projections for the MAgPIE scenarios and the RCP pathways provided in the work of Jantz et al. (2015). Graph (b) additionally shows results for the RCP-SSP hybrid scenarios found by Chaudhary and Mooers (2017). ‘Bioenergy demand’ includes bioenergy produced from traditional and modern feedstock and includes bioenergy with and without carbon capture and storage depending on the scenario. Bioenergy demand values, for comparison to results by Jantz et al. (2015), have been taken from the work of van Vuuren et al. (2011). Values for RCP 2.6 SSP1 IMAGE, RCP 3.4 SSP4 GCAM and RCP 6 SSP4 GCAM have been taken from the SSP database (IIASA, 2018b).

Together, findings from the three studies show a weak but somewhat positive correlation between bioenergy deployment and number of species committed to extinction by 2100. The complexity of this correlation can be explained by several causes. Though increased mitigation and socioeconomic efforts are generally shown to result in less loss of natural vegetation cover, in some instances this is not the case. For example, the most ambitious mitigation scenario RCP2.6 still yields intermediate levels of natural vegetation loss, and thus species loss, implying that climate mitigation and habitat protection are not always directly linked. In addition, species loss from the SSP1 (RCP2.6 IMAGE) scenario in the work of Chaudhary and Mooers (2017) is not dissimilar to species loss calculated for the SSP2 MAgPIE scenarios in this work, a scenario with supposedly less land-use regulations and socio-economic restrictions. Outlying estimates, such as those for Bio-REDD from this work and RCP 4.5 GCAM calculated by Jantz et al. (2015), can be attributed to substantially less natural vegetation loss, and therefore habitat loss, occurring within these scenarios compared to other scenarios. With regards to the GCAM model, this is partly due to demographics being fixed, with around 3 billion fewer people in the world in RCP8.5 GCAM relative to RCP 8.5 MESSAGE, as shown in the work of Riahi et al. (2011). Further, the pricing of LUC emissions in both the RCP 4.5 GCAM and Bio-REDD scenarios acts to discourage the removal of forest. In fact, for all SSP pathways following RCP4.5 and RCP2.6, GCAM has been shown to produce the largest amount of forest expansion compared to other models (Popp et al., 2017). Contrastingly, the effects of a lack of forest regulation (particularly in low income countries) is depicted in findings for the RCP 6 SSP4 GCAM, in which species loss is highest out of all scenarios even though bioenergy deployment is low.

#### **5.4.4 Impacts of a REDD+ Scheme**

Restrictive land-use change policies that aim to conserve natural forests, such as the REDD+ scheme, can be used as an option to mitigate climate change and prevent the conversion of important land ecosystems. As shown previously in **Figure 5.14**, trade-offs between bioenergy expansion and endemic species loss can be significantly reduced with the incorporation of REDD+. This, however, is not the case for endangered and critically endangered species. In total, an additional 9 AZE species are impacted in the Bio-REDD scenario compared to the Bio scenario. Dissimilarities between analyses could be due to several factors. For instance, not all AZE sites are located within biodiversity hotspots, with those that are, not necessarily being

situated within primary or secondary forests (see **Figure 5.15**). Thus, impacts of REDD+ seen in the hotspot analysis would not apply to these AZE sites.

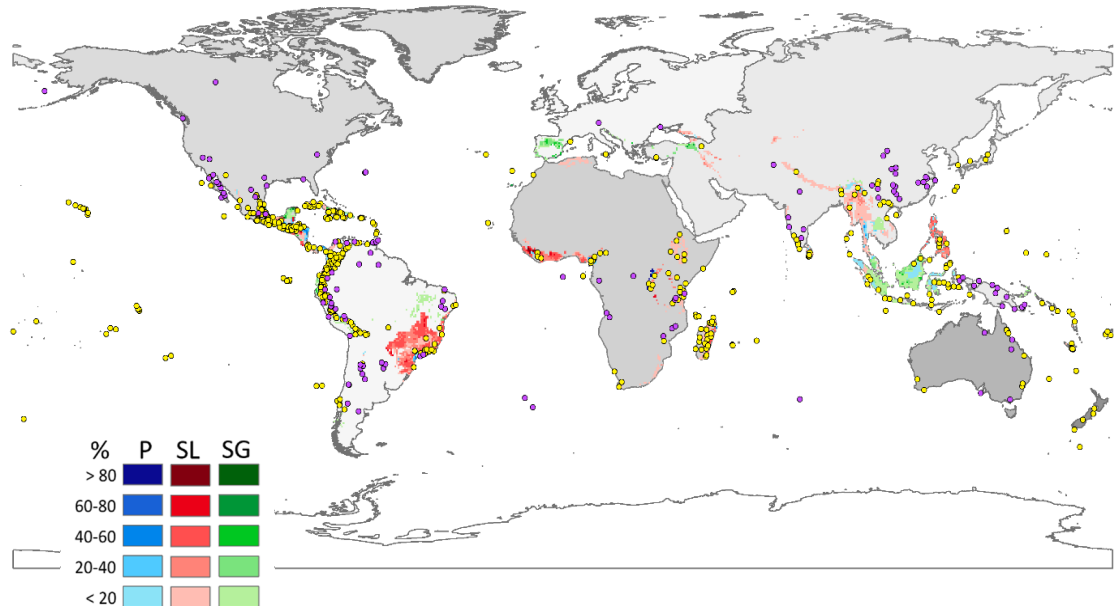


**Figure 5.15:** Alliance for Zero Extinction sites inside (yellow dots) and outside (purple pots) biodiversity hotspots, overlaid onto changes in primary (P-blue) and secondary forest (SL/SG-red/green) between 2005 and 2100.

As discussed in previous chapters, the expansion of cropland into forests and other carbon-rich ecosystems is restrained in the Bio-REDD scenario by putting a price on CO<sub>2</sub> emissions from land-use change. The prevention of costly conversion of these carbon-rich ecosystems in the MAGPIE scenarios leads to cropland being spread out over a wider area of land. Consequently, more ‘non-forest’ areas are used for cropland expansion (see *Chapter 3*), thus increasing the chances of overlap with AZE sites. These areas include natural vegetation, such as shrublands, savannas, grasslands, and pastures, which contain important ecosystems that may also be rich in carbon. Shrublands and savannas, can store considerable amounts of aboveground carbon and are largely found across Africa, Latin America and parts of Asia (Baccini et al., 2012). Natural grasslands and pastures are permanent vegetation, unlike cropland, and therefore promote soil carbon storage, a major part of the overall terrestrial carbon balance (Guo and Gifford, 2002; Smith, 2008; Don et al., 2011). In the literature, the shift of land-use pressure to non-forest ecosystems has been termed ‘non-forest leakage’ and is one of the major concerns regarding REDD+ implementation (A. Popp, Humpenöder, et al., 2014).

As discussed in *Chapter 4*, changes in cropland distribution in the MAgPIE scenarios result in increased terrestrial CO<sub>2</sub> emissions from conversion of, not only forest, but also shrubland and grassland. This corroborates findings from previous work, which demonstrate that in order to achieve ambitious targets for global climate change mitigation, terrestrial carbon policies need to cover the full range of carbon-rich ecosystems (M. Wise et al., 2009; Reilly et al., 2012; A. Popp, Humpenöder, et al., 2014). Findings in this chapter show that such policies could provide co-benefits for biodiversity in non-forest ecosystems, such as the tropical savannas of the Brazilian Cerrado hotspot, which are increasingly threatened under incomplete schemes (Myers et al., 2000; Miles and Kapos, 2008; Stickler et al., 2009)

Operation of land-use policies would require identifying and protecting non-forest ecosystems of high value for carbon and biodiversity. These would further need to be incorporated into the National Biodiversity Strategies and Action Plans (NBSAPs), strategic documents developed by countries which implement the objectives of the Convention on Biological Diversity (CBD) (CBD, 2023). To do this, future work could use finer resolution scenarios of cropland conversion, combined with satellite and ground survey data, to determine non-forested ecosystems most at risk. In addition, government financing structures would need to include conservation investment for a wide range of land types not covered by REDD+ funding (Miles and Kapos, 2008). Popp et al (2014) indicate the potential challenges that will need to be overcome if cropland expansion is restricted for land conservation. Enhanced land-use competition will likely occur, resulting in high production costs and food prices (M.A. Wise et al., 2009; Popp, Dietrich, et al., 2011; Popp et al., 2012). Further, increased agricultural productivity will be needed to compensate for reduced land availability. This could involve the closing of yield gaps through more efficient land management and technological innovations in agriculture (Popp, Dietrich, et al., 2011; Mueller et al., 2012). Demand-side measures, such as changes towards more plant-based diets, could also make more land available. Regardless of which policies and actions are implemented, global participation will be needed for them to work.

High numbers of impacted AZE species in the Bio-REDD scenario could also be due to how “impacted sites” are defined within the calculations. As stated in Section 5.2.2.2, this study assumes that AZE sites containing cropland conversion higher than zero are counted as impacted. Therefore, although REDD+ leads to lower conversion on some AZE sites, these sites are still considered impacted. Molotoks et al. (2018) use the same AZE method, in combination with the IMAGE 3.0 SSP2 scenario, and show that almost 50% of all AZE species

(455 out of 920) will experience habitat loss from cropland conversion by 2050. In addition to this, they calculate the intensity of these impacts for each site that is affected, finding that higher numbers of species tend to occur in areas of low conversion to cropland. In this study it is likely that lower converted AZE sites occur more frequently in the Bio-REDD scenario than in the Bio scenario. If this were the case, the impact of Bio-REDD on biodiversity may be considered lower than it appears.

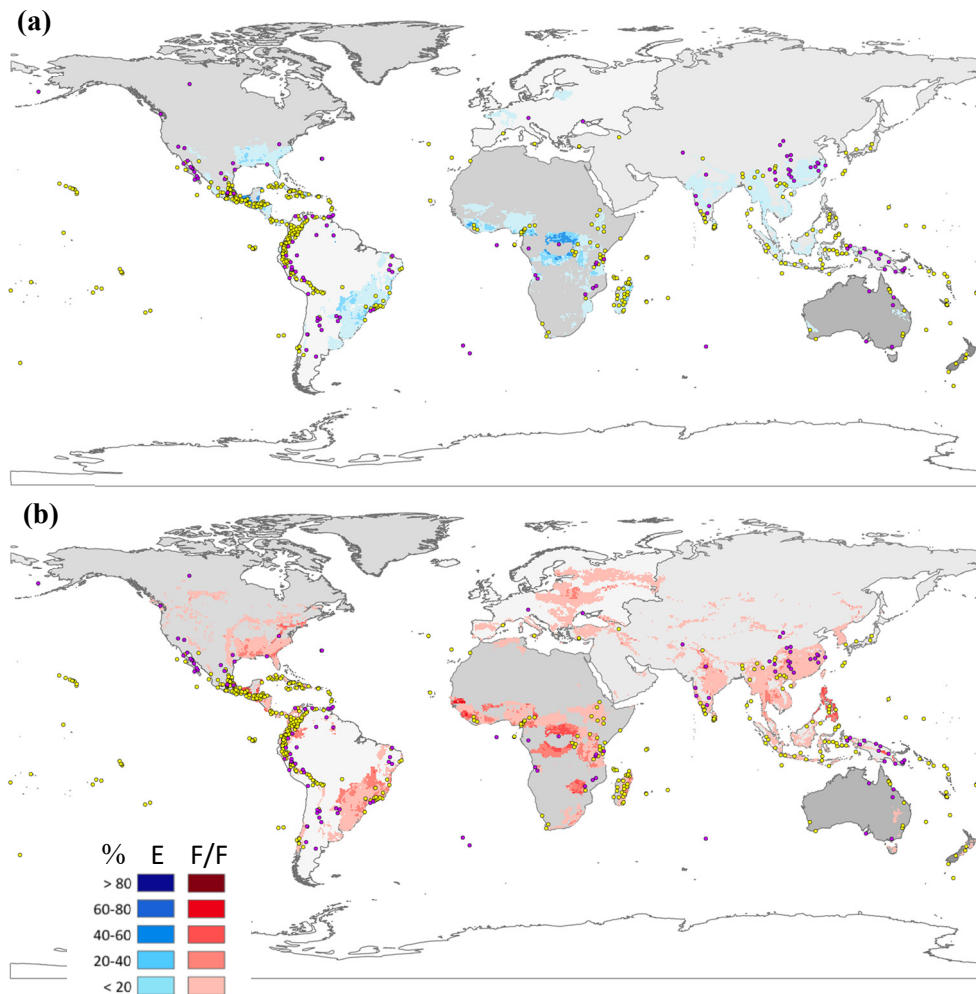


**Figure 5.16:** Percentage reductions in energy “E” (a) and food/feed “F/F” (b) cropland intensity due to the implementation of a REDD+ policy, calculated as the difference between cropland expansions in the Bio-REDD and Bio scenarios between 2005 and 2100. Increases in cropland expansion from REDD+ are not shown. Yellow and purple dots are the AZE sites inside and outside of biodiversity hotspots, respectively.

Differences between cropland in the two scenarios can show where cropland conversion is lower in the Bio-REDD scenario than in the Bio scenario (see **Figure 5.16**). Overall, 487 sites consist of reduced energy cropland conversion due to REDD+. For food/feed cropland, this occurs across 529 sites. Increased cropland cover is also seen from REDD+ incorporation in some regions, however, occurs over a smaller number of AZE sites (energy cropland: 216 sites; food/food cropland: 322 sites). These findings could therefore infer that REDD+ has a positive impact for AZE species due to reduced intensity of cropland expansion on over half of the AZE sites. Future work could carry out a similar analysis to that shown by Molotoks et al. (2018) to determine exact intensities of cropland expansion over AZE sites, and how these vary between the Bio-REDD and Bio scenarios.

### 5.4.5 Impacts of a Water Protection Scheme

The overall impact of a water protection policy is a small reduction of species loss. Globally, the greatest benefits are therefore seen when combining REDD+ and water protection policies, with around 16,058–19,539 plant species and 953–1,451 vertebrate species prevented from extinction globally in the hotspot analysis (see Section 5.3.1.4.1). However, water protection benefits are mainly influenced by results for the Caribbean Islands hotspot. Though the Caribbean Islands is one of the smallest biodiversity hotspots, it harbours the sixth highest number of endemic species out of all the hotspots. Over the century, energy cropland expansion in this hotspot is projected to decline by approximately 7,000 km<sup>2</sup> with the addition of water protection, compared to bioenergy deployment on its own (see **Figure 5.13**). Food/feed cropland is completely prevented from expanding, instead this land is used for expansion of other land-use types, such as energy cropland and secondary forest regrowth. The overall impact is reduced deforestation and subsequently a prevention of 72% of species being lost compared to a scenario without water protection (the Bio scenario).

This contraction of species loss, however, does not depict findings in other hotspots. In total, out of the sixteen hotspots undergoing extinctions, ten show an increase in species loss after the addition of a water protection policy. Some of the largest increases are seen in the Coastal Forests of East Africa, Eastern Afrotropical, Madagascar, and Atlantic Forest. These hotspots are located in dry regions; where water is less available for irrigation (Goodman et al., 2005; Mittermeier et al., 2011; Cunha et al., 2015; Bonsch et al., 2016). As discussed in previous chapters, the implementation of water protection prohibits irrigation of bioenergy production, making it hard to produce high yields per unit area. As a result, significantly more land is

needed to utilise rainwater and thus fulfil energy cropland demands. Such land requirements are partly fulfilled at the expense of pasture areas, however, as shown in this work, expansion can also occur onto natural forests. In either case, the impact of this land conversion could lead to the loss of important ecosystems featuring high biodiversity, carbon storage potential and water flow regulation, if strict land-use change regulations are not implemented (Alkemade et al., 2013; Conant et al., 2017).

Certification schemes (Fehrenbach, 2011) and government incentives (e.g., taxes and subsidies; Moraes et al. (2011)) for rainfed bioenergy can be useful in protecting water resources, however, neglect potential trade-offs with land ecosystems. Rather than implementing only rainfed bioenergy, water use for energy cropland could instead be restricted to sustainable levels (Bonsch et al., 2016). This would require site-specific understanding of how much water is needed for human consumption and environmental purposes (or environmental flows) (Smakhtin et al., 2004; Poff et al., 2010; Bonsch et al., 2015). Findings would determine where water resources are available for energy cropland irrigation, and thus reduce land requirements and subsequent impacts on ecosystems and biodiversity. This information could feed into countries contributions to National Biodiversity Strategies and Action Plans (NBSAPs) (CBD, 2023). The Convention on Biological Diversity (CBD) does not explicitly require NBSAPs to address water protection (or REDD+). However, many countries recognise the importance of freshwater ecosystems and the need to incorporate water-related measures into their biodiversity conservation efforts. If implemented carefully, the combination of water protection policies with forest protection policies, such as REDD+, has the potential to significantly reduce trade-offs between bioenergy expansion and land ecosystems.

#### **5.4.6 Limitations in Methodological Approaches**

The assessments used in this chapter have been well-established in previous literature, thus were considered most appropriate for determining global land-use impacts on biodiversity. However, biodiversity modelling as a whole is still relatively new (particularly in comparison to climate modelling), and the approaches demonstrated in this chapter have their limitations.

The EAR model is an improvement on its predecessor, the SAR model, which tends to overestimate species extinctions. However, the EAR approach still has its drawbacks (which also occur for the SAR approach). For instance, it only captures the direct effects of habitat

conversion on endemic species, in which species loss is assumed to be immediate. It also relies on the assumption that habitat is uniform i.e., that  $z$  (and thus  $z'$ ) does not change across the region being studied. In reality, cropland expansion in a particular area could have repercussions on neighbouring areas, and result in degradation of other ecosystem services. The result is habitat fragmentation, creation of edges, and the closing of habitat corridors (Kinzig and Harte, 2000). To estimate these impacts, site-specific monitoring using finer resolution data within countries would be needed. Further, individual responses of species to land-use change may vary as some species are more sensitive than others. Thus, ignoring these contextual factors could have resulted in inaccurate predictions or interpretations of species richness patterns. Previous work has tried to combat this issue by developing a Matrix SAR model, which accounts for habitat heterogeneity and acknowledges that some species can tolerate human-modified habitats (De Baan et al., 2013; Chaudhary et al., 2015; Chaudhary and Brooks, 2018). However, these models are based on the SAR and thus do not accurately account for species distributions within habitats. Future work could develop a combined model which encompasses the benefits of this matrix approach, with the EAR model used in this chapter.

Limitations also exist within the AZE analysis, whereby indirect impacts of cropland expansion have been excluded. It is important to further note that, since the time that this analysis was carried out, the AZE dataset has changed to include wider boundaries, whereby each site is a polygon shapefile rather than a location point. Hence, findings in this study may under-estimate impacts of cropland expansion on endangered and critically endangered species. Future impact assessments would thus need to incorporate cropland expansion over the total area of each site. Another limitation in the AZE analysis is the assumption that AZE sites containing cropland conversion higher than zero are counted as impacted. This method therefore neglects the different intensities of cropland conversion on each site that is affected and is possibly one of the reasons why species loss is higher in the Bio-REDD scenario than the Bio scenario. Preliminary analysis in Section 5.4.4 illustrates the likelihood that lower converted AZE sites occur more frequently in the Bio-REDD scenario than in the Bio scenario, thus indicating that REDD+ could potentially have a positive impact for some of these sites. By incorporating intensities of conversion into the analysis, as carried out by Molotoks et al. (2018), future work could provide a more comprehensive understanding of the role of REDD+ in preventing or exacerbating species loss within the AZE sites.



While the metrics and models used in this analysis have been well-established and peer reviewed, other less-used biodiversity indicators (e.g., mean species abundance, Biodiversity Intactness Index, species distribution), datasets (e.g., other priority areas for conservation; Brooks et al. (2006)), and methodologies (e.g., GLOBIO modelling, species distribution modelling, PREDICTS data analysis) could be implemented in future work, with some studies emphasising the importance of incorporating a variety of biodiversity metrics in land use impact assessments (Grenyer et al., 2006; Davies and Cadotte, 2011; Souza et al., 2015; Gabel et al., 2016; Marquardt et al., 2019; Molotoks et al., 2020). However, each model has its limitations, and the approach used here was decided most suitable for this assessment, with the resources available.

In both the biodiversity hotspot and AZE analyses, the conversion of habitat to energy cropland is considered a loss of biodiversity. However, bioenergy systems can also positively affect biodiversity (as well as carbon storage and other ecosystem services), depending how the land is used. Economic incentives can be carefully designed to promote bioenergy systems that minimise biodiversity losses and deliver multiple benefits. Bottom-up processes using finer resolution data and field surveys can be used to determine priorities of habitats and whether there are possibilities for land-sharing approaches to biofuel production (Barbier et al., 1997; Lotze-Campen et al., 2010; Phalan et al., 2011).

Finally, this study only investigates the impacts of LUC from bioenergy expansion on species loss. Global and regional climate change is also expected to have dramatic consequences for biodiversity over the next century. Findings from *Chapter 4* could indicate that the cooling effect of substituting fossil fuel emissions via bioenergy production may alleviate this crisis, however also that regional biogeophysical and biogeochemical changes due to energy cropland expansion could exacerbate it. As shown in *Chapter 2*, previous literature indicates mixed findings, with most concluding that reduced species richness from bioenergy expansion outweighs the benefits of prevented climate change (Powell and Lenton, 2013; Heck et al., 2018; Hof et al., 2018; Hanssen et al., 2022), but that over longer periods of time (e.g., 80 years) this could switch (Hanssen et al., 2022). It is evident that significant uncertainty remains in this field, and that there is large scope for further research. Preliminary work by the author has highlighted a couple of possible avenues that could be carried out:

- Further research could use bioenergy scenarios (such as the MAgPIE scenarios) to calculate endemic species loss due to disappearing and novel climates within the

biodiversity hotspots. This would require the use of a GCM to produce high resolution projections of climate indicators (e.g., temperature and precipitation), and the standardized Euclidian distance (SED) method, developed by Williams et al. (2007), to determine climatic dissimilarity across hotspots (Bellard et al., 2014). Findings could then be compared to the number of extinctions resulting from LUC (such as those calculated in *Chapter 5*) to determine whether biodiversity loss from limiting climate change through bioenergy incorporation compensates for biodiversity loss due to LUC for bioenergy.

- Another possible method would be to utilise pre-calculated values of extinction-risk relative to °C of warming in combination with GCM predictions of temperature change and LUC emissions for certain bioenergy scenarios (e.g., the MAgPIE scenarios). For example, Hanssen et al. (2022) estimate the percentage of species saved per °C of warming prevented due to bioenergy incorporation using extinction-risk values based on a meta-regression analysis of vertebrates, plants and insects carried out by Urban (2015). By incorporating the effect of negative emissions from different bioenergy scenarios on global temperature change, they further calculate how bioenergy-based negative emissions impact species loss prevention.

## 5.5 Summary and Conclusions

As the global population increases, cropland expansion is expected to play a key role in the provision of food and energy security. However, as shown in this chapter, it can also have significant trade-offs with biodiversity. On top of food/feed cropland impacts, the expansion of energy cropland ( $2.49 \times 10^6$  km<sup>2</sup>) from implementation of second-generation bioenergy could lead to a loss of around 12,300–15,500 (7.5–9.5%) endemic species in the biodiversity hotspots, relative to 2005, whereby plants account for 94% of this loss. Across the AZE sites, 557 endangered and critically endangered species are projected to experience habitat destruction from conversion to energy cropland, with amphibians being most affected. In comparison to the baseline scenario excluding bioenergy (but including food/feed cropland expansion), 40% of endangered and critically endangered species (10 conifer and 362 vertebrate) are impacted by shifts cropland expansion due to bioenergy incorporation.

Most threatened species are located across tropical regions of Africa, Asia, and Latin America, with the largest numbers and percentages of endemic species extinctions occurring in

Madagascar and the Philippines, respectively. These countries have some of the highest levels of endemism out of all the hotspots, partly because they are island systems. However, due to increases in population size and corresponding agricultural and wood demands, these hotspots have experienced significant declines in natural forest area. Mexico contains the highest number of threatened endangered and critically endangered species in comparison to all other countries, accounting for more than half of the total species impacted by cropland expansion in North America. Without land-use regulations and commitment to conservation, the addition of a new land-use sector could lead to unsalvageable consequences for these hotspots.

REDD+ schemes are projected to significantly reduce trade-offs between bioenergy expansion and endemic species loss, resulting from the almost complete prevention of cropland expansion into forests. However, the dispersal of cropland away from forests could result in even more endangered and critically endangered species sites being affected. This shift of agriculture onto other equally biodiverse ecosystems, such as shrublands, savannas, grasslands, and pastures, is a prime example of ‘non-forest leakage’, one of the major concerns regarding REDD+. Land-use policies concerning emissions and biodiversity should therefore cover the full range of carbon-rich ecosystems.

The overall impact of a water protection policy is a small reduction in endemic species loss. Thus, globally, the greatest benefits are seen when combining REDD+ and water protection policies, with around 16,778 – 20,717 and 233-273 species prevented from extinction when applying REDD+ and water protection policies, respectively, to the bioenergy scenario. The benefits of water protection are, however, largely skewed by findings for the Caribbean Islands hotspot. On closer inspection, almost two-thirds of all hotspots undergoing extinctions result in higher species loss when water protection is applied. The largest threats occur in Coastal Forests of East Africa, Eastern Afromontane, Madagascar, and Atlantic Forest, due to larger areas of land needed for rainfed cropland. Like the REDD+ policy, implementation of a global water protection policy is complex. Site-specific understanding of how much water is needed for human and environmental use could help determine the amount (if any) available for bioenergy irrigation, thus reducing land needed for rainfed cropland in certain regions.

The assessments carried out in this chapter provide tools for evaluating potential global impacts of large-scale bioenergy expansion regarding threats to biodiversity. However, it also indicates limitations within biodiversity modelling, including availability of up-to-date species data, simplifications of complex ecological processes and environmental conditions, and difficulties

in predicting future impacts. It also highlights challenges associated with implementing conservation of non-forest land and water protection, which need to be addressed in the National Biodiversity Strategies and Action Plans (NBSAPs).

## Chapter 6 Conclusions and Future Work

### 6.1 Summary of Findings

Large-scale second-generation bioenergy deployment plays a key role in the 1.5 °C and 2 °C mitigation pathways. However, the expansion of another large land-use sector could have negative sustainability implications, and therefore may conflict with the Sustainable Development Goal (SDG) agenda. Two major concerns are the impacts of land-use changes on climate and biodiversity. Yet, with regards to bioenergy, these two areas remain relatively understudied. Using scenarios based on the SSP2 (“middle of the road”) and 1.5–2 °C pathways, this thesis has explored the potential impacts of large-scale bioenergy deployment on climate and biodiversity, with the aims of furthering knowledge of bioenergy’s role within SDGs 13: “Climate Action”, and 15: “Life on Land”.

In *Chapter 4*, the UVic Earth System Climate Model (v2.9) was used to determine climate impacts of land-use changes associated with large-scale bioenergy deployment (300EJyr<sup>-1</sup> by 2100). One of the main findings in this chapter is that the global cooling effect of substituting fossil fuel emissions via BECCS production ((–)0.44 °C by 2100) is significantly dominant over the global biogeochemical warming effect from increased LUC emissions due to bioenergy expansion ((+)0.0087 °C by 2075–2100). In addition, it takes approximately 11 years (between 2005 and 2016) for CO<sub>2</sub> savings from incorporating bioenergy to compensate the 5 GtCO<sub>2</sub> of LUC emissions produced by 2075–2100. Cooling from altered biogeophysical effects further dampens this biogeochemical warming, resulting in a small net global cooling of (–)0.0063 °C by 2075–2100, relative to 2005. Together these findings indicate that deployment of large-scale BECCS has an overall beneficial impact on global climate change over the 21<sup>st</sup> century, confirming the extensive use of BECCS in ambitious mitigation pathways.

However, at the regional scale impacts of bioenergy-induced LUC on climate become more pronounced, causing both disturbances and benefits. Biogeochemical warming responses to LUC emissions from bioenergy expansion are projected to be largest in the extratropics

(averaging at 0.016 °C by 2075–2100 relative to 2005), with signs of polar amplification occurring. However, this is partially compensated for by reductions in biogeophysical warming when compared to the control scenario excluding bioenergy. This biogeophysical warming occurs as more fossil fuel-derived CO<sub>2</sub> gases are emitted, reducing snowpack and sea ice, thus lowering albedo in the mid- to high- latitudes (particularly in the North Atlantic oceans).

In contrast, global biogeophysical cooling due to bioenergy expansion is higher in the tropics (–0.013 °C by 2075–2100 relative to 2005), with stronger patterns occurring locally near to where deforestation has occurred. This cooling is the result of effects such as increases in surface albedo, drier conditions, higher soil temperatures and reduced sensible heat fluxes, which are enhanced as deforestation increases and are specific to tropical deforestation (Longobardi et al., 2016). Regions most impacted by biogeophysical effects from bioenergy expansion are those that undergo large-scale energy and food/feed cropland expansion, namely Latin America, Central Africa, and East/Southeast Asia. In these regions, localised cooling can reach up to (–)0.090 °C (by 2075–2100 relative to 2005) due to bioenergy expansion. Though this cooling will be somewhat compensated by increases in biogeochemical warming, fluctuations in biogeophysical effects and drier conditions will likely be felt at the local level in these regions and may lead to more extreme weather such as heatwaves, droughts and extreme rainfall events (Jia et al., 2019). Further analysis indicates sensitivity of energy cropland growth to CO<sub>2</sub> concentration and climate temperature changes, whereby CO<sub>2</sub> fertilisation enhances growth across the globe, whereas temperature increases dampen this effect in the tropics.

*Chapter 5* explored the impacts of bioenergy expansion on biodiversity using two approaches: the calculation of species extinctions across biodiversity hotspots using the Endemics-Area Relationship model, and the estimation of impacted species across the Alliance for Zero Extinction (AZE) sites. In both analyses, significant trade-offs between bioenergy and biodiversity are demonstrated. Extensive habitat loss due to bioenergy expansion (0.819 x 10<sup>6</sup> km<sup>2</sup>) leads to a loss of approximately 11,600–14,500 (10.5–13%) endemic plant species and 686–1060 endemic vertebrate species (8.8–13%) across the biodiversity hotspots by 2100. In addition, 557 endangered and critically endangered AZE species are projected to experience habitat destruction from conversion to energy cropland. In comparison to the baseline scenario excluding bioenergy (but including food/feed cropland expansion), 40% of endangered and

critically endangered species (10 conifer and 362 vertebrate) are impacted by shifts in cropland expansion across the AZE sites in the bioenergy scenario.

As in the case for climate impacts, most threatened species are located across tropical regions of Africa, Asia, and Latin America. More specifically, the largest number of endemic species extinctions occur in Madagascar (6,699 species) and the largest number of endangered and critically endangered species impacted are in Mexico (87 species), as a result of large-scale bioenergy incorporation. These countries are very biodiverse and contain some of the highest levels of endemism (Madagascar) and numbers of threatened species (Mexico) across the globe. In addition, these regions are expected to undergo significant changes in biogeophysical climate effects resulting from both energy and food/feed cropland expansion (see *Chapters 3 and 4*). The expansion of bioenergy will thus require strong land-use regulation policies and commitment to conservation within these regions.

Significant losses occur across all species classes; however, conservation schemes will need to pay particular attention to plant species, which are shown to be worst affected by bioenergy expansion in this work. Plants are especially vulnerable during habitat destruction, due to their inability to disperse to new habitat patches. In addition, the significant number of plant species means that they are often overlooked during land conversion. Among the vertebrate species, amphibians are most heavily impacted by bioenergy expansion when considering both AZE and hotspot analyses. By 2100, around 272 endemic and 246 endangered and critically endangered amphibian species are projected to be lost due to bioenergy expansion. Increasingly rapid declines in amphibian species indicate the urgency for their conservation, particularly if bioenergy deployment is to progress globally.

The implementation of REDD+ and water protection schemes have, in previous work, proven to help prevent the loss of important terrestrial and freshwater ecosystems (Harvey et al., 2010; Bonsch et al., 2016; Humpenöder et al., 2018a; Morita and Matsumoto, 2018). The climate and biodiversity assessments carried out in *Chapters 4 and 5* indicate both benefits and trade-offs when incorporating these two measures alongside bioenergy expansion. As expected, incorporation of REDD+ dampens climate impacts associated with bioenergy-induced LUC, with reductions in both global biogeochemical warming (of 0.010 °C) and biogeophysical cooling (of 0.0081 °C) occurring by the end of the century. Better representation of forest distributions in the modelled interpretation of the REDD+ scenario would, however, likely exacerbate this impact. Significant benefits are predicted for endemic species loss, with around

18,700 fewer species committed to extinction across the biodiversity hotspots as a result of REDD+ incorporation. However, shifting of cropland away from forests could have dramatic consequences for endangered and critically endangered species located in non-forested, yet equally biodiverse ecosystems, such as shrublands, savannas, grasslands, and pastures.

Incorporation of a water protection scheme leads to mixed results in both climate and biodiversity assessments. Globally, its implementation has little effect on climate impacts of bioenergy expansion, resulting in a small reduction of biogeochemical warming (0.0010°C) and biogeophysical cooling (0.0024 °C) by the end of the century. However, changes in regional surface temperatures become more spread out, encompassing wider areas, due to increased land area required for rainfed cropland expansion. Similarly, regional species loss is exacerbated, with almost two-thirds of biodiversity hotspots negatively impacted by water protection. An exception to this is the Caribbean Islands hotspot, which experiences significant reductions in species loss (72%) due to declines in energy and food/feed cropland expansion. Previous work has further indicated that prohibiting irrigated energy cropland production could substantially increase food prices (de Fraiture and Wichelns, 2010; Bonsch et al., 2015). That said, globally, implementation of water protection leads to the prevention of around 253 plant and vertebrate species going extinct by 2100.

## 6.2 Contributions to Knowledge

This thesis contributes to existing knowledge in two main ways. Firstly, new methodologies have been created for projecting impacts of bioenergy expansion on two major sustainability indicators: climate regulation and biodiversity. Secondly, findings provide further knowledge of bioenergy's role within the Sustainable Development Goal (SDG) agenda, particularly with regards to SDG's 13: "Climate Action" and 15: "Life on Land".

Recent advancements in projected spatial energy cropland distributions, proposed in SSP and RCP pathways, have enabled opportunities for isolating impacts related to bioenergy expansion within these pathways. In this thesis, such distributions were portrayed by the MAgPIE scenarios, recently developed by Humpenöder et al. (2018a). For the first time, this data has been used for predicting potential impacts of bioenergy-induced land-use changes on the climate system and biodiversity habitats. The assessments shown in *Chapters 4* and *5* provide



useful methodologies for determining these impacts and can be replicated in future scenario work.

The UVic Earth System Climate Model v2.9, applied in the climate analysis (*Chapter 4*), is a model of intermediate complexity. Compared to global climate models of high complexity (e.g., HadGEM2-ES, MPI-ESM-LR), the UVic model produces outputs in much quicker timescales (though at lower resolutions). This is highly beneficial for carrying out numerous simulations at a time, thus works well with the LUCID-CMIP5 protocol analysis which requires multiple runs for the same scenario (i.e., PC and TL). This work therefore presents an effective tool for determining climate impacts of multiple bioenergy scenarios with different input parameters, such as bioenergy deployment potentials, fossil fuel emissions, global warming targets, climate sensitivity, and fossil fuel emissions. Written in the Fortran programming language, the model can also be modified to, more accurately, portray existing scenario data e.g., forest and cropland distributions.

*Chapter 5* further presents two novel approaches for determining biodiversity impacts of future bioenergy scenarios. Modifications to established statistical models have been performed to further enhance findings of species loss. To the authors knowledge, this is the first study to have incorporated proportions of primary forest species existing in secondary forest, dependant on the age of the secondary forest. Together with the use of the EAR model rather than the SAR model, this work aims to provide more accurate representations of species distributions and therefore species loss. Further, the end models generated are relatively simple and can be easily replicated for batch processing of multiple bioenergy scenarios in GIS or programming software. Overall, the methods presented in this thesis can be used as efficient tools for broadly determining the sustainability implications of bioenergy with regards to climate and biodiversity impacts. For a more in-depth understanding, regional or local level assessments will need to be carried out using finer-resolution data or field surveys. However, the global analyses shown here provide a starting point for finding key locations that need further research and conservation.

In *Chapter 1* of this thesis, an analysis of linkages between bioenergy and the sustainable development goals indicated that research into bioenergy's role within SDG's 13: "Climate Action" and 15: "Life on Land" contains significant gaps, and thus needs further work. Findings from both the literature review in *Chapter 2*, and the assessments in *Chapters 4* and *5*, provide further insight into these two areas. As discussed in Section 6.1, the results show

that land-use change for bioenergy expansion has relatively low global impacts on climate, however that regionally changes in climate become more significant and varied. Findings also demonstrate substantial loss of some of the most vulnerable and irreplaceable species across the world, due to habitat destruction for second-generation energy cropland. However, the impact of large-scale bioenergy on both climate and biodiversity is altered by the incorporation of global water protection and REDD+ policies, with dramatic changes occurring from the latter. The significant influence of REDD+ in reducing negative climate and biodiversity impacts indicates that, if implemented conscientiously, second-generation bioenergy could be a sustainable solution to combatting climate change mitigation and energy security. Contrastingly, water protection measures have the potential to somewhat increase negative impacts, though further research and site-specific understanding could prevent this.

Considering all findings, it can be deduced that the expansion of large-scale bioenergy deployment over the 21<sup>st</sup> century could *counteract* with aims in SDGs 13 (*medium confidence*), and 15 (*high confidence*), however, that this is highly dependent on the land-use policy (see **Figure 6.1**). With forest conservation policies put into place, results may be substantially more positive, though without them could lead to *cancelling* effects, which will mostly be felt at the local level.

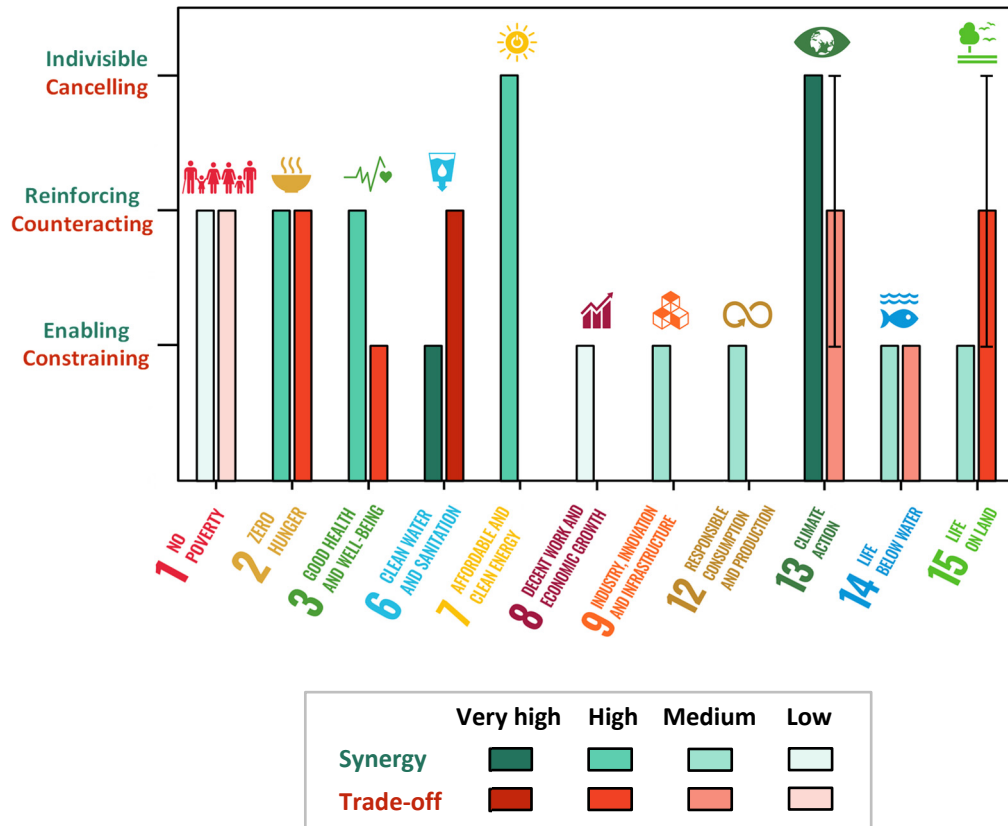


**Figure 6.1:** Findings in this study for the relationship between bioenergy expansion and SDGs 13 and 15, alongside results indicated in existing literature, as previously discussed in Chapter 1 (Figure 1.3). Overall, bioenergy expansion could counteract with aims in SDGs 13 (medium confidence), and 15 (high confidence). Length of bars indicate the strength of the synergies and trade-offs, and shading indicates confidence in impact assessments. Results other than those from this study have been taken from the works of van Leeuwen (2017), GBEP (2018), Roy et al. (2018).

### 6.3 Limitations and Future Recommendations

Findings presented in this thesis display multiple options for future work. While the assessments used here are based off peer-reviewed methods, large uncertainties indicate that there is scope for improvements. This section highlights overall limitations within climate and biodiversity modelling, as well as potential options for translating modelled outputs into policy and conservation schemes.

### 6.3.1 Modelling and Metrics

The inherent complexity and variability of climate and biodiversity dynamics makes modelling these two phenomena a challenging task. Analyses are therefore often limited to using specific indicators (e.g., species richness or abundance in biodiversity modelling), somewhat outdated data, and models that can over-simplify climate feedbacks and species distributions. Global modelling can further mask fine-scale patterns and miss important temporal dynamics and lagged effects. That said, climate and biodiversity models have made significant progress in recent years (whereby climate modelling is generally more established). Global models, in particular, can provide a broad overview of the most vulnerable regions and are thus useful for scenario work.

To further refine global outputs, this thesis focuses on certain climatic regions (i.e., the tropics and extratropics), and high priority habitat areas (i.e., the biodiversity hotspots and AZE sites). To improve on accuracy, this work uses well-regarded models and methods, such as the EAR model, the UVic model, and the LUCID-CMIP5 protocol. In addition, relatively up-to-date initialisation datasets are used, such as the HYDE 3.1 historical land cover dataset (Goldewijk et al., 2011), the AZE database (AZE, 2010), and the Conservation International biodiversity hotspot database (Mittermeier et al., 2005; Conservation International, 2011). However, further improvements can be made in both the climate and biodiversity assessments used here. As discussed in *Chapter 4*, these include better representation of present-day forest and cropland distributions, use of a higher resolution Earth system model, incorporation of cloud dynamics, and modelling of dynamic nitrogen and phosphorous cycles. Regarding the biodiversity assessment in *Chapter 5*, a wider range of biodiversity indicators and datasets could be utilised, as well as improvements made to the EAR model analysis to incorporate a larger range of land-use types and different species dispersal abilities.

Overall, findings from both the climate and biodiversity assessments indicate that future efforts and funding in modelling should be targeted towards enhancing areas such as data collection (e.g., satellite imagery, field surveys, remote sensing, and citizen science initiatives), spatial resolution and scale, species interactions and ecological processes (e.g., predator-prey relationships, nutrient cycling, species adaptability in different habitats), biogeophysical climate effects, and social and economic drivers of land-use change. The interrelated nature of

biodiversity and climate effects further highlights the importance of integrating these two fields.

### **6.3.2 Policies and Conservation Schemes**

The role of second-generation bioenergy production in addressing climate change extends beyond the traditional concept of CO<sub>2</sub> mitigation, which generally neglects local and global climate regulation services provided by land and biodiversity. This work demonstrates the overall importance of including land-based biodiversity and climate impact analyses within future bioenergy assessments, and highlights areas that need further investigation yet are lacking in current policy frameworks.

A key challenge is translating impacts found in modelling assessments into local policy actions. It is clear from this work (and previous work) that for second-generation bioenergy expansion to occur sustainably, measures to conserve forests and other natural land are required. The REDD+ initiative, created by the United Nations Framework Convention on Climate Change (UNFCCC), is a recognised tool for promoting sustainable forest practices and enhancing carbon sequestration, and is thus incorporated into many modelling studies, such as this work. However, as previously discussed, REDD+ primarily focuses on reduction of greenhouse gas emissions, often overlooking the broader range of ecosystem services provided by forests, including biodiversity conservation, water regulation, soil protection, and cultural values. Future work could therefore focus on integrating these other non-carbon benefits into REDD+ initiatives and modelling analyses to enhance the overall resilience of forest ecosystems.

The inherent nature of REDD+ means that biogeophysical effects of forests are generally ignored in policies and conservation schemes incorporating this initiative. It is becoming increasingly clear through both local and global model assessments that biogeophysical effects of forest cover can contribute significantly to solving local adaptation challenges, such as extreme heat and flooding, at all latitudes. However, lack of simple calculation metrics and uncertainties in estimates have delayed progress in implementing these effects within UNFCCC targets. Ideally, biogeophysical effects should be included in future scenario assessments incorporating bioenergy, as well as within Nationally Determined Contributions (NDCs) provided by individual countries each year. They could also be used, alongside REDD+ and water protection analyses as evidence to indicate priority regions within countries

National Biodiversity Strategies and Action Plans (NBSAPs), and ultimately strengthen conservation schemes for different countries.

Cropland ‘leakage’ resulting in unintended loss of forest or other biodiverse- and carbon-rich land is another concern when implementing REDD+, as demonstrated in *Chapter 5*. However, REDD+ and biodiversity conservation can be mutually reinforcing if implemented carefully. For instance, landscape-level planning can be used to identify priority areas for REDD+ activities that also have high biodiversity value. This would incorporate not only forest land but the full range of carbon-rich ecosystems (A. Popp, Humpenöder, et al., 2014). Environmental and social safeguards set out by the UNFCCC framework need to also be enforced, ensuring the conservation of biodiversity while including the participation of local communities and indigenous people. Financial mechanisms and incentives play a crucial role in promoting the cooperation between REDD+ and biodiversity conservation. These include grants for local communities, incorporation of co-benefit indicators into financial rewards, dedicated funding streams specifically focused on biodiversity conservation, and assigning economic value to biodiversity benefits (IPBES, 2019).

Accounting for both climate and biodiversity impacts of land-use change is imperative for effective conservation and sustainable management of natural resources. The expansion of second-generation bioenergy will require a careful balance of efforts in these two areas, and consistent monitoring and reporting systems that assess both carbon emissions and biodiversity conservation outcomes of corresponding changes in and preservation of land cover. A multi land-use approach will also be needed to integrate bioenergy expansion alongside REDD+, water protection, and biodiversity conservation. Examples of this include promoting agroforestry systems, sustainable forest management, increasing irrigation efficiency, and establishing protected areas or wildlife corridors within REDD+ project areas. Countries across the globe have indicated commitment to this approach e.g., Indonesia’s national REDD+ strategy (Masripatin et al., 2021), Costa Rica’s PES program (Malavasi and Kellenberg, 2002), Brazil’s Amazon Fund (Ferraz et al., 2023), and Sweden and Finland’s sustainable forest management schemes (IRENA, 2019), with 65 countries currently signed up to the UN-REDD Programme, and certification systems such as the Roundtable on Sustainable Biofuel (RSB) and Forest Stewardship Council (FSC) helping to execute these commitments (see *Chapter 2*, Section 2.5.1). However, land prioritisation is complex and continuous development of

identification methods, including bottom-up processes (e.g., engaging stakeholders) as well as local to global modelling, is needed to provide robust evidence for these schemes.

Furthermore, initiatives protecting freshwater ecosystems from degradation due to bioenergy production need to be designed, in which trade-offs between ecosystems and economic incentives opposing sustainable water use are covered (see Section 2.5.2). Most land conservation schemes (in addition to the Alliance for Water Stewardship) incorporate water conservation to varying degrees, with many incentivising rainfed bioenergy production. However, as demonstrated in this work, this can lead to complications with displaced deforestation, and thus further threats to biodiversity and local climate regulation. Site-specific understanding of human and environmental water consumption, increased irrigation efficiency through improvements in water storage and transport, and better land management practices can help increase crop yields and reduce the need for large areas of rainfed cropland.

It is important to note that climate change and biodiversity are interconnected, whereby changes to one can have dramatic consequences for the other. Integrating biodiversity and climate change within conservation planning and policy has become increasingly acknowledged in various international frameworks, such as the Convention on Biological Diversity (CBD) and the UNFCCC, which have called for coordinated actions (UNFCCC et al., 2022). Modelling of this integration has also become more advanced. For instance, the concept of climate-smart conservation assesses the vulnerability of species and ecosystems to climate change and implements adaptive management strategies (Stein et al., 2014).

Despite limitations and divergence in modelling assessments, an overall picture is appearing in which a few regions, particularly in the tropics, are consistently emphasized as priorities for biodiversity conservation and climate regulation. It is thus important that the global donor community channel efforts to these regions, with much finer scale analysis needed for immediate effects.

## 6.4 Closing Comments

Without a complete assessment of all aims within the SDG agenda, it is impossible to determine the overall sustainability of bioenergy expansion. However, this thesis provides further insight into the role of bioenergy in achieving SDGs 13: “Climate Action”, and 15: “Life on Land”. In addition, it highlights areas most at risk and in need of continued conservation policies.

Conflicts may also occur with multiple other sustainability criteria not accounted for in this study, such as food security, health, air quality and economic growth, though, uncertainties around environmental impacts remain the largest.

Some trade-offs are inevitable but, as discussed, in many cases negative impacts can be mitigated or reduced through careful planning and conservation. Increasing crop yields and use of wastes and residues, improving conversion efficiencies, and developing advanced biotechnologies could further help alleviate these issues (Henry et al., 2018). Carbon dioxide removal technologies, such as BECCS, will be required, though to be effective should be implemented imminently. In addition, international trade may be needed to support a global bioeconomy. For such large changes to occur, strong institutional and economic structures will need to be put in place, domestically and internationally (Fuss et al., 2014; Muratori et al., 2016; Fridahl and Lehtveer, 2018).

Despite the key role of BECCS in future mitigation pathways, acceptability of bioenergy is low compared to other renewable energy sources such as solar and wind (Poortinga et al., 2013; Peterson et al., 2015; Ma et al., 2015; EPCC, 2017). Successful implementation of BECCS will depend on government intervention to support both bioenergy and CCS. Demand side incentives could create a market for second-generation bioenergy, however, the final decision to plant energy cropland comes down to individual landowner preferences, with the help of financial incentives and guaranteed support. Bridging gaps in knowledge between scientific research, policy frameworks, and end land-use decisions will ultimately lead to a better understanding of sustainable bioenergy practices.



## References

- Aatola, H., Larmi, M., Sarjovaara, T. and Mikkonen, S. 2009. Hydrotreated vegetable Oil (HVO) as a renewable diesel fuel: Trade-off between NO<sub>x</sub>, particulate emission, and fuel consumption of a heavy duty engine. *SAE International Journal of Engines*. **1**(1), pp.1251–1262.
- Abdenur, A.E. 2022. *The Glasgow Leaders' Declaration on Forest: Déjà Vu or Solid Restart?* United Nations University, New York.
- Achten, W.M.J. and Verchot, L. V. 2011. Implications of biodiesel-induced land-use changes for CO<sub>2</sub> emissions: Case studies in Tropical America, Africa, and Southeast Asia. *Ecology and Society*. **16**(4).
- Ahlgren, S. and Di Lucia, L. 2016. Indirect land use changes of biofuel production – a review of modelling efforts and policy developments in the European Union. *Biotechnology for Biofuels*. **9**(1), pp.1–10.
- Ahlswede, B.J. and Thomas, R.Q. 2017. Community earth system model simulations reveal the relative importance of afforestation and forest management to surface temperature in Eastern North America. *Forests*. **8**(12).
- Ai, Z., Hanasaki, N., Heck, V., Hasegawa, T. and Fujimori, S. 2021. Global bioenergy with carbon capture and storage potential is largely constrained by sustainable irrigation. *Nature Sustainability*. **4**(10), pp.884–891.
- Alexander, K. and Easterbrook, S.M. 2015. The software architecture of climate models: a graphical comparison of CMIP5 and EMICAR5 configurations. *Geoscientific Model Development*. **8**(4), pp.1221–1232.
- Alexandratos, N. and Bruinsma, J. 2012. *World agriculture towards 2030/2050: the 2012 revision* [Online]. Available from: <http://www.fao.org/economic/esa>.
- Alkama, R. and Cescatti, A. 2016. Climate change: Biophysical climate impacts of recent changes in global forest cover. *Science*. **351**(6273), pp.600–604.
- Alkemade, R., Van Oorschot, M., Miles, L., Nellemann, C., Bakkenes, M. and Ten Brink, B. 2009. GLOBIO3: A framework to investigate options for reducing global terrestrial biodiversity loss. *Ecosystems*. **12**(3), pp.374–390.
- Alkemade, R., Reid, R.S., Van Den Berg, M., De Leeuw, J. and Jeuken, M. 2013. Assessing the impacts of livestock production on biodiversity in rangeland ecosystems. *Proceedings of the National Academy of Sciences of the United States of America*. **110**(52), pp.20900–20905.
- Allnutt, T.F., Ferrier, S., Manion, G., Powell, G.V.N., Ricketts, T.H., Fisher, B.L., Harper, G.J., Irwin, M.E., Kremen, C., Labat, J.-N., Lees, D.C., Pearce, T.A. and Rakotondrainibe, F. 2008. A method for quantifying biodiversity loss and its application to a 50-year record of deforestation across Madagascar. *Conservation Letters*. **1**(4), pp.173–181.
- Anderson, C.J., Anex, R.P., Arritt, R.W., Gelder, B.K., Khanal, S., Herzmann, D.E. and Gassman, P.W. 2013. Regional climate impacts of a biofuels policy projection. *Geophysical Research Letters*. **40**(6), pp.1217–1222.
- Apps, J.A., Zheng, L., Zhang, Y., Xu, T. and Birkholzer, J.T. 2010. Evaluation of potential changes in groundwater quality in response to CO<sub>2</sub> leakage from deep geologic storage.

- Transport in Porous Media*. **82**(1), pp.215–246.
- Aratrakorn, S., Thunhikorn, S. and Donald, P.F. 2006. Changes in bird communities following conversion of lowland forest to oil palm and rubber plantations in southern Thailand. *Bird Conservation International*. **16**(1), pp.71–82.
- Arias, P.A., Bellouin, N., Coppola, E., Jones, R.G., Krinner, G., Marotzke, J., Naik, V., Palmer, M.D., Plattner, G.-K., Rogelj, J., Rojas, M., Sillmann, J., Storelvmo, T., Thorne, P.W. and Trewin, B. 2021. *Technical Summary*. In *Climate Change 2021: The Physical Science Basis. Contribution of Working Group I to the Sixth Assessment Report of the Intergovernmental Panel on Climate Change [V. Masson-Delmotte et al (eds.)]*. Cambridge University Press, Cambridge, United Kingdom and New York, NY, USA.
- Arndt, C., Msangi, S. and Thurlow, J. 2010. Are Biofuels good for African Development?
- Arora, V.K. and Boer, G.J. 2010. Uncertainties in the 20th century carbon budget associated with land use change. *Global Change Biology*. **16**(12), pp.3327–3348.
- Arora, V.K., Katavouta, A., Williams, R.G., Jones, C.D., Brovkin, V., Friedlingstein, P., Schwinger, J., Bopp, L., Boucher, O., Cadule, P., Chamberlain, M.A., Christian, J.R., Delire, C., Fisher, R.A., Hajima, T. and ... 2020. Carbon-concentration and carbon-climate feedbacks in CMIP6 models. *Biogeosciences*. **17**(16), pp.4173–4222.
- Arora, V.K., Scinocca, J.F., Boer, G.J., Christian, J.R., Denman, K.L., Flato, G.M., Kharin, V. V., Lee, W.G. and Merryfield, W.J. 2011. Carbon emission limits required to satisfy future representative concentration pathways of greenhouse gases. *Geophysical Research Letters*. **38**(5), pp.3–8.
- Arrhenius, O. 1921. Species and Area. *Journal of Ecology*. **9**(1), pp.95–99.
- Asher, C. 2019. Brazil's New Forest Code puts vast areas of protected Amazon forest at risk. *Mongobay*. [Online]. Available from: <https://news.mongabay.com/2019/03/brazils-new-forest-code-puts-vast-areas-of-protected-amazon-forest-at-risk/>.
- Ashworth, K., Folberth, G., Hewitt, C.N. and Wild, O. 2012. Impacts of near-future cultivation of biofuel feedstocks on atmospheric composition and local air quality. *Atmospheric Chemistry and Physics*. **12**(2), pp.919–939.
- Ashworth, P., Bradbury, J., Wade, S., Ynke Feenstra, C.F.J., Greenberg, S., Hund, G. and Mikunda, T. 2012. What's in store: Lessons from implementing CCS. *International Journal of Greenhouse Gas Control*. **9**, pp.402–409.
- Atchley, A.L., Maxwell, R.M. and Navarre-Sitchler, A.K. 2013. Human health risk assessment of CO<sub>2</sub> leakage into overlying aquifers using a stochastic, geochemical reactive transport approach. *Environmental Science and Technology*. **47**(11), pp.5954–5962.
- Atmadja, S. and Verchot, L. 2012. A review of the state of research, policies and strategies in addressing leakage from reducing emissions from deforestation and forest degradation (REDD+). *Mitigation and Adaptation Strategies for Global Change*. **17**(3), pp.311–336.
- Avitabile, V., Herold, M., Heuvelink, G.B.M., Lewis, S.L., Phillips, O.L., Asner, G.P., Armston, J., Ashton, P.S., Banin, L., Bayol, N., Berry, N.J., Boeckx, P., de Jong, B.H.J., Devries, B. and ... 2016. An integrated pan-tropical biomass map using multiple reference datasets. *Global Change Biology*. **22**(4), pp.1406–1420.
- AZE 2010. Alliance for Zero Extinction (AZE) (2010). AZE Update. Available from: [www.zeroextinction.org](http://www.zeroextinction.org).
- Azevedo, A.A., Rajão, R., Costa, M.A., Stabile, M.C.C., Macedo, M.N., Dos Reis, T.N.P., Alencar, A., Soares-Filho, B.S. and Pacheco, R. 2017. Limits of Brazil's Forest Code as

- a means to end illegal deforestation. *Proceedings of the National Academy of Sciences of the United States of America*. **114**(29), pp.7653–7658.
- De Baan, L., Mutel, C.L., Curran, M., Hellweg, S. and Koellner, T. 2013. Land use in life cycle assessment: Global characterization factors based on regional and global potential species extinction. *Environmental Science and Technology*. **47**(16), pp.9281–9290.
- Baccini, A., Goetz, S.J., Walker, W.S., Laporte, N.T., Sun, M., Sulla-Menashe, D., Hackler, J., Beck, P.S.A., Dubayah, R., Friedl, M.A., Samanta, S. and Houghton, R.A. 2012. Estimated carbon dioxide emissions from tropical deforestation improved by carbon-density maps. *Nature Climate Change*. **2**(3), pp.182–185.
- Baccini, A., Walker, W., Carvalho, L., Farina, M. and Houghton, R.A. 2017. Tropical forests are a net carbon source based on aboveground measurements of gain and loss. *Science*. **358**, pp.230–234.
- Bailey, R. 2013. *The Handbook of Global Energy Policy, Chapter 16: The “Food Versus Fuel” Nexus*.
- Bailis, R.E. and Baka, J.E. 2010. Greenhouse gas emissions and land use change from *Jatropha curcas*-based jet fuel in Brazil. *Environmental Science and Technology*. **44**(22), pp.8684–8691.
- Bala, G., Caldeira, K., Wickett, M., Phillips, T.J., Lobell, D.B., Delire, C. and Mirin, A. 2007. Combined climate and carbon-cycle effects of large-scale deforestation. *Proceedings of the National Academy of Sciences*. **104**(16), pp.6550–6555.
- Barbier, E.B., Burgess, J.C., Economics, S.L., May, N., Barbier, E.B. and Burgess, J.C. 1997. *The Economics of Tropical Forest Land Use Options* Published by: University of Wisconsin Press Stable URL : <https://www.jstor.org/stable/3147281> The Economics of Tropical Forest Land Use Options. . **73**(2), pp.174–195.
- Bárcena, T.G., Kiær, L.P., Vesterdal, L., Stefánsdóttir, H.M., Gundersen, P. and Sigurdsson, B.D. 2014. Soil carbon stock change following afforestation in Northern Europe: A meta-analysis. *Global Change Biology*. **20**(8), pp.2393–2405.
- Barlow, J., Gardner, T.A., Araujo, I.S., Avila-Pires, T.C., Bonaldo, A.B., Costa, J.E., Esposito, M.C., Ferreira, L. V., Hawes, J., Hernandez, M.I.M., Hoogmoed, M.S., Leite, R.N., Loman-Hung, N.F., Malcolm, J.R., Martins, M.B. and ... 2007. Quantifying the biodiversity value of tropical primary, secondary, and plantation forests. *Proceedings of the National Academy of Sciences*. **104**(47), pp.18555–18560.
- Barnes, A.D., Jochum, M., Mumme, S., Haneda, N.F., Farajallah, A., Widarto, T.H. and Brose, U. 2014. Consequences of tropical land use for multitrophic biodiversity and ecosystem functioning. *Nature Communications*. **5**, pp.1–7.
- Barney, J. 2012. Best Management Practices for bioenergy crops: reducing the invasion risk. , pp.1–8.
- Barney, J.N. 2014. Bioenergy and Invasive Plants: Quantifying and Mitigating Future Risks. *Invasive Plant Science and Management*. **7**(2), pp.199–209.
- Barthlott, W., Lauer, W. and Placke, A. 1996. Global distribution of species diversity in vascular plants: Towards a world map of phytodiversity. *Erdkunde*. **50**, pp.317–327.
- Bashkin, M.A. and Binkley, D.A.N. 2017. Changes in Soil Carbon following Afforestation in Hawaii Author ( s ): Michael A . Bashkin and Dan Binkley Published by : Wiley on behalf of the Ecological Society of America Stable URL : <https://www.jstor.org/stable/176582> REFERENCES Linked references ar. . **79**(3), pp.828–833.

- Bathiany, S., Claussen, M., Brovkin, V., Raddatz, T. and Gayler, V. 2010. Combined biogeophysical and biogeochemical effects of large-scale forest cover changes in the MPI earth system model. *Biogeosciences*. **7**(5), pp.1383–1399.
- Bauer, N., Baumstark, L. and Leimbach, M. 2012. The REMIND-R model: The role of renewables in the low-carbon transformation-first-best vs. second-best worlds. *Climatic Change*. **114**(1), pp.145–168.
- Bayrak, M.M. and Marafa, L.M. 2016. Ten years of REDD+: A critical review of the impact of REDD+ on forest-dependent communities. *Sustainability (Switzerland)*. **8**(7), pp.1–22.
- Beaumont, L.J., Pitman, A., Perkins, S., Zimmermann, N.E., Yoccoz, N.G. and Thuiller, W. 2011. Impacts of climate change on the world's most exceptional ecoregions. *Proceedings of the National Academy of Sciences of the United States of America*. **108**(6), pp.2306–2311.
- Beca, G., Vancine, M.H., Carvalho, C.S., Pedrosa, F., Alves, R.S.C., Buscariol, D., Peres, C.A., Ribeiro, M.C. and Galetti, M. 2017. High mammal species turnover in forest patches immersed in biofuel plantations. *Biological Conservation*. **210**, pp.352–359.
- Behrman, K.D., Juenger, T.E., Kiniry, J.R. and Keitt, T.H. 2015. Spatial land use trade-offs for maintenance of biodiversity, biofuel, and agriculture. *Landscape Ecology*. **30**(10), pp.1987–1999.
- Bellard, C., Bertelsmeier, C., Leadley, P., Thuiller, W. and Courchamp, F. 2012. Impacts of climate change on the future of biodiversity. *Ecology Letters*. **15**(4), pp.365–377.
- Bellard, C., Leclerc, C., Leroy, B., Bakkenes, M., Veloz, S., Thuiller, W. and Courchamp, F. 2014. Vulnerability of biodiversity hotspots to global change. *Global Ecology and Biogeography*. **23**(12), pp.1376–1386.
- Bennett, E.M., Carpenter, S.R. and Caraco, N.F. 2001. Human impact on erodable phosphorus and eutrophication: A global perspective. *BioScience*. **51**(3), pp.227–234.
- Benton, T.G., Vickery, J.A. and Wilson, J.D. 2003. Farmland biodiversity: Is habitat heterogeneity the key? *Trends in Ecology and Evolution*. **18**(4), pp.182–188.
- Bergl, R.A., Oates, J.F. and Fotso, R. 2007. Distribution and protected area coverage of endemic taxa in West Africa's Biafran forests and highlands. *Biological Conservation*. **134**(2), pp.195–208.
- Beringer, T., Lucht, W. and Schaphoff, S. 2011. Bioenergy production potential of global biomass plantations under environmental and agricultural constraints. *GCB Bioenergy*. **3**(4), pp.299–312.
- Berndes, G. 2002. Bioenergy and water — the implications of large-scale bioenergy production for water use and supply. *Global Environmental Change*. **12**, pp.253–271.
- Betts, R. 2001. Biogeophysical impacts of land use on present-day climate: near-surface temperature change and radiative forcing. *Atmospheric Science Letters*. **2**(1–4), pp.39–51.
- Betts, R. a., Falloon, P.D., Goldewijk, K.K. and Ramankutty, N. 2007. Biogeophysical effects of land use on climate: Model simulations of radiative forcing and large-scale temperature change. *Agricultural and Forest Meteorology*. **142**(2–4), pp.216–233.
- Biomass Technology Group 2008. *Sustainability Criteria & Certification Systems for Biomass Production* [Online]. Enschede, Netherlands. Available from: [http://ec.europa.eu/energy/renewables/bioenergy/doc/sustainability\\_criteria\\_and\\_certification\\_systems.pdf](http://ec.europa.eu/energy/renewables/bioenergy/doc/sustainability_criteria_and_certification_systems.pdf).

- BIP 2010. *Guidance for National Biodiversity Indicator Development and Use* [Online]. Biodiversity Indicators Partnership, Cambridge. Available from: [www.bipnational.net](http://www.bipnational.net).
- BirdLife International 2022. Data Zone: Species distribution data request. *BirdLife International*. [Online]. Available from: <http://datazone.birdlife.org/species/requestdis>.
- Bodirsky, B.L., Popp, A., Lotze-Campen, H., Dietrich, J.P., Rolinski, S., Weindl, I., Schmitz, C., Müller, C., Bonsch, M., Humpenöder, F., Biewald, A. and Stevanovic, M. 2014. Reactive nitrogen requirements to feed the world in 2050 and potential to mitigate nitrogen pollution. *Nature Communications*. **5**.
- Bodirsky, B.L., Rolinski, S., Biewald, A., Weindl, I., Popp, A. and Lotze-Campen, H. 2015. Global Food Demand Scenarios for the 21st Century. *PLoS ONE*. **10**(11).
- Bonan, G.B., Pollard, D. and Thompson, S.L. 1992. Effects of Boreal Forest Vegetation on Global Climate. *Nature*. **359**(6397), pp.716–718.
- Bondeau, A., Smith, P. and Zaehle, S. 2007. Modelling the role of agriculture for the 20th century global terrestrial carbon balance. *Global Change Biology*. **13**, pp.679–706.
- Bonsch, M. 2015. *Land and water for agriculture - future prospects and trade-offs*. Technical University of Berlin, Berlin, Germany.
- Bonsch, M., Humpenöder, F., Popp, A., Bodirsky, B., Dietrich, J.P., Rolinski, S., Biewald, A., Lotze-Campen, H., Weindl, I., Gerten, D. and Stevanovic, M. 2016. Trade-offs between land and water requirements for large-scale bioenergy production. *GCB Bioenergy*. **8**(1), pp.11–24.
- Bonsch, M., Popp, A., Biewald, A., Rolinski, S., Schmitz, C., Weindl, I., Stevanovic, M., Högner, K., Heinke, J., Ostberg, S., Dietrich, J.P., Bodirsky, B., Lotze-Campen, H. and Humpenöder, F. 2015. Environmental flow provision: Implications for agricultural water and land-use at the global scale. *Global Environmental Change*. **30**, pp.113–132.
- Botello, F., Sarkar, S. and Sánchez-Cordero, V. 2015. Impact of habitat loss on distributions of terrestrial vertebrates in a high-biodiversity region in Mexico. *Biological Conservation*. **184**, pp.59–65.
- Bounoua, L., DeFries, R., Collatz, G.J., Sellers, P. and Khan, H. 2002. Effects of land cover conversion on surface climate. *Clim. Change*. **52**, pp.29–64.
- Bouwman, A.F., Beusen, A.H.W. and Billen, G. 2009. Human alteration of the global nitrogen and phosphorus soil balances for the period 1970–2050. *Global Biogeochemical Cycles*. **23**(4).
- Bovo, A.A. de A., Magioli, M., Percequillo, A.R., Kruszynski, C., Alberici, V., Mello, M.A.R., Correa, L.S., Gebin, J.C.Z., Ribeiro, Y.G.G., Costa, F.B., Ramos, V.N., Benatti, H.R., Lopes, B., Martins, M.Z.A., Diniz-Reis, T.R. and ... 2018. Human-modified landscape acts as refuge for mammals in atlantic forest. *Biota Neotropica*. **18**(2).
- Boysen, L.R., Brovkin, V., Arora, V.K., Cadule, P., De Noblet-Ducoudré, N., Kato, E., Pongratz, J. and Gayler, V. 2014. Global and regional effects of land-use change on climate in 21st century simulations with interactive carbon cycle. *Earth System Dynamics*. **5**(2), pp.309–319.
- Boysen, L.R., Brovkin, V., Pongratz, J., Lawrence, D.M., Lawrence, P., Vuichard, N., Peylin, P., Liddicoat, S., Hajima, T., Zhang, Y., Rocher, M., Delire, C., Séférian, R., Arora, V.K., Nieradzick, L., Anthoni, P., Thiery, W., Laguë, M.M., Lawrence, D. and Lo, M.H. 2020. Global climate response to idealized deforestation in CMIP6 models. *Biogeosciences*. **17**(22), pp.5615–5638.

- Bracmort, K. 2014. *The Renewable Fuel Standard (RFS): Cellulosic Biofuels* [Online]. Congressional Research Service, US. Available from: [www.crs.gov](http://www.crs.gov).
- Brando, P., Trumbore, S., Silvério, D., Macedo, M., Beck, P. and Coe, M. 2016. Climate impacts of expanded soy agriculture in the arc of deforestation in Brazil. *Geophysical Research Abstracts*. **18**, pp.10631–1.
- Bright, R.M. 2015. Metrics for biogeophysical climate forcings from land use and land cover changes and their inclusion in life cycle assessment: A critical review. *Environmental Science and Technology*. **49**(6), pp.3291–3303.
- Bright, R.M., Davin, E., O'Halloran, T., Pongratz, J., Zhao, K. and Cescatti, A. 2017. Local temperature response to land cover and management change driven by non-radiative processes. *Nature Climate Change*. **7**(4), pp.296–302.
- Brooks, T.M., Mittermeier, R.A., da Fonseca, G.A.B., Gerlach, J., Hoffmann, M., JLamoreux, J.F., Mittermeier, C.G., Pilgrim, J.D. and Rodrigues, A.S.L. 2006. Global Biodiversity Conservation Priorities. *Science*. **313**, pp.58–62.
- Brooks, T.M., Mittermeier, R.A., Mittermeier, C.G., da Fonseca, G.A.B., Rylands, A.B., Konstant, W.R., Flick, P., Pilgrim, J., Oldfield, S., Magin, G. and Hilton-Taylor, C. 2002. Habitat Loss and Extinction in the Hotspots of Biodiversity. *Conservation Biology*. **16**(4), pp.909–923.
- Broucke, S. Vanden, Luyssaert, S., Davin, E.L., Janssens, I. and Lipzig, N. van 2015. New insights in the capability of climate models to simulate the impact of LUC based on temperature decomposition of paired site observations. *Journal of Geophysical Research: Atmospheres*. **120**(11), pp.5417–5436.
- Brovkin, V., Boysen, L., Arora, V.K., Boisier, J.P., Cadule, P., Chini, L., Claussen, M., Friedlingstein, P., Gayler, V., Van den hurk, B.J.J.M., Hurtt, G.C., Jones, C.D., Kato, E., De noblet-ducoudre, N., Pacifico, F., Pongratz, J. and Weiss, M. 2013. Effect of anthropogenic land-use and land-cover changes on climate and land carbon storage in CMIP5 projections for the twenty-first century. *Journal of Climate*. **26**(18), pp.6859–6881.
- Brovkin, V., Claussen, M., Driesschaert, E., Fichet, T., Kicklighter, D., Loutre, M.F., Matthews, H.D., Ramankutty, N., Schaeffer, M. and Sokolov, A. 2006. Biogeophysical effects of historical land cover changes simulated by six Earth system models of intermediate complexity. *Climate Dynamics*. **26**(6), pp.587–600.
- Brovkin, V., Ganopolski, A., Claussen, M., Kubatzki, C. and Petoukhov, V. 1999. Modelling climate response to historical land cover change. *Global Ecology and Biogeography*. **8**(6), pp.509–517.
- Brovkin, V., Ganopolski, A. and Svirezhev, Y. 1997. A continuous climate-vegetation classification for use in climate-biosphere studies. *Ecological Modelling*. **101**, pp.251–261.
- Brovkin, V., Pugh, T., Robertson, E., Bathiany, S., Jones, C. and Arneeth, A. 2015. Cooling biogeophysical effect of large-scale tropical deforestation in three Earth System models. *EGU General Assembly Conference Abstracts*. **17**(8903).
- Brovkin, V., Raddatz, T., Reick, C.H., Claussen, M. and Gayler, V. 2009. Global biogeophysical interactions between forest and climate. *Geophysical Research Letters*. **36**(7), pp.1–5.
- Bruinsma, J. 2003. *Crop Production and Natural Resource Use. In: World Agriculture: Towards 2015/2030, An FAO Perspective*.

- Brutsaert, W. 1982. *Evaporation into the Atmosphere*. Boston: D. Reidel.
- Buchanan, G.M., Butchart, S.H.M., Dutson, G., Pilgrim, J.D., Steininger, M.K., Bishop, K.D. and Mayaux, P. 2008. Using remote sensing to inform conservation status assessment: Estimates of recent deforestation rates on New Britain and the impacts upon endemic birds. *Biological Conservation*. **141**, pp.56–66.
- Butchart, S.H.M., Walpole, M., Collen, B., Van Strien, A., Scharlemann, J.P.W., Almond, R.E.A., Baillie, J.E.M., Bomhard, B., Brown, C., Bruno, J., Carpenter, K.E., Carr, G.M., Chanson, J., Chenery, A.M., Csirke, J. and ... 2010. Global biodiversity: Indicators of recent declines. *Science*. **328**(5982), pp.1164–1168.
- Butler, R.A. 2016. The top 10 most biodiverse countries. *Mongabay*. [Online]. Available from: <https://news.mongabay.com/2016/05/top-10-biodiverse-countries/>.
- Cacho, J.F., Negri, M.C., Zumpf, C.R. and Campbell, P. 2018. Introducing perennial biomass crops into agricultural landscapes to address water quality challenges and provide other environmental services. *Wiley Interdisciplinary Reviews: Energy and Environment*. **7**(2), pp.1–11.
- Caiazzo, F., Malina, R., Staples, M.D., Wolfe, P.J., Yim, S.H.L. and Barrett, S.R.H. 2014. Quantifying the climate impacts of albedo changes due to biofuel production: a comparison with biogeochemical effects. *Environmental Research Letters*. **9**(2), pp.1–10.
- Calvin, K., Wise, M., Kyle, P., Patel, P., Clarke, L. and Edmonds, J. 2014. Trade-offs of different land and bioenergy policies on the path to achieving climate targets. *Climatic Change*. **123**(3–4), pp.691–704.
- Canadell, J.G., Kirschbaum, M.U.F., Kurz, W.A., Sanz, M.J., Schlamadinger, B. and Yamagata, Y. 2007. Factoring out natural and indirect human effects on terrestrial carbon sources and sinks. *Environmental Science and Policy*. **10**(4), pp.370–384.
- Canadell, J.G., Monteiro, P.M.S., Costa, M.H., Cotrim da Cunha, L., Cox, P.M., Eliseev, A. V., Henson, S., Ishii, M., Jac- card, S., Koven, C., Lohila, A., Patra, P.K., Piao, S., Rogelj, J., Syampungani, S., Zaehle, S. and Zickfeld, K. 2022. *Global Carbon and other Biogeochemical Cycles and Feedbacks, in: Climate Change 2021: The Physical Science Basis, Contribution of Working Group I to the Sixth Assessment Report of the Intergovernmental Panel on Climate Change, edited by: Masson- Delmotte,*. Cambridge.
- Canadell, J.G. and Schulze, E.D. 2014. Global potential of biospheric carbon management for climate mitigation. *Nature Communications*. **5**(1), pp.1–12.
- Cantrell, K.B., Ducey, T., Ro, K.S. and Hunt, P.G. 2008. Livestock waste-to-bioenergy generation opportunities. *Bioresource Technology*. **99**(17), pp.7941–7953.
- Cantú, C., Wright, R.G., Scott, J.M. and Strand, E. 2004. Assessment of current and proposed nature reserves of Mexico based on their capacity to protect geophysical features and biodiversity. *Biological Conservation*. **115**(3), pp.411–417.
- Cardona, C.A., Quintero, J.A. and Paz, I.C. 2010. Production of bioethanol from sugarcane bagasse: Status and perspectives. *Bioresource Technology*. **101**(13), pp.4754–4766.
- Carlson, K.M., Curran, L.M., Ratnasari, D., Pittman, A.M., Soares-Filho, B.S., Asner, G.P., Trigg, S.N., Gaveau, D.A., Lawrence, D. and Rodrigues, H.O. 2012. Committed carbon emissions, deforestation, and community land conversion from oil palm plantation expansion in West Kalimantan, Indonesia. *Proceedings of the National Academy of Sciences of the United States of America*. **109**(19), pp.7559–7564.
- Carpenter, S.R., Caraco, N.F., Correll, D.L., Howarth, R.W., Sharpley, A.N. and Smith, V.H.

1998. Nonpoint Pollution of Surface Waters with Phosphorus and Nitrogen. *Ecological Applications*. **8**(3), pp.559–568.
- Carvalhais, N., Forkel, M., Khomik, M., Bellarby, J., Jung, M., Migliavacca, M., Mingquan, M., Saatchi, S., Santoro, M., Thurner, M., Weber, U., Ahrens, B., Beer, C., Cescatti, A., Randerson, J.T. and Reichstein, M. 2014. Global covariation of carbon turnover times with climate in terrestrial ecosystems. *Nature*. **514**, pp.213–217.
- Carvalho, F.M.V., De Marco, P. and Ferreira, L.G. 2009. The Cerrado into-pieces: Habitat fragmentation as a function of landscape use in the savannas of central Brazil. *Biological Conservation*. **142**(7), pp.1392–1403.
- Casson, A. 2003. *Oil palm, soybeans and critical habitat loss*. WWF Forest Conversion Initiative, Switzerland.
- CBD 2010. *Global Biodiversity Outlook 3* [Online]. Secretariat of the Convention on Biological Diversity, Montreal, Quebec, Canada. Available from: <https://www.cbd.int/gbo3>.
- CBD 2023. National Biodiversity Strategies and Action Plans (NBSAPs). *Convention on Biological Diversity*. [Online]. Available from: <https://www.cbd.int/nbsap/>.
- CCS Norway 2020. Longship CCS. *Fortum Oslo Varme*. [Online]. Available from: <https://ccsnorway.com/>.
- Chagnon, F.J.F., Bras, R.L. and Wang, J. 2004. Climatic shift in patterns of shallow clouds over the Amazon. *Geophysical Research Letters*. **31**(24), pp.1–4.
- Chang, Y., Li, G., Yao, Y., Zhang, L. and Yu, C. 2016. Quantifying the water-energy-food nexus: Current status and trends. *Energies*. **9**(2), pp.1–17.
- Chase, T.N., Pielke, R.A., Kittel, S. á T.G.F., Nemani, R.R. and Running, S.W. 2000. Simulated impacts of historical land cover changes on global climate in northern winter. *Climate Dynamics*. **16**, pp.93–105.
- Chase, T.N., Sr, R.A.P., Kittel, T.G.F.M., Pitman, A.J., Running, S.W. and Nemani, R.R. 2001. Relative climatic effects of landcover change and A comparison of model results and observations. . **106**, pp.685–691.
- Chaudhary, A. and Brooks, T.M. 2018. Land Use Intensity-Specific Global Characterization Factors to Assess Product Biodiversity Footprints. *Environmental Science and Technology*. **52**(9), pp.5094–5104.
- Chaudhary, A. and Mooers, A.O. 2017. Biodiversity loss under future global socio-economic and climate scenarios.
- Chaudhary, A., Verones, F., De Baan, L. and Hellweg, S. 2015. Quantifying Land Use Impacts on Biodiversity: Combining Species-Area Models and Vulnerability Indicators. *Environmental Science and Technology*. **49**(16), pp.9987–9995.
- Chazdon, R.L., Peres, C.A., Dent, D., Sheil, D., Lugo, A.E., Lamb, D., Stork, N.E. and Miller, S.E. 2009. The potential for species conservation in tropical secondary forests. *Conservation Biology*. **23**(6), pp.1406–1417.
- Chevin, L.M., Lande, R. and Mace, G.M. 2010. Adaptation, plasticity, and extinction in a changing environment: Towards a predictive theory. *PLoS Biology*. **8**(4).
- Chongkhong, S., Tongurai, C., Chetpattanonondh, P. and Bunyakan, C. 2007. Biodiesel production by esterification of palm fatty acid distillate. *Biomass and Bioenergy*. **31**(8), pp.563–568.



- Chua, K.H., Cheah, W.L., Tan, C.F. and Leong, Y.P. 2013. Harvesting biogas from wastewater sludge and food waste. *IOP Conference Series: Earth and Environmental Science*. **16**(1), pp.8–12.
- Chum, H., Faaij, A., Moreira, J., Berndes, G., Dhamija, P., Dong, H., Gabrielle, B., Eng, A.G., Lucht, W., Mapako, M., Cerutti, O.M., McIntyre, T., Minowa, T. and Pingoud, K. 2011. *Bioenergy*. In: *IPCC Special Report on Renewable Energy Sources and Climate Change Mitigation* [O. Edenhofer et al. (eds.)]. Cambridge University Press, Cambridge, United Kingdom and New York, USA.
- Ciais, P., Sabine, C., Bala, G., Bopp, L., Brovkin, V., Canadell, J., Chhabra, A., DeFries, R., Galloway, J., Heimann, M., Jones, C., Quéré, C. Le, Myneni, R.B., Piao, S. and Thornton, P. 2013. *Carbon and Other Biogeochemical Cycles*. In: *Climate Change 2013: The Physical Science Basis. Contribution of Working Group I to the Fifth Assessment Report of the Intergovernmental Panel on Climate Change* [T.F. Stocker et al. (eds.)]. Cambridge University Press, Cambridge, United Kingdom and New York, NY, USA.
- Cincotta, R.P., Wisnewski, J. and Engelman, R. 2000. Human population in the biodiversity hotspots. *Nature*. **404**, pp.990–992.
- Clarke, L., Jiang, K., Akimoto, K., Babiker, M., Blanford, G., Fisher-Vanden, K., Hourcade, J.-C., Krey, V., Kriegler, E., Löschel, A., McCollum, D., Paltsev, S., Rose, S., Shukla, P.R., Tavoni, M., Zwaan, B.C.C. van der and Vuuren, D.P. van 2014. *Assessing Transformation Pathways*. In: *Climate Change 2014: Mitigation of Climate Change. Contribution of Working Group III to the Fifth Assessment Report of the Intergovernmental Panel on Climate Change* [O. Edenhofer et al. (eds.)]. Cambridge University Press, Cambridge, United Kingdom and New York, NY, USA.
- Clarke, L., Wei, Y.-M., Navarro, A.D.L.V., Garg, A., Hahmann, A.N., Khennas, S., Azevedo, I.M.L., Löschel, A., Singh, A.K., Steg, L., Strbac, G. and Wada, K. 2022. *Energy Systems*. In *IPCC, 2022: Climate Change 2022: Mitigation of Climate Change. Contribution of Working Group III to the Sixth Assessment Report of the Intergovernmental Panel on Climate Change* [P.R. Shukla et al. (eds.)]. Cambridge University Press, Cambridge, UK and New York, NY, USA.
- Claussen, M., Brovkin, V. and Ganopolski, A. 2001. Biogeophysical versus biogeochemical feedbacks of large-scale land cover change. *Geophysical Research Letters*. **28**(6), pp.1011–1014.
- Claussen, M., Mysak, L., Weaver, A., Crucifix, M., Fichefet, T., Loutre, M.F., Weber, S., Alcamo, J., Alexeev, V., Berger, A., Calov, R., Ganopolski, A., Goosse, H., Lohmann, G., Lunkeit, F. and ... 2002. Earth system models of intermediate complexity: Closing the gap in the spectrum of climate system models. *Climate Dynamics*. **18**(7), pp.579–586.
- CMIP5 2009. CMIP5 Coupled Model Intercomparison Project. *WCRP*. [Online]. Available from: [http://cmip-pcmdi.llnl.gov/cmip5/forcing.html#land-use\\_data](http://cmip-pcmdi.llnl.gov/cmip5/forcing.html#land-use_data).
- Coca, N. 2020. As palm oil for biofuel rises in Southeast Asia, tropical ecosystems shrink. *China Dialogue*. [Online]. Available from: <https://chinadialogue.net/en/energy/11957-as-palm-oil-for-biofuel-rises-in-southeast-asia-tropical-ecosystems-shrink/>.
- Codesido, M., González-Fischer, C. and Bilenca, D. 2011. Distributional changes of landbird species in agroecosystems of central Argentina. *Condor*. **113**(2), pp.266–273.
- Collins, M., Knutti, R., Arblaster, J., Dufresne, J.-L., Fichefet, T., Friedlingstein, P., Gao, X., Gutowski, W.J., Johns, T., Krinner, G., Shongwe, M., Tebaldi, C., Weaver, A.J. and Wehner, M. 2013. *Long-term Climate Change: Projections, Commitments and Irreversibility*. In: *Climate Change 2013: The Physical Science Basis. Contribution of*

- Working Group I to the Fifth Assessment Report of the Intergovernmental Panel on Climate Change [T.F. Stocker ...].* Cambridge University Press, Cambridge, United Kingdom and New York, USA.
- COM 2006. *Biofuels progress report: Report on the progress made in the use of biofuels and other renewable fuels in the member states of the European Union.* Brussels.
- Conant, R.T., Cerri, C.E.P., Osborne, B.B. and Paustian, K. 2017. Grassland management impacts on soil carbon stocks: A new synthesis: A. *Ecological Applications*. **27**(2), pp.662–668.
- de Coninck, H., Revi, A., Babiker, M., Bertoldi, P., Buckeridge, M., Cartwright, A., Dong, W., Ford, J., Fuss, S., Hourcade, J.-C., Mechler, R., Newman, P., Revokatova, A., Schultz, S., Steg, L. and Sugiyama, T. 2018. *Strengthening and Implementing the Global Response. In: Global Warming of 1.5°C. An IPCC Special Report on the impacts of global warming of 1.5°C above pre-industrial levels and related global greenhouse gas emission pathways, in the context of strengthen.* Cambridge University Press, Cambridge, United Kingdom and New York, USA.
- Conservation International 2011. Biodiversity Hotspots Revisited, Creators: Conservation Synthesis and Center for Applied Biodiversity Science at Conservation International. Available from: <https://databasin.org/datasets/23fb5da1586141109fa6f8d45de0a260>.
- Consoli, C. 2019. *Bioenergy and Carbon Capture and Storage.*
- Corsten, M., Ramírez, A., Shen, L., Koornneef, J. and Faaij, A. 2013. Environmental impact assessment of CCS chains - Lessons learned and limitations from LCA literature. *International Journal of Greenhouse Gas Control*. **13**, pp.59–71.
- Costa, M. and Piazzullo, D. 2018. Biofuel Powering of Internal Combustion Engines: Production Routes, Effect on Performance and CFD Modeling of Combustion. *Frontiers in Mechanical Engineering*. **4**, pp.1–14.
- Cox, P.M. 2001. Description of the " TRIFFID " Dynamic Global Vegetation Model. *Hadley Centre technical note*. **24**, pp.1–17.
- Cox, P.M., Betts, R.A., Bunton, C.B., Essery, R.L.H., Rowntree, P.R. and Smith, S.J. 1999. The impact of new land surface physics on the GCM simulation of climate and climate sensitivity. *Climate Dynamics*. **15**(3), pp.183–203.
- Cox, P.M., Huntingford, C. and Harding, R.J. 1998. A canopy conductance and photosynthesis model for use in a GCM land surface scheme. *Journal of Hydrology*. **212–213**(1–4), pp.79–94.
- Crawley, M.J. and Harral, J.E. 2001. Scale Dependence in Plant Biodiversity. . **291**(February), pp.864–868.
- Creative Commons 2022. Attribution-NonCommercial 3.0 Unported (CC BY-NC 3.0). Available from: <https://creativecommons.org/licenses/by-nc/3.0/>.
- Creutzig, F., Ravindranath, N.H., Berndes, G., Bolwig, S., Bright, R., Cherubini, F., Chum, H., Corbera, E., Delucchi, M., Faaij, A., Fargione, J., Haberl, H., Heath, G., Lucon, O., Plevin, R. and ... 2015. Bioenergy and climate change mitigation: An assessment. *GCB Bioenergy*. **7**(5), pp.916–944.
- Cunha, A.P.M.A., Alvalá, R.C.S., Kubota, P.Y. and Vieira, R.M.S.P. 2015. Impacts of land use and land cover changes on the climate over Northeast Brazil. *Atmospheric Science Letters*. **16**(3), pp.219–227.
- Curtis, P.G., Slay, C.M., Harris, N.L., Tyukavina, A. and Hansen, M.C. 2018. Classifying

- drivers of global forest loss. *Science*. **361**(6407), pp.1108–1111.
- Cushman, S.A. 2006. Effects of habitat loss and fragmentation on amphibians: A review and prospectus. *Biological Conservation*. **128**(2), pp.231–240.
- Daioglou, V. 2016. *The role of biomass in climate change mitigation - Assessing the long-term dynamics of bioenergy and biochemicals in the land and energy systems*. [Online] Available from: <https://dspace.library.uu.nl/handle/1874/333999>.
- Daioglou, V., Doelman, J.C., Wicke, B., Faaij, A. and van Vuuren, D.P. 2019. *Integrated assessment of biomass supply and demand in climate change mitigation scenarios* [Online]. Elsevier Ltd. Available from: <https://doi.org/10.1016/j.gloenvcha.2018.11.012>.
- Daioglou, V., Stehfest, E., Wicke, B., Faaij, A. and van Vuuren, D.P. 2016. Projections of the availability and cost of residues from agriculture and forestry. *GCB Bioenergy*. **8**(2), pp.456–470.
- van Dam, J., Faaij, A.P.C., Hilbert, J., Petruzzi, H. and Turkenburg, W.C. 2009. Large-scale bioenergy production from soybeans and switchgrass in Argentina. Part B. Environmental and socio-economic impacts on a regional level. *Renewable and Sustainable Energy Reviews*. **13**(8), pp.1679–1709.
- Van Dam, J., Junginger, M. and Faaij, A.P.C. 2010. From the global efforts on certification of bioenergy towards an integrated approach based on sustainable land use planning. *Renewable and Sustainable Energy Reviews*. **14**(9), pp.2445–2472.
- Danielsen, F., Beukema, H., Burgess, N., Parish, F., Brühl, C., Donald, P., Murdiyarto, D., Phalan, B., Reijnders, L., Struebig, M. and Fitzherbert, E. 2009. Biofuel plantations on forested lands: Double jeopardy for biodiversity and climate. *IOP Conference Series: Earth and Environmental Science*. **6**(24), p.242014.
- Dauber, J., Jones, M.B. and Stout, J.C. 2010. The impact of biomass crop cultivation on temperate biodiversity. *GCB Bioenergy*. **2**(6), pp.289–309.
- Davies-Barnard, T., Valdes, P.J., Singarayer, J.S., Pacifico, F.M. and Jone, C.D. 2014. Full effects of land use change in the representative concentration pathways. *Environmental Research Letters*. **9**(11).
- Davies, T.J. and Cadotte, M.W. 2011. *Quantifying Biodiversity: Does It Matter What We Measure? In: Biodiversity Hotspots*. Springer, Berlin, Germany.
- Davin, E.L. and de Noblet-Ducoudre, N. 2010. Climatic impact of global-scale Deforestation: Radiative versus nonradiative processes. *Journal of Climate*. **23**(1), pp.97–112.
- Davis, S.C., Boddey, R.M., Alves, B.J.R., Cowie, A.L., George, B.H., Ogle, S.M., Smith, P., van Noordwijk, M. and van Wijk, M.T. 2013. Management swing potential for bioenergy crops. *GCB Bioenergy*. **5**(6), pp.623–638.
- Dawson, T.P., Jackson, S.T., House, J.I., Prentice, I.C. and Mace, G.M. 2011. Beyond predictions: Biodiversity conservation in a changing climate. *Science*. **332**(6025), pp.53–58.
- DeFries, R., Hansen, A., Newton, A.C. and Hansen, M.C. 2005. Increasing isolation of protected areas in tropical forests over the past twenty years. *Ecological Applications*. **15**(1), pp.19–26.
- Defries, R.S. and Townshend, J.R. 1994. Ndvi-Derived Land Cover Classifications At a Global Scale. *International Journal of Remote Sensing*. **15**(17), pp.3567–3586.
- Delzeit, R., Zabel, F., Meyer, C. and Václavík, T. 2017. Addressing future trade-offs between biodiversity and cropland expansion to improve food security. *Regional Environmental*

- Change*. **17**(5), pp.1429–1441.
- Deng, L., Liu, G. bin and Shangguan, Z. ping 2014. Land-use conversion and changing soil carbon stocks in China's 'Grain-for-Green' Program: A synthesis. *Global Change Biology*. **20**(11), pp.3544–3556.
- Devaraju, N., Bala, G. and Nemani, R. 2015. Modelling the influence of land-use changes on biophysical and biochemical interactions at regional and global scales. *Plant, Cell and Environment*. **38**(9), pp.1931–1946.
- Diamond, J.M. 1972. Biogeographic Kinetics: Estimation of Relaxation Times for Avifaunas of Southwest Pacific Islands. *Proceedings of the National Academy of Sciences (USA)*. **69**(11), pp.3199–3203.
- Díaz, S., Settele, J., Brondízio, E.S., Ngo, H.T., Agard, J., Arneth, A., Balvanera, P., Brauman, K.A., Butchart, S.H.M., Chan, K.M.A., Lucas, A.G., Ichii, K., Liu, J., Subramanian, S.M., Midgley, G.F. and ... 2019. Pervasive human-driven decline of life on Earth points to the need for transformative change. *Science*. **366**(6471).
- Dietrich, J.P., Schmitz, C., Lotze-Campen, H., Popp, A. and Müller, C. 2014. Forecasting technological change in agriculture-An endogenous implementation in a global land use model. *Technological Forecasting and Social Change*. **81**(1), pp.236–249.
- Dietrich, J.P., Schmitz, C., Müller, C., Fader, M., Lotze-Campen, H. and Popp, A. 2012. Measuring agricultural land-use intensity - A global analysis using a model-assisted approach. *Ecological Modelling*. **232**, pp.109–118.
- Diochon, A., Kellman, L. and Beltrami, H. 2009. Looking deeper: An investigation of soil carbon losses following harvesting from a managed northeastern red spruce (*Picea rubens* Sarg.) forest chronosequence. *Forest Ecology and Management*. **257**(2), pp.413–420.
- Domac, J., Richards, K. and Risovic, S. 2005. Socio-economic drivers in implementing bioenergy projects. *Biomass and Bioenergy*. **28**(2), pp.97–106.
- Don, A., Osborne, B., Hastings, A., Skiba, U., Carter, M.S., Drewer, J., Flessa, H., Freibauer, A., Hyvönen, N., Jones, M.B., Lanigan, G.J., Mander, Ü., Monti, A., Djomo, S.N., Valentine, J., Walter, K., Zegada-Lizarazu, W. and Zenone, T. 2012. Land-use change to bioenergy production in Europe: Implications for the greenhouse gas balance and soil carbon. *GCB Bioenergy*. **4**(4), pp.372–391.
- Don, A., Schumacher, J. and Freibauer, A. 2011. Impact of tropical land use change on soil organic carbon stocks - a meta-analysis. *Global Change Biology*. **17**(4), p.1658.
- Dornburg, V., Faaij, A.P.C. and Verweij, P.A. 2008. *Climate Change Scientific Assessment and Policy Analysis. Biomass Assessment – Assessment of Global Biomass Potentials and Their Links to Food, Water, Biodiversity, Energy Demand and Economy, Inventory and Analysis of Existing Studies*. Netherlands Environmental Assessment Agency (MNP), Bilthoven, The Netherlands.
- Dornburg, V., Vuuren, D. van, Ven, G. van de, Langeveld, H., Meeusen, M., Banse, M., Oorschot, M. van, Ros, J., Born, G.J. van den, Aiking, H., Londo, M., Mozaffarian, H., Verweij, P., Lyseng, E. and Faaij, A. 2010. Bioenergy revisited: Key factors in global potentials of bioenergy. *Energy and Environmental Science*. **3**(3), p.253.
- Drax 2020. Carbon dioxide now being captured in first of its kind BECCS pilot. *Drax*. [Online]. Available from: [https://www.drax.com/press\\_release/world-first-co2-beccs-ccus/](https://www.drax.com/press_release/world-first-co2-beccs-ccus/).
- Drax Group plc 2021. *Innovating for a positive future, Drax Group plc Annual report and accounts 2021*. Selby, North Yorkshire.

- Duden, A.S., Verweij, P.A., Faaij, A.P.C., Baisero, D., Rondinini, C. and van der Hilst, F. 2020. Biodiversity impacts of increased ethanol production in Brazil. *Land*. **9**(1).
- Duden, A.S., Verweij, P.A., Kraak, Y. V., van Beek, L.P.H., Wanders, N., Karssenberg, D.J., Sutanudjaja, E.H. and van der Hilst, F. 2021. Hydrological impacts of ethanol-driven sugarcane expansion in Brazil. *Journal of Environmental Management*. **282**(June 2020), p.111942.
- Dudgeon, D., Arthington, A.H., Gessner, M.O., Kawabata, Z., Naiman, R.J., Knowler, D.J. and Le, C. 2015. Freshwater biodiversity: importance, threats, status and conservation challenges. (2006), pp.163–182.
- Dunderdale, M., Muller, J.P. and Cox, P.M. 1999. *Sensitivity of the Hadley Centre climate model to different earth observation and cartographically derived land surface data-sets. The Contribution of POLDER and New Generation Spaceborne Sensors to Global Change Studies*. Meribel, France.
- Dung, T.N.B., Sen, B., Chen, C.C., Kumar, G. and Lin, C.Y. 2014. Food waste to bioenergy via anaerobic processes. *Energy Procedia*. **61**, pp.307–312.
- Dunn, R.R. 2004. Recovery of Faunal Communities During Tropical Forest Regeneration. . **18**(2), pp.302–309.
- Durán, A.P., Green, J.M.H., West, C.D., Visconti, P., Burgess, N.D., Virah-Sawmy, M. and Balmford, A. 2020. A practical approach to measuring the biodiversity impacts of land conversion. *Methods in Ecology and Evolution*. **11**(8), pp.910–921.
- Durieux, L., Toledo Machado, L.A. and Laurent, H. 2003. The impact of deforestation on cloud cover over the Amazon arc of deforestation. *Remote Sensing of Environment*. **86**(1), pp.132–140.
- Duveiller, G., Caporaso, L., Abad-Viñas, R., Perugini, L., Grassi, G., Arneth, A. and Cescatti, A. 2020. Local biophysical effects of land use and land cover change: towards an assessment tool for policy makers. *Land Use Policy*. **91**(December 2019), p.104382.
- Duveiller, G., Forzieri, G., Robertson, E., Li, W., Georgievski, G., Lawrence, P., Wiltshire, A., Ciais, P., Pongratz, J., Sitch, S., Arneth, A. and Cescatti, A. 2018. Biophysics and vegetation cover change: A process-based evaluation framework for confronting land surface models with satellite observations. *Earth System Science Data*. **10**(3), pp.1265–1279.
- Duveiller, G., Hooker, J. and Cescatti, A. 2018. The mark of vegetation change on Earth's surface energy balance. *Nature Communications*. **9**(1).
- E.I.A 2019. How much carbon dioxide is produced when different fuels are burned? *U.S Energy Information Administration*. [Online]. Available from: <https://www.eia.gov/tools/faqs/faq.php?id=73&t=11>.
- Eby, M., Zickfeld, K., Montenegro, A., Archer, D., Meissner, K.J. and Weaver, A.J. 2009. Lifetime of anthropogenic climate change: Millennial time scales of potential CO<sub>2</sub> and surface temperature perturbations. *Journal of Climate*. **22**(10), pp.2501–2511.
- Eggers, J., Tröltzsch, K., Falcucci, A., Maiorano, L., Verburg, P.H., Framstad, E., Louette, G., Maes, D., Nagy, S., Ozinga, W. and Delbaere, B. 2009. Is biofuel policy harming biodiversity in Europe? *GCB Bioenergy*. **1**(1), pp.18–34.
- Eitelberg, D.A., van Vliet, J. and Verburg, P.H. 2015. A review of global potentially available cropland estimates and their consequences for model-based assessments. *Global Change Biology*. **21**(3), pp.1236–1248.

- Elliott Campbell, J., Lobell, D.B., Genova, R.C. and Field, C.B. 2008. The global potential of bioenergy on abandoned agricultural lands. *Environ. Sci. Technol.* **42**(15), pp.5791–5794.
- Elmore, A.J. and Asner, G.P. 2006. Effects of grazing intensity on soil carbon stocks following deforestation of a Hawaiian dry tropical forest. *Global Change Biology.* **12**(9), pp.1761–1772.
- Elshout, P.M.F., Van Zelm, R., Balkovic, J., Obersteiner, M., Schmid, E., Skalsky, R., Van Der Velde, M. and Huijbregts, M.A.J. 2015. Greenhouse-gas payback times for crop-based biofuels. *Nature Climate Change.* **5**(6), pp.604–610.
- EPA 2010. *EPA lifecycle analysis of greenhouse gas emissions from renewable fuels.* Environmental Protection Agency, Ann Arbor, MI.
- Erb, K.H., Gaube, V., Krausmann, F., Plutzar, C., Bondeau, A. and Haberl, H. 2007. A comprehensive global 5 min resolution land-use data set for the year 2000 consistent with national census data. *Journal of Land Use Science.* **2**(3), pp.191–224.
- Erb, K.H., Haberl, H. and Plutzar, C. 2012. Dependency of global primary bioenergy crop potentials in 2050 on food systems, yields, biodiversity conservation and political stability. *Energy Policy.* **47**, pp.260–269.
- Eschmeyer, W.M. 1998. *Catalog of Fishes.* San Francisco: California Academy of Sciences.
- EUBIA 2020. Biomass processing technologies. *European Biomass Industry Association.* [Online]. Available from: <https://www.eubia.org/cms/wiki-biomass/biomass-processing-technologies/>.
- Ewen, T.L., Weaver, A.J., Eby, M., Ewen, T.L., Weaver, A.J., Eby, M., Ewen, T.L., Weaver, A.J. and Eby, M. 2004. Sensitivity of the Inorganic Ocean Carbon Cycle to Future Climate Warming in the UVic Coupled Model. *Atmosphere-Ocean.* **5900**, pp.1480–9214.
- Eyring, V., Gillett, N.P., Achuta Rao, K.M., Barimalala, R., Barreiro Parrillo, M., Bellouin, N., Cassou, C., Durack, P.J., Kosaka, Y., McGregor, S., Min, S., Morgenstern, O. and Sun, Y. 2021. *Human Influence on the Climate System. In Climate Change 2021: The Physical Science Basis. Contribution of Working Group I to the Sixth Assessment Report of the Intergovernmental Panel on Climate Change [V. P. Masson-Delmotte et al, (eds.)].* Cambridge University Press, Cambridge, United Kingdom and New York, USA.
- Fahrig, L., Baudry, J., Brotons, L., Burel, F.G., Crist, T.O., Fuller, R.J., Sirami, C., Siriwardena, G.M. and Martin, J.L. 2011. Functional landscape heterogeneity and animal biodiversity in agricultural landscapes. *Ecology Letters.* **14**(2), pp.101–112.
- Fajardy, M., Koberle, A., Mac Dowell, N. and Fantuzzi, A. 2019. BECCS deployment: a reality check. *Grantham Institute.* **28**(28), pp.1–14.
- FAO 2015. FAO Statistical Database. *Food and Agriculture Organization of the United Nations.* [Online]. Available from: <https://www.fao.org/statistics/en/>.
- FAO 2006. *Livestock's Long Shadow. Environmental Issues and Options.*
- FAO 2022. *The State of the World's Forests 2022. Forest pathways for green recovery and building inclusive, resilient and sustainable economies.* [Online]. Available from: <https://doi.org/10.4060/cb9360en>.
- FAO and UNEP 2020. *The State of the World's Forests 2020. Forests, Biodiversity and People* [Online]. Rome. Available from: <https://doi.org/10.4060/ca8642en>.
- Fargione, J., Hill, J., Tilman, D., Polasky, S. and Hawthorne, P. 2008. Land Clearing and the Biofuel Carbon Debt. *Science.* **319**, pp.1235–1238.

- FDP 2023. What is the New York Declaration on Forests? *Forest Declaration Platform*. [Online]. Available from: <https://forestdeclaration.org/about/new-york-declaration-on-forests/>.
- Feddema, J.J. 2005. The Importance of Land-Cover Change in Simulating Future Climates. *Science*. **310**(5754), pp.1674–1678.
- Fehrenbach, H. 2011. How bioenergy related water impacts are considered by certification schemes. *Biofuels, Bioproducts and Biorefining*. **5**, pp.464–473.
- Fernandes, G.W., Vale, M.M., Overbeck, G.E., Bustamante, M.M.C., Grelle, C.E.V., Bergallo, H.G., Magnusson, W.E., Akama, A., Alves, S.S., Amorim, A., Araújo, J., Barros, C.F., Bravo, F., Carim, M.J.V., Cerqueira, R. and ... 2017. Dismantling Brazil's science threatens global biodiversity heritage. *Perspectives in Ecology and Conservation*. **15**(3), pp.239–243.
- Ferraz, J.C., Santiago, J. and Ramos, L. 2023. Policy innovation for sustainable development: the case of the Amazon Fund. *Review of Evolutionary Political Economy*.
- Ferrier, S., Pressey, R.L. and Barrett, T.W. 2000. A new predictor of the irreplaceability of areas for achieving a conservation goal, its application to real-world planning, and a research agenda for further refinement. *Biological Conservation*. **93**(3), pp.303–325.
- Findell, K.L., Pitman, A.J., England, M.H. and Pegen, P.J. 2009. Regional and global impacts of land cover change and sea surface temperature anomalies. *Journal of Climate*. **22**(12), pp.3248–3269.
- Fischer, J., Abson, D.J., Butsic, V., Chappell, M.J., Ekroos, J., Hanspach, J., Kuemmerle, T., Smith, H.G. and von Wehrden, H. 2014. Land sparing versus land sharing: Moving forward. *Conservation Letters*. **7**(3), pp.149–157.
- Fischlin, A., Midgley, G.F., Price, J.T., Leemans, R., Gopal, B., Turley, C., Rounsevell, M.D.A., Dube, O.P., Tarazona, J. and Velichko, A.A. 2007. *Ecosystems, their properties, goods and services*. In: *Climate change 2007: impacts, adaptation and vulnerability* [M. L. Parry (eds.)]. Cambridge University Press, Cambridge, UK.
- Fisher, B. and Christopher, T. 2007. Poverty and biodiversity: Measuring the overlap of human poverty and the biodiversity hotspots. *Ecological Economics*. **62**(1), pp.93–101.
- Fisher, M.C., Garner, T.W.J. and Walker, S.F. 2009. Global emergence of Batrachochytrium dendrobatidis and amphibian chytridiomycosis in space, time and host. *Ann Rev Microbiol* **63**. **63**, pp.291–310.
- Fitzherbert, E.B., Struebig, M.J., Morel, A., Danielsen, F., Brühl, C.A., Donald, P.F. and Phalan, B. 2008. How will oil palm expansion affect biodiversity? *Trends in Ecology and Evolution*. **23**(10), pp.538–545.
- Flather, C.H. and Bevers, M. 2002. Patchy reaction-diffusion and population abundance: The relative importance of habitat amount and arrangement. *American Naturalist*. **159**(1), pp.40–56.
- Foley, J.A., Defries, R., Asner, G.P., Barford, C., Bonan, G., Carpenter, S.R., Chapin, F.S., Coe, M.T., Daily, G.C., Gibbs, H.K., Helkowski, J.H., Holloway, T., Howard, E.A., Kucharik, C.J., Monfreda, C. and ... 2005. Global Consequences of Land Use. *Science*. **309**(5734), pp.570–574.
- Foley, J.A., Prentice, I.C., Ramankutty, N., Levis, S., Pollard, D., Sitch, S. and Haxeltine, A. 1996. An integrated biosphere model of land surface processes, terrestrial carbon balance, and vegetation dynamics. *Global Biogeochemical Cycles*. **10**(4), pp.603–628.

- Foley, J.A., Ramankutty, N., Brauman, K.A., Cassidy, E.S., Gerber, J.S., Johnston, M., Mueller, N.D., O'Connell, C., Ray, D.K., West, P.C., Balzer, C., Bennett, E.M., Carpenter, S.R., Hill, J., Monfreda, C. and ... 2011. Solutions for a cultivated planet. *Nature*. **478**(7369), pp.337–342.
- Foust, T. d., Arent, D., Macedo, I. de C., Goldemberg, J., Hoysala, C., Filho, R.M., Nigro, F.E.B., Richard, T.L., Saddler, J., Samseth, J. and Somerville, and C.R. 2017. *Chapter 3: Energy security. In: The Palgrave Handbook of Security, Risk and Intelligence.*
- Fox-Kemper, B., Hewitt, H.T., Xiao, C., Aðalgeirsdóttir, G., Drijfhout, S.S., Edwards, T.L., Gollledge, N.R., Hemer, M., Kopp, R.E., Krinner, G., Mix, A., Notz, D., Nowicki, S., Nurhati, I.S., Ruiz, L. and ... 2021. *Ocean, Cryosphere and Sea Level Change. In Climate Change 2021: The Physical Science Basis. Contribution of Working Group I to the Sixth Assessment Report of the Intergovernmental Panel on Climate Change [V. P. Masson-Delmotte et al. (eds.)].* Cambridge University Press, Cambridge, United Kingdom and New York, USA.
- de Fraiture, C. and Wichelns, D. 2010. Satisfying future water demands for agriculture. *Agricultural Water Management*. **97**(4), pp.502–511.
- Frank, S., Havlík, P., Soussana, J.F., Levesque, A., Valin, H., Wollenberg, E., Kleinwechter, U., Fricko, O., Gusti, M., Herrero, M., Smith, P., Hasegawa, T., Kraxner, F. and Obersteiner, M. 2017. Reducing greenhouse gas emissions in agriculture without compromising food security? *Environmental Research Letters*. **12**(10).
- Franz, M., Schlitz, N. and Schumacher, K.P. 2018. Globalization and the water-energy-food nexus – Using the global production networks approach to analyze society-environment relations. *Environmental Science and Policy*. **90**(December 2017), pp.201–212.
- Freepnging 2022. Free PNG image icons. Available from: <https://freepngimg.com/icon>.
- Freudmann, A., Mollik, P., Tschapka, M. and Schulze, C.H. 2015. Impacts of oil palm agriculture on phyllostomid bat assemblages. *Biodiversity and Conservation*. **24**(14), pp.3583–3599.
- Friedlingstein, P., Betts, R., Bopp, L., Bloh, W. Von, Brovkin, V., Doney, S., Eby, M., Fung, I., Govindasamy, B., John, J., Jones, C., Joos, F., Kato, T., Kawamiya, M., Knorr, W. and ... 2006. Climate-carbon cycle feedback analysis, results from the C4MIP model intercomparison. *Journal of Climate*. **19**, pp.3337–3353.
- Friedlingstein, P., Houghton, R.A., Marland, G., Hackler, J., Boden, T.A., Conway, T.J., Canadell, J.G., Raupach, M.R., Ciais, P. and Le Quéré, C. 2010. Update on CO2 emissions. *Nature Geoscience*. **3**(12), pp.811–812.
- Friedlingstein, P., Jones, M.W., Sullivan, M.O., Andrew, R.M., Bakker, D.C.E., Hauck, J., Quéré, C. Le, Peters, G.P. and Peters, W. 2022. Global Carbon Budget 2021. *Earth System Science Data*. **14**, pp.4811–4900.
- Friedlingstein, P., O'Sullivan, M., Jones, M.W., Andrew, R.M., Hauck, J., Olsen, A., Peters, G.P., Peters, W., Pongratz, J., Sitch, S., Le Quéré, C., Canadell, J.G., Ciais, P., Jackson, R.B., Alin, S. and ... 2020. Global Carbon Budget 2020. *Earth System Science Data*. **12**(4), pp.3269–3340.
- Friend, A.D., Stevens, A.K., Knox, R.G. and Cannell, M.G.R. 1997. A process-based, terrestrial biosphere model of ecosystem dynamics (Hybrid v3.0). *Ecological Modelling*. **95**(2–3), pp.249–287.
- Fritsche, U.R., Hünecke, K., Hermann, A., Schulze, F. and Wiegmann, K. 2006. *Sustainability Standards for Bioenergy*. WWF, Frankfurt am Main, Germany.



- Fritz, S., See, L., Van Der Velde, M., Nalepa, R.A., Perger, C., Schill, C., McCallum, I., Schepaschenko, D., Kraxner, F., Cai, X., Zhang, X., Ortner, S., Hazarika, R., Cipriani, A., Di Bella, C. and ... 2013. Downgrading recent estimates of land available for biofuel production. *Environmental Science and Technology*. **47**(3), pp.1688–1694.
- De Frutos, A., Olea, P.P. and Mateo-Tomás, P. 2015. Responses of medium- and large-sized bird diversity to irrigation in dry cereal agroecosystems across spatial scales. *Agriculture, Ecosystems and Environment*. **207**, pp.141–152.
- Fuss, S., Canadell, J.G., Peters, G.P., Tavoni, M., Andrew, R.M., Ciais, P., Jackson, R.B., Jones, C.D., Kraxner, F., Nakicenovic, N., Le Quere, C., Raupach, M.R., Sharifi, A., Smith, P., Yamagata, Y. and ... 2014. Betting on negative emissions. *Nature Clim. Change*. **4**(10), pp.850–853.
- Gabel, V.M., Meier, M.S., Köpke, U. and Stolze, M. 2016. The challenges of including impacts on biodiversity in agricultural life cycle assessments. *Journal of Environmental Management*. **181**, pp.249–260.
- Gambhir, A., Butnar, I., Li, P.H., Smith, P. and Strachan, N. 2019. A review of criticisms of integrated assessment models and proposed approaches to address these, through the lens of BECCs. *Energies*. **12**(9), pp.1–21.
- Ganopolski, A., Petoukhov, V., Rahmstorf, S., Brovkin, V., Claussen, M., Eliseev, A. and Kubatzki, C. 2001. CLIMBER-2: a climate system of intermediate complexity. Part II: model sensitivity. *Clim. \ Dyn.* **17**, pp.735–751.
- Gao, Y., Skutsch, M., Masera, O. and Pacheco, P. 2011. A global analysis of deforestation due to biofuel development. *Center for International Forestry Research*., p.86.
- Garcia, R.A., Cabeza, M., Altwegg, R. and Araújo, M.B. 2016. Do projections from bioclimatic envelope models and climate change metrics match? *Global Ecology and Biogeography*. **25**(1), pp.65–74.
- Gascon, C., Collins, J.P., Moore, R.D., Church, D.R., McKay, J.E. and Mendelson III, J.R. 2007. *Amphibian Conservation Action Plan*. IUCN/SSC Amphibian Specialist Group, IUCN/SSC Amphibian Specialist Group.
- Gasparatos, A., Borzoni, M. and Abramovay, R. 2012. *The Brazilian bioethanol and biodiesel programs: Drivers, policies and impacts*. In: *Socioeconomic and Environmental Impacts of Biofuels: Evidence from Developing Nations*. A. Gasparatos P. Stromberg, ed. Cambridge University Press, Cambridge, England.
- Gasparatos, A., Stromberg, P. and Takeuchi, K. 2013. Sustainability impacts of first-generation biofuels. *Animal Frontiers*. **3**(2), pp.12–26.
- Gasser, T. and Ciais, P. 2013. A theoretical framework for the net land-to-atmosphere CO<sub>2</sub> flux and its implications in the definition of ‘emissions from land-use change’. *Earth System Dynamics*. **4**(1), pp.171–186.
- GBEP 2018. *Linkages between the Sustainable Development Goals (SDGs) and the GBEP Sustainability Indicators for Bioenergy (GSI)* [Online]. IINAS & IFEU, Darmstadt, Berlin, Heidelberg. Available from: <http://www.globalbioenergy.org/events1/events->
- GEA 2012. *Global energy assessment (GEA) - Toward a Sustainable Future*. Cambridge University Press, Cambridge UK and New York, NY, USA and the International Institute for Applied Systems Analysis, Laxenburg, Austria.
- Geiger, F., Bengtsson, J., Berendse, F., Weisser, W.W., Emmerson, M., Morales, M.B., Ceryngier, P., Liira, J., Tschardtke, T., Winqvist, C., Eggers, S., Bommarco, R., Pärt, T.,

- Bretagnolle, V., Plantegenest, M. and ... 2010. Persistent negative effects of pesticides on biodiversity and biological control potential on European farmland. *Basic and Applied Ecology*. **11**(2), pp.97–105.
- Georgescu, M., Lobell, D.B. and Field, C.B. 2011. Direct climate effects of perennial bioenergy crops in the United States. *Proceedings of the National Academy of Sciences*. **108**(11), pp.4307–4312.
- Gerbens-Leenes, P.W. 2017. Bioenergy water footprints, comparing first, second and third generation feedstocks for bioenergy supply in 2040. *European Water*. **59**, pp.373–380.
- Gerbens-leenes, W., Hoekstra, A.Y. and Meer, T.H. Van Der 2009. The water footprint of bioenergy. . **2009**(23).
- Gerten, D., Hoff, H., Rockstrom, J., Kummu, M. and Pastor, A. V 2013. Towards a revised planetary boundary for consumptive freshwater use: role of environmental flow requirements.
- GetData 2019. GetData Graph Digitizer. Available from: <http://getdata-graph-digitizer.com/index.php>.
- Ghazoul, J., Butler, R.A., Mateo-Vega, J. and Koh, L.P. 2010. REDD: A reckoning of environment and development implications. *Trends in Ecology and Evolution*. **25**(7), pp.396–402.
- Gibbard, S., Caldeira, K., Bala, G., Phillips, T.J. and Wickett, M. 2005. Climate effects of global land cover change. *Geophysical Research Letters*. **32**(23), pp.1–4.
- Gibbons, J.W., Scott, E., Ryan, T.J., Buhlmann, K.A., Tuberville, T.D., Metts, B.S., Greene, J.L., Mills, T., Leiden, Y., Poppy, S. and Winne, C.T. 2000. The Global Decline of Reptiles, Déjà vu amphibians. *Bioscience*. **50**(8), pp.653–666.
- Gibbs, H.K., Rausch, L., Munger, J., Schelly, I., Morton, D.C., Noojipady, P., Soares-Filho, B., Barreto, P., Micol, L. and Walker, N.F. 2015. Brazil's Soy Moratorium: Supply-chain governance is needed to avoid deforestation. *Science*. **347**(6220), pp.377–378.
- Gibson, L., Lee, T.M., Koh, L.P., Brook, B.W., Gardner, T.A., Barlow, J., Peres, C.A., Bradshaw, C.J.A., Laurance, W.F., Lovejoy, T.E. and Sodhi, N.S. 2011. Primary forests are irreplaceable for sustaining tropical biodiversity. *Nature*. **478**(7369), pp.378–381.
- Gillett, N.P., Arora, V.K., Matthews, D. and Allen, M.R. 2013. Constraining the ratio of global warming to cumulative CO<sub>2</sub> emissions using CMIP5 simulations. *Journal of Climate*. **26**(18), pp.6844–6858.
- Gilman, S.E., Urban, M.C., Tewksbury, J., Gilchrist, G.W. and Holt, R.D. 2010. A framework for community interactions under climate change. *Trends in Ecology and Evolution*. **25**(6), pp.325–331.
- Glaw, F. and Köhler, J. 1998. Amphibian species diversity exceeds that of mammals. *Herpetological Review*. **29**(1), pp.11–12.
- Gleick, P.H. and Cooley, H. 2009. *The World's Water 2008–2009: The Biennial Report on Freshwater Resources*. Washington, DC: Island Press.
- Goh, C.S., Saito, O. and Yamagata, Y. 2020. Developing sustainable bioenergy systems with local bio-resources: cases in Asia. *Sustainability Science*. **15**(5), pp.1449–1453.
- Goldewijk, K.K., Beusen, A., Van Dreht, G. and De Vos, M. 2011. The HYDE 3.1 spatially explicit database of human-induced global land-use change over the past 12,000 years. *Global Ecology and Biogeography*. **20**(1), pp.73–86.

- Goll, D.S., Brovkin, V., Parida, B.R., Reick, C.H., Kattge, J., Reich, P.B., Van Bodegom, P.M. and Niinemets, Ü. 2012. Nutrient limitation reduces land carbon uptake in simulations with a model of combined carbon, nitrogen and phosphorus cycling. *Biogeosciences*. **9**(9), pp.3547–3569.
- Goodman, S.M., Andriafidison, D., Andrianaivoarivelo, R., Cardiff, S.G., Ifticene, E., Jenkins, R.K.B., Kofoky, A., Mbohoahy, T., Rakotondravony, D. and Ranivo, J. 2005. The distribution and conservation of bats in the dry regions of Madagascar. *Animal Conservation forum*. **8**(2), pp.153–165.
- Gorter, H. De, Drabik, D. and Just, D.R. 2013. The perverse effects of biofuel public-sector policies. *Annual Review of Resource Economics*. **5**(November 2012), pp.463–483.
- Gotangco Castillo, C.K., Raymond, L. and Gurney, K.R. 2012. REDD+ and climate: Thinking beyond carbon. *Carbon Management*. **3**(5), pp.457–466.
- Grassi, G., House, J., Dentener, F., Federici, S., Den Elzen, M. and Penman, J. 2017. The key role of forests in meeting climate targets requires science for credible mitigation. *Nature Climate Change*. **7**(3), pp.220–226.
- Grassi, G., House, J., Kurz, W.A., Cescatti, A., Houghton, R.A., Peters, G.P., Sanz, M.J., Viñas, R.A., Alkama, R., Arneth, A., Bondeau, A., Dentener, F., Fader, M., Federici, S., Friedlingstein, P. and ... 2018. Reconciling global-model estimates and country reporting of anthropogenic forest CO<sub>2</sub> sinks. *Nature Climate Change*. **8**(10), pp.914–920.
- Gray, V. 2007. Climate change 2007: The physical science basis summary for policymakers. *Energy and Environment*. **18**(3–4), pp.433–440.
- Grenyer, R., Orme, C.D.L., Jackson, S.F., Thomas, G.H., Davies, R.G., Davies, T.J., Jones, K.E., Olson, V.A., Ridgely, R.S., Rasmussen, P.C., Ding, T.S., Bennett, P.M., Blackburn, T.M., Gaston, K.J., Gittleman, J.L. and Owens, I.P.F. 2006. Global distribution and conservation of rare and threatened vertebrates. *Nature*. **444**(7115), pp.93–96.
- Griscom, B.W., Adams, J., Ellis, P.W., Houghton, R.A., Lomax, G., Miteva, D.A., Schlesinger, W.H., Shoch, D., Siikamäki, J. V., Smith, P., Woodbury, P., Zganjar, C., Blackman, A., Campari, J. and ... 2017. Natural climate solutions. *Proceedings of the National Academy of Sciences of the United States of America*. **114**(44), pp.11645–11650.
- Groombridge, B. and Jenkins, M. 2000. *Global Biodiversity: Earth's Living Resources in the 21st Century*. Cambridge, U.K.
- Guisan, A. and Zimmermann, N.E. 2000. Predictive habitat distribution models in ecology. *Ecological Modelling*. **135**(2–3), pp.147–186.
- Guo, L.B. and Gifford, R.M. 2002. Soil carbon stocks and land use change: A meta analysis. *Global Change Biology*. **8**(4), pp.345–360.
- Hallgren, W., Schlosser, A. and Monier, E. 2012. Impacts of Land Use and Biofuels Policy on Climate: Temperature and Localized Impacts. . (227).
- Hallgren, W., Schlosser, C.A., Monier, E., Kicklighter, D., Sokolov, A. and Melillo, J. 2013. Climate impacts of a large-scale biofuels expansion. *Geophysical Research Letters*. **40**(8), pp.1624–1630.
- Hansen, M.C., Potapov, P. V., Moore, R., Hancher, M., Turubanova, S.A., Tyukavina, A., Thau, D., Stehman, S. V., Goetz, S.J., Loveland, T.R., Kommareddy, A., Egorov, A., Chini, L., Justice, C.O. and Townshend, J.R.G.G. 2013. High-resolution global maps of 21st-century forest cover change. *Science (New York, N.Y.)*. **342**(6160), pp.850–853.
- Hansis, E., Davis, S.J. and Pongratz, J. 2015. Relevance of methodological choices for

- accounting of land use change carbon fluxes. *Global Biogeochemical Cycles*. **29**(8), pp.1230–1246.
- Hanssen, S. V., Daioglou, V., Steinmann, Z.J.N., Frank, S., Popp, A., Brunelle, T., Lauri, P., Hasegawa, T., Huijbregts, M.A.J. and Van Vuuren, D.P. 2020. Biomass residues as twenty-first century bioenergy feedstock—a comparison of eight integrated assessment models. *Climatic Change*. **163**(3), pp.1569–1586.
- Hanssen, S. V., Steinmann, Z.J.N., Daioglou, V., Čengić, M., Van Vuuren, D.P. and Huijbregts, M.A.J. 2022. Global implications of crop-based bioenergy with carbon capture and storage for terrestrial vertebrate biodiversity. *GCB Bioenergy*. **14**(3), pp.307–321.
- Hanssen, S. V., Daioglou, V., Steinmann, Z.J.N., Doelman, J.C., Vuuren, D.P. Van and Huijbregts, M.A.J. 2020. The climate change mitigation potential of bioenergy with carbon capture and storage. *Nature Climate Change*. **10**, pp.1023–1029.
- Harding, K.J., Twine, T.E., VanLoocke, A., Bagley, J.E. and Hill, J. 2016. Impacts of second-generation biofuel feedstock production in the central U.S. on the hydrologic cycle and global warming mitigation potential. *Geophysical Research Letters*. **43**(20), 10,773–10,781.
- Harper, A.B., Powell, T., Cox, P.M., House, J., Huntingford, C., Lenton, T.M., Sitch, S., Burke, E., Chadburn, S.E., Collins, W.J., Comyn-Platt, E., Daioglou, V., Doelman, J.C., Hayman, G., Robertson, E. and ... 2018. Land-use emissions play a critical role in land-based mitigation for Paris climate targets. *Nature Communications*. **9**(1).
- Harris, E., Ladreiter-Knauss, T., Butterbach-Bahl, K., Wolf, B. and Bahn, M. 2018. Land-use and abandonment alters methane and nitrous oxide fluxes in mountain grasslands. *Science of the Total Environment*. **628–629**, pp.997–1008.
- Harris, Z.M., Spake, R. and Taylor, G. 2015. Land use change to bioenergy: A meta-analysis of soil carbon and GHG emissions. *Biomass and Bioenergy*. **82**, pp.27–39.
- Harte, J. and Kinzig, A.P. 1997. On the Implications of Species-Area Relationships for Endemism, Spatial Turnover, and Food Web Patterns. *Oikos*. **80**(3), pp.417–427.
- Hartman, J.C., Nippert, J.B., Orozco, R.A. and Springer, C.J. 2011. Potential ecological impacts of switchgrass (*Panicum virgatum* L.) biofuel cultivation in the Central Great Plains, USA. *Biomass and Bioenergy*. **35**(8), pp.3415–3421.
- Harvey, C.A., Dickson, B. and Kormos, C. 2010. Opportunities for achieving biodiversity conservation through REDD. *Conservation Letters*. **3**(1), pp.53–61.
- Haughton, A.J., Bohan, D.A., Clark, S.J., Mallott, M.D., Mallott, V., Sage, R. and Karp, A. 2016. Dedicated biomass crops can enhance biodiversity in the arable landscape. *GCB Bioenergy*. **8**(6), pp.1071–1081.
- Havlík, P., Schneider, U.A., Schmid, E., Böttcher, H., Fritz, S., Skalský, R., Aoki, K., Cara, S. De, Kindermann, G., Kraxner, F., Leduc, S., McCallum, I., Mosnier, A., Sauer, T. and Obersteiner, M. 2011. Global land-use implications of first and second generation biofuel targets. *Energy Policy*. **39**(10), pp.5690–5702.
- Haxeltine, A. and Prentice, I.C. 1996. BIOME3: An equilibrium terrestrial biosphere model based on ecophysiological constraints, resource availability, and competition among plant functional types. *Global Biogeochemical Cycles*. **10**(4), pp.693–709.
- Haxeltine, A., Prentice, I.C. and Creswell, I.D. 1996. A coupled carbon and water flux model to predict vegetation structure. *Journal of Vegetation Science*. **7**(5), pp.651–666.

- He, F. and Hubbell, S.P. 2011. Species-area relationships always overestimate extinction rates from habitat loss. , pp.3–6.
- Heald, C.L. and Geddes, J.A. 2016. The impact of historical land use change from 1850 to 2000 on secondary particulate matter and ozone. *Atmospheric Chemistry and Physics*. **16**(23), pp.14997–15010.
- Heck, V., Gerten, D., Lucht, W. and Popp, A. 2018. Biomass-based negative emissions difficult to reconcile with planetary boundaries. *Nature Climate Change*. **8**(2), pp.151–155.
- Heilmayr, R., Rausch, L.L., Munger, J. and Gibbs, H.K. 2020. Brazil's Amazon Soy Moratorium reduced deforestation. *Nature Food*. **1**(12), pp.801–810.
- Heimann, M. and Reichstein, M. 2008. Terrestrial ecosystem carbon dynamics and climate feedbacks. *Nature*. **451**(7176), pp.289–292.
- Hellmann, F. and Verburg, P.H. 2010. Impact assessment of the European biofuel directive on land use and biodiversity. *Journal of Environmental Management*. **91**(6), pp.1389–1396.
- Henry, R.C., Engström, K., Olin, S., Alexander, P., Arneeth, A. and Rounsevell, M.D.A. 2018. Food supply and bioenergy production within the global cropland planetary boundary. *PLoS ONE*. **13**(3), pp.1–17.
- Hertwich, E.G., Aaberg, M., Singh, B. and Strømman, A.H. 2008. Life-cycle Assessment of Carbon Dioxide Capture for Enhanced Oil Recovery. *Chinese Journal of Chemical Engineering*. **16**(3), pp.343–353.
- Hewitt, C.N., MacKenzie, A.R., Di Carlo, P., Di Marco, C.F., Dorsey, J.R., Evans, M., Fowler, D., Gallagher, M.W., Hopkins, J.R., Jones, C.E., Langford, B., Lee, J.D., Lewis, A.C., Lim, S.F. and ... 2009. Nitrogen management is essential to prevent tropical oil palm plantations from causing ground-level ozone pollution. *Proceedings of the National Academy of Sciences of the United States of America*. **106**(44), pp.18447–18451.
- Highina, B.K., Bugaje, I.M., State, B., Umar, B. and State, B. 2014. A review on second generation biofuel: a comparison of its carbon footprints. *European Journal of Engineering and Technology*. **2**(2), pp.117–125.
- Hill, J., Nelson, E., Tilman, D., Polasky, S. and Tiffany, D. 2006. Environmental, economic, and energetic costs and benefits of biodiesel and ethanol biofuels. *Proceedings of the National Academy of Sciences of the United States of America*. **103**(30), pp.11206–11210.
- Van Der Hilst, F., Lesschen, J.P., Van Dam, J.M.C., Riksen, M., Verweij, P.A., Sanders, J.P.M. and Faaij, A.P.C. 2012. Spatial variation of environmental impacts of regional biomass chains. *Renewable and Sustainable Energy Reviews*. **16**(4), pp.2053–2069.
- Hof, C., Voskamp, A., Biber, M.F., Böhning-gaese, K. and Katharina, E. 2018. Bioenergy cropland expansion may offset positive effects of climate change mitigation for global vertebrate diversity.
- Holland, M.M. and Bitz, C.M. 2003. Polar amplification of climate change in coupled models. *Climate Dynamics*. **21**(3–4), pp.221–232.
- Houghton, R.A. and Hackler, J.L. 2008. *Carbon Flux to the Atmosphere from Land-Use Changes: 1850 to 1990*.
- Houghton, R.A., Hobbie, J.E., Melillo, J.M., Moore, B., Peterson, B.J., Shaver, G.R. and Woodwell, G.M. 1983. Changes in the Carbon Content of Terrestrial Biota and Soils between 1860 and 1980: A Net Release of CO<sub>2</sub> to the Atmosphere. *Ecological Society of America*. **53**(3), pp.235–262.
- Houghton, R.A., House, J.I., Pongratz, J., Van Der Werf, G.R., Defries, R.S., Hansen, M.C.,

- Le Quéré, C. and Ramankutty, N. 2012. Carbon emissions from land use and land-cover change. *Biogeosciences*. **9**(12), pp.5125–5142.
- Houghton, R.A. and Nassikas, A.A. 2017. Global and regional fluxes of carbon from land use and land cover change 1850–2015. *Global Biogeochemical Cycles*. **31**(3), pp.456–472.
- Hsu, T., French, K. and Major, R. 2010. Avian assemblages in eucalypt forests, plantations and pastures in northern NSW, Australia. *Forest Ecology and Management*. **260**(6), pp.1036–1046.
- Hua, W., Chen, H., Sun, S. and Zhou, L. 2015. Assessing climatic impacts of future land use and land cover change projected with the CanESM2 model. *International Journal of Climatology*. **35**(12), pp.3661–3675.
- Hudson, L.N., Newbold, T., Contu, S., Hill, S.L.L., Lysenko, I., De Palma, A., Phillips, H.R.P., Alhusseini, T.I., Bedford, F.E., Bennett, D.J., Booth, H., Burton, V.J., Chng, C.W.T., Choimes, A., Correia, D.L.P. and ... 2017. The database of the PREDICTS (Projecting Responses of Ecological Diversity In Changing Terrestrial Systems) project. *Ecology and Evolution*. **7**(1), pp.145–188.
- Humpenöder, F., Popp, A., Bodirsky, B.L., Weindl, I., Biewald, A., Lotze-Campen, H., Dietrich, J.P., Klein, D., Kreidenweis, U., Müller, C., Rolinski, S. and Stevanovic, M. 2018a. Large-scale bioenergy production: how to resolve sustainability trade-offs? *Environ. Res. Lett.* **13**.
- Humpenöder, F., Popp, A., Bodirsky, B.L., Weindl, I., Biewald, A., Lotze-Campen, H., Dietrich, J.P., Klein, D., Kreidenweis, U., Müller, C., Rolinski, S. and Stevanovic, M. 2018b. Supplementary Information: Large-scale bioenergy production: how to resolve sustainability trade-offs? *Environmental Research Letters*. **13**.
- Huppmann, D., Kriegler, E., Krey, V., Riahi, K., Rogelj, J., Calvin, K., Humpenoeder, F., Popp, A., Rose, S.K., Weyant, J., Bauer, N., Bertram, C., Bosetti, V., Doelman, J., Drouet, L. and ... 2019. IAMC 1.5°C scenario explorer and data hosted by IIASA. In: Integrated Assessment Modeling Consortium & International Institute for Applied Systems Analysis. *IIASA*.
- Hurt, G.C., Chini, L.P., Frohling, S., Betts, R. a., Feddema, J., Fischer, G., Fisk, J.P., Hibbard, K., Houghton, R. a., Janetos, a., Jones, C.D., Kindermann, G., Kinoshita, T., Klein Goldewijk, K., Riahi, K., Shevliakova, E., Smith, S., Stehfest, E., Thomson, a., Thornton, P., van Vuuren, D.P. and Wang, Y.P. 2011. Harmonization of land-use scenarios for the period 1500-2100: 600 years of global gridded annual land-use transitions, wood harvest, and resulting secondary lands. *Climatic Change*. **109**(1), pp.117–161.
- Hurt, G.C., Chini, L.P., Frohling, S., Betts, R., Feddema, J., Fischer, G., Goldewijk, K.K., Hibbard, K., Janetos, A., Jones, C., Kindermann, G., Kinoshita, T., Riahi, K., Shevliakova, E. and Smith, S. 2009. Harmonisation of global land-use scenarios for the period 1500–2100 for IPCC-AR5. *iLEAPS*. (7), pp.6–8.
- I.E.A 2016. Key world energy statistics. *International Energy Agency*.
- IEA 2009. *Bioenergy – a sustainable and reliable energy source: a review of status and prospects*. Ausilio Bauen, Göran Berndes, Martin Junginger, François Vuille.
- IEA 2017. *Technology Roadmap: Delivering Sustainable Bioenergy*.
- IEA 2020. *World Energy Outlook 2020* [Online]. Available from: <https://iea.blob.core.windows.net/assets/a72d8abf-de08-4385-8711-b8a062d6124a/WEO2020.pdf>.

- IIASA 2009. International Institute for Applied Systems Analysis - RCP Database (version 2.0.5). Available from: <https://tntcat.iiasa.ac.at/RcpDb/dsd?Action=htmlpage&page=about>.
- IIASA 2018a. International Institute for Applied Systems Analysis - SSP Database (Shared Socioeconomic Pathways) - Version 2.0. Available from: <https://tntcat.iiasa.ac.at/SspDb/dsd?Action=htmlpage&page=about>.
- IIASA 2018b. Shared Socioeconomic Pathway (SSP) Database 2.0. Available from: <https://tntcat.iiasa.ac.at/SspDb/dsd?Action=htmlpage&page=about>.
- Immerzeel, D.J., Verweij, P.A., van der Hilst, F. and Faaij, A.P.C. 2014. Biodiversity impacts of bioenergy crop production: A state-of-the-art review. *GCB Bioenergy*. 6(3), pp.183–209.
- IPBES 2019. *Global assessment report on biodiversity and ecosystem services of the Intergovernmental Science-Policy Platform on Biodiversity and Ecosystem Services*, Brondizio, E. S., Díaz, S., Settele, J., Ngo, H. T. (eds) [Online]. Bonn, Germany. Available from: <https://doi.org/10.5281/zenodo.3553458>.
- IPCC 2013. *Climate Change 2013: The Physical Science Basis. Contribution of Working Group I to the Fifth Assessment Report of the Intergovernmental Panel on Climate Change* [T. F. Stocker et al. (eds.)]. Cambridge University Press, Cambridge, United Kingdom and New York, NY, USA.
- IPCC 2014. *Climate Change 2014: Synthesis Report. Contribution of Working Groups I, II and III to the Fifth Assessment Report of the Intergovernmental Panel on Climate Change* [R.K. Pachauri et al. (eds.)]. Cambridge University Press, Cambridge, United Kingdom and New York, NY, USA.
- IPCC 2021. *Climate Change 2021: The Physical Science Basis. Contribution of Working Group I to the Sixth Assessment Report of the Intergovernmental Panel on Climate Change* [V. P. Masson-Delmotte et al. (eds.)]. Cambridge University Press, Cambridge, United Kingdom and New York, NY, USA.
- IPCC 2022a. *Climate Change 2022: Impacts, Adaptation, and Vulnerability. Contribution of Working Group II to the Sixth Assessment Report of the Intergovernmental Panel on Climate Change* [H.-O. Pörtner et al. (eds.)]. Cambridge University Press, Cambridge, United Kingdom and New York, NY, USA.
- IPCC 2022b. *Climate Change 2022: Mitigation of Climate Change. Contribution of Working Group III to the Sixth Assessment Report of the Intergovernmental Panel on Climate Change* [P.R. Shukla et al. (eds.)]. Cambridge University Press, Cambridge, UK and New York, NY, USA.
- IPCC 2019. *Climate Change and Land: an IPCC special report on climate change, desertification, land degradation, sustainable land management, food security, and greenhouse gas fluxes in terrestrial ecosystems* [P.R. Shukla et al. (eds.)]. Cambridge University Press, Cambridge, UK and New York, USA.
- IPCC 2018. *Global Warming of 1.5°C. An IPCC Special Report on the impacts of global warming of 1.5°C above pre-industrial levels and related global greenhouse gas emission pathways, in the context of strengthening the global response to the threat of climate change*. Cambridge University Press, Cambridge, United Kingdom and New York, USA.
- IPCC 2005. *IPCC Special Report on Carbon Dioxide Capture and Storage*. [B. O. Metz (eds.)]. Prepared by Working Group III of the Intergovernmental Panel on Climate Change. Cambridge University Press, Cambridge, United Kingdom and New York, NY, USA.

- IPCC 2012. *Renewable Energy Sources and Climate Change Mitigation: Special Report of the Intergovernmental Panel on Climate Change*, [O. Edenhofer et al. (eds.)]. Cambridge University Press, Cambridge, United Kingdom and New York, NY, USA.
- IPCC 2011. *Summary for Policymakers*. In: *IPCC Special Report on Renewable Energy Sources and Climate Change Mitigation* [O. Edenhofer, R. Pichs-Madruga, Y. Sokona, K. Seyboth, P. Matschoss, S. Kadner, T. Zwickel, P. Eickemeier, G. Hansen, S. Schlömer, C. von Stechow. Cambridge, United Kingdom and New York, NY, USA.
- IRENA 2019. *Bioenergy from boreal forests: Swedish approach to sustainable wood use*. International Renewable Energy Agency, Abu Dhabi.
- IUCN 2018. International Union for Conservation of Nature (IUCN) Red List of Threatened Species.
- IUCN 2022a. IUCN Red List of Threatened Species: Spatial Data Download. *IUCN Red List*. [Online]. Available from: <https://www.iucnredlist.org/resources/spatial-data-download>.
- IUCN 2022b. The IUCN Red List of Threatened Species. Summary Statistics. Available from: <https://www.iucnredlist.org/resources/summary-statistics#Summary Tables>.
- Jackson, L.P., Grinsted, A. and Jevrejeva, S. 2018. 21st Century Sea-Level Rise in Line with the Paris Accord. *Earth's Future*. **6**(2), pp.213–229.
- Jantz, S.M., Barker, B., Brooks, T.M., Chini, L.P., Huang, Q., Moore, R.M., Noel, J. and Hurtt, G.C. 2015. Future habitat loss and extinctions driven by land-use change in biodiversity hotspots under four scenarios of climate-change mitigation. *Conservation Biology*. **29**(4), pp.1122–1131.
- Jetz, W., Wilcove, D.S. and Dobson, A.P. 2007. Projected impacts of climate and land-use change on the global diversity of birds. *PLoS Biology*. **5**(6), pp.1211–1219.
- Jevrejeva, S., Grinsted, A. and Moore, J.C. 2014. Upper limit for sea level projections by 2100. *Environmental Research Letters*. **9**(10).
- Jia, G., Shevliakova, E., Artaxo, P., Noblet-Ducoudré, N. De, Houghton, R., House, J., Kitajima, K., Lennard, C., Popp, A., Sirin, A., Sukumar, R. and Verchot, L. 2019. *Land–climate interactions*. In: *Climate Change and Land: an IPCC special report on climate change, desertification, land degradation, sustainable land management, food security, and greenhouse gas fluxes in terrestrial ecosystems* [P.R. Shukla ...].
- Johns, T.C., Gregory, J.M., Ingram, W.J., Johnson, C.E., Jones, A., Lowe, J.A., Mitchell, J.F.B., Roberts, D.L., Sexton, D.M.H., Stevenson, D.S., Tett, S.F.B. and Woodage, M.J. 2003. Anthropogenic climate change for 1860 to 2100 simulated with the HadCM3 model under updated emissions scenarios. *Climate Dynamics*. **20**(6), pp.583–612.
- Johnston, M., Foley, J. a, Holloway, T., Gibbs, H.K., Johnston, M., Foley, J. a, Holloway, T., Monfreda, C., Ramankutty, N. and Zaks, D. 2008. Carbon payback times for crop-based biofuel expansion in the tropics: the effects of changing yield and technology. *Environmental Research Letters*. **3**(3), p.034001.
- Jones, A.D., Collins, W.D., Edmonds, J., Torn, M.S., Janetos, A., Calvin, K. V., Thomson, A., Chini, L.P., Mao, J., Shi, X., Thornton, P., Hurtt, G.C. and Wise, M. 2013. Greenhouse gas policy influences climate via direct effects of land-use change. *Journal of Climate*. **26**(11), pp.3657–3670.
- Jones, C.D., Ciais, P., Davis, S.J., Friedlingstein, P., Gasser, T., Peters, G.P., Rogelj, J., van Vuuren, D.P., Canadell, J.G., Cowie, A., Jackson, R.B., Jonas, M., Kriegler, E., Littleton, E., Lowe, J.A., Milne, J., Shrestha, G., Smith, P., Torvanger, A. and Wiltshire, A. 2016.



- Simulating the Earth system response to negative emissions. *Environmental Research Letters*. **11**(9), p.095012.
- Kaplan, J.O. 2001. *Geophysical Applications of Vegetation Modeling*.
- Keller, D.P., Lenton, A., Scott, V., Vaughan, N.E., Bauer, N., Ji, D., Jones, C.D., Kravitz, B., Muri, H. and Zickfeld, K. 2018. The Carbon Dioxide Removal Model Intercomparison Project (CDRMIP): Rationale and experimental protocol for CMIP6. *Geoscientific Model Development*. **11**(3), pp.1133–1160.
- Kessler, J.J., Rood, T., Tekelenburg, T. and Bakkenes, M. 2007. Biodiversity and socioeconomic impacts of selected agro-commodity production systems. *Journal of Environment and Development*. **16**(2), pp.131–160.
- Kicklighter, D.W., Gurgel, A.C., Melillo, J.M., Reilly, J.M. and Paltsev, S. 2012. *Potential Direct and Indirect Effects of Global Cellulosic Biofuel Production on Greenhouse Gas Fluxes from Future Land-Use Change*. Joint Program Report Series Report 210.
- Kim, S. and Dale, B.E. 2005. Life cycle assessment of various cropping systems utilized for producing biofuels: Bioethanol and biodiesel. *Biomass and Bioenergy*. **29**(6), pp.426–439.
- Kim, S., Dale, B.E., Heijungs, R., Azapagic, A., Darlington, T. and Kahlbaum, D. 2014. Indirect land use change and biofuels: Mathematical analysis reveals a fundamental flaw in the regulatory approach. *Biomass and Bioenergy*. **71**, pp.408–412.
- Kinzig, A.P. and Harte, J. 2000. Implications of Endemics-Area Relationships for Estimates of Species Extinctions. *Ecology*. **81**(12), p.3305.
- Kline, K.L., Msangi, S., Dale, V.H., Woods, J., Souza, G.M., Osseweijer, P., Clancy, J.S., Hilbert, J.A., Johnson, F.X., McDonnell, P.C. and Muger, H.K. 2017. Reconciling food security and bioenergy: priorities for action. *GCB Bioenergy*. **9**(3), pp.557–576.
- Klink, C.A. and Machado, R.B. 2005. Conservation of the Brazilian Cerrado. *Conservation Biology*. **19**(3), pp.707–713.
- Köberle, A.C. 2019. The Value of BECCS in IAMs: a Review. *Current Sustainable/Renewable Energy Reports*. **6**(4), pp.107–115.
- Koh, L.P., Miettinen, J., Liew, S.C. and Ghazoul, J. 2011. Remotely sensed evidence of tropical peatland conversion to oil palm. *Proceedings of the National Academy of Sciences of the United States of America*. **108**(12), pp.5127–5132.
- Koh, L.P. and Wilcove, D.S. 2008. Is oil palm agriculture really destroying tropical biodiversity? *Conservation Letters*. **1**(2), pp.60–64.
- Krause, A., Bayer, A.D., Pugh, T.A.M., Doelman, J.C., Humpenöder, F., Anthoni, P., Olin, S., Bodirsky, B.L., Popp, A., Stehfest, E. and Arneeth, A. 2017. Global consequences of afforestation and bioenergy cultivation on ecosystem service indicators. *Biogeosciences Discussions*. (May), pp.1–42.
- Krause, M., Lotze-Campen, H., Popp, A., Dietrich, J.P. and Bonsch, M. 2013. Conservation of undisturbed natural forests and economic impacts on agriculture. *Land Use Policy*. **30**(1), pp.344–354.
- Kraxner, F., Nordström, E.M., Havlík, P., Gusti, M., Mosnier, A., Frank, S., Valin, H., Fritz, S., Fuss, S., Kindermann, G., McCallum, I., Khabarov, N., Böttcher, H., See, L., Aoki, K., Schmid, E., Máthé, L. and Obersteiner, M. 2013. Global bioenergy scenarios - Future forest development, land-use implications, and trade-offs. *Biomass and Bioenergy*. **57**, pp.86–96.

- Kriegler, E., Edmonds, J., Hallegatte, S., Ebi, K.L., Kram, T., Riahi, K., Winkler, H. and van Vuuren, D.P. 2014. A new scenario framework for climate change research: The concept of shared climate policy assumptions. *Climatic Change*. **122**(3), pp.401–414.
- Kularathne, I.W., Gunathilake, C.A., Rathneweera, A.C., Kalpage, C.S. and Rajapakse, S. 2019. The effect of use of biofuels on environmental pollution-A review. *International Journal of Renewable Energy Research*. **9**(3), pp.1355–1367.
- Kumar, R.R., Rao, P.H. and Arumugam, M. 2015. Lipid extraction methods from microalgae: A comprehensive review. *Frontiers in Energy Research*. **3**(JAN).
- Kurz, W.A., Dymond, C.C., White, T.M., Stinson, G., Shaw, C.H., Rampley, G.J., Smyth, C., Simpson, B.N., Neilson, E.T., Trofymow, J.A., Metsaranta, J. and Apps, M.J. 2009. CBM-CFS3: A model of carbon-dynamics in forestry and land-use change implementing IPCC standards. *Ecological Modelling*. **220**(4), pp.480–504.
- Kvalevåg, M.M., Myhre, G. and Levis, S. 2012. Anthropogenic land cover changes in a GCM with surface albedo changes based on MODIS data. . **2117**(September 2009), pp.2105–2117.
- Ladanai, S. and Vinterbäck, J. 2010. Certification Criteria for Sustainable Biomass for Energy. , p.45.
- Laguë, M.M. and Swann, A.L.S. 2016. Progressive midlatitude afforestation: Impacts on clouds, global energy transport, and precipitation. *Journal of Climate*. **29**(15), pp.5561–5573.
- Lal, R. 2004. Soil carbon sequestration impacts on global climate change and food security. *Science*. **304**(5677), pp.1623–1627.
- Lapola, D.M., Schaldach, R., Alcamo, J., Bondeau, A., Koch, J. and Koelking, C. 2010. Indirect land-use changes can overcome carbon savings from biofuels in Brazil. *PNAS*. **107**(8), pp.3388–3393.
- Lardon, L., Hélias, A., Sialve, B., Steyer, J.P. and Bernard, O. 2009. Life-cycle assessment of biodiesel production from microalgae. *Environmental Science and Technology*. **43**(17), pp.6475–6481.
- Larson, E.D. 2006. A review of life-cycle analysis studies on liquid biofuel systems for the transport sector. *Energy for Sustainable Development*. **10**(2), pp.109–126.
- Laurance, W.F., Carolina Useche, D., Rendeiro, J., Kalka, M., Bradshaw, C.J.A., Sloan, S.P., Laurance, S.G., Campbell, M., Abernethy, K., Alvarez, P., Arroyo-Rodriguez, V., Ashton, P., Benítez-Malvido, J., Blom, A. and ... 2012. Averting biodiversity collapse in tropical forest protected areas. *Nature*. **489**(7415), pp.290–293.
- Lauri, P., Forsell, N., Gusti, M., Korosuo, A., Havlík, P. and Obersteiner, M. 2019. Global Woody Biomass Harvest Volumes and Forest Area Use under Different SSP-RCP Scenarios. *Journal of Forest Economics*. **34**(3–4), pp.285–309.
- Lawrence, D., Coe, M., Walker, W., Verchot, L. and Vandecar, K. 2022. The Unseen Effects of Deforestation: Biophysical Effects on Climate. *Frontiers in Forests and Global Change*. **5**(March), pp.1–13.
- Lawrence, D. and Vandecar, K. 2015. Effects of tropical deforestation on climate and agriculture. *Nature Climate Change*. **5**(1), pp.27–36.
- Lawrence, P.J., Feddema, J.J., Bonan, G.B., Meehl, G.A., O'Neill, B.C., Oleson, K.W., Levis, S., Lawrence, D.M., Kluzek, E., Lindsay, K. and Thornton, P.E. 2012. Simulating the biogeochemical and biogeophysical impacts of transient land cover change and wood

- harvest in the Community Climate System Model (CCSM4) from 1850 to 2100. *Journal of Climate*. **25**(9), pp.3071–3095.
- Lawrence, P.J., Lawrence, D.M. and Hurtt, G.C. 2018. Attributing the Carbon Cycle Impacts of CMIP5 Historical and Future Land Use and Land Cover Change in the Community Earth System Model (CESM1). *Journal of Geophysical Research: Biogeosciences*. **123**(5), pp.1732–1755.
- Leadley, P., Pereira, H.M., Alkemade, R., Fernandez-Manjarres, J.F., Proenca, V. and Scharlemann, J.P.W. 2010. *Biodiversity scenarios: projections of 21st century change in biodiversity and associated ecosystem services*. In: *Secretariat of the Convention on Biological Diversity (ed. Diversity SotCoB)*. Secretariat of the Convention on Biological Diversity, Montreal, Canada.
- Leal, M.R.L.V., Duft, D.G., Hernandez, T.A.D. and Bordonal, R.O. 2017. Brazilian sugarcane expansion and deforestation. *European Biomass Conference and Exhibition Proceedings*. **2017**(25thEUBCE), pp.1476–1483.
- Leclère, D., Obersteiner, M., Alkemade, R., Almond, R., Barrett, M., Bunting, G., Burgess, N.D., Butchart, S.H.M., Chaudhary, A., Cornell, S., De Palma, A., DeClerk, F.A.J., Fujimori, S., Grooten, M., Harfoot, M., Harwood, T., Hasegawa, T., Havlík, P., Hellweg, S., Herrero, M. and Hilbers, J.P. 2018. *Towards pathways bending the curve of terrestrial biodiversity trends within the 21st century*. IIASA, Laxenburg, Austria.
- Lee, X., Goulden, M.L., Hollinger, D.Y., Barr, A., Black, T.A., Bohrer, G., Bracho, R., Drake, B., Goldstein, A., Gu, L., Katul, G., Kolb, T., Law, B.E., Margolis, H., Meyers, T., Monson, R., Munger, W., Oren, R., Paw U, K.T., Richardson, A.D., Schmid, H.P., Staebler, R., Wofsy, S. and Zhao, L. 2011. Observed increase in local cooling effect of deforestation at higher latitudes. *Nature*. **479**(7373), pp.384–387.
- van Leeuwen, J. 2017. Synergies and trade-offs between bioenergy use and the UN sustainable development goals.
- Leimbach, M., Bauer, N. and Baumstark, L. 2010. Technological Change and International Trade – Insights from REMIND-R. *The Energy Journal*. **31**(1), pp.1786–1793.
- Leimbach, M., Bauer, N., Baumstark, L. and Edenhofer, O. 2010. Mitigation costs in a globalized world: Climate policy analysis with REMIND-R. *Environmental Modeling and Assessment*. **15**(3), pp.155–173.
- Lemma, B., Kleja, D.B., Nilsson, I. and Olsson, M. 2006. Soil carbon sequestration under different exotic tree species in the southwestern highlands of Ethiopia. *Geoderma*. **136**(3–4), pp.886–898.
- Li, D., Niu, S. and Luo, Y. 2012. Global patterns of the dynamics of soil carbon and nitrogen stocks following afforestation: A meta-analysis. *New Phytologist*. **195**(1), pp.172–181.
- Li, W., Ciais, P., Peng, S., Yue, C., Wang, Y., Thurner, M. and Saatchi, S.S. 2017. Land-use and land-cover change carbon emissions between 1901 and 2012 constrained by biomass observations. . (May), pp.5053–5067.
- Li, Y., Zhao, M., Motesharrei, S., Mu, Q., Kalnay, E. and Li, S. 2015. Local cooling and warming effects of forests based on satellite observations. *Nature Communications*. **6**.
- Liao, W., Rigden, A.J. and Li, D. 2018. Attribution of Local Temperature Response to Deforestation. *Journal of Geophysical Research: Biogeosciences*. **123**(5), pp.1572–1587.
- Lima, M., Skutsch, M. and de Medeiros Costa, G. 2011. Deforestation and the social impacts of soy for biodiesel: Perspectives of farmers in the south Brazilian Amazon. *Ecology and*

*Society*. **16**(4).

- Loarie, S.R., Lobell, D.B., Asner, G.P., Mu, Q. and Field, C.B. 2011. Direct impacts on local climate of sugar-cane expansion in Brazil. *Nature Climate Change*. **1**(2), pp.105–109.
- Loh, J. 2000. *Living Planet Report 2000*. Gland, Switzerland.
- Longobardi, P., Montenegro, A., Beltrami, H. and Eby, M. 2016. Deforestation induced climate change: Effects of spatial scale. *PLoS ONE*. **11**(4).
- Lorenzen, E.D., Nogués-Bravo, D., Orlando, L., Weinstock, J., Binladen, J., Marske, K.A., Ugan, A., Borregaard, M.K., Gilbert, M.T.P., Nielsen, R., Ho, S.Y.W., Goebel, T., Graf, K.E., Byers, D. and Stenderup, J.T. 2011. Species-specific responses of Late Quaternary megafauna to climate and humans. *Nature*. **479**(7373), pp.359–364.
- Lotze-Campen, H., Müller, C., Bondeau, A., Rost, S., Popp, A. and Lucht, W. 2008. Global food demand, productivity growth, and the scarcity of land and water resources: A spatially explicit mathematical programming approach. *Agricultural Economics*. **39**(3), pp.325–338.
- Lotze-Campen, H., Popp, A., Beringer, T., Müller, C., Bondeau, A., Rost, S. and Lucht, W. 2010. Scenarios of global bioenergy production: The trade-offs between agricultural expansion, intensification and trade. *Ecological Modelling*. **221**(18), pp.2188–2196.
- Louette, G., Maes, D., Alkemade, J.R.M., Boitani, L., de Knegt, B., Eggers, J., Falcucci, A., Framstad, E., Hagemeijer, W., Hennekens, S.M., Maiorano, L., Nagy, S., Serradilla, A.N., Ozinga, W.A., Schaminée, J.H.J., Tsiaousi, V., van Tol, S. and Delbaere, B. 2010. BioScore-Cost-effective assessment of policy impact on biodiversity using species sensitivity scores. *Journal for Nature Conservation*. **18**(2), pp.142–148.
- Loyn, R.H., McNabb, E.G., Macak, P. and Noble, P. 2007. Eucalypt plantations as habitat for birds on previously cleared farmland in south-eastern Australia. *Biological Conservation*. **137**(4), pp.533–548.
- Luderer, G., Leimbach, M., Bauer, N., Kriegler, E., Aboumahboub, T., Curras, A., Baumstark, L., Bertram, C., Giannousakis, A., Hilaire, J., Klein, D., Mouratiadou, I., Pietzcker, R., Piontek, F., Roming, N., Schwanitz, V.J. and Strefler, J. 2013. *Description of the REMIND model (Version 1 . 5)*. Potsdam Institute for Climate Impact Research (PIK), Potsdam, Germany.
- Luysaert, S., Jammot, M., Stoy, P.C., Estel, S., Pongratz, J., Ceschia, E., Churkina, G., Don, A., Erb, K., Ferlicoq, M., Gielen, B., Grünwald, T., Houghton, R.A., Klumpp, K. and ... 2014. Land management and land-cover change have impacts of similar magnitude on surface temperature. *Nature Climate Change*. **4**(5), pp.389–393.
- Maddox, T., Priatna, D., Gemita, E. and Salampessy, A. 2007. *The conservation of tigers and other wildlife in oil palm plantations*. The Zoological Society of London, Regents Park, London.
- Malavasi, E.O. and Kellenberg, J. 2002. *Program of Payments for Ecological Services in Costa Rica* [Online]. Costa Rica, United Kingdom. Available from: [http://ecosystemmarketplace.com/documents/cms\\_documents/lr\\_ortiz\\_kellenberg\\_ext.pdf](http://ecosystemmarketplace.com/documents/cms_documents/lr_ortiz_kellenberg_ext.pdf).
- Malcolm, J.R., Liu, C., Neilson, R.P., Hansen, L. and Hannah, L. 2006. Global warming and extinctions of endemic species from biodiversity hotspots. *Conservation Biology*. **20**(2), pp.538–548.
- Manabe, S. 1969. Climate and the ocean circulation, I, the atmospheric circulation and the

- hydrology of the earth's surface. *Monthly Weather Review*. **97**(11), pp.739–774.
- Margules, C.R. and Pressey, R.L. 2000. Systematic conservation planning. *Nature*. **405**(6783), pp.243–253.
- Marland, G., Boden, T.A. and J., A.R. 2013. Global, Regional and National Fossil Fuel CO<sub>2</sub> Emissions. *Carbon Dioxide Information Analysis Center (CDIAC)*. [Online]. Available from: [http://cdiac.esd.ornl.gov/trends/emis/em\\_cont.html](http://cdiac.esd.ornl.gov/trends/emis/em_cont.html).
- Marland, G., Pielke, R.A., Apps, M., Avissar, R., Betts, R.A., Davis, K.J., Frumhoff, P.C., Jackson, S.T., Joyce, L.A., Kauppi, P., Katzenberger, J., MacDicken, K.G., Neilson, R.P., Niles, J.O., Niyogi, D.S., Norby, R.J., Pena, N., Sampson, N. and Xue, Y. 2003. The climatic impacts of land surface change and carbon management, and the implications for climate-change mitigation policy. *Climate Policy*. **3**(2), pp.149–157.
- Marquardt, S.G., Guindon, M., Wilting, H.C., Steinmann, Z.J.N., Sim, S., Kulak, M. and Huijbregts, M.A.J. 2019. Consumption-based biodiversity footprints – Do different indicators yield different results? *Ecological Indicators*. **103**, pp.461–470.
- Martinelli, L.A. and Filoso, S. 2008. Expansion of sugarcane ethanol production in Brazil: Environmental and social challenges. *Ecological Applications*. **18**(4), pp.885–898.
- Masripatin, N., Kurniawati, E.T., Zamzani, F., Budiharto, Asaad, I., Gunawan, W., Bagiono, R., Albar, I., Wibowo, H., Indrihastuti, D., Putra, A.P., Tosiani, A., Cipta, J.D., Oktavia, E.R., Carolyn, R.D., Wijanarka, K., Amelgia, R., Martadijaya, T.I. and Suyitno 2021. *Indonesia: REDD+ National Strategy 2021-2030*.
- Matthews, H.D. 2007. Implications of CO<sub>2</sub> fertilization for future climate change in a coupled climate – carbon model. *Global Change Biology*. **13**, pp.1068–1078.
- Matthews, H.D. 2004. *Land Cover Change, Vegetation Dynamics and The Global Carbon Cycle: Experiments with the UVic Earth System Climate Model*.
- Matthews, H.D., Gillett, N.P., Stott, P.A. and Zickfeld, K. 2009. The proportionality of global warming to cumulative carbon emissions. *Nature*. **459**, pp.10–14.
- Matthews, H.D., Weaver, a. J., Meissner, K.J., Gillett, N.P. and Eby, M. 2004. Natural and anthropogenic climate change: incorporating historical land cover change, vegetation dynamics and the global carbon cycle. *Climate Dynamics*. **22**, pp.461–479.
- Matthews, H.D., Weaver, A.J., Eby, M. and Meissner, K.J. 2003. Radiative forcing of climate by historical land cover change. *Geophysical Research Letters*. **30**(2), pp.25–28.
- May, R.M., Lawton, J.H. and Stork, N.E. 1995. *Assessing Extinction Rates in Extinction Rates*. Oxford, UK: Oxford University Press.
- Mayani-Parás, F., Botello, F., Castañeda, S., Munguía-Carrara, M. and Sánchez-Cordero, V. 2021. Cumulative habitat loss increases conservation threats on endemic species of terrestrial vertebrates in Mexico. *Biological Conservation*. **253**(June 2020).
- Mbow, C., Rosenzweig, C., Barioni, L.G., Benton, T.G., Herrero, M., Krishnapillai, M., E. Liwenga, P., Pradhan, M.G., Rivera-Ferre, Sapkota, T., Tubiello, F.N. and Xu, Y. 2019. *Food Security*. In: *Climate Change and Land: an IPCC special report on climate change, desertification, land degradation, sustainable land management, food security, and greenhouse gas fluxes in terrestrial ecosystems [P.R. Shukla et al. (eds.)]* [Online]. Available from: <https://burundi-food-securityhealthywealthywise.weebly.com/food-security.html>.
- McConnell, W.J. and Kull, C.A. 2014. Deforestation in Madagascar: Debates over the island's forest cover and challenges of measuring forest change. *Conservation and Environmental*

- Management in Madagascar.*, pp.67–104.
- McDonald, R.I., Kareiva, P. and Forman, R.T.T. 2008. The implications of current and future urbanization for global protected areas and biodiversity conservation. *Biological Conservation*. **141**(6), pp.1695–1703.
- McLeman, R. 2011. *Climate change, migration and critical international security considerations*.
- McMahon, S.M., Harrison, S.P., Armbruster, W.S., Bartlein, P.J., Beale, C.M., Edwards, M.E., Kattge, J., Midgley, G., Morin, X. and Prentice, I.C. 2011. Improving assessment and modelling of climate change impacts on global terrestrial biodiversity. *Trends in Ecology and Evolution*. **26**(5), pp.249–259.
- MEA 2005. *Ecosystems and human well-being -Synthesis of the Millennium Ecosystem Assessment*. Island Press, Washington, DC.
- Meehan, T.D., Hurlbert, A.H. and Gratton, C. 2010. Bird communities in future bioenergy landscapes of the Upper Midwest. *Proceedings of the National Academy of Sciences of the United States of America*. **107**(43), pp.18533–18538.
- Meehan, T.D., Werling, B.P., Landis, D.A. and Gratton, C. 2011. Agricultural landscape simplification and insecticide use in the Midwestern United States. *Proceedings of the National Academy of Sciences of the United States of America*. **108**(28), pp.11500–11505.
- Mehmood, M.A., Ibrahim, M., Rashid, U., Nawaz, M., Ali, S., Hussain, A. and Gull, M. 2017. Biomass production for bioenergy using marginal lands. *Sustainable Production and Consumption*. **9**, pp.3–21.
- Meier, J., Zabel, F. and Mauser, W. 2018. A global approach to estimate irrigated areas - A comparison between different data and statistics. *Hydrology and Earth System Sciences*. **22**(2), pp.1119–1133.
- Meijaard, E., J., G.-U., Sheil, D., Wich, S.A., Carlson, K.M., Juffe-Bignoli, D. and Brooks, T.. 2018. *Oil palm and biodiversity: a situation analysis by the IUCN Oil Palm Task Force*. Gland, Switzerland.
- Meissner, K.J., Weaver, A.J., Matthews, H.D. and Cox, P.M. 2003. The role of land surface dynamics in glacial inception: a study with the UVic Earth System Model. *Climate Dynamics*. **21**, pp.515–537.
- Melara, A.J., Singh, U. and Colosi, L.M. 2020. Is aquatic bioenergy with carbon capture and storage a sustainable negative emission technology? Insights from a spatially explicit environmental life-cycle assessment. *Energy Conversion and Management*. **224**, p.113300.
- Melillo, J.M., Gurgel, A.C., Kicklighter, D.W., Reilly, J.M., Cronin, T.W., Felzer, B.S., Paltsev, S., Schlosser, C., Sokolov, A.P. and Wang, X. 2009. *Unintended Environmental Consequences of a Global Biofuels Program*. MIT Joint Program on the Science and Policy of Global Change, Cambridge MA.
- Melillo, J.M., Reilly, J.M., Kicklighter, D.W., Gurgel, A.C., Cronin, T.W., Paltsev, S., Felzer, B.S., Wang, X., Sokolov, A.P. and Schlosser, C.A. 2009. Indirect Emissions from Biofuels: How Important? *Science*. **326**(5958), pp.1397–1399.
- Meller, L., van Vuuren, D.P. and Cabeza, M. 2015. Quantifying biodiversity impacts of climate change and bioenergy: the role of integrated global scenarios. *Regional Environmental Change*. **15**(6), pp.961–971.
- Mello, F.F.C., Cerri, C.E.P., Davies, C.A., Holbrook, N.M., Paustian, K., Maia, S.M.F.,

- Galdos, M. V., Bernoux, M. and Cerri, C.C. 2014. Payback time for soil carbon and sugar-cane ethanol. *Nature Climate Change*. **4**(7), pp.605–609.
- Menichetti, E. and Otto, M. 2009. Energy balance & greenhouse gas emissions of biofuels from a life cycle perspective. *Biofuels: Environmental consequences and interactions with changing land use*. (5), pp.81–109.
- Miles, L. and Kapos, V. 2008. Reducing greenhouse gas emissions from deforestation and forest degradation: Global land-use implications. *Science*. **320**(5882), pp.1454–1455.
- Millet, D.B., Apel, E., Henze, D.K., Hill, J., Marshall, J.D., Singh, H.B. and Tessum, C.W. 2012. Response to comment on ‘natural and anthropogenic ethanol sources in north America and potential atmospheric impacts of ethanol fuel use’. *Environmental Science and Technology*. **46**, 8484–8492.
- Minang, P.A., Van Noordwijk, M., Duguma, L.A., Alemagi, D., Do, T.H., Bernard, F., Agung, P., Robiglio, V., Catacutan, D., Suyanto, S., Armas, A., Silva Aguad, C., Feudjio, M., Galudra, G., Maryani, R., White, D., Widayati, A., Kahurani, E., Namirembe, S. and Leimona, B. 2014. REDD+ Readiness progress across countries: time for reconsideration. *Climate Policy*. **14**(6), pp.685–708.
- Mittermeier, R.A., van Dijk, P.P., Rhodin, A.G.J. and Nash, S.D. 2005. Hotspots Revisited: Earth’s Biologically Richest and Most Endangered Ecoregions. *Chelonian Conservation and Biology*. **14**(1), p.200.
- Mittermeier, R.A., Turner, W.R., Larsen, F.W., Brooks, T. and Gascon, C. 2011. *Global Biodiversity Conservation: The Critical Role of Hotspots*. In: *Biodiversity Hotspots* [Online]. Springer, Berlin, Germany. Available from: <http://www.springerlink.com/index/10.1007/978-3-642-20992-5>.
- Molden, D., Oweis, T., Steduto, P., Bindraban, P., Hanjra, M.A. and Kijne, J. 2010. Improving agricultural water productivity: Between optimism and caution. *Agricultural Water Management*. **97**(4), pp.528–535.
- Molotoks, A., Green, J. and West, C. 2020. Evaluating aspects of biodiversity loss, and associated indicators, for application to the assessment of the impacts of agricultural commodity trade. . (November), pp.1–38.
- Molotoks, A., Kuhnert, M., Dawson, T.P. and Smith, P. 2017. Global hotspots of conflict risk between food security and biodiversity conservation. *Land*. **6**(4), pp.1–15.
- Molotoks, A., Stehfest, E., Doelman, J., Albanito, F., Fitton, N., Dawson, T.P. and Smith, P. 2018. Global projections of future cropland expansion to 2050 and direct impacts on biodiversity and carbon storage. *Global Change Biology*. **24**(12), pp.5895–5908.
- Mondiale, B. 2008. *Rising food prices : Policy options and World Bank response* [Online]. Available from: <http://scholar.google.com/scholar?hl=en&btnG=Search&q=intitle:Rising+food+prices:+Policy+options+and+World+Bank+response#1>.
- Monteith, J.L. and Unsworth, M.H. 2008. *Microclimatology of Radiation (i)*. In *Principles of Environmental Physics*. Academic Press.
- Montenegro, A., Eby, M., Mu, Q., Mulligan, M., Weaver, A.J., Wiebe, E.C. and Zhao, M. 2009. The net carbon drawdown of small scale afforestation from satellite observations. *Global and Planetary Change*. **69**(4), pp.195–204.
- Moraes, M.M.G.A., Ringler, C. and Cai, X. 2011. Policies and instruments affecting water use for bioenergy production. Biofuels, Bioproducts and Biorefining, 5,. *Biofuels*,

- Bioproducts and Biorefining*. **5**, pp.431–444.
- Morita, K. and Matsumoto, K. 2018. REDD+ financing to enhance climate change mitigation and adaptation and biodiversity co-benefits: Lessons from the global environment facility. *AGRIVITA Journal of Agricultural Science*. **40**(1), pp.118–130.
- Morton, D.C., DeFries, R.S., Shimabukuro, Y.E., Anderson, L.O., Arai, E., Del Bon Espirito-Santo, F., Freitas, R. and Morisette, J. 2006. Cropland expansion changes deforestation dynamics in the southern Brazilian Amazon. *Proceedings of the National Academy of Sciences of the United States of America*. **103**(39), pp.14637–14641.
- Morton, S. and Hill, R. 2014. *Biodiversity. Chapter 1: What is biodiversity and why is it important?* [Online]. Collingwood VIC. Available from: <https://www.publish.csiro.au/book/6967>.
- MPI 2009. LUCID-CMIP5 protocol. *Max-Planck-Institut für Meteorologie*. [Online]. Available from: <https://www.mpimet.mpg.de/en/science/the-land-in-the-earth-system/working-groups/climate-biogeosphere-interaction/lucid-cmip5/>.
- Mueller, N.D., Gerber, J.S., Johnston, M., Ray, D.K., Ramankutty, N. and Foley, J.A. 2012. Closing yield gaps through nutrient and water management. *Nature*. **490**(7419), pp.254–257.
- Müller, C. and Robertson, R.D. 2014. Projecting future crop productivity for global economic modeling. *Agricultural Economics (United Kingdom)*. **45**(1), pp.37–50.
- Muratori, M., Bauer, N., Rose, S.K., Wise, M., Daioglou, V., Cui, Y., Kato, E., Gidden, M., Streffer, J., Fujimori, S., Sands, R.D., van Vuuren, D.P. and Weyant, J. 2020. EMF-33 insights on bioenergy with carbon capture and storage (BECCS). *Climatic Change*. **163**(3), pp.1621–1637.
- Muri, H. 2018. The role of large-scale BECCS in the pursuit of the 1.5°C target: An Earth system model perspective. *Environmental Research Letters*. **13**(4).
- Myers, N., Fonseca, G.A.B., Mittermeier, R. a, Fonseca, G.A.B. and Kent, J. 2000. Biodiversity hotspots for conservation priorities. *Nature*. **403**(6772), pp.853–858.
- Nabuurs, G.-J., Mrabet, R., Abu, A.H., Bustamante, M., Clark, H., Havlík, P., House, J., Mbow, C., Ninan, K.N., Popp, A., Roe, S., Sohngen, B. and Towprayoon, S. 2022. *Agriculture, Forestry and Other Land Uses (AFOLU)*. In *IPCC, 2022: Climate Change 2022: Mitigation of Climate Change. Contribution of Working Group III to the Sixth Assessment Report of the Intergovernmental Panel on Climate Change [P.R. Shukla, J. Skea, R. Cambridge, UK and New York, NY, USA*.
- Nair, P.K.R., Kumar, B.M. and Nair, V.D. 2009. Agroforestry as a strategy for carbon sequestration. *Journal of Plant Nutrition and Soil Science*. **172**(1), pp.10–23.
- Nakićenović, N., Victor, N. and Morita, T. 1998. Emissions Scenarios Database and Review of Scenarios. *Mitigation and Adaptation Strategies for Global Change*. (3), pp.95–131.
- Narayanan, G.B. and Walmsley, T.L. 2008. Global Trade, Assistance, and Production: The GTAP 7 Data Base. *Center for Global Trade Analysis: Purdue University*.
- Nassar, A.M., Harfuch, L., Moreira, M.M.R., Bachion, L.C. and Antoniazzi, L.B. 2009. *Impacts on land use and GHG emissions from a shock on Brazilian sug- arcane ethanol exports to the United States using the Brazilian Land Use Model (BLUM)*. *Institute for International Trade Negotiations (ICONE)*. São Paulo, Brazil.
- National Snow and Ice Data Center 2019. State of the Cryosphere. Available from: [https://nsidc.org/cryosphere/sotc/sea\\_ice.html](https://nsidc.org/cryosphere/sotc/sea_ice.html).



- Nave, L.E., Vance, E.D., Swanston, C.W. and Curtis, P.S. 2010. Harvest impacts on soil carbon storage in temperate forests. *Forest Ecology and Management*. **259**(5), pp.857–866.
- Negash, M. and Swinnen, J.F.M. 2013. Biofuels and food security: Micro-evidence from Ethiopia. *Energy Policy*. **61**, pp.963–976.
- Nelson, A. 2008. Estimated travel time to the nearest city of 50,000 or more people in year 2000. *Global Environment Monitoring Unit - Joint Research Centre of the European Commission: Ispra Italy*.
- Newbold, T., Hudson, L.N., Hill, S.L.L., Contu, S., Lysenko, I., Senior, R.A., Börger, L., Bennett, D.J., Choimes, A., Collen, B., Day, J., De Palma, A., Díaz, S., Echeverria-Londoño, S., Edgar, M.J. and ... 2015. Global effects of land use on local terrestrial biodiversity. *Nature*. **520**(7545), pp.45–50.
- Nguyen, Q., Bowyer, J., Howe, J., Bratkovich, S., Groot, H., Pepke, E. and Fernholz, K. 2017. Global Production of Second Generation Biofuels: Trends and Influences. *Biofuels/Biorefinery Development Report Card*. (265896), pp.1–15.
- Nijssen, M., Smeets, E., Stehfest, E. and van Vuuren, D.P. 2012. An evaluation of the global potential of bioenergy production on degraded lands. *GCB Bioenergy*. **4**(2), pp.130–147.
- De Noblet-Ducoudré, N., Boisier, J.P., Pitman, A., Bonan, G.B., Brovkin, V., Cruz, F., Delire, C., Gayler, V., Van Den Hurk, B.J.J.M., Lawrence, P.J., Van Der Molen, M.K., Müller, C., Reick, C.H., Strengers, B.J. and Voldoire, A. 2012. Determining robust impacts of land-use-induced land cover changes on surface climate over North America and Eurasia: Results from the first set of LUCID experiments. *Journal of Climate*. **25**(9), pp.3261–3281.
- Noh, J. kyoung, Echeverría, C., Pauchard, A. and Cuenca, P. 2019. Extinction debt in a biodiversity hotspot: the case of the Chilean Winter Rainfall-Valdivian Forests. *Landscape and Ecological Engineering*. **15**(1), pp.1–12.
- Noone, K.J., Chaplin III, F.S., Persson, Å. and Folke, C. 2013. A safe operating space for humanity. *Nature*. **461**.
- Nowak, R.M. 1999. *Walker's Mammals of the World*. Baltimore, Maryland: Johns Hopkins University Press.
- Núñez-Regueiro, M.M., Siddiqui, S.F. and Fletcher, R.J. 2021. Effects of bioenergy on biodiversity arising from land-use change and crop type. *Conservation Biology*. **35**(1), pp.77–87.
- Nunez, S., Arets, E., Alkemade, R., Verwer, C. and Leemans, R. 2019. Assessing the impacts of climate change on biodiversity: is below 2 °C enough? *Climatic Change*. **154**(3–4), pp.351–365.
- O'Neill, B.C., Kriegler, E., Ebi, K.L., Kemp-Benedict, E., Riahi, K., Rothman, D.S., Van Ruijven, B.J., Van Vuuren, D.P., Birkmann, J., Kok, K., Levy, M. and Solecki, W. 2015. The roads ahead: Narratives for shared socioeconomic pathways describing world futures in the 21st century. *Global Environmental Change*.
- O'Neill, B.C., Kriegler, E., Riahi, K., Ebi, K.L., Hallegatte, S., Carter, T.R., Mathur, R. and van Vuuren, D.P. 2014. A new scenario framework for climate change research: The concept of shared socioeconomic pathways. *Climatic Change*. **122**(3), pp.387–400.
- Obersteiner, M., Walsh, B., Frank, S., Havlík, P., Cantele, M., Liu, J., Palazzo, A., Herrero, M., Lu, Y., Mosnier, A., Valin, H., Riahi, K., Kraxner, F., Fritz, S. and Van Vuuren, D. 2016. Assessing the land resource–food price nexus of the Sustainable Development

Goals. *Science Advances*. **2**(9).

- Obidzinski, K., Andriani, R., Komarudin, H. and Andrianto, A. 2012. Environmental and social impacts of oil palm plantations and their implications for biofuel production in Indonesia. *Ecology and Society*. **17**(1).
- Odgaard, M. V., Knudsen, M.T., Hermansen, J.E. and Dalgaard, T. 2019. Targeted grassland production – A Danish case study on multiple benefits from converting cereal to grasslands for green biorefinery. *Journal of Cleaner Production*. **223**, pp.917–927.
- Oki, T. and Kanae, S. 2006. Global hydrological cycles and world water resources. *Science*. **313**(5790), pp.1068–1072.
- Oliver, R.J., Finch, J.W. and Taylor, G. 2009. Second generation bioenergy crops and climate change : a review of the effects of elevated atmospheric CO<sub>2</sub> and drought on water use and the implications for yield. *GCB Bio*. **1**, pp.97–114.
- Olsen, J. and Watts, J. 1982. *Major World Ecosystem Complexes Ranked by Carbon in Live Vegetation (Map)*. Oak Ridge, Tennessee.
- Openshaw, K. 2010. Biomass energy : Employment generation and its contribution to poverty alleviation. *Biomass and Bioenergy*. **34**(3), pp.365–378.
- Pahl-Wostl, C., Arthington, A., Bogardi, J., Bunn, S.E., Hoff, H., Lebel, L., Nikitina, E., Palmer, M., Poff, L.R.N., Richards, K., Schlüter, M., Schulze, R., St-Hilaire, A., Tharme, R., Tockner, K. and Tsegai, D. 2013. Environmental flows and water governance: Managing sustainable water uses. *Current Opinion in Environmental Sustainability*. **5**(3–4), pp.341–351.
- Parnesan, C. 2006. Ecological and Evolutionary Responses to Recent Climate Change. *Annual Review of Ecology Evolution and Systematics*. **37**(1), pp.637–669.
- Parnesan, C., Morecroft, M.D., Trisurat, Y., Adrian, R., Anshari, G.Z., Arneth, A., Gao, Q., Gonzalez, P., Harris, R., Price, J., Stevens, N. and Talukdarr, G.. 2022. *Terrestrial and Freshwater Ecosystems and Their Services. In: Climate Change 2022: Impacts, Adaptation and Vulnerability. Contribution of Working Group II to the Sixth Assessment Report of the Intergovernmental Panel on Climate Change [H.-O. Pörtner ...]*. Cambridge University Press, Cambridge, United Kingdom and New York, NY, USA.
- Pastor, A. V., Ludwig, F., Biemans, H., Hoff, H. and Kabat, P. 2014. Accounting for environmental flow requirements in global water assessments. *Hydrology and Earth System Sciences*. **18**(12), pp.5041–5059.
- Pearson, R.G. and Dawson, T.P. 2003. Predicting the impacts of climate change on the distribution of species: Are bioclimate envelope models useful? *Global Ecology and Biogeography*. **12**(5), pp.361–371.
- Peh, K.S.H., Sodhi, N.S., De Jong, J., Sekercioglu, C.H., Yap, C.A.M. and Lim, S.L.H. 2006. Conservation value of degraded habitats for forest birds in southern Peninsular Malaysia. *Diversity and Distributions*. **12**(5), pp.572–581.
- Pena, N. 2008. Biofuels for Transportation: a Climate Perspective. , p.32.
- Pereira, H.M., Leadley, P.W., Proença, V., Alkemade, R., Scharlemann, J.P.W., Fernandez-Manjarrés, J.F., Araújo, M.B., Balvanera, P., Biggs, R., Cheung, W.W.L., Chini, L., Cooper, H.D., Gilman, E.L., Guénette, S., Hurr, G.C., Huntington, H.P., Mace, G.M., Oberdorff, T., Revenga, C., Rodrigues, P., Scholes, R.J., Sumaila, U.R. and Walpole, M. 2010. Scenarios for global biodiversity in the 21st century. *Science*. **330**(6010), pp.1496–1501.

- Pereira, H.M., Navarro, L.M. and Martins, I.S. 2012. *Global biodiversity change: The bad, the good, and the unknown*. Annual Review of Environment and Resources, Lisboa, Portugal.
- Perlack, R.D., Wright, L.L., Turhollow, A.F. and Graham, R.L. 2005. *Biomass as Feedstock for a Bioenergy and Bioproducts Industry: The Technical Feasibility of a Billion-Ton Annual Supply*. U.S. Department of Energy & U.S. Department of Agriculture. [Online]. Available from: [http://www1.eere.energy.gov/biomass/pdfs/final\\_billionton\\_vision\\_report2.pdf](http://www1.eere.energy.gov/biomass/pdfs/final_billionton_vision_report2.pdf).
- Perugini, L., Caporaso, L., Marconi, S., Cescatti, A., Quesada, B., De Noblet-Ducoudré, N., House, J.I. and Arneth, A. 2017. Biophysical effects on temperature and precipitation due to land cover change. *Environmental Research Letters*. **12**(5).
- Peura, M., Burgas, D., Eyvindson, K., Repo, A. and Mönkkönen, M. 2018. Continuous cover forestry is a cost-efficient tool to increase multifunctionality of boreal production forests in Fennoscandia. *Biological Conservation*. **217**, pp.104–112.
- Phalan, B., Onial, M., Balmford, A. and Green, R.E. 2011. Reconciling food production and biodiversity conservation: Land sharing and land sparing compared. *Science*. **333**(6047), pp.1289–1291.
- Phillipson, P., Schatz, G., Lowry, P.I. and Labat, J.-N. (2006) 2006. A catalogue of the vascular plants of Madagascar. In: S.A. Ghazanfar & H.J. Beentje (eds), Taxonomy and ecology of African plants, their conservation and sustainable use. *Royal Botanic Gardens, Kew.*, pp.613–627.
- Pielke, R.A., Marland, G., Betts, R.A., Chase, T.N., Eastman, J.L., Niles, J.O., Niyogi, D. d. S. and Running, S.W. 2002. The influence of land-use change and landscape dynamics on the climate system: relevance to climate-change policy beyond the radiative effect of greenhouse gases. *Philosophical Transactions of the Royal Society A: Mathematical, Physical and Engineering Sciences*. **360**(1797), pp.1705–1719.
- Pielke, R.A., Pitman, A., Niyogi, D., Mahmood, R., McAlpine, C., Hossain, F., Goldewijk, K.K., Nair, U., Betts, R., Fall, S., Reichstein, M., Kabat, P. and de Noblet, N. 2011. Land use/land cover changes and climate: Modeling analysis and observational evidence. *Wiley Interdisciplinary Reviews: Climate Change*. **2**(6), pp.828–850.
- PIK 2022. MAgPIE – Model of Agricultural Production and its Impact on the Environment. *Potsdam Institute for Climate Impact Research*. [Online]. Available from: <https://www.pik-potsdam.de/en/institute/departments/activities/land-use-modelling/magpie/magpie-2013-model-of-agricultural-production-and-its-impact-on-the-environment>.
- Pimm, S.L. and Askins, R.A. 1995. Forest losses predict bird extinctions in eastern North America. *Proceedings of the National Academy of Sciences of the United States of America*. **92**(20), pp.9343–9347.
- Pimm, S.L., Russell, G.J., Gittleman, J.L. and Brooks, T.M. 1995. The future of biodiversity. *Science*. **269**(5222), pp.347–350.
- Pinsonneault, A.J., Matthews, H.D., Kothavala, Z., Pinsonneault, A.J., Matthews, H.D., Kothavala, Z., Pinsonneault, A.J., Matthews, H.D. and Kothavala, Z. 2011. Benchmarking Climate-Carbon Model Simulations against Forest FACE Data. *Atmosphere-Ocean*. **49**(1), pp.41–50.
- Pitman, A.J., De Noblet-Ducoudré, N., Cruz, F.T., Davin, E.L., Bonan, G.B., Brovkin, V., Claussen, M., Delire, C., Ganzeveld, L., Gayler, V., Van Den Hurk, B.J.J.M., Lawrence, P.J., Van Der Molen, M.K., Müller, C., Reick, C.H., Seneviratne, S.I., Strengen, B.J. and

- Voltaire, A. 2009. Uncertainties in climate responses to past land cover change: First results from the LUCID intercomparison study. *Geophysical Research Letters*. **36**(14), pp.1–6.
- Plevin, R.J., Beckman, J., Golub, A.A., Witcover, J. and O’Hare, M. 2015. Carbon accounting and economic model uncertainty of emissions from biofuels-induced land use change. *Environmental Science and Technology*. **49**(5), pp.2656–2664.
- Poff, N.L., Richter, B.D., Arthington, A.H., Bunn, S.E., Naiman, R.J., Kendy, E., Acreman, M., Apse, C., Bledsoe, B.P., Freeman, M.C., Henriksen, J., Jacobson, R.B., Kennen, J.G., Merritt, D.M., O’Keeffe, J.H., Olden, J.D., Rogers, K., Tharme, R.E. and Warner, A. 2010. The ecological limits of hydrologic alteration (ELOHA): A new framework for developing regional environmental flow standards. *Freshwater Biology*. **55**(1), pp.147–170.
- Pongratz, J., Reick, C.H., Houghton, R.A. and House, J.I. 2014. Terminology as a key uncertainty in net land use and land cover change carbon flux estimates. *Earth System Dynamics*. **5**(1), pp.177–195.
- Pongratz, J., Reick, C.H., Raddatz, T. and Claussen, M. 2010. Biogeophysical versus biogeochemical climate response to historical anthropogenic land cover change. *Geophysical Research Letters*. **37**(8), pp.1–5.
- Pongratz, J., Reick, C.H., Raddatz, T. and Claussen, M. 2009. Effects of anthropogenic land cover change on the carbon cycle of the last millennium. *Global Biogeochemical Cycles*. **23**(4), pp.1–13.
- Popp, A., Calvin, K., Fujimori, S., Havlik, P., Humpenöder, F. I., Stehfest, E., Bodirsky, B.L., Dietrich, J.P., Doelmann, J.C., Gusti, M., Hasegawa, T., Kyle, P., Obersteiner, M., Tabau, A., Takahashi, K. and ... 2017. Land-use futures in the shared socio-economic pathways. *Global Environmental Change*. **42**, pp.331–345.
- Popp, A., Dietrich, J.P., Lotze-Campen, H., Klein, D., Bauer, N., Krause, M., Beringer, T., Gerten, D. and Edenhofer, O. 2011. The economic potential of bioenergy for climate change mitigation with special attention given to implications for the land system. *Environmental Research Letters*. **6**(3).
- Popp, A., Humpenöder, F., Weindle, I., Bodirsky, B.L., Bonsch, M., Lotze-Campen, H., Müller, C., Biewald, A., Rolinski, S., Stevanovic, M. and Dietrich, J.P. 2014. Land-use protection for climate change mitigation. *Nature Climate Change*. **4**(12), pp.1095–1098.
- Popp, A., Krause, M., Dietrich, J.P., Lotze-Campen, H., Leimbach, M., Beringer, T. and Bauer, N. 2012. Additional CO<sub>2</sub> emissions from land use change - Forest conservation as a precondition for sustainable production of second generation bioenergy. *Ecological Economics*. **74**, pp.64–70.
- Popp, A., Lotze-Campen, H. and Bodirsky, B. 2010. Food consumption, diet shifts and associated non-CO<sub>2</sub> greenhouse gases from agricultural production. *Global Environmental Change*. **20**(3), pp.451–462.
- Popp, A., Lotze-Campen, H., Leimbach, M., Knopf, B., Beringer, T., Bauer, N. and Bodirsky, B. 2011. On sustainability of bioenergy production: Integrating co-emissions from agricultural intensification. *Biomass and Bioenergy*. **35**(12), pp.4770–4780.
- Popp, A., Rose, S.K., Calvin, K., Van Vuuren, D.P., Dietrich, J.P., Wise, M., Stehfest, E., Humpenoder, F., Kyle, P., Van Vliet, J., Bauer, N., Lotze-Campen, H., Klein, D. and Kriegler, E. 2014. Land-use transition for bioenergy and climate stabilization: Model comparison of drivers, impacts and interactions with other land use based mitigation

- options. *Climatic Change*. **123**(3–4), pp.495–509.
- Popp, A., Weindl, I., Bodirsky, B.L., Bonsch, M., Lotze-Campen, H., Müller, C., Biewald, A., Rolinski, S., Stevanovic, M. and Dietrich, J.P. 2014. Land-use protection for climate change mitigation. *Nature Climate Change*. **4**(12), pp.1095–1098.
- Popp, J., Lakner, Z., Harangi-Rákos, M. and Fári, M. 2014. The effect of bioenergy expansion: Food, energy, and environment. *Renewable and Sustainable Energy Reviews*. **32**, pp.559–578.
- Porter, J., Costanza, R., Sandhu, H., Sigsgaard, L. and Wratten, S. 2009. The value of producing food, energy, and ecosystem services within an agro-ecosystem. *Ambio*. **38**(4), pp.186–193.
- Posa, M.R.C., Diesmos, A.C., Sodhi, N.S. and Brooks, T.M. 2008. Hope for threatened tropical biodiversity: Lessons from the Philippines. *BioScience*. **58**(3), pp.231–240.
- Post W. M. and Kwon K. C. 2000. Soil Carbon Sequestration and Land-use Change: Processes and Potential. *Global Change Biology*. **6**, pp.317–327.
- Postel, S.L., Daily, G.C. and Ehrlich, P.. 2008. Human Appropriation of Renewable Fresh Water Author ( s ): Sandra L . Postel , Gretchen C . Daily , Paul R . Ehrlich Published by : American Association for the Advancement of Science Stable URL : <http://www.jstor.org/stable/2889886>. *Science*. **271**(5250), pp.785–788.
- Potter, G.L., Ellsaesser, H.W., Maccracken, M.C. and Ellis, J.S. 1981. Albedo change by man: Test of climatic effects. *Nature*. **291**(5810), pp.47–49.
- Potter, G.L., Ellsaesser, H.W., Maccracken, M.C. and Luther, F.M. 1975. Possible climatic impact of tropical deforestation. *Nature*. **258**, pp.697–698.
- Pounds, J.A., Bustamante, M.R., Coloma, L.A., Consuegra, J.A., Fogden, M.P.L., Foster, P.N., La Marca, E., Masters, K.L., Merino-Viteri, A., Puschendorf, R., Ron, S.R., Sánchez-Azofeifa, G.A., Still, C.J. and Young, B.E. 2006. Widespread amphibian extinctions from epidemic disease driven by global warming. *Nature*. **439**(7073), pp.161–167.
- Pour, N., Webley, P.A. and Cook, P.J. 2018. Potential for using municipal solid waste as a resource for bioenergy with carbon capture and storage (BECCS). *International Journal of Greenhouse Gas Control*. **68**(February 2017), pp.1–15.
- Powell, T.W.R. and Lenton, T.M. 2013. Scenarios for future biodiversity loss due to multiple drivers reveal conflict between mitigating climate change and preserving biodiversity. *Environmental Research Letters*. **8**(2).
- Prentice, I.C., Cramer, W., Harrison, S.P., Leemans, R., Monserud, R.A. and Solomon, A.M. 1992. A global biome model based on plant physiology and dominance, soil properties and climate. *Journal of Biogeography*. **19**(2), pp.117–134.
- Prevedello, J.A., Winck, G.R., Weber, M.M., Nichols, E. and Sinervo, B. 2019. Impacts of forestation and deforestation on local temperature across the globe. *PLoS ONE*. **14**(3), pp.1–18.
- Pugh, T.A.M., Arneth, A., Olin, S., Ahlström, A., Bayer, A.D., Klein Goldewijk, K., Lindeskog, M. and Schurgers, G. 2015. Simulated carbon emissions from land-use change are substantially enhanced by accounting for agricultural management. *Environmental Research Letters*. **10**(12), pp.1–10.
- Quesada, B., Arneth, A. and De Noblet-Ducoudré, N. 2017. Atmospheric, radiative, and hydrologic effects of future land use and land cover changes: A global and multimodel climate picture. *Journal of Geophysical Research*. **122**(10), pp.5113–5131.

- Rajagopal, D. and Plevin, R.J. 2013. Implications of market-mediated emissions and uncertainty for biofuel policies. *Energy Policy*. **56**(2013), pp.75–82.
- Randerson, J.T., Liu, H., Flanner, M.G., Chambers, S.D., Jin, Y., Hess, P.G., Pfister, G., Mack, M.C., Treseder, K.K., Welp, L.R., Chapin, F.S., Harden, J.W., Goulden, M.L., Lyons, E., Neff, J.C., Schuur, E.A.G. and Zender, C.S. 2006. The impact of boreal forest fire on climate warming. *Science*. **314**(5802), pp.1130–1132.
- Reilly, J., Melillo, J., Cai, Y., Kicklighter, D., Gurgel, A., Paltsev, S., Cronin, T., Sokolov, A. and Schlosser, A. 2012. Using land to mitigate climate change: Hitting the target, recognizing the trade-offs. *Environmental Science and Technology*. **46**(11), pp.5672–5679.
- REN21 2021. *Renewables 2021 Global Status Report*. REN21 Secretariat, Paris, France.
- Riahi, K., Rao, S., Krey, V., Cho, C., Chirkov, V., Fischer, G., Kindermann, G., Nakicenovic, N. and Rafaj, P. 2011. RCP 8.5-A scenario of comparatively high greenhouse gas emissions. *Climatic Change*. **109**(1), pp.33–57.
- Riahi, K., Schaeffer, R., Arango, J., Calvin, K., Guivarch, C., Hasegawa, T., Jiang, K., Kriegler, E., Matthews, R., Peters, G., Rao, A., Robertson, S., Sebbit, A.M., Steinberger, J., Tavoni, M. and Vuuren, D. van 2022. *Mitigation pathways compatible with long-term goals. In IPCC, 2022: Climate Change 2022: Mitigation of Climate Change. Contribution of Working Group III to the Sixth Assessment Report of the Intergovernmental Panel on Climate Change [P.R. Shukla eds.]*. Cambridge, UK and New York, NY, USA.
- Riahi, K., van Vuuren, D.P., Kriegler, E., Edmonds, J., O'Neill, B.C., Fujimori, S., Bauer, N., Calvin, K., Dellink, R., Fricko, O., Lutz, W., Popp, A., Cuaresma, J.C., KC, S., Leimbach, M. and ... 2017. The Shared Socioeconomic Pathways and their energy, land use, and greenhouse gas emissions implications: An overview. *Global Environmental Change*. **42**, pp.153–168.
- Ricketts, T.H., Dinerstein, E., Boucher, T., Brooks, T.M., Butchart, S.H.M., Hoffmann, M., Lamoreux, J.F., Morrison, J., Parr, M., Pilgrim, J.D., Rodrigues, A.S.L., Sechrest, W., Wallace, G.E., Berlin, K., Bielby, J. and ... 2005. Pinpointing and preventing imminent extinctions. *Proceedings of the National Academy of Sciences of the United States of America*. **102**(51), pp.18497–18501.
- Robertson, A.D., Zhang, Y., Sherrod, L.A., Rosenzweig, S.T., Ma, L., Ahuja, L. and Schipanski, M.E. 2018. Climate Change Impacts on Yields and Soil Carbon in Row Crop Dryland Agriculture. *Journal of Environmental Quality*. **47**(4), pp.684–694.
- Robertson, B.A., Doran, P.J., Loomis, E.R., Robertson, J.R. and Schemske, D.W. 2011. Avian use of perennial biomass feedstocks as post-breeding and migratory stopover habitat. *PLoS ONE*. **6**(3).
- Robertson, G.P., Hamilton, S.K., Barham, B.L., Dale, B.E., Izaurrealde, R.C., Jackson, R.D., Landis, D.A., Swinton, S.M., Thelen, K.D. and Tiedje, J.M. 2017. Cellulosic biofuel contributions to a sustainable energy future: Choices and outcomes. *Science*. **356**(6345).
- Rocha, G.F., Ferreira Jr., L.G., Ferreira, N.C. and Ferreira, M.E. 2011. Detecção de desmatamentos no bioma Cerrado entre 2002 e 2009: Padrões, tendências e impactos. *Revista Brasileira de Cartografia*. **63**, pp.341–349.
- Rockström, B.J., Gaffney, O., Rogelj, J., Meinshausen, M., Nakicenovic, N. and Joachim, H. 2017. A roadmap for rapid decarbonization Emissions. *Science*. **355**(6331), pp.1269–1271.
- Rogelj, J., Popp, A., Calvin, K. V., Luderer, G., Emmerling, J., Gernaat, D., Fujimori, S.,

- Hasegawa, J., Tomoko, S., Marangoni, G., Krey, V., Kriegler, E., Riahi, K., Vuuren, D.P. van, Doelman, J., Drouet, L., Edmonds, J., Fricko, O., Harmsen, M., Havlík, P., Humpenöder, F., Stehfest, E. and Tavoni, M. 2018. Scenarios towards limiting global mean temperature increase below 1.5 °C. *Nature Climate Change*. **8**(4), pp.325–332.
- Rogelj, J., Shindell, D., Jiang, K., Fifita, S., Forster, P., Ginzburg, V., Handa, C., Kheshgi, H., Kobayashi, S., Kriegler, E., Mundaca, L., Séférian, R. and Vilariño, M. V. 2018. Mitigation Pathways Compatible with 1.5°C in the Context of Sustainable Development. Chapter 2 of The Special Report on Global Warming of 1.5°C.
- Roos 2002. *Policy and institutional factors affecting forest energy*. In: *Bioenergy from Sustainable Forestry - Guiding Principles and Practice* [J. Richardson, R. Björheden, P. Hakkila, A. T. Lowe, C. T. Smith, (eds.)]. Forestry Sciences, Kluwer Academic Publishers.
- Rose, S.K., Bauer, N., Popp, A., Weyant, J., Fujimori, S., Havlik, P., Wise, M. and van Vuuren, D.P. 2020. An overview of the Energy Modeling Forum 33rd study: assessing large-scale global bioenergy deployment for managing climate change. *Climatic Change*. **163**(3), pp.1539–1551.
- Rose, S.K., Kriegler, E., Bibas, R., Calvin, K., Popp, A., van Vuuren, D.P. and Weyant, J. 2014. Bioenergy in energy transformation and climate management. *Climatic Change*. **123**(3–4), pp.477–493.
- Rose, S.K., Popp, A., Fujimori, S., Havlik, P., Weyant, J., Wise, M., van Vuuren, D., Brunelle, T., Cui, R.Y., Daioglou, V., Frank, S., Hasegawa, T., Humpenöder, F., Kato, E., Sands, R.D., Sano, F., Tsutsui, J., Doelman, J., Muratori, M., Prudhomme, R., Wada, K. and Yamamoto, H. 2022. Global biomass supply modeling for long-run management of the climate system. *Climatic Change*. **172**(1–2), pp.1–27.
- Rosenzweig, C., Elliott, J., Deryng, D., Ruane, A.C., Müller, C. and Arneth, A. 2014. Assessing agricultural risks of climate change in the 21st century in a global gridded crop model intercomparison. *PNAS*. **111**(9), pp.4–9.
- Rosenzweig, M.L. 2003a. Applying Species-area Relationships to the Conservation of Species Diversity Michael. *Ibs*. **53**(9), pp.1689–1699.
- Rosenzweig, M.L. 2001. Loss of speciation rate will impoverish future diversity. *Proceedings of the National Academy of Sciences*. **98**(10), pp.5404–5410.
- Rosenzweig, M.L. 2003b. Reconciliation ecology and the future of species diversity. *Oryx*. **37**(2), pp.194–205.
- Rosenzweig, M.L. 1995. *Species diversity in space and time*. Cambridge, UK.
- Rost, S., Gerten, D., Bondeau, A., Lucht, W., Rohwer, J. and Schaphoff, S. 2008. Agricultural green and blue water consumption and its influence on the global water system. *Water Resources Research*. **44**(9), pp.1–17.
- Rowe, H., Withers, P.J.A., Baas, P., Chan, N.I., Doody, D., Holiman, J., Jacobs, B., Li, H., MacDonald, G.K., McDowell, R., Sharpley, A.N., Shen, J., Taheri, W., Wallenstein, M. and Weintraub, M.N. 2016. Integrating legacy soil phosphorus into sustainable nutrient management strategies for future food, bioenergy and water security. *Nutrient Cycling in Agroecosystems*. **104**(3), pp.393–412.
- Roy, J., Saugier, B. and Mooney, H.A. 2001. *Terrestrial Global Productivity*. Academic Press.
- Roy, J., Tschakert, P., Waisman, H., Halim, S.A., Antwi-Agyei, P., Dasgupta, P., Hayward, B., Kanninen, M., Liverman, D., Okereke, C., Pinho, P., Riahi, K. and Suarez Rodriguez, A. 2018. *Sustainable Development, Poverty Eradication and Reducing Inequalities*. In:

*Global Warming of 1.5°C. An IPCC Special Report on the impacts of global warming of 1.5°C above pre-industrial levels and related global greenhouse gas emission pathways, in the c.* Cambridge University Press, Cambridge, United Kingdom and New York, NY, USA.

- Rudorff, B.F.T., de Aguiar, D.A., da Silva, W.F., Sugawara, L.M., Adami, M. and Moreira, M.A. 2010. Studies on the rapid expansion of sugarcane for ethanol production in São Paulo state (Brazil) using Landsat data. *Remote Sensing*. **2**(4), pp.1057–1076.
- Rulli, M.C., Bellomi, D., Cazzoli, A., De Carolis, G. and D’Odorico, P. 2016. The water-land-food nexus of first-generation biofuels. *Scientific Reports*. **6**, pp.1–10.
- Sagan, C., Toon, O.B. and Pollack, J.B. 1979. Anthropogenic albedo changes and the Earth’s climate. *Science*. **206**(4425), pp.1363–1368.
- Sala, O.E., Chapin, F.S., Armesto, J.J., Berlow, E., Bloomfield, J., Dirzo, R., Huber-Sanwald, E., Huenneke, L.F., Jackson, R.B., Kinzig, A., Leemans, R., Lodge, D.M., Mooney, H.A., Oesterheld, M., Poff, L. and ... 2000. Biodiversity - Global biodiversity scenarios for the year 2100. *Science*. **287**(5459), pp.1770–1774.
- Sampaio, G., Nobre, C., Costa, M.H., Satyamurty, P., Soares-Filho, B.S. and Cardoso, M. 2007. Regional climate change over eastern Amazonia caused by pasture and soybean cropland expansion. *Geophysical Research Letters*. **34**(17), pp.1–7.
- Scarpore, F.V., Hernandez, T.A.D., Ruiz-Corrêa, S.T., Picoli, M.C.A., Scanlon, B.R., Chagas, M.F., Duft, D.G. and Cardoso, T. de F. 2016. Sugarcane land use and water resources assessment in the expansion area in Brazil. *Journal of Cleaner Production*. **133**, pp.1318–1327.
- Schaphoff, S., Forkel, M., Müller, C., Knauer, J., Von Bloh, W., Gerten, D., Jägermeyr, J., Lucht, W., Rammig, A., Thonicke, K. and Waha, K. 2018. LPJmL4 - A dynamic global vegetation model with managed land - Part 2: Model evaluation. *Geoscientific Model Development*. **11**(4), pp.1377–1403.
- Schipper, A.M., Hilbers, J.P., Meijer, J.R., Antão, L.H., Benítez-López, A., de Jonge, M.M.J., Leemans, L.H., Scheper, E., Alkemade, R., Doelman, J.C., Mylius, S., Stehfest, E., van Vuuren, D.P., van Zeist, W.J. and Huijbregts, M.A.J. 2020. Projecting terrestrial biodiversity intactness with GLOBIO 4. *Global Change Biology*. **26**(2), pp.760–771.
- Schmitz, C., Biewald, A., Lotze-Campen, H., Popp, A., Dietrich, J.P., Bodirsky, B., Krause, M. and Weindl, I. 2012. Trading more food: Implications for land use, greenhouse gas emissions, and the food system. *Global Environmental Change*. **22**(1), pp.189–209.
- Scholes, R.J. and Biggs, R. 2005. A biodiversity intactness index. *Nature*. **434**(7029), pp.45–49.
- Schröder, P., Beckers, B., Daniels, S., Gnädinger, F., Maestri, E., Marmiroli, N., Mench, M., Millan, R., Obermeier, M.M., Oustriere, N., Persson, T., Poschenrieder, C., Rineau, F., Rutkowska, B., Schmid, T., Szulc, W., Witters, N. and Sæbø, A. 2018. Intensify production, transform biomass to energy and novel goods and protect soils in Europe—A vision how to mobilize marginal lands. *Science of the Total Environment*. **616–617**, pp.1101–1123.
- Schultz, N.M., Lawrence, P.J. and Lee, X. 2017. Global satellite data highlights the diurnal asymmetry of the surface temperature response to deforestation. *Journal of Geophysical Research: Biogeosciences*. **122**(4), pp.903–917.
- Schulz, U., Brauner, O. and Größ, H. 2009. Animal diversity on short-rotation coppices - A review. *Landbauforschung Volkenrode*. **59**(3), pp.171–182.



- Schwietzke, S., Kim, Y., Ximenes, E., Mosier, N. and Ladisch, M. 2009. Ethanol production from maize. *Biotechnology in Agriculture and Forestry*. **63**(January), pp.347–364.
- Scott, C.E., Monks, S.A., Spracklen, D. V., Arnold, S.R., Forster, P.M., Rap, A., Carslaw, K.S., Chipperfield, M.P., Reddington, C.L.S. and Wilson, C. 2017. Impact on short-lived climate forcers (SLCFs) from a realistic land-use change scenario via changes in biogenic emissions. *Faraday Discussions*. **200**, pp.101–120.
- Searchinger, T., Heimlich, R., Houghton, R.A., Dong, F., Elobeid, A., Fabiosa, J., Tokgoz, S., Hayes, D. and Yu, T. 2008. Use of U.S. Croplands for Biofuels Increases Greenhouse Gases Through Emissions from Land-Use Change. *Science*. **423**, pp.1238–1240.
- Sellers, P.J., Meeson, B.W., Closs, J., Collatz, J., Corprew, F., Dazlich, D., Hall, F.G., Kerr, Y., Koster, R., Los, S., Mitchell, K., McManus, J., Myers, D., Sun, K.J. and Try, P. 1996. The ISLSCP initiative I global datasets: Surface boundary conditions and atmospheric forcings for land-atmosphere studies. *Bulletin of the American Meteorological Society*. **77**(9), pp.1987–2005.
- Seneviratne, S.I., Zhang, X., Adnan, M., Badi, W., Dereczynski, C., Luca, A. Di, Ghosh, S., Iskandar, I., Kossin, J., Lewis, S., Otto, F., Pinto, I., Satoh, M., Vicente-Serrano, S.M., Wehner, M. and Zhou, B. 2021. *Weather and Climate Extreme Events in a Changing Climate. In Climate Change 2021: The Physical Science Basis. Contribution of Working Group I to the Sixth Assessment Report of the Intergovernmental Panel on Climate Change [V. P. Masson-Delmotte (eds.)]*. Cambridge University Press, Cambridge, United Kingdom and New York, NY, USA,.
- Settele, J. 2014. *Terrestrial and inland water systems. In Climate change 2014: impacts, adaptation, and vulnerability. Part A: Global and sectoral aspects. Contribution of Working Group II to the Fifth Assessment Report of the Intergovernmental Panel on Climate Change*. Cambridge University Press, Cambridge, UK and New York, NY, USA.
- Shackley, S., Reiner, D., Upham, P., de Coninck, H., Sigurthorsson, G. and Anderson, J. 2009. The acceptability of CO<sub>2</sub> capture and storage (CCS) in Europe: An assessment of the key determining factors. Part 2. The social acceptability of CCS and the wider impacts and repercussions of its implementation. *International Journal of Greenhouse Gas Control*. **3**(3), pp.344–356.
- Sheldon, F.H., Styring, A. and Hosner, P.A. 2010. Bird species richness in a Bornean exotic tree plantation: A long-term perspective. *Biological Conservation*. **143**(2), pp.399–407.
- Shevliakova, E., Pacala, S.W., Malyshev, S., Hurtt, G.C., Milly, P.C.D., Caspersen, J.P., Sentman, L.T., Fisk, J.P., Wirth, C. and Crevoisier, C. 2009. Carbon cycling under 300 years of land use change: importance of the secondary vegetation sink. *Global Biogeochemical Cycles*. **23**(2), pp.1–16.
- Shi, H., Singh, A., Kant, S., Zhu, Z. and Waller, E. 2005. Integrating habitat status, human population pressure, and protection status into biodiversity conservation priority setting. *Conservation Biology*. **19**(4), pp.1273–1285.
- Shukla, J. and Mintz, Y. 1982. Influence of land-surface evapotranspiration on the Earth's climate. *Science*. **215**, pp.1498–1502.
- Sibley, C.G. and Monroe, B.L. 1990. *Distribution and Taxonomy of Birds of the World*. New Haven, Connecticut: Yale University Press.
- Siirila, E.R., Navarre-Sitchler, A.K., Maxwell, R.M. and McCray, J.E. 2012. A quantitative methodology to assess the risks to human health from CO<sub>2</sub> leakage into groundwater. *Advances in Water Resources*. **36**, pp.146–164.

- Simmons, C.T. and Matthews, H.D. 2016. Assessing the implications of human land-use change for the transient climate response to cumulative carbon emissions. *Environmental Research Letters*. **11**(3), p.35001.
- Singh, B., Strømman, A.H. and Hertwich, E.G. 2011. Comparative life cycle environmental assessment of CCS technologies. *International Journal of Greenhouse Gas Control*. **5**(4), pp.911–921.
- Sitch, S., Brovkin, V., von Bloh, W., van Vuuren, D., Eickhout, B. and Ganopolski, A. 2005. Impacts of future land cover changes on atmospheric CO<sub>2</sub> and climate. *Global Biogeochemical Cycles*. **19**(2), pp.1–15.
- Sitch, S., Smith, B., Prentice, I.C., Arneth, A., Bondeau, A., Cramer, W., Kaplan, J.O., Levis, S., Lucht, W., Sykes, M.T., Thonicke, K. and Venevsky, S. 2003. Evaluation of ecosystem dynamics, plant geography and terrestrial carbon cycling in the LPJ dynamic global vegetation model. *Global Change Biology*. **9**(2), pp.161–185.
- Smakhtin, V., Revenga, C. and Döll, P. 2004. A Pilot Global Assessment of Environmental Water Requirements and Scarcity. **29**(3), pp.1–12.
- Smith, P. 2008. Land use change and soil organic carbon dynamics. *Nutrient Cycling in Agroecosystems*. **81**(2), pp.169–178.
- Smith, P., Bustamante, M., Ahammad, H., Clark, H., Dong, H., Elsiddig, E.A., Haberl, H., Harper, R., House, J., Jafari, M., Masera, O., Mbow, C., Ravindranath, N.H.H., Rice, C.W.W., Abad, C.R., Romanovskaya, A., Sperling, F., Tubiello, F., P., S., Bustamante, M., Ahammad, H., Clark, H., Dong, H., Elsiddig, E.A., Haberl, H., Harper, R., House, J., Jafari, M., Masera, O., Mbow, C., Ravindranath, N.H.H., Rice, C.W.W., Abad, C.R., Romanovskaya, A., Sperling, F. and Tubiello, F. 2014. *Agriculture, Forestry and Other Land Use (AFOLU)*. In: *Climate Change 2014: Mitigation of Climate Change. Contribution of Working Group III to the Fifth Assessment Report of the Intergovernmental Panel on Climate Change [Edenhofer, O., R. Pichs-Madruga, Y. Cambridge, United Kingdom and New York, NY, USA.*
- Smith, P., Davis, S.J., Creutzig, F., Fuss, S., Minx, J., Gabrielle, B., Kato, E., Jackson, R.B., Cowie, A., Kriegl, E., van Vuuren, D.P., Rogelj, J., Ciais, P., Milne, J. and ... 2016. Biophysical and economic limits to negative CO<sub>2</sub> emissions. *Nature Clim. Change*. **6**(1), pp.42–50.
- Smith, P., Haberl, H., Popp, A., Erb, K.H., Lauk, C., Harper, R., Tubiello, F.N., De Siqueira Pinto, A., Jafari, M., Sohi, S., Masera, O., Böttcher, H., Berndes, G., Bustamante, M., Ahammad, H., Clark, H., Dong, H., Elsiddig, E.A., Mbow, C., Ravindranath, N.H., Rice, C.W., Robledo Abad, C., Romanovskaya, A., Sperling, F., Herrero, M., House, J.I. and Rose, S. 2013. How much land-based greenhouse gas mitigation can be achieved without compromising food security and environmental goals? *Global Change Biology*. **19**(8), pp.2285–2302.
- Smith, P., Nkem, J., Calvin, K., Campbell, D., Cherubini, F., Grassi, G., Korotkov, V., Hoang, A.L., Lwasa, S., McElwee, P., Nkonya, E., Saigusa, N., Soussana, J.-F. and Taboada, M.A. 2019. *Interlinkages Between Desertification, Land Degradation, Food Security and Greenhouse Gas Fluxes: Synergies, Trade-offs and Integrated Response Options*. In: *Climate Change and Land: an IPCC special report on climate change, desertification*. Cambridge University Press, Cambridge, United Kingdom and New York, NY, USA.
- Smith, P., Price, J., Molotoks, A., Warren, R. and Malhi, Y. 2018. Impacts on terrestrial biodiversity of moving from a 2°C to a 1.5°C target. *Philosophical Transactions of the Royal Society A: Mathematical, Physical and Engineering Sciences*. **376**(2119), pp.1–18.

- Snyder, P.K., Delire, C. and Foley, J.A. 2004. Evaluating the influence of different vegetation biomes on the global climate. *Climate Dynamics*. **23**(3–4), pp.279–302.
- Sodhi, N.S., Koh, L.P., Brook, B.W. and Ng, P.K.L. 2004. Southeast Asian biodiversity: An impending disaster. *Trends in Ecology and Evolution*. **19**(12), pp.654–660.
- Sodhi, N.S., Posa, M.R.C., Lee, T.M., Bickford, D., Koh, L.P. and Brook, B.W. 2010. The state and conservation of Southeast Asian biodiversity. *Biodiversity and Conservation*. **19**(2), pp.317–328.
- Sokolov, A.P., Kicklighter, D.W., Melillo, J.M., Felzer, B.S., Schlosser, C.A. and Cronin, T.W. 2008. Consequences of considering carbon-nitrogen interactions on the feedbacks between climate and the terrestrial carbon cycle. *Journal of Climate*. **21**(15), pp.3776–3796.
- Souza, D.M., Teixeira, R.F.M. and Ostermann, O.P. 2015. Assessing biodiversity loss due to land use with Life Cycle Assessment: Are we there yet? *Global Change Biology*. **21**(1), pp.32–47.
- Spracklen, D.V., Arnold, S.R. and Taylor, C.M. 2012. Observations of increased tropical rainfall preceded by air passage over forests. *Nature*. **489**(7415), pp.282–285.
- Staples, M.D., Barrett, R.M. and H, S.R. 2017. The limits of bioenergy for mitigating global life-cycle greenhouse gas emissions from fossil fuels. *Nature Energy*. **2**(16202).
- Steffen, W., Richardson, K., Rockström, J., Cornell, S.E., Fetzer, I., Bennett, E.M., Biggs, R., Carpenter, S.R., De Vries, W., De Wit, C.A., Folke, C., Gerten, D., Heinke, J., Mace, G.M., Persson, L.M., Ramanathan, V., Reyers, B. and Sörlin, S. 2015. Planetary boundaries: Guiding human development on a changing planet. *Science*. **347**(6223), pp.1–10.
- Stein, B.A., Glick, P., Edelson, N. and Staudt, A. 2014. *Climate-smart conservation: putting adaptation principles into practice* [Online]. Washington D.C. Available from: <https://pubs.er.usgs.gov/publication/70093621>.
- Stibig, H.J., Achard, F., Carboni, S., Raši, R. and Miettinen, J. 2014. Change in tropical forest cover of Southeast Asia from 1990 to 2010. *Biogeosciences*. **11**(2), pp.247–258.
- Stickler, C.M., Nepstad, D.C., Coe, M.T., Mcgrath, D.G., Rodrigues, H.O., Walker, W.S., Soares-Filho, B.S. and Davidson, E.A. 2009. The potential ecological costs and cobenefits of REDD: a critical review and case study from the Amazon region. *Global Change Biology*. **15**(12), pp.2803–2824.
- Stocker, B.D., Zscheischler, J., Keenan, T.F., Prentice, I.C., Seneviratne, S.I. and Peñuelas, J. 2019. Drought impacts on terrestrial primary production underestimated by satellite monitoring. *Nature Geoscience*. **12**(4), pp.264–270.
- Stoms, D.M., Davis, F.W., Jenner, M.W., Nogueira, T.M. and Kaffka, S.R. 2012. Modeling wildlife and other trade-offs with biofuel crop production. *GCB Bioenergy*. **4**(3), pp.330–341.
- Stoy, A.P.C., Ahmed, S., Jarchow, M., Rashford, B., Swanson, D., Albeke, S., Brookshire, E.N.J., Dixon, M.D., Haggerty, J., Peyton, B., Royem, A., Spangler, L., Straub, C. and Poulter, B. 2018. Opportunities and Trade-offs among BECCS and the Food, Water, Energy, Biodiversity, and Social Systems Nexus at Regional Scales. *BioScience*. **68**(2), pp.100–111.
- Strandberg, G. and Kjellström, E. 2019. Climate impacts from afforestation and deforestation in Europe. *Earth Interactions*. **23**(1), pp.1–27.

- Strassmann, K.M., Joos, F. and Fischer, G. 2008. Simulating effects of land use changes on carbon fluxes: Past contributions to atmospheric CO<sub>2</sub> increases and future commitments due to losses of terrestrial sink capacity. *Tellus, Series B: Chemical and Physical Meteorology*. **60**(4), pp.583–603.
- Stratton, R.W., Wong, H.M. and Hileman, J.I. 2010. *Life Cycle Greenhouse Gas Emissions from Alternative Jet Fuels. Partner Project 28 report. Version 1.2*. Cambridge, Massachusetts.
- Stromberg, P. and Gasparatos, A. 2012. *Biofuels at the Confluence of Energy Security, Rural Development, and Food Security: A Developing Country Perspective in Socioeconomic and Environmental Impacts of Biofuels*. Cambridge, UK: Cambridge University Press.
- Stuart, S.N., Chanson, J.S., Cox, N.A., Young, B.E., Rodrigues, A.S.L., Fischman, D.L. and Waller, R.W. 2004. States and Trends of Amphibian Declines and Extinctions Worldwide. *Science*. **306**(5702), pp.1783–1786.
- Sunderlin, W.D., Sills, E.O., Duchelle, A.E., Ekaputri, A.D., Kweka, D., Toniolo, M.A., Ball, S., Doggart, N., Pratama, C.D., Padilla, J.T., Enright, A. and Otsyina, R.M. 2015. REDD+ at a Critical Juncture: Assessing the Limits of Polycentric Governance for Achieving Climate Change Mitigation. *International Forestry Review*. **17**(4), pp.400–413.
- Taheripour, F. and Tyner, W.E. 2013. Induced Land Use Emissions due to First and Second Generation Biofuels and Uncertainty in Land Use Emission Factors. *Economics Research International*. **2013**, pp.1–12.
- Terborgh, J. 1999. *Requiem for nature*. Island Press, Washington, DC.
- Tharammal, T., Bala, G., Narayanappa, D. and Nemani, R. 2018. Potential roles of CO<sub>2</sub> fertilization, nitrogen deposition, climate change, and land use and land cover change on the global terrestrial carbon uptake in the twenty-first century. *Climate Dynamics*. **52**(7–8), pp.4393–4406.
- Thomas, C.D., Cameron, A., Green, R.E., Bakkeness, M., Beaumont, L.J., Collingham, Y.C., Erasmus, B.F.N., Ferreira de Siqueira, M., Grainger, A., Hannah, L., Hughes, L., Huntley, B., van Jaarsveld, A.S., Midgley, G.F., Miles, L. and ... 2004. Extinction risk from climate change. *Nature*. **427**, pp.145–148.
- Thornton, P.E., Doney, S.C., Lindsay, K., Moore, J.K., Mahowald, N., Randerson, J.T., Fung, I., Lamarque, J.F., Feddes, J.J. and Lee, Y.H. 2009. Carbon-nitrogen interactions regulate climate-carbon cycle feedbacks: Results from an atmosphere-ocean general circulation model. *Biogeosciences*. **6**(10), pp.2099–2120.
- Thuiller, W., Lavergne, S., Roquet, C., Boulangeat, I., Lafourcade, B. and Araujo, M.B. 2011. Consequences of climate change on the tree of life in Europe. *Nature*. **470**(7335), pp.531–534.
- Tilman, D., Hill, J. and Lehman, C. 2006. Carbon-Negative Biofuels from Low-Input High-Diversity Grassland Biomass. *Science*. **314**(5805), pp.1598–1600.
- Tilman, D., May, R.M., Lehman, C.L. and Nowak, M.A. 1994. Habitat destruction and the extinction debt. *Nature*. **371**, pp.65–66.
- Tokarska, K.B. and Zickfeld, K. 2015. The effectiveness of net negative carbon dioxide emissions in reversing anthropogenic climate change. *Environmental Research Letters*. **10**(9).
- Tölle, M.H., Gutjahr, O., Busch, G. and Thiele, J.C. 2014. Increasing bioenergy production on arable land: Does the regional and local climate respond? Germany as a case study.

- Journal of Geophysical Research Atmospheres*. **119**(6), pp.2711–2724.
- Toshiba 2019. Construction Work Progresses at Large-Scale Carbon Capture Demonstration Facility. *Toshiba ESS*. [Online]. Available from: <https://www.toshiba-energy.com/en/thermal/topics/ccs-1.htm>.
- Townsend, A.R., Howarth, R.W., Bazzaz, F.A., Booth, M.S., Cleveland, C.C., Collinge, S.K., Dobson, A.P., Epstein, P.R., Holland, E.A., Keeney, D.R., Mallin, M.A., Rogers, C.A., Wayne, P. and Wolfe, A.H. 2003. Human health effects of a changing global nitrogen cycle. *Frontiers in Ecology and the Environment*. **1**(5), pp.240–246.
- Tsao, C.C., Campbell, J.E., Mena-Carrasco, M., Spak, S.N., Carmichael, G.R. and Chen, Y. 2012. Increased estimates of air-pollution emissions from Brazilian sugar-cane ethanol. *Nature Climate Change*. **2**(1), pp.53–57.
- Tscharntke, T., Clough, Y., Wanger, T.C., Jackson, L., Motzke, I., Perfecto, I., Vandermeer, J. and Whitbread, A. 2012. Global food security, biodiversity conservation and the future of agricultural intensification. *Biological Conservation*. **151**(1), pp.53–59.
- Tubiello, F.N., Salvatore, M., Rossi, S., Ferrara, A., Fitton, N. and Smith, P. 2013. The FAOSTAT database of greenhouse gas emissions from agriculture. *Environmental Research Letters*. **8**(1).
- Tudge, S.J., Purvis, A. and De Palma, A. 2021. The impacts of biofuel crops on local biodiversity: a global synthesis. *Biodiversity and Conservation*. **30**(11), pp.2863–2883.
- Turner, W.R., Brandon, K., Brooks, T.M., Gascon, C., Gibbs, H.K., Lawrence, K.S., Mittermeier, R.A. and Selig, E.R. 2012. Global biodiversity conservation and the alleviation of poverty. *BioScience*. **62**(1), pp.85–92.
- Tyukavina, A., Baccini, A., Hansen, M.C., Potapov, P. V., Stehman, S. V., Houghton, R.A., Krylov, A.M., Turubanova, S. and Goetz, S.J. 2015. Aboveground carbon loss in natural and managed tropical forests from 2000 to 2012. *Environmental Research Letters*. **10**(7).
- Uetz, P. and Etzold, T. 1996. The EMBL/EBI reptile database. *Herpetological Review*. **27**(4), pp.174–175.
- UN 2015. *Transforming Our World: The 2030 Agenda for Sustainable Development*. New York, NY.
- UNEP 2004. *Indicators for assessing progress towards, and communicating, the 2010 target at the global level*. Convention on Biological Diversity.
- UNFCCC 2011a. *Decision 2/CMP.7: Land Use, Land-use Change and Forestry. Publication FCCC/KP/CMP/2011/10/Add.1*.
- UNFCCC 2023. Nationally Determined Contributions (NDCs). *United Nations Framework Convention on Climate Change*. [Online]. Available from: <https://unfccc.int/process-and-meetings/the-paris-agreement/nationally-determined-contributions-ndcs>.
- UNFCCC 2011b. *Report of the Conference of the Parties on its sixteenth session, held in Cancun from 29 November to 10 December 2010. Addendum. Part two: Action taken by the Conference of the Parties at its sixteenth session. Technical Report*.
- UNFCCC, CBD, IISD, GIZ, UNEP and SwedBio 2022. *Promoting synergies between climate change adaptation and biodiversity through the National Adaptation Plan (NAP) and National Biodiversity Strategies and Action Plan (NBSAP) processes*. Terton, A., Qi, J. and Zúñiga, G. (authors). United Nations Climate Change Secretariat. Bonn.
- United Nations 2015. *Adoption of the Paris Agreement. 21st Conference of the Parties* [Online]. Available from: <http://unfccc.int/resource/docs/2015/cop21/eng/109r01.pdf>,

FCCC/CP/ 2015/L.9/Rev.1.

- Upham, P., Thornley, P., Tomei, J. and Boucher, P. 2009. Substitutable biodiesel feedstocks for the UK: a review of sustainability issues with reference to the UK RTFO. *Journal of Cleaner Production*. **17**(SUPPL. 1), pp.S37–S45.
- Valdez, Z.P., Hockaday, W.C., Masiello, C.A., Gallagher, M.E. and Philip Robertson, G. 2017. Soil Carbon and Nitrogen Responses to Nitrogen Fertilizer and Harvesting Rates in Switchgrass Cropping Systems. *Bioenergy Research*. **10**(2), pp.456–464.
- Valin, H., Peters, D., Berg, M. van den, Frank, S., Havlik, P., Forsell, N. and Hamelinck, C. 2015. *The land use change impact of biofuels in the EU: Quantification of area and greenhouse gas impacts*. ECOFYS, Kanaalweg, Utrecht, Netherlands.
- VanLoocke, A., Bernacchi, C. and Twine, T. 2010. The impacts of *Miscanthus*×*giganteus* production on the Midwest US hydrologic cycle. *GCB Bioenergy*. **2**, pp.180–191.
- Vaughan, N.E. and Gough, C. 2016. Expert assessment concludes negative emissions scenarios may not deliver. *Environmental Research Letters*. **11**(9).
- Veltman, K., Singh, B. and Hertwich, E.G. 2010. Human and environmental impact assessment of postcombustion CO<sub>2</sub> capture focusing on emissions from amine-based scrubbing solvents to air. *Environmental Science and Technology*. **44**(4), pp.1496–1502.
- Vesterdal, L., Ritter, E. and Gundersen, P. 2002. Change in soil organic carbon following afforestation of former arable land. *Forest Ecology and Management*. **169**(1–2), pp.137–147.
- Visconti, P., Pressey, R.L., Giorgini, D., Maiorano, L., Bakkenes, M., Boitani, L., Alkemade, R., Falcucci, A., Chiozza, F. and Rondinini, C. 2011. Future hotspots of terrestrial mammal loss. *Philosophical Transactions of the Royal Society B: Biological Sciences*. **366**(1578), pp.2693–2702.
- Van Der Voet, E., Lifset, R.J. and Luo, L. 2010. Life-cycle assessment of biofuels, convergence and divergence. *Biofuels*. **1**(3), pp.435–449.
- Volpato, G.H., Prado, V.M. and dos Anjos, L. 2010. What can tree plantations do for forest birds in fragmented forest landscapes? A case study in southern Brazil. *Forest Ecology and Management*. **260**(7), pp.1156–1163.
- van Vuuren, D.P., Edmonds, J., Kainuma, M., Riahi, K., Thomson, A., Hibbard, K., Hurtt, G.C., Kram, T., Krey, V., Lamarque, J.F., Masui, T., Meinshausen, M., Nakicenovic, N., Smith, S.J. and Rose, S.K. 2011. The representative concentration pathways: An overview. *Climatic Change*. **109**(5), pp.5–31.
- van Vuuren, D.P., Kriegler, E., O'Neill, B.C., Ebi, K.L., Riahi, K., Carter, T.R., Edmonds, J., Hallegatte, S., Kram, T., Mathur, R. and Winkler, H. 2014. A new scenario framework for Climate Change Research: Scenario matrix architecture. *Climatic Change*.
- van Vuuren, D.P., Sala, O.E. and Pereira, H.M. 2006. The future of vascular plant diversity under four global scenarios. *Ecology and Society*. **11**(2), p.25.
- Wang, M. 2007. *Ethanol: The complete energy lifecycle picture*. U.S Department of Energy, Energy Efficiency and Renewable Energy, Washington D.C, US.
- Wang, M., Wagner, M., Miguez-Macho, G., Kamarianakis, Y., Mahalov, A., Moustou, M., Miller, J., VanLoocke, A., Bagley, J.E., Bernacchi, C.J. and Georgescu, M. 2017. On the long-term hydroclimatic sustainability of perennial bioenergy crop expansion over the United States. *Journal of Climate*. **30**(7), pp.2535–2557.
- Wang, S. and Jaffe, P.R. 2004. Dissolution of a mineral phase in potable aquifers due to CO<sub>2</sub>

- releases from deep formations; Effect of dissolution kinetics. *Energy Conversion and Management*. **45**(18–19), pp.2833–2848.
- Wang, X., Biewald, A., Dietrich, J.P., Schmitz, C., Lotze-Campen, H., Humpenöder, F., Bodirsky, B.L. and Popp, A. 2016. Taking account of governance: Implications for land-use dynamics, food prices, and trade patterns. *Ecological Economics*. **122**, pp.12–24.
- Wang, Y.P., Zhang, Q., Pitman, A.J. and Dai, Y. 2015. Nitrogen and phosphorous limitation reduces the effects of land use change on land carbon uptake or emission. *Environmental Research Letters*. **10**(1).
- Warren, R., Vanderwal, J., Price, J., Welbergen, J.A., Atkinson, I., Ramirez-Villegas, J., Osborn, T.J., Jarvis, A., Shoo, L.P., Williams, S.E. and Lowe, J. 2013. Quantifying the benefit of early climate change mitigation in avoiding biodiversity loss. *Nature Climate Change*. **3**(7), pp.678–682.
- WBA 2020. *Global Bioenergy Statistics 2020*, World Bioenergy Association [Online]. Stockholm, Sweden. Available from: [https://worldbioenergy.org/uploads/201210\\_WBA\\_GBS\\_2020.pdf](https://worldbioenergy.org/uploads/201210_WBA_GBS_2020.pdf).
- WBA 2021. *Global Bioenergy Statistics 2021*, World Bioenergy Association. Stockholm, Sweden.
- WCED 1987. *Our Common Future: The Bruntland Report*. Oxford University Press from the New York, NY.
- Wearn, O.R., Carbone, C., Rowcliffe, J.M., Bernard, H. and Ewers, R.M. 2016. Grain-dependent responses of mammalian diversity to land use and the implications for conservation set-aside. *Ecological Applications*. **26**, pp.1409–1420.
- Weaver, A.J., Eby, M., Wiebe, E.C., Bitz, C.M., Duffy, P.B., Ewen, T.L., Fanning, A.F., Holland, M.M., Macfadyen, A., Matthews, H.D., Meissner, K.J., Saenko, O., Schmittner, A., Wang, H. and Yoshimori, M. 2001. The UVic Earth System Climate Model : Model Description , Climatology , and Applications to Past , Present and Future Climates. . **39**(4), pp.1–68.
- von Wehrden, H., Abson, D.J., Beckmann, M., Cord, A.F., Klotz, S. and Seppelt, R. 2014. Realigning the land-sharing/land-sparing debate to match conservation needs: Considering diversity scales and land-use history. *Landscape Ecology*. **29**(6), pp.941–948.
- West, P.C., Narisma, G.T., Barford, C.C., Kucharik, C.J. and Foley, J.A. 2011. An alternative approach for quantifying climate regulation by ecosystems. *Frontiers in Ecology and the Environment*. **9**(2), pp.126–133.
- Whitaker, J., Field, J.L., Bernacchi, C.J., Cerri, C.E.P., Ceulemans, R., Davies, C.A., DeLucia, E.H., Donnison, I.S., McCalmont, J.P., Paustian, K., Rowe, R.L., Smith, P., Thornley, P. and McNamara, N.P. 2018. Consensus, uncertainties and challenges for perennial bioenergy crops and land use. *GCB Bioenergy*. **10**(3), pp.150–164.
- WHO/UNICEF 2014. *Progress on Drinking Water and Sanitation: 2014 Update, Joint Water Supply and Sanitation Monitoring Programme*. World Health Organization & United Nations Children's Fund (UNICEF).
- WHO 2018. Frequently Asked Questions: Ambient and Household Air Pollution and Health. *World Health Organisation*. [Online]. Available from: [http://www.who.int/phe/health\\_topics/outdoorair/databases/faqs\\_air\\_pollution.pdf?ua=1](http://www.who.int/phe/health_topics/outdoorair/databases/faqs_air_pollution.pdf?ua=1)

- Wicke, B., Verweij, P., Van Meijl, H., Van Vuuren, D.P. and Faaij, A.P.C. 2012. Indirect land use change: Review of existing models and strategies for mitigation. *Biofuels*. **3**(1), pp.87–100.
- Wiens, J., Fargione, J. and Hill, J. 2011. Biofuels and biodiversity. *Ecological Applications*. **21**(4), pp.1085–1095.
- Wilcove, D.S., Giam, X., Edwards, D.P., Fisher, B. and Koh, L.P. 2013. Navjot's nightmare revisited: logging, agriculture, and biodiversity in Southeast Asia. *Trends in Ecology and Evolution*. **28**(9), pp.531–540.
- Williams, B.A., Grantham, H.S., Watson, J.E.M., Alvarez, S.J., Simmonds, J.S., Rogéiz, C.A., Da Silva, M., Forero-Medina, G., Etter, A., Nogales, J., Walschburger, T., Hyman, G. and Beyer, H.L. 2020. Minimising the loss of biodiversity and ecosystem services in an intact landscape under risk of rapid agricultural development. *Environmental Research Letters*. **15**(1).
- Williams, J.W., Jackson, S.T. and Kutzbach, J.E. 2007. Projected distributions of novel and disappearing climates by 2100 AD. *Proceedings of the National Academy of Sciences*. **104**(14), pp.5738–5742.
- Wiloso, E.I., Heijungs, R., Huppel, G. and Fang, K. 2016. Effect of biogenic carbon inventory on the life cycle assessment of bioenergy: Challenges to the neutrality assumption. *Journal of Cleaner Production*. **125**, pp.78–85.
- Wise, M., Calvin, K., Thomson, A., Clarke, L., Bond-Lamberty, B., Sands, R., Smith, S., Janetos, A. and Edmonds, J. 2009. Implications of limiting CO<sub>2</sub> Concentrations for Land Use and Energy. *Science*. **324**(1), pp.1183–1186.
- Wise, M.A., Calvin, K. V., Thomson, A.M., Clarke, L.E., Bond-Lamberty, B., Sands, R.D., Smith, S.J., Janetos, A.C. and Edmonds, J.A. 2009. *The Implications of Limiting CO<sub>2</sub> Concentrations for Agriculture, Land Use, Land-use Change Emissions and Bioenergy*. Pacific Northwest National Laboratory, University of Maryland, Maryland, US.
- World Bank 2021. World Bank Open Data. Available from: <https://data.worldbank.org/>.
- WRI 2022a. Indicators of Forest Extent: Forest Loss. *World Resource Institute*. [Online]. Available from: <https://research.wri.org/gfr/forest-extent-indicators/primary-forest-loss>.
- WRI 2022b. Indicators of Forest Extent: Primary Forest Loss. *World Resource Institute*. [Online]. Available from: <https://research.wri.org/gfr/forest-extent-indicators/primary-forest-loss>.
- Wright, A.J., Barry, K.E., Lortie, C.J. and Callaway, R.M. 2021. Biodiversity and ecosystem functioning: Have our experiments and indices been underestimating the role of facilitation? *Journal of Ecology*. **109**(5), pp.1962–1968.
- Wright, S.J. and Muller-Landau, H.C. 2006. The Future of Tropical Forest Species. *Biotropica*. **38**(3), pp.287–301.
- WWF 2012. *Living planet report 2012 – biodiversity, biocapacity and making better choices*. Support. Gland, Switzerland.
- Xu, H., Li, Y., Liu, S., Zang, R., He, F. and Spence, J.R. 2015. Partial recovery of a tropical rain forest a half-century after clear-cut and selective logging. *Journal of Applied Ecology*. **52**(4), pp.1044–1052.
- Yanai, A.M., Fearnside, P.M., Graça, P.M.L. de A. and Nogueira, E.M. 2012. Avoided deforestation in Brazilian Amazonia: Simulating the effect of the Juma Sustainable Development Reserve. *Forest Ecology and Management*. **282**, pp.78–91.



- Yang, Y., Luo, Y. and Finzi, A.C. 2011. Carbon and nitrogen dynamics during forest stand development: A global synthesis. *New Phytologist*. **190**(4), pp.977–989.
- Yee, K.F., Tan, K.T., Abdullah, A.Z. and Lee, K.T. 2009. Life cycle assessment of palm biodiesel: Revealing facts and benefits for sustainability. *Applied Energy*. **86**(SUPPL. 1), pp.S189–S196.
- Zabel, F., Delzeit, R., Schneider, J.M., Seppelt, R., Mauser, W. and Václavík, T. 2019. Global impacts of future cropland expansion and intensification on agricultural markets and biodiversity. *Nature Communications*. **10**(1), pp.1–10.
- Zaehle, S., Friedlingstein, P. and Friend, A.D. 2010. Terrestrial nitrogen feedbacks may accelerate future climate change. *Geophysical Research Letters*. **37**(1), pp.1–5.
- Zhang, K., Dang, H., Zhang, Q. and Cheng, X. 2015. Soil carbon dynamics following land-use change varied with temperature and precipitation gradients: evidence from stable isotopes. *Global Change Biology*. **21**(7), pp.2762–2772.
- Zhang, M., Lee, X., Yu, G., Han, S., Wang, H., Yan, J., Zhang, Y., Li, Y., Ohta, T., Hirano, T., Kim, J., Yoshifuji, N. and Wang, W. 2014. Response of surface air temperature to small-scale land clearing across latitudes. *Environmental Research Letters*. **9**(3).
- Zhang, Q., Pitman, A.J., Wang, Y.P., Dai, Y.J. and Lawrence, P.J. 2013. The impact of nitrogen and phosphorous limitation on the estimated terrestrial carbon balance and warming of land use change over the last 156 yr. *Earth System Dynamics*. **4**(2), pp.333–345.
- Zhao, M. and Pitman, A.J. 2002. The impact of land cover change and increasing carbon dioxide on the extreme and frequency of maximum temperature and convective precipitation. *Journal of Climate*. **15**(6), pp.2–5.
- Zickfeld, K., Azevedo, D., Mathesius, S. and Matthews, H.D. 2021. Asymmetry in the climate–carbon cycle response to positive and negative CO<sub>2</sub> emissions. *Nature Climate Change*. **11**(7), pp.613–617.
- Zilberman, D. 2017. Indirect land use change: much ado about (almost) nothing. *GCB Bioenergy*. **9**(3), pp.485–488.
- Zomer, R.J., Trabucco, A., Bossio, D.A. and Verchot, L. V. 2008. Climate change mitigation: A spatial analysis of global land suitability for clean development mechanism afforestation and reforestation. *Agriculture, Ecosystems and Environment*. **126**(1–2), pp.67–80.